Mineral Investigation of the Rare-Earth-Element-Bearing Deposits, Red Cloud Mining District, Gallinas Mountains, Lincoln County, New Mexico

By Russell A. Schreiner
Intermountain Field Operations Center

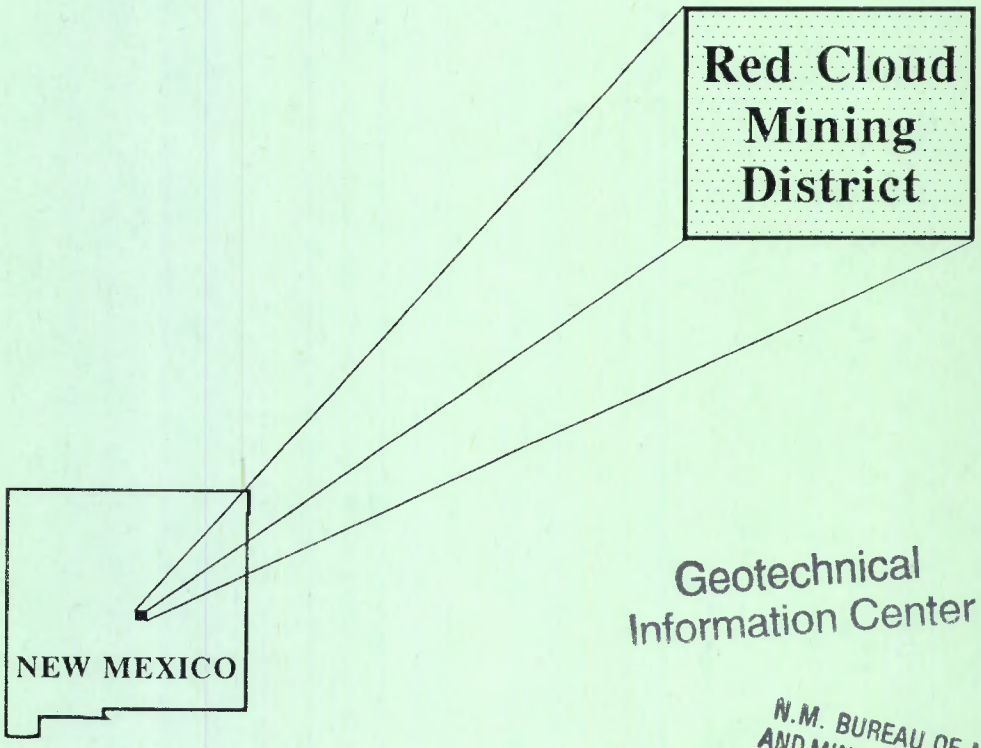

UNITED STATES DEPARTMENT OF THE INTERIOR
Bruce Babbitt, Secretary

BUREAU OF MINES
Hermann Enzer, Acting Director

OFR 99-93

This open-file report summarizes the results of a Bureau of Mines' site specific study. The report has not been edited or reviewed for conformity with the Bureau of Mines' editorial standards. This study was conducted by personnel from the Resource Evaluation Branch, Intermountain Field Operations Center, P. O. Box 25086, Denver Federal Center, Denver, CO 80225.

Table of Contents

ILLUSTRATIONS

TABLES

UNIT OF MEASURE ABBREVIATIONS USED IN THIS REPORT

cps	count per second
°C	degree celsius
ft	foot
in.	inch
mi	mile
mi^2	square mile
mm	millimeter
cm	centimeter
ppb	part per billion
ppm	part per million
%	percent
st	short tons
ft^3/st	cubic feet per short ton
oz	troy ounce
oz/st	troy ounce per short ton
lb	pound

MINERAL INVESTIGATION OF THE RARE-EARTH-ELEMENT-BEARING DEPOSITS, RED CLOUD MINING DISTRICT, GALLINAS MOUNTAINS, LINCOLN COUNTY, NEW MEXICO

By Russell A. Schreiner

ABSTRACT

In 1990 and 1991, the U. S. Bureau of Mines conducted a field investigation to evaluate the rare-earth and associated element resources in the Red Cloud mining district, Gallinas Mountains, Lincoln County, New Mexico. Bureau personnel mapped and sampled mines, prospects, and mineralized zones to appraise the mineral resources. Two hundred sixty samples were taken primarily from rare-earth-element-bearing fluorite-barite-quartz deposits in intrusive and fault breccias.

Subeconomic inferred resources were identified at the Old Hickory, Eagles Nest, Last Chance, and Conqueror No. 4-Hilltop prospects in fault breccia deposits. The deposits are small, 32,000 to 348,000 short tons, and contain low- to high-grade fluorite, 25% to 49%, and low-grade rare-earth-oxides, 0.8% to 2.3%.

Bureau personnel identified potassic and sodic fenitization and carbonatization in intrusive breccia pipes and adjacent country rocks. The presence of light-rare-earth-element-bearing fluorite-barite-quartz deposits and associated fenitization and carbonatization suggest that the Red Cloud district is the upper hydrothermal level of a carbonatite system. Although no economic resources were identified, significant concentrations of rare-earth-elements, fluorite, gold, silver, lead, copper, and zinc are present at the surface. The intrusive breccia pipes have not been fully explored and appear to be the best targets for rare-earth-elements, and precious and base metals. Although no carbonatites were identified on the surface they are inferred to be present at depth. A carbonatite body may contain increased concentrations of rare-earth-elements and base metals.

INTRODUCTION

The U.S. Bureau of Mines, in cooperation with the New Mexico Bureau of Mines and Mineral Resources and the U.S. Geological Survey, is conducting an investigation to evaluate the rare-earth element (REE) and associated metal resources of Tertiary alkaline intrusive complexes in New Mexico and Colorado. The deposits associated with Tertiary alkaline intrusive complexes have been classified as Great Plains Margin deposits by North and McLemore (1988). Great Plains Margin deposits, as defined by North and McLemore, contain precious, base, and REE and associated metals deposited in veins, breccias, skarns, and placers associated with alkaline intrusive complexes. The intrusions occur as stocks, laccoliths, dikes, and sills of middle to late Tertiary age along and near the margin between the Great Plains and the Rocky Mountain or Basin and Range physiographic provinces. It is generally believed that these intrusive complexes have formed from magmas generated by partial melting of the upper mantle or lower crust along a subduction zone as outlined by Clark and others (1982). Tertiary alkaline intrusive complexes occur in the Lincoln County Porphyry Belt, the Ortiz Mountains, the Cornudas Mountains and the Laughlin Peak area in New Mexico, and the Spanish Peaks/Huerfano Park and Cripple Creek areas in Colorado.

These Tertiary alkaline intrusive complexes have been mined primarily for gold (e.g., Cripple Creek, Colo.; Ortiz and White Oaks, N. Mex. districts) but also contain concentrations of REE and associated elements (McLemore and others, 1988a, b). Complete analytical data have not been published on the REE and associated element contents of many of these deposits. Tertiary alkaline intrusive complexes in New Mexico and Colorado may contain significant resources of REE, scandium, strontium, niobium, zirconium, hafnium, beryllium, and titanium, which are considered strategic and critical minerals by the Critical and Strategic Minerals Stockpiling Act (50 U.S.C. 98 et seq.) (1988-89) and Anti-Apartheid Act, Section 504 (1986). This report presents the results of a field investigation conducted in June and August of 1990, and May of 1991 in one of these alkaline intrusive complexes in the Gallinas Mountains, Lincoln County, N. Mex.

Geographic Setting

The Gallinas Mountains are in Lincoln County, in central New Mexico, approximately 40 mi north of Carrizozo, and 10 mi west of Corona (fig. 1). The Gallinas Mountains are part of the Basin and Range physiographic province near the margin with the Great Plains physiographic province. The Gallinas Mountains consist of a 15 mi long by 5 mi wide range that rises above the surrounding plains from approximately 6,800 ft to 8,637 ft on Gallinas Peak. The area investigated contains almost all of the known deposits in the Red Cloud mining district and comprises approximately 20,000 acres in the southern part of the Gallinas Mountains (pl. 1) and part of the Cibola National Forest administered by the U.S. Forest Service Mountainair Ranger District. Access to the area is by Forest Service dirt roads 99, 104, and 161, off of U.S. Highway 54.

Method of Investigation

Literature pertaining to the Gallinas Mountains was reviewed to obtain information concerning geology, mineral occurrences, and mining activity. Two geologists spent 54 days mapping and sampling prospects and mineralized zones. Two hundred and sixty rock-chip or grab samples were taken.

Analytical determinations were made by Bondar Clegg, Inc., Lakewood, Colo. All samples were analyzed three times and averaged for fourteen REE or nine REE (praseodymium, gadolinium, dysprosium, holmium, and erbium were not analyzed in some samples), scandium, thorium, and uranium by instrumental neutron activation analysis. All samples were also analyzed for gold by fire assay with an atomic absorption spectroscopy finish; antimony, arsenic, bismuth, chromium, cobalt, copper, iron, lead, manganese, molybdenum, nickel, silver, tungsten, and zinc by inductively coupled plasma emission spectroscopy with a nitric-hydrochloric acid hot extraction; barium, strontium, and yttrium by X-ray fluorescence; and mercury by cold vapor atomic absorption spectroscopy with a nitric-hydrochloric-tin sulfate acid extraction. Selected samples were analyzed for fluorine by specific ion method or distillation, iron by titrametric method, niobium by X-ray fluorescence, tellurium by atomic absorption spectroscopy, and whole rock components by borate fusion plasma emission spectroscopy. Reported analytical

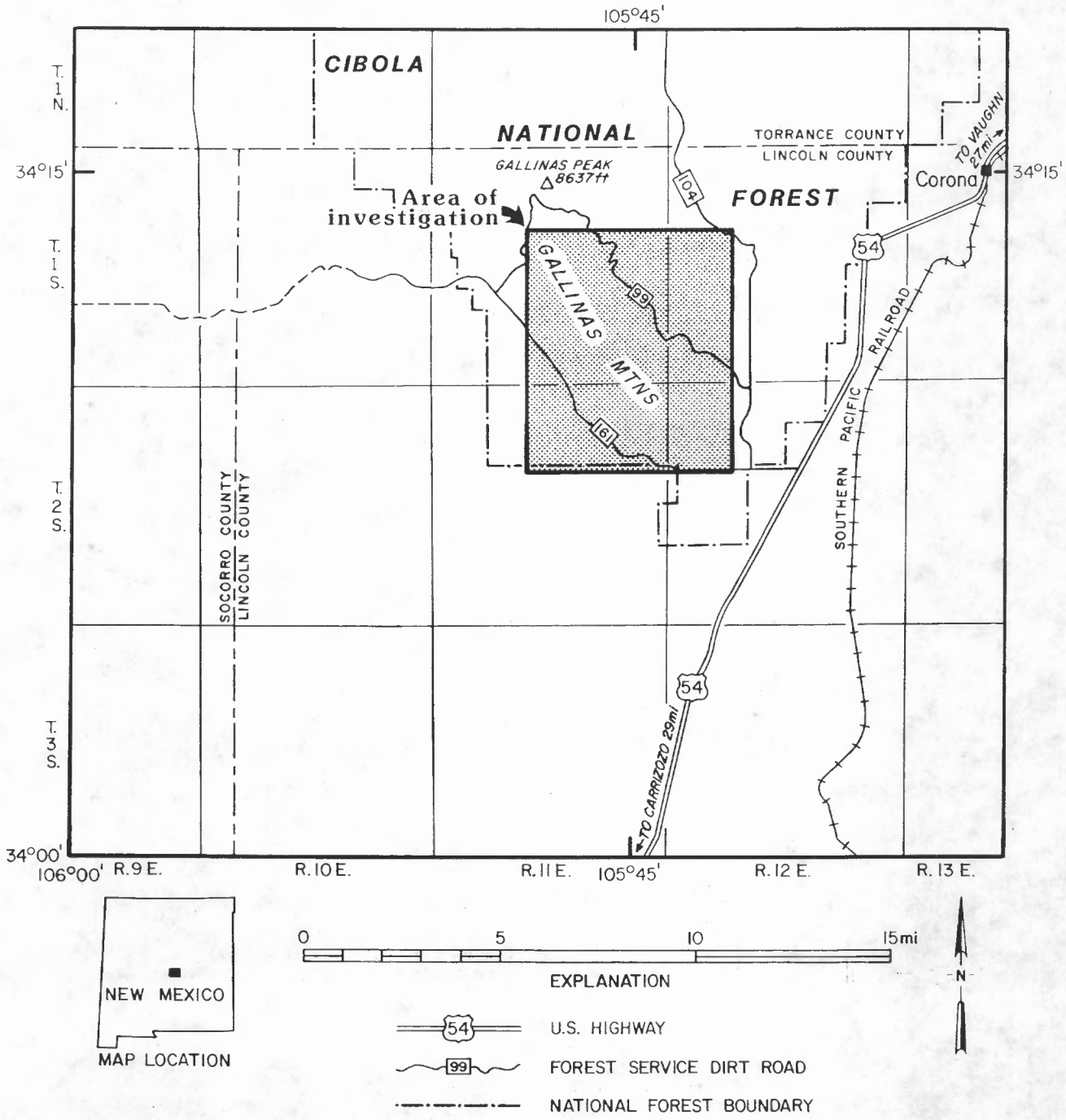

Figure 1. Index map of area of investigation in the Red Cloud mining district, Gallinas Mountains, Lincoln County, N. Mex.

concentrations are in the Appendix A; analytical data shown in the text are rounded to appropriate significant figures. The weight percent fluorite concentrations were calculated from the measured fluorine concentrations. The reported total rare-earth-oxide (REO) concentrations were calculated by converting the REE, including yttrium, to oxides (REE_2O_3) and then summed.

In addition to the analytical determinations, 32 polished thin sections and 4 thin sections of samples from mineralized zones and host rocks were examined using a petrographic microscope.

Scanning electron microscope-energy dispersive x-ray (SEM-EDX) analysis was done by James Sjoberg, U.S. Bureau of Mines, Reno Research Center, Reno, Nev., using a JEOL T-300 equipped with a Princeton Gamma Tech System 4 x-ray analyzer, with an Omega SLS x-ray detector. The SEM-EDX analysis should be considered semiquantitative and was conducted to verify petrographic mineral determinations and to help identify extremely fine-grained minerals. Additional semiquantitative SEM-EDX analysis was done on a Cambridge Stereoscan 250 MK 2 with the aid of Peter Modreski, U.S. Geological Survey, Denver, Colo.

Cathodoluminescence (CL) was observed on the polished thin sections and rock slabs using a Technosyn Model 8200 MK11 cathodoluminescence stage. CL is a process in which a sample is bombarded by an electron beam from a cold cathode gun resulting in the emission of light of various wavelengths. The wavelength and the intensity of the light emission characterize the mineral and the impurities, known as activators, within it (Marshall, 1988, p. 2). CL is an extremely useful tool in the examination of rocks altered by incipient fenitization (Mariano, 1978, p. 47-49).

Fenitization is a metasomatic process in which alkalis are introduced, from the late residual fluids of an alkalic magma, into previously crystallized rocks resulting in the replacement of the original minerals and the removal of silica. The original quartz, feldspar and mafic minerals are usually replaced by fenite feldspar, sodic pyroxene, and sodic amphibole. Incipient fenitization appears most commonly as veinlets consisting of fenite feldspar. Fenitization is best seen under CL due to the red-luminescing behavior of fenite feldspar, resulting

from ferric iron (Fe^{3+}) activation, which is formed by the invading fenite fluids crystallizing under conditions of high alkalinity and moderate to high temperatures (Mariano, 1978, p. 47 and 1988, p. 112-113). Almost all feldspars from igneous and metamorphic rocks show luminescence under CL. In nonalkaline rocks, potassium feldspars commonly luminesce bright blue, attributed to titanium (Ti^{4+}) activation and plagioclase feldspars commonly luminesce bright greenish yellow due to manganese (Mn^{2+}) and/or ferrous iron (Fe^{2+}) activation (Mariano, 1978, p. 47-49; Marshall, 1988, p. 57-66). In the Red Cloud district all fenite albite luminesces a brilliant red due to ferric iron activation. The fenite potassium feldspar in the Red Cloud district most commonly luminesces tan but it can vary from gray to bluish gray to tan to reddish tan to red and is also dominated by ferric iron activation. The tan and variable CL of the fenite potassium feldspar is very unusual and probably due to a defect in the crystal structure of the mineral (Anthony N. Mariano, consultant, oral commun., March 1992). Incipient fenitization is most commonly found in host rocks in contact with carbonatites and their related rocks (McKie, 1966, p. 261).

Apatite is a common accessory mineral in all igneous and metamorphic rocks. The color of luminescing apatite due to various impurities or activators observed under CL, can be an indicator of its trace element content and origin. The impurities are in concentrations too low to be detected by routine SEM analysis. The blue, violet, or lavender luminescence of apatite most frequently observed in primary apatite from carbonatites and related rocks is attributed to dominance of light-rare-earth-elements (LREE) activators. Apatite from normal granites and other nonalkaline rocks usually shows a yellow CL from manganese (Mn^{2+}) activation or a dominance of heavy-rare-earth-element (HREE) activators.(See Mariano, 1978, p. 41-47 and 1988, P. 101-102; Roeder and others, 1987.)

Considerable variation may be present in the colors seen under CL. The CL color and intensity of the color of a mineral varies with the activator, its concentration, and crystallographic or other factors. Spectrum scans of a mineral and correlation of the spectrum with that of the mineral that has been synthesized in the laboratory are required to determine the specific activator

or cause of the CL color. While it has been established that certain activators in specific minerals cause a certain CL color, research has been carried out for only a few materials, e.g., ferric iron activation causes the red luminescence in feldspars.(Compiled from Mariano and others, 1973; Geake and others, 1973; Marshall, 1988; and Anthony N. Mariano, consultant, Carlisle, Mass., oral commun., March 1992.)

CL photomicrographs were used in conjunction with SEM analysis of polished thin sections to identify the colors that characterize the various mineral phases. CL observations are included in this report. CL emission spectrographic analysis was done on a few selected samples to identify the activators responsible for the color of the luminescing mineral phase in selected samples. Anthony N. Mariano (consultant, Carlisle, Mass.) was consulted on interpretations of the CL of various minerals or mineral phases and provided the CL emission spectrographic analysis. The instrumentation used to generate the CL emission spectrographic analysis includes a MAAS Inc. (Nuclide) Luminoscope with a cold cathode electron gun and were obtained using a Spex Industries Inc., 1681B Spectrophotometer.

Inferred resources calculated for the REE-bearing fluorite barite-quartz deposits are only estimates of the tonnage and grade from the available data. For calculations, a projection of surface mapping and sample data to a depth of 200 ft was used because the larger adits and shafts show that mineralization was fairly continuous to this depth. Drilling by Molycorp Inc. has shown that high-grade REE-bearing-fluorite mineralized rock (greater than 5% REO) is present at depths over 400 ft and there is no reason to believe that the grade of the deposits decreases with depth. In addition, the reported inferred resource tonnage and grade does not represent a limit, and it is possible that similar mineralization extends laterally, as well as at depth beyond the calculated resource.

Scintillometer readings were taken with a Geometrics, model GR-101A gamma ray scintillometer.

The brand names referenced above do not imply endorsement by the Bureau of Mines.

Previous Investigations

The first detailed examination of the mineral deposits and geology in the Red Cloud (Gallinas) mining district was conducted in 1943 by the U.S. Bureau Of Mines and U. S. Geological Survey as part of the War Minerals Reports, in order to provide essential information to the U.S. Government and to assist owners and operators of mining properties in production of minerals vital to the war effort. Four reports describing the fluorite deposits and the geology were published, two by the U.S. Bureau of Mines (Soule, 1943; 1946) and two prepared by the U.S. Geological Survey (Kelley and others, 1946; Rothrock and others 1946). Glass and Smalley (1945) and Adams (1965) reported on the occurrence of bastnaesite in the fluorite deposits. Kelley (1949) and Harrer and Kelly (1963) discussed the iron deposits. Griswold (1959) reported on the history and production of the Red Cloud district and described some of the fluorite and iron deposits. McAnulty (1978) and Williams (1963) discussed the fluorite deposits. The first detailed map of the entire Gallinas Mountains and detailed petrographic work on the rocks and mineral deposits were published by Perhac (1960 and 1970). Perhac and Heinrich (1964) discussed the fluorite-bastnaesite deposits and bastnaesite paragenesis. DeMark (1980) and Modreski (1983) reported on the various minerals identified at the Red Cloud Copper and Red Cloud Fluorite Mines. McLemore and others (1988a, b) and McLemore (1991) contain general discussions on the Red Cloud mining district. Woodward and Fulp (1991) discuss gold mineralization in the district.

Acknowledgements

The Bureau thanks Anthony N. Mariano for assistance with the CL examination of polished thin sections and for furnishing the CL emission spectra and some CL photomicrographs. The Bureau also thanks Peter Modreski, U.S. Geological Survey, Denver, Colo. for help with additional SEM analysis of polished thin sections. The Bureau's work was facilitated by discussions with James G. Clark, Supervisor of Specialty Minerals Exploration, Hecla Mining Company, Coeur

d'Alene, Idaho, concerning the mineralization in the Red Cloud mining district. The manuscript benefitted from reviews by James Clark; Anthony N. Mariano, Consultant, Carlisle, Mass.; and Peter Modreski, Geologist, U. S. Geological Survey, Denver, Colo. Jan Groeneboer, photographer, U.S. Bureau of Mines, Denver, Colo. developed and color balanced all photographs in this report.

GEOLOGIC SETTING

The Gallinas Mountains are the northernmost of several intrusive domal uplifts of the Lincoln County Porphyry Belt on the north-south trending Mescalero-Pedernal Arch in Lincoln County. The range is elliptical in shape with the major axis trending northwest. A major fault in Red Cloud Canyon strikes parallel to this axis and is steeply dipping. (See Perhac, 1970, p. 31-32.)

The Gallinas Mountains consist of Precambrian basement gneissic granite, gneiss, and quartz diorite, overlain by Permian sedimentary rocks, predominantly sandstones, that have been intruded by Oligocene-age hypabyssal rocks (fig. 2). Oligocene-age intrusive rocks consist of rhyolite, trachyte, and latite porphyries and several intrusive breccia pipes. The rhyolite and trachyte occur as distinct laccoliths as well as sills and dikes that form the major part of the range, while the latite occurs only at Cougar Mountain, a small isolated mountain to the northeast. One andesite dike has been identified on the surface and one basalt dike is reported in a mine working. (See Perhac, 1970, p. 7.)

Many of the rocks in the area investigated by the Bureau are fenitized, a feature that was not reported in previous literature, and therefore rock descriptions citing the original mineral composition in these areas may be suspect. The recognition of fenitized rocks in the field is difficult except in some cases of strong fenitization. Polished thin sections and rock slabs examined using CL were usually required to positively identify fenitization. A study of all the rocks in the Gallinas Mountains is beyond the scope of this report and a short description of those that occur outside of the area investigated is given for background. Almost all of the rocks examined were

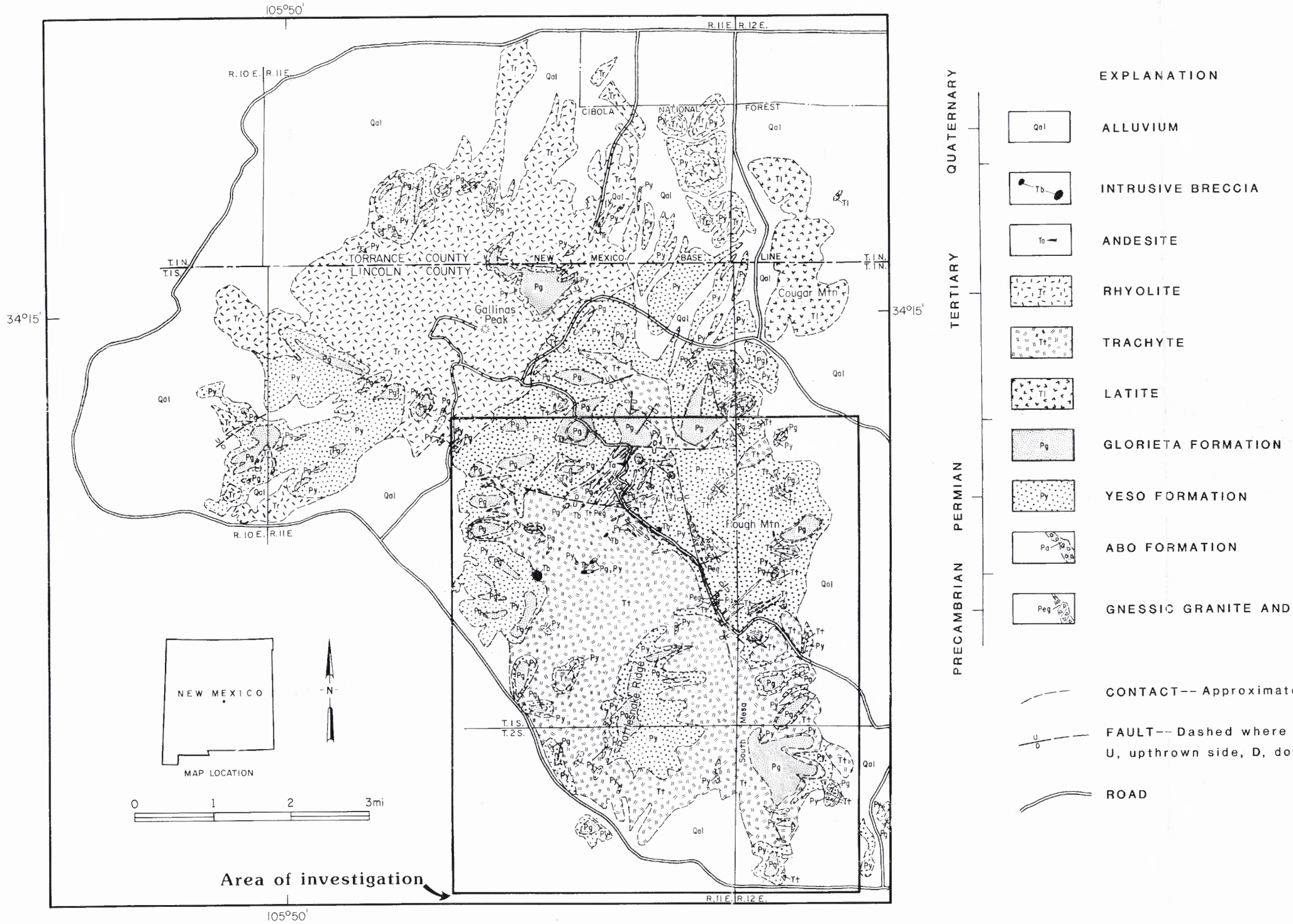

EXPLANATION

QUATERNARY

- Qal — ALLUVIUM

TERTIARY

- Tb — INTRUSIVE BRECCIA
- Ta — ANDESITE
- Tr — RHYOLITE
- Tt — TRACHYTE
- Tl — LATITE

PERMIAN

- Pg — GLORIETA FORMATION
- Py — YESO FORMATION
- Pa — ABO FORMATION

PRECAMBRIAN

- Peg — GNESSIC GRANITE AND GNEISS

CONTACT-- Approximately located

FAULT-- Dashed where approximately located, U, upthrown side, D, downthrown side

ROAD

Figure 2. Generalized geologic map of the Gallinas Mountains, Lincoln County, N. Mex. (from Perhac, 1970).

altered by incipient fenitization and only a few samples of relatively unaltered rocks were taken for comparison.

Precambrian Basement Rocks

Gneissic Granite

Precambrian gneissic granite is exposed in a few scattered outcrops in two upfaulted blocks along a fault in Red Cloud Canyon. The best exposures are found on the east side canyon wall south of the Red Cloud Fluorite Mine and in the drainage east of the Helen S Prospect (sample sites 105 and 106). The gneissic granite is a foliated light gray to pinkish gray, fine-grained (less than 1 mm), commonly equigranular rock. It consists of quartz, microcline, oligoclase, minor biotite, and accessory zircon, sphene, and apatite (Perhac, 1960, p. 18) Hornblende was also reported in thin sections examined by Molycorp (Curtis Serviss, 1981, Red Cloud district project report, Molycorp Inc., obtained from claim-owner Mrs. Edna L. Davis, 1746 Caudor Street, Encinitas, CA). In some areas the granite contains porphyroblasts of feldspar and quartz as much as 3 cm in diameter; the porphyroblasts locally form crude bands.

Although no polished thin sections were made from Bureau samples taken from the gneissic granite, two rock slabs were examined under CL. A sample from an outcrop in the drainage approximately 300 ft due east of the Helen S Prospect (sample sites 105 and 106) showed no evidence of fenitization, while the slabbed rock sample taken at site 239 showed brilliant red-luminescing fenite feldspar veinlets and a few patches of orange luminescing calcite along fractures under CL, an indication of alteration by incipient fenitization. Whole rock analytical results of sample 239 are in Appendix B. Chemically the sample plots on the granite-alkali granite boundary of the De La Roche R_1R_2 grid classification (Appendix C).

Gneiss

Gneiss is poorly exposed and much of the information on its character is from scattered outcrops and float fragments (sample sites 29, 30, 32-34, and 41) that are found in the upfaulted block north of the All American Prospect where

it has been altered by incipient fenitization. A small outcrop of gneiss is also found in the drainage approximately 300 ft due east of the Helen S Prospect (sample sites 105 and 106), where it has not been fenitized. The gneiss is a heterogeneous, irregularly banded rock, generally consisting of various proportions of medium- to coarse-grained (1 to 10 mm) plagioclase (albite), orthoclase, quartz, and minor biotite. It contains some myrmekite, minor microperthite, and accessory zircon, sphene, and apatite. In some areas it contains porphryroblasts of quartz and feldspar as long as 5 cm.

The gneiss contains local schistose bands at sample site 32 and in some float fragments scattered over the upfaulted block north of the All American Prospect. The schistose bands contain abundant biotite, plagioclase (andesine), orthoclase, and quartz. Some of the schistose fragments contain a few feldspar porphyroblasts.

At the small outcrop in the drainage east of the Helen S Prospect, augen gneiss is exposed and appears to be a xenolith within the gneissic granite. The augen gneiss consists of pink microcline porphyroblasts in a schistose groundmass of biotite, gray quartz, and white plagioclase feldspar.

Quartz Diorite

Quartz diorite was identified by Molycorp Inc. only in drill core from the eastern part of the Gallinas Mountains. It is a fine- to medium-grained rock consisting of plagioclase, microcline, hornblende, quartz and accessory biotite, sphene, rutile, pyrite, chalcopyrite, magnetite, and apatite (Curtis Serviss, 1981, Red Cloud district project report, Molycorp Inc., obtained from claim-owner Mrs. Edna L. Davis, 1746 Caudor Street, Encinitas, CA).

Incipient fenitization of the diorite was identified in drill core by Molycorp Inc. and is described in the mining history section.

Permian Sedimentary Rocks

Abo Formation

The Precambrian rocks are overlain by a red basal conglomeratic arkose and interbedded red shale, siltstone, sandstone, and conglomerate of the Permian Abo

Formation. The Abo Formation is best exposed in the upfaulted block east of the Helen S Prospect. The Abo Formation is as thick as 150 ft and the gradational contact with the overlying Yeso Formation has been arbitrarily defined by the complete disappearance of conglomeratic material. (See Perhac, 1970, p. 8).

Yeso Formation

The Permian Yeso Formation is the predominant rock type in the eastern part of the area investigated. It consists of tan, fine-grained feldspathic sandstone and minor interbedded siltstone, shale, limestone and dolomitic limestone. The Yeso Formation is approximately 1,500 ft thick, and the upper contact is marked by the appearance of distinct quartzose Glorieta Sandstone.(See Perhac, 1970, p. 9-10). Incipient fenitization of the sandstone was identified by the Bureau in two polished thin sections from sample sites 30 and 42 near the intrusive breccia north of the All American Prospect.

Glorieta Sandstone

The Permian Glorieta Sandstone caps many of the mountain tops in the area investigated by the Bureau. It is a white to light gray, coarse-grained orthoquartzite. Part of the formation has been eroded, but the remaining portion has a maximum thickness of approximately 250 ft on South Mesa in the Gallinas Mountains. (See Perhac, 1970, p. 11-12).

Oligocene Intrusive Rocks

Rhyolite

Rhyolite is present in the northwestern part of the Gallinas Mountains outside of the area investigated. Its greatest thickness and probable laccolithic center is around Gallinas Peak. The rhyolite is a white to buff porphyritic rock primarily consisting of albite phenocrysts, 0.5-1.5 mm in length, in an aphanitic groundmass. The groundmass, averaging 0.2 mm in grain size, consists of orthoclase, quartz, and some albite. Sparse biotite (as much as 3% locally) and rare aegirine or aegirine-augite make up the mafic minerals. Accessory minerals are apatite, sphene, magnetite, ilmenite, zircon, and muscovite. (See Perhac, 1970, p. 21-31).

Latite

A small stock of latite is present at Cougar Mountain. The latite is a light gray porphyritic rock consisting of oligoclase and hornblende phenocrysts, 2-5 mm in length, in an aphanitic groundmass. The groundmass, averaging 0.2 mm in length, consists of orthoclase feldspar and minor plagioclase. Accessory minerals are quartz, magnetite, apatite, zircon, and sphene.(See Perhac, 1970, p. 14).

Trachyte

Trachyte occurs in the southern part of the Gallinas Mountains and is the major rock type in the western part of the area investigated. The thickest section of trachyte and the probable laccolithic center, is exposed north of Rattlesnake Ridge (Perhac, 1970, p. 31). The trachyte is a white to light-gray, porphyritic rock that is variable in composition. It consists of subhedral to euhedral albite and subordinate potassium feldspar phenocrysts, ranging from 1 to 7 mm in length, in a aphanitic groundmass. The aphanitic groundmass consists of anhedral to subhedral laths of albite and potassium feldspar averaging 0.05-0.3 mm in length, with a pilotaxitic to trachytic texture. The mafic minerals occur as phenocrysts making up 2% to 10% of the rock. They are usually totally altered to hematite and limonite and appear to have been either biotite or hornblende as determined from the crystal outlines. The trachyte contains accessory apatite, quartz, zircon, and iron oxide. The apatite crystals are commonly prismatic ranging from 0.05-2 mm in length. The large apatite crystals, as large as some of the phenocrysts and commonly associated with them, were seen only in the trachyte dike at sample site 258.

The trachyte, though variable in composition, is predominantly sodic. The variable composition is reflected in three samples (54, 95, and 258) of relatively unaltered trachyte that were analyzed by whole rock analysis (Appendix B). Sample 95 from the trachyte laccolith and sample 258 from a trachyte dike contained 0.98% potassium oxide (K_2O) and 9.41% sodium oxide (Na_2O), and 2.45% K_2O and 8.35% Na_2O, respectively. Sample 54 from the trachyte laccolith contained much higher potassium, 5.52% K_2O, and lower sodium, 6.75% Na_2O, concentrations.

Chemically all three samples plot in the trachyte field of the De La Roche R_1R_2 grid classification although they are scattered (Appendix C).

No polished thin section was made from sample site 95, but a polished thin section from sample site 258 contains albite phenocrysts in a predominantly albite groundmass. Observed under CL the thin section consists of yellowish green luminescing albite and orangish yellow luminescing apatite and showed no evidence of fenitization.

A polished thin section from sample site 54 contains twinned albite phenocrysts altering to sericite, rimmed by turbid potassium feldspar, and subordinate potassium feldspar phenocrysts. The groundmass consists of stubby crystals and laths of potassium feldspar and albite, with some interstitial anhedral quartz. It appears that late quartz was introduced. Euhedral crystals as long as 0.4 mm, some containing numerous inclusions, were found lining the walls of a few vugs.

Observation under CL shows tan-luminescing potassium feldspar, dark brown or gray-luminescing albite, and brilliant red-luminescing albite with Fe^{3+} activation in the groundmass. The phenocrysts are rimmed with tan-luminescing potassium feldspar with cores of dull dark brown- or gray-luminescing albite. The rims are often an intergrowth of tan- and dark brown-luminescing feldspars. A few of the phenocrysts are blue-luminescing potassium feldspar. Some phenocrysts contain red-luminescing albite in cracks and two small areas of fine, 0.01 mm, brilliant red-luminescing albite in vugs suggest possible weak incipient fenitization, but no distinct veinlets of red-luminescing fenite feldspar are visible in the groundmass. It is interesting to note that fenitized trachyte country rock at the M and E No. 13 Prospect (sample site 85), also contains introduced quartz. Apatite crystals luminesce yellow. Quartz luminesces a bluish gray.

In the absence of distinct red-luminescing feldspar veinlets it is possible that the red luminescence of the groundmass albite could be due to internal fenitization. Internal fenitization is a condition in which residual fluids become enriched in alkalis during crystallization resulting in the stabilization

of ferric iron. The later crystallizing groundmass feldspar is red-luminescing due to ferric iron activation and earlier formed feldspar phenocrysts are commonly subject to peripheral replacement by ferric iron activated feldspar. Internal fenitization occurs without introduction of foreign fluids, and it is not specific to carbonatite-associated alkaline igneous rocks. (See Mariano, 1988, p. 113-116).

The tan-luminescing original potassium feldspar is unusual. Spectrum scans of the tan luminescencing potassium feldspar showed a broad intrinsic band characteristic of a defect in the crystal structure of the feldspar (Anthony N. Mariano, consultant, Carlisle, Mass., oral commun., March, 1992).

Alteration of the trachyte by incipient fenitization was identified at the M and E No. 13 Prospect (sample sites 83 and 85), in a dike and in float fragments at the intrusive breccia north of the All American Prospect (sample site 26 and 32), in a dike at the Rio Tinto Mine (sample sites 252 and 258), in a dike exposed in the road cut in Red Cloud Canyon (sample site 22), and in what appears to have been a syenite (sample site 23). The geographic extent of fenitization of the trachyte was not determined in this investigation but it appears to be present around the intrusive breccia pipes and along faults where the fenitizing fluids gained access to the rocks. Perhac (1970, p. 14-20) reported aegirine-augite and aegirine as subhedral to euhedral crystals in the trachyte and aegirine-augite and tiny euhedral crystals of riebeckite in the microsyenite phase, but they were identified only in fenitized rocks during this investigation.

Andesite

One dike of altered andesite approximately 28 ft in width, striking N. 55° to 75° W., and steeply dipping, intrudes sandstone near the Sky High Prospect. The dike is exposed in the main road up Red Cloud Canyon (pl. 1), and some fragments were found near a bulldozed area at the Sky High Prospect (sample site 21). It is a porphyritic rock, consisting of subhedral to euhedral phenocrysts (as long as 2 cm) of zoned hornblende, calcic pyroxene (probably salite, $Mg_{30.0}$ $Fe_{19.5}$ $Ca_{50.5}$), and plagioclase (albite-oligoclase) in a fine-grained groundmass of

anhedral to subhedral alkali and plagioclase feldspar. The mafic phenocrysts are unaltered. The plagioclase phenocrysts are sericitized and some are partially replaced by veinlets of fine-grained, clear potassium feldspar. Potassium feldspar was also found rimming some vugs, a possible indication of potassic fenitization. Prismatic apatite crystals as long as 1.5 mm and minor amounts of biotite are also present. A calcium-aluminum-silicate mineral rims some vugs, and calcite is found filling vugs.

The andesite showed no brilliant red-luminescing feldspar when examined under CL. The fenite potassium feldspar veinlets luminesces a dull reddish gray or gray. The polished thin section consists of yellowish green-luminescing plagioclase phenocrysts in a gray to reddish gray groundmass. The apatite luminesces yellow and the calcite orange. The calcium-aluminum-silicate mineral luminesces a brilliant yellow due to manganese (Mn^{2+}) activation (Anthony N. Mariano, consultant, Carlisle, MA, oral commun., March, 1992). Whole rock analysis from sample site 21 is in Appendix B, and the sample plots as a trachyandesite on the De La Roche R_1R_2 diagram (Appendix C).

Basalt

A dike of olivine basalt along the west side of the fault in Red Cloud Canyon at the Red Cloud Fluorite Mine was mapped by Smalley (Rothrock and others, 1946, p. 112 and plate 13).

Intrusive breccia

The term intrusive breccia as used in this report is defined as a heterogeneous mixture of angular to rounded fragments in a matrix of clastic material, which has been mobilized and intruded into its present position (Bates and Jackson, 1980). The intrusive breccias are believed to have been formed by the release of carbon dioxide under pressure and by a process of gas fluidization as described by McCallum (1985, p. 1525).

Intrusive breccias occur as pipes, roughly elliptical in shape, in the western part of the area investigated and form a northeast-trending belt 2 mi

long and 1/2 mi wide near the center of the trachyte laccolith. The intrusive breccia pipes also occur along a northwest-striking fault in Red Cloud Canyon that cuts across the northeastern part of this belt (pl. 1). Sixteen intrusive breccia pipes were primarily identified by mapping float, although some are probably connected, and all contacts are approximate. The pipes cut Precambrian basement rocks, Permian sedimentary rocks, and Oligocene trachyte. The largest pipe occurs north of the M and E No. 13 Prospect in the western part of the area and is approximately 1,000 ft wide and 2,000 ft long.

The identified intrusive breccia pipes, except for two pipes at the M and E. No. 13 Prospect and part of a pipe at the Sky High Prospect, are matrix supported. They consist of angular to rounded granite, gneiss, trachyte, sandstone, and limestone clasts (as much as 6 in. in diameter), and crystal fragments in a aphanitic matrix. The matrix consists of a fine-grained (less than 0.01 mm) mass of anhedral to subhedral feldspar, sometimes with a trachytic texture. Some of the matrix appears to be porphyritic and contains feldspar and mafic phenocrysts, although most appear to be crystal fragments from the intruded rocks. The mafic minerals are altered to hematite-limonite.

The two pipes at the M and E No. 13 Prospect (pl. 1) are clast-supported intrusive breccias. The breccias consist predominantly of angular to subangular trachyte clasts and subordinate angular to rounded sandstone and granitic clasts. The clast-supported breccias occur within a few hundred feet of the matrix-supported breccias and may grade into them, but this could not be determined due to soil and colluvial cover. The same appears to be the case at the Sky High Prospect where only part of the intrusive breccia contains an aphanitic matrix. These breccias are interpreted as intrusive breccia pipes because of their shape and the presence of angular to rounded clasts of sandstone and granite. The presence of granite clasts indicates that they have been carried upward to their present position. The absence of the aphanitic matrix and dominance of clasts from the surrounding country rock suggest that these pipes, or parts of these pipes, did not completely blow out at this level and that mixing of the clasts

by fluidization was incomplete. It is also possible that the pipes formed along pre-existing faults.

Most of the intrusive breccias are highly weathered; the aphanitic matrix commonly has a bleached tan color and is stained by limonite. All of the intrusive breccias appear to have been altered. Weak to strong incipient fenitization was identified in intrusive breccias at the M and E No. 13 Prospect, north of the All American Prospect, the Sky High Prospect, and the 17 No. 2 Prospect, as well as in polished thin sections or rock slabs from the intrusive breccias at sample sites 44, 55, 56, and 68. Observation under CL showed red luminescing fenite feldspar veinlets cutting both the matrix and the clasts of the intrusive breccias.

Carbonatization (replacement by carbonates) was observed in the intrusive breccias at the intrusive breccia north of the All American Prospect, at the M and E No. 13 Prospect, at the Sky High Prospect, the 17 No. 2 Prospect, and at the intrusive breccia at sample site 43.

MINING HISTORY

The Red Cloud, Buckhorn, and Summit mining claims, were located in 1881 and were the first claims staked for precious and base metals. Eighteen claims were subsequently patented in the eastern part of the district from 1891 through 1952 (fig. 3). From 1909 through 1953, 5,086 st of ore was sold or treated containing 5.58 oz gold, 23,526 oz silver, 383,344 lb copper, 1,717,570 lb lead, and 19,029 lb zinc (Table 1) (U. S. Bureau of Mines, production record files). The ore contained an average grade of 4.6 oz/st silver, 3.9% copper, and 16.9% lead. No zinc was produced prior to 1948. Base and precious metal production came mainly from the Red Cloud Copper Mine (Corona Queen Mine, Deadwood Mine) with minor production from the Rio Tinto Mine (Conqueror Mine) and Buckhorn Mine (Little Wonder Adit). The Buckhorn Mine produced a total of 50 st of ore during 1951 and 1953, containing an average grade of 4.3 oz/st silver, 9.4% copper, 19.2% lead, and 1.7% zinc. McLemore (1991, p. 64) also reported production of 23 st containing 45 oz silver and 7,900 lb lead in 1954 and 250 st containing 1 oz

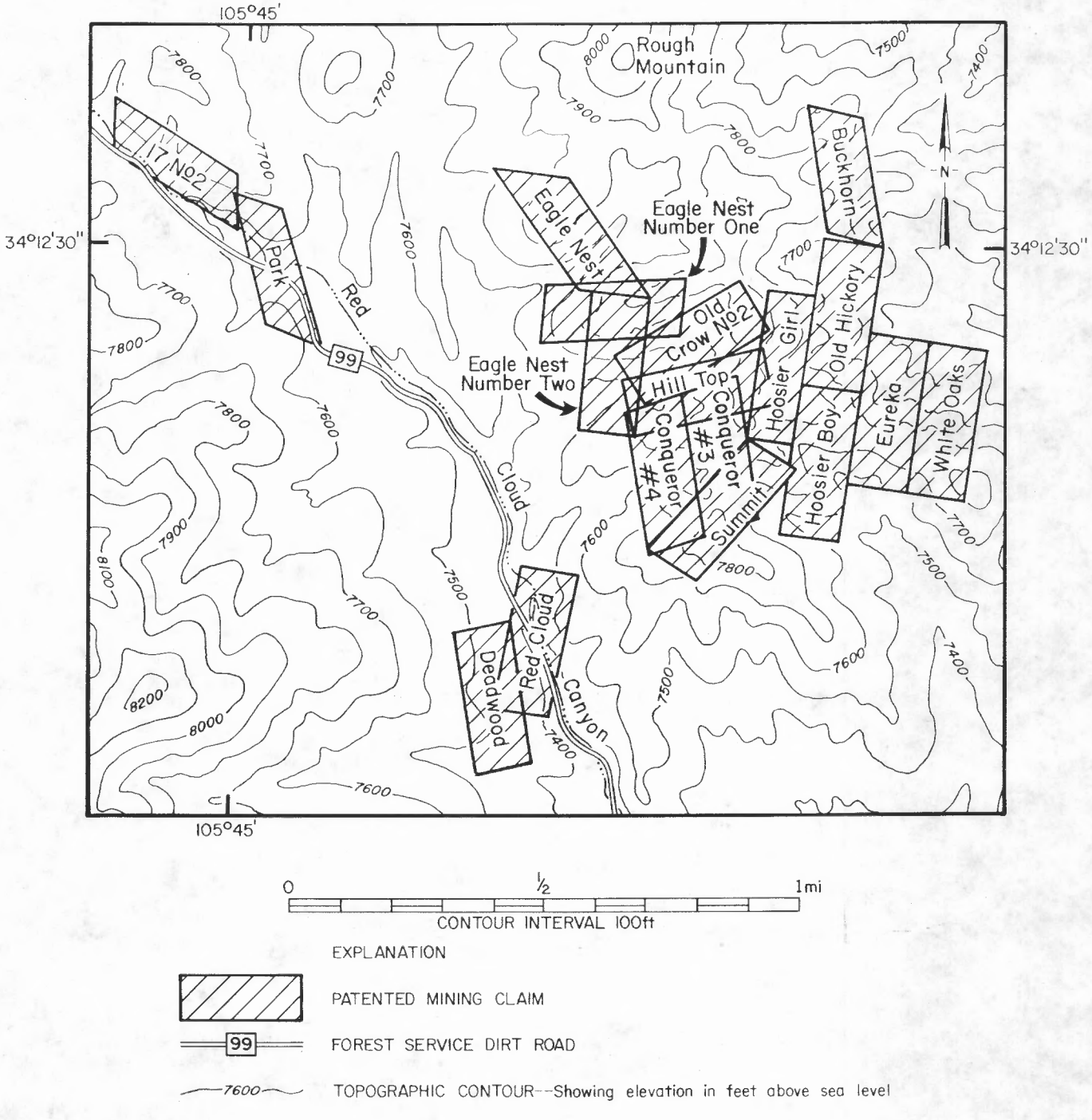

Figure 3. Map showing patented claims in the Red Cloud mining district, Gallinas Mountains, Lincoln County, N. Mex.

Table 1-- Recorded precious and base metal annual production for the Red Cloud mining district, Lincoln County, N. Mex. (Data from Bureau of Mines production files.)

[np, no production; na, not applicable; st, short ton; oz, ounce; lb, pound]

Year	Ore sold or treated (st)	Gold (oz)	Silver (oz)	Copper (lb)	Lead (lb)	Zinc (lb)
1909	14	np	42	361	7,907	np
1910	np	np	np	np	np	np
1911	8	np	70	555	6,620	np
1912	131	np	879	8,337	103,911	np
1913	157	0.18	895	7,068	94,010	np
1914	82	3.44	649	15,068	10,641	np
1915	46	.11	243	5,091	13,277	np
1916-19	np	np	np	np	np	np
1920	363	np	1,345	11,386	171,925	np
1921	378	np	2,552	49,240	155,222	np
1922	1,893	np	11,015	213,072	700,072	np
1923	578	np	3,065	38,966	232,657	np
1924	121	np	409	8,596	26,912	np
1925-26	np	np	np	np	np	np
1927	60	np	381	3,382	21,683	np
1928	18	np	77	667	7,000	np
1929	np	np	np	np	np	np
1930	23	.19	151	700	12,000	np
1931	np	np	np	np	np	np
1932	24	.58	103	1,000	11,500	np
1933	42	.39	103	1,000	14,000	np
1934	30	.29	221	4,400	13,850	np
1935	61	.40	185	2,000	17,300	np
1936-47	np	np	np	np	np	np
1948	1,015	np	927	13,085	77,891	17,685
1949-50	np	np	np	np	np	np
1951*	11	np	32	4,841	4,841	369
1952	np	np	np	np	np	np
1953*	39	np	182	4,529	14,351	1,344
Total	5,086	5.58	23,526	393,344	1,717,570	19,029

{Almost all production indicated as being from Red Cloud Copper (Deadwood) Mine.}

Red Cloud mining district

	Silver	Copper	Lead
Average grade	4.6 oz/st	3.9 %	16.9 %

Buckhorn (Little Wonder) Mine

	Silver	Copper	Lead	Zinc
Average grade	4.3 oz/st	9.4 %	19.2 %	1.7 %

* - Production from Buckhorn (Little Wonder) Mine

gold, 205 oz silver, and 7,900 lb lead in 1955 from the district.

In 1942 and 1943, 2,785 st containing 56.2% iron and 1,159 st containing 54.5% iron were produced from the American Iron Mine, respectively (table 2) (Kelley, 1949, p. 173). In 1942, 6,410 st containing 48.7% iron were produced from the Red Cliff Mine (Corona, Gallinas, Iron Chief) (Kelley, 1949, p. 177). The Bureau of Mines conducted trenching and sampling at the American Iron Mine and the Little Marie Iron Prospect in 1943, but no additional ore was produced (Harrer and Kelly, 1963, p. 47).

In 1942, fluorite was discovered during the construction of a road to the American Iron Mine at the site of the All American Mine. The Bureau of Mines conducted an exploratory program to identify fluorite reserves that could contribute to the supply needed for the war effort in 1943 and 1944. The Bureau excavated 2,887 ft of trenches, 161 ft of shafts, 280 ft of test pits, 35.5 ft of raises, 663.5 ft of drifting and crosscutting; and drilled 175 ft of wagon drill holes and 967 ft of diamond drill holes. In addition, the Bureau took 450 samples that were analyzed for fluorite and in some cases barite, and performed processing tests for the recovery of fluorite and by-product bastnaesite. The work was done on the Red Cloud Fluorite Mine (Conqueror No. 9 Claim), Old Hickory Prospect, Hoosier Girl North Prospect, Eureka Prospect, Eagles Nest Prospect, Hilltop Prospect, Conqueror No. 4 Prospect, All American Prospect, and Bottleneck Prospect (Soule, 1946). Production of 1,608 st of fluorite was recorded in 1951, 1953, and 1954 (table 2)(Griswold, 1959, p. 64). The fluorite was produced from the Red Cloud Fluorite Mine and Conqueror No. 10 Mine. In 1956, approximately 300 st of copper-lead-fluorspar ore was reported to have been mined from the Rio Tinto Mine by the New Mexico Copper Corporation (Griswold, 1959, p. 64). McAnulty (1978, P. 18) estimated 129 st of fluorite was produced from the All American Prospect.

During the fluorite exploration project, the rare-earth-element fluorocarbonate bastnaesite was first identified in the Red Cloud district, but only two samples from the Red Cloud Fluorite Mine were analyzed for REE (Soule, 1946). From 1954 though 1956, 142,000 lb of bastnaesite was produced from the

Table 2-- Recorded iron, fluorspar, and bastnaesite production for the Red Cloud mining district, Lincoln County, N. Mex. (Data from Griswold, 1959, p. 64 and Kelley, 1949, p. 172)

[np, no production; st, short ton; lb, pound]

Year	Iron ore (st)	Fluorspar (st)	Bastnaesite concentrate (lb)
1942	9,195	np	np
1943	1,159	np	np
1944-50	np	np	np
1951	np	80	np
1952	np	np	np
1953	np	674	np
1954	np	854	40,000
1955	np	np	84,000
1956	np	np	22,000
Total	10,354	1,608	146,000

Red Cloud Fluorite Mine and the Conqueror No. 10 Mine (table 2)(Griswold, 1959, p. 64). The concentrate from the Red Cloud Fluorite Mine ore was processed in a small mill owned by United States Rare Earths Inc. at Gallinas.

Since the 1950's, little exploration has taken place in the district. In 1980, Phelps Dodge drilled one inclined core hole to a depth of 532 ft at the Rio Tinto Mine and penetrated no significant mineralized rock; additional information on the project was not available.

In 1980 and 1981, Molycorp Inc. conducted a geochemical survey and a ground magnetic survey in the eastern part of the district (Curtis Serviss, 1981, Red Cloud district project report, Molycorp Inc., obtained from claim-owner Mrs. Edna L. Davis, 1746 Caudor Street, Encinitas, CA). Subsequently, two diamond drill holes were drilled on a magnetic high found during the survey. Hole no. 1 was drilled due west and inclined at 45° at the Eureka Prospect to a total depth of 404 ft, and hole no. 2 was drilled S. 30° W. and inclined at 53° at the Old Hickory Prospect to a total depth of 888 ft. Precambrian quartz diorite was penetrated at 203 ft in hole no. 1 and at 157 ft in hole no. 2. Mineralized rock was penetrated only in hole no. 2 at 445 ft where a 4-ft-thick zone of brecciated quartz diorite with a fluorite matrix contained 1.34% REO, and from 497.5 ft to 558 ft where a zone of fractured and brecciated diorite in a fluorite-barite-quartz matrix was penetrated. Four samples of core from parts of this zone contained erratic REO concentrations. Intercepts; 497.5-507.5 ft contained 0.77% REO, 519-524 ft contained 0.21% REO, 538-545 ft contained 5.20% REO, and 556-558 ft contained 0.27% REO. Incipient fenitization of the diorite was observed by CL in core samples from both holes. In hole no. 1, incipient fenitization was identified from a core sample containing calcite veinlets in the diorite at 334.6 ft. The calcite veinlets have a selvage of potassium feldspar replacing diorite; hornblende was replaced by riebeckite. In hole no. 2, a core sample of a fluorite veinlet in the diorite at 418.2 ft, contained veinlets of potassium feldspar replacing diorite roughly normal to the fluorite veinlet with calcite patches in trace amounts.

In 1989, Canyon Resources conducted mapping and a geochemical survey as part of a gold exploration program. Hecla Mining Company acquired the property in a joint venture with Canyon Resources in 1991 and is conducting additional mapping and geochemical sampling and had drilled seven shallow reverse circulation holes during October 1991 (James G. Clark, Supervisor of Specialty Metals Exploration, Hecla Mining Company, Coeur d'Alene, Idaho, oral commun., August 1991). Additional work was conducted in 1992. As of 1991, American Copper and Nickel Inc. and Romana Resources were also conducting gold exploration in the district.

MINERAL DEPOSITS

Two types of mineral deposits have been identified in the Red Cloud district, REE-bearing, fluorite-barite-quartz breccia deposits and iron replacement deposits. The fluorite-barite-quartz breccia deposits usually contain minor concentrations of precious and base metals, although three of the deposits are lead, copper, silver, and arsenic rich.

The REE-bearing, fluorite-barite-quartz deposits were deposited as open-space filling in the breccias that were formed after the solidification of the trachyte magma. The breccias are divided into two types; mineralized intrusive breccia deposits formed by explosive activity probably by carbon dioxide gas and mineralized fault breccia deposits formed by tectonic activity probably due to the intrusion of the magmas.

Although all of the intrusive breccias appear to have been fenitized only a few are mineralized. Mineralized intrusive breccias were identified in and around the trachyte laccolith in the western part of the area investigated. All of the mineralized intrusive breccias are also carbonatized.

The fault breccia deposits are located mainly in the eastern part of the district, away from the center of the trachyte laccolith in the more highly fractured and faulted sandstones. No fenitization was found associated with the fault breccia deposits and only minor replacement of the wallrocks and rock fragments by pyrite, fluorite, calcite, and quartz was observed.

The iron deposits are pyrometasomatic replacements that occur in limestone in contact with trachyte and they are the oldest mineral deposits in the district formed during the intrusion of the trachyte magma.

Intrusive Breccia Deposits

Fenitized and carbonatized, weakly to strongly mineralized intrusive breccia pipes at the M and E No. 13 Prospect, Sky High Prospect, and at a little prospected intrusive breccia north of the All American Prospect are discussed in the text below. Nineteen samples (43-45, 55-57, 60, 62, and 65-70) taken from twelve other identified pipes contained low REO and gold concentrations. REO concentrations ranged from 439 to 1,085 ppm. Eight of these samples from five intrusive breccia pipes contained elevated (greater than 5 ppb) gold concentrations ranging from 7 to 23 ppb. Two smaller mineralized intrusive breccia pipes, at the Park and the 17 No. 2 Prospects are summarized in table 3 and shown on plate 1 and on figure 26.

M and E No. 13 Prospect

Description

The M and E No. 13 Prospect (pl. 2, sample sites 71-85) consists of a caved shaft, an 18-ft-deep shaft, 3 pits, and a 70- by 50-ft bulldozed area. The workings are located on the southern edge of a horseshoe-shaped intrusive breccia pipe approximately 700 ft long on the east side and 350 ft long on the west side that wraps around the nose of a ridge. The extent of the pipe was difficult to determine due to the presence of more abundant intrusive breccia float from a large pipe on the ridge above (pl. 1); it is possible that the two pipes are connected. The width of the pipe ranges from 150 to 350 ft. Mapping of the pipe was done mostly by float because outcrops are small and scattered, therefore contacts are approximate.

The intrusive breccia is clast supported and consists primarily of angular and a few rounded trachyte clasts; some outcrops consist only of brecciated trachyte. Rounded to angular sandstone fragments generally 2-4 in. in diameter, although one fragment at least 3 ft in diameter was found, are found scattered over the pipe. At the outcrop at sample site 73, a 2 in. diameter rounded granitic clast was found. At the two ends of the horseshoe-shaped pipe the float fragments appear to grade into an aphanitic matrix-supported intrusive breccia with some granitic clasts, but this may represent float from the large matrix supported intrusive breccia pipe on the ridge above.

Abundant fluorite, barite, and calcite occur in the matrix of the intrusive breccia in the southern part of the pipe. The mineralized rock is exposed over a 100 ft diameter area in workings at sample sites 76-82. Fluorite-barite-quartz mineralized rock is also present in outcrop over a distance of 7 ft at sample site 71, 400 ft to the north in the northeastern part of the pipe. A few pieces of fluorite-barite-quartz float were found in the drainage at sample site 75 and on the east side of the drainage. The extent of mineralization and the relationship of these two areas could not be determined due to soil cover.

In addition to the horseshoe-shaped pipe, a smaller elliptical shaped intrusive breccia pipe was found 300 ft to the east at sample sites 86 and 87 (pl. 1). The pipe is approximately 300 ft long and 120 ft wide; determined by mapping of float. The breccia exposed in a small pit at sample site 87 consists of bleached white angular clasts of trachyte; fluorite and some barite were visible in cavities.

Scintillometer readings over most of the large intrusive breccia were slightly anomalous, averaging 75 cps and ranging from 50 to 380 cps. Scintillometer readings over most of the trachyte in the area ranged from 50 to 60 cps; readings increased to 100 cps in some areas near and at the edges of the pipe. Scintillometer readings over the smaller pipe ranged from 60 to 130 cps.

Mineralogy

Fluorite, barite, quartz, calcite, pyrite, bastnaesite, and xenotime occur mainly as open-space fillings in the intrusive breccia at the M and E No. 13 Prospect. Minor chrysocolla and malachite coating vugs were noted at a few sites.

Bastnaesite occurs as brownish yellow to greenish yellow hexagonal plates with a waxy luster. At sample sites 76 and 80, the bastnaesite occurs as cracked and broken anhedral to euhedral crystals, as long as 1.3 cm (fig. 4). At sample site 71, the bastnaesite occurs as 0.1- to 0.5-mm long, commonly broken, stubby platy crystals and as clusters of smaller crystals, 0.01-0.05 mm in length. SEM-EDX analysis of 6 points on bastnaesite crystals from sample sites 71, 76, and 80 detected an average of 31.8% La_2O_3, 31.7% Ce_2O_3, 4.3% Pr_2O_3, 7.6% Nd_2O_3, 0.3% Sm_2O_3, 1.0% Gd_2O_3, 0.6% CaO, 4.8% F, and 17.7% CO_3. In addition to the bastnaesite, an unidentified REE-bearing mineral occurs in 10-micron long acicular bundles and appears to be a secondary mineral in vugs and cracks. SEM analysis detected 23.8% La_2O_3, 33.5% Ce_2O_3, 4.4% Pr_2O_3, 9.3% Nd_2O_3, 1.0% Sm_2O_3, 1.2% Gd_2O_3, 3.9% CaO, 4.9% F, and 18.1% CO_3. The difference in composition from the bastnaesite is the increased calcium oxide content. The mineral could be parisite, a calcium and REE-bearing fluorocarbonate; however the calcium oxide content is lower and REO content is higher than reported parisite analyses.

Xenotime occurs as 10- to 50-micron, subhedral to euhedral crystals at sample sites 71 and 80. SEM analysis of one crystal from sample site 80 detected 46.6% Y_2O_3, 2.4% Dy_2O_3, 3.8% Er_2O_3, 5.4% Yb_2O_3, 1.9% CaO, and 39.9% P_2O_5. Xenotime crystals commonly luminesce yellow under CL, but a few of the small crystals did not luminesce.

Purple fluorite occurs most commonly as cracked or broken, anhedral to euhedral, zoned cubic crystals, as much as 3 mm and averaging 1 mm in diameter. These larger fluorite crystals commonly have deeper purple rims with smaller, 0.01-0.05 mm, subhedral to euhedral cubic fluorite rimming them. Both the coarse- and fine-grained crystals of fluorite are found deposited on rock clasts. The fine-grained fluorite also occurs as spotty replacements in rock clasts.

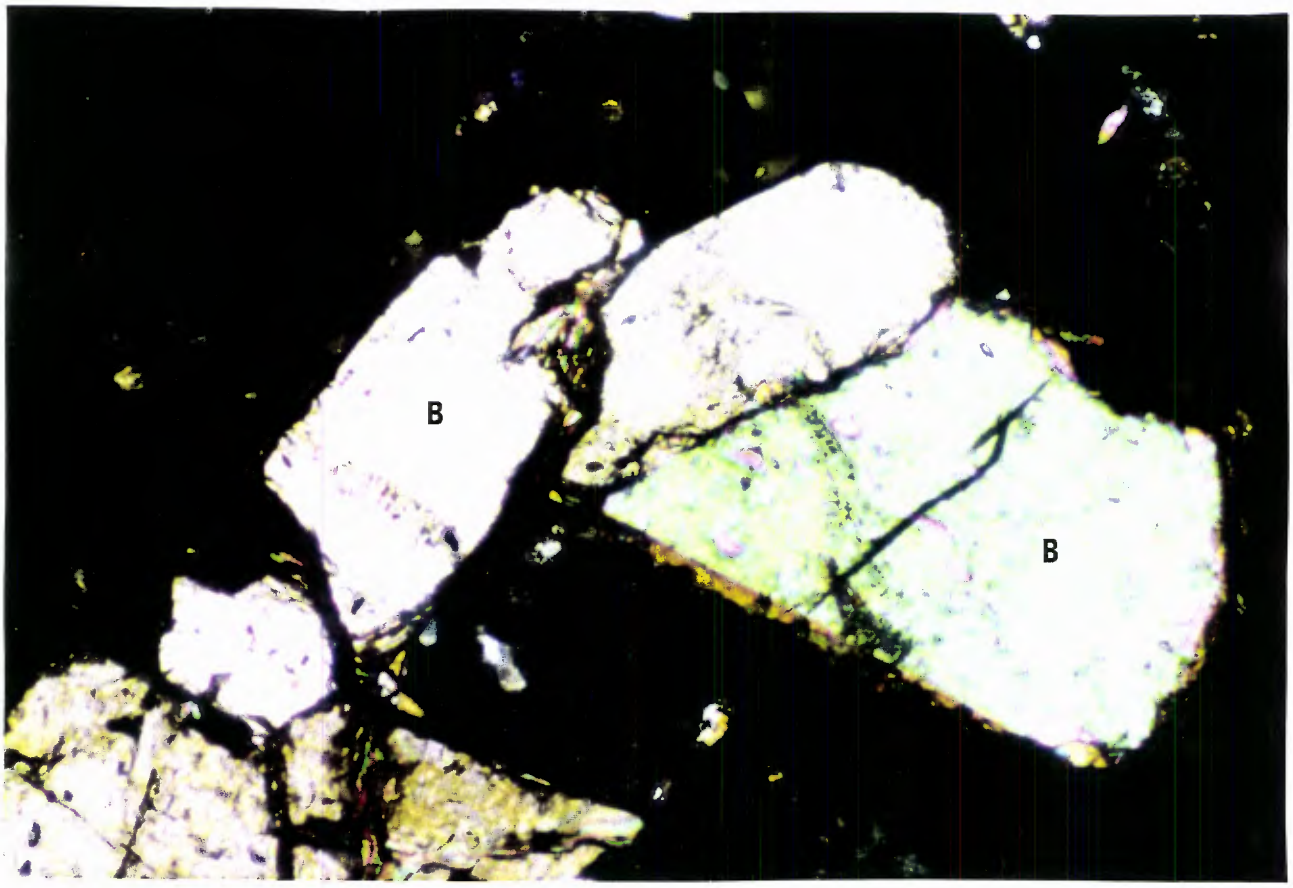

Figure 4. Photomicrograph of a polished thin section of intrusive breccia from sample site 80 at the M and E No. 13 Prospect, Red Cloud mining district, Lincoln County, N. Mex., Magnification X 112.5, crossed nicols, showing fractured bastnaesite (B) crystals in a fluorite matrix.

Fluorite crystals exhibit luminescent zoning from deep blue to pale purple under CL. Some of the interiors of the larger crystals showed a greenish luminescence. In environments enriched in LREE, fluorite commonly is blue luminescing (Mariano, 1988, p. 108).

Barite occurs as fine- to coarse-grained, bluish white, anhedral to subhedral, corroded crystals scattered throughout the matrix of the intrusive breccia at sample sites 76 and 80. At sample site 71, abundant barite occurs in crude bands, oriented N. 54° E., with fluorite. The barite ranges from bands of coarse, corroded, tabular, broken, and cracked bluish white crystals, as long as 2.5 cm, to finer corroded crystals, less than 2 mm in length. Although most of the barite crystals did not luminesce under CL, a few crystals contained areas that luminesced a dark deep blue.

Quartz occurs as subhedral to euhedral, prismatic crystals, as long as 2 mm, at sample sites 76 and 80. Most of the crystals are corroded around the edges, contain inclusions of fluorite, barite, manganese-rich calcite, and iron and manganese oxides. One inclusion of xenotime and several fine needle-shaped inclusions of bastnaesite were also identified. At sample site 73, quartz rims fluorite, barite, and bastnaesite crystals, as late-forming bands of small zoned crystals , less than 0.1 mm in diameter. The zoning is due to numerous fine inclusions that form turbid bands in the quartz crystals. They commonly have overgrowths of cryptocrystalline quartz, that are found rimming vugs.

Pyrite commonly occurs as cubes and pyritohedrons, as much as 8 mm and averaging 1 mm in diameter, that commonly have crystallized on rock clasts. Pyrite is most commonly completely altered to hematite-limonite.

Calcite at sample site 76 occurs as anhedral masses in the matrix, averaging 0.05 mm in diameter and as subhedral crystals in cavities and fractures, as much as 0.4 mm in diameter. Calcite forms most of the matrix, surrounding and rimming fluorite and quartz crystals, and has crystallized on earlier fluorite rimming rock clasts. Calcite is found in amounts ranging from a few percent to 44% at sample sites 76-82 (Appendix B). No calcite is present at sample site 71. Most of the calcite luminesces bright orange to dull orange

under CL. In some of the larger crystals cyclic zoning of nonluminescing and dull orange luminescing calcite were present. The orange luminescence is probably due to manganese (Mn^{2+}) activation (Mariano, 1988, p. 105-109).

Alteration

The intrusive breccia as well as the trachyte country rock around the intrusive breccia pipe have been altered by two episodes of incipient fenitization. The rocks have been altered by a period of sodic fenitization followed by a later period of potassic fenitization. The extent of the fenitization of the trachyte host rock was not determined, but it is present around the pipes extending for a distance of at least 100 ft from the edge of the intrusive breccia pipe. The southern part of the intrusive breccia pipe has also been carbonatized.

Intrusive Breccia

In most outcrops the intrusive breccia has been bleached white by incipient fenitization. Only at sample site 78, a block of trachyte in the center of the bulldozed area, is the trachyte not bleached but is a dark brown. The trachyte is carbonatized, and the groundmass is brown in color, while the feldspar phenocrysts are bleached white. The mafic phenocrysts are altered to hematite-limonite.

Polished thin sections of samples 72 and 73 in the intrusive breccia contain trachyte, sandstone, and granitic clasts replaced by fenite feldspar. The fenite feldspars are albite and potassium feldspar and occur in veinlets and in patches replacing the original minerals. Early fenite albite is replaced by fenite potassium feldspar (Appendix D) that commonly makes up most of the polished thin section. Hematite-limonite pseudomorphs after pyrite are common in the veinlets and within the clasts. Minor sericite occurs from alteration of the original albite, most commonly along the fenite veinlets. Monazite occurs as prismatic crystals, as long as 0.04 mm, in the fenite feldspar veinlets. SEM-EDX analysis of two crystals detected an average of 16.9% La_2O_3, 26.3% Ce_2O_3, 3.0% Pr_2O_3, 10.8% Nd_2O_3, 1.4% Sm_2O_3, and 41.7% P_2O_5. Prismatic zircon crystals, as long

as 0.28 mm, were commonly found in the fenite veinlets. A few weathered anhedral masses of titanium oxide, probably rutile, were also found in the fenite veinlets. Crystals of svanbergite, a compound phosphate, as much as 0.02 mm in diameter, were identified. SEM-EDX analysis of two crystals averaged 1.9% K_2O, 1.4% CaO, 1.8% La_2O_3, 1.7% Ce_2O_3, 24.0% SrO, 16.8% Al_2O_3, 9.8% SO_4, 14.7% P_2O_5, and 12.7% OH. Similar phosphates, such as goyazite, have been noted in several carbonatite complexes where they are formed during supergene conditions (McKie, 1962; Mariano, 1989, p. 332).

Polished thin sections of samples 72 and 73 examined under CL showed brilliant red-luminescing albite and tan-luminescing fenite potassium feldspar that have partially replaced the clasts. Spectrum scans by Anthony Mariano indicated that the brilliant red luminescence of the albite observed under CL is due to ferric iron activation. Spectrum scans of the unusual tan-luminescing fenite potassium feldspar also showed activation due to ferric iron but also contained a broad intrinsic band that is probably due to a defect in the crystal structure of the feldspar (Appendix E) (Anthony Mariano, consultant, Carlisle, Mass., oral commun., March 1992). Tan-luminescing fenite potassium feldspar has almost completely replaced some areas of the trachyte clasts, leaving only remnants of red-luminescing fenite-albite-replaced phenocrysts. A polished thin section of sample 73 contains a granitic clast and shows early red-luminescing fenite albite veinlets have replaced the blue-luminescing orthoclase, yellowish green-luminescing albite, and bluish gray-luminescing quartz in the clast. Late fenite potassium feldspar veinlets are tan-luminescing and replace fenite albite and the original minerals (fig. 5). Zircon crystals luminesce bright yellow or dark blue with bright white rims. A few patches of orange-luminescing calcite are present in vugs.

In two polished thin sections, trachyte clasts in the intrusive breccia at sample sites 76 and 80 are partially replaced by fine-grained albite and fenite potassium feldspar. The fenite feldspars occur in veinlets and as rims and patches replacing the original feldspars. The original feldspars are turbid where partially replaced by veinlets and patches of fenite feldspar. Fenite

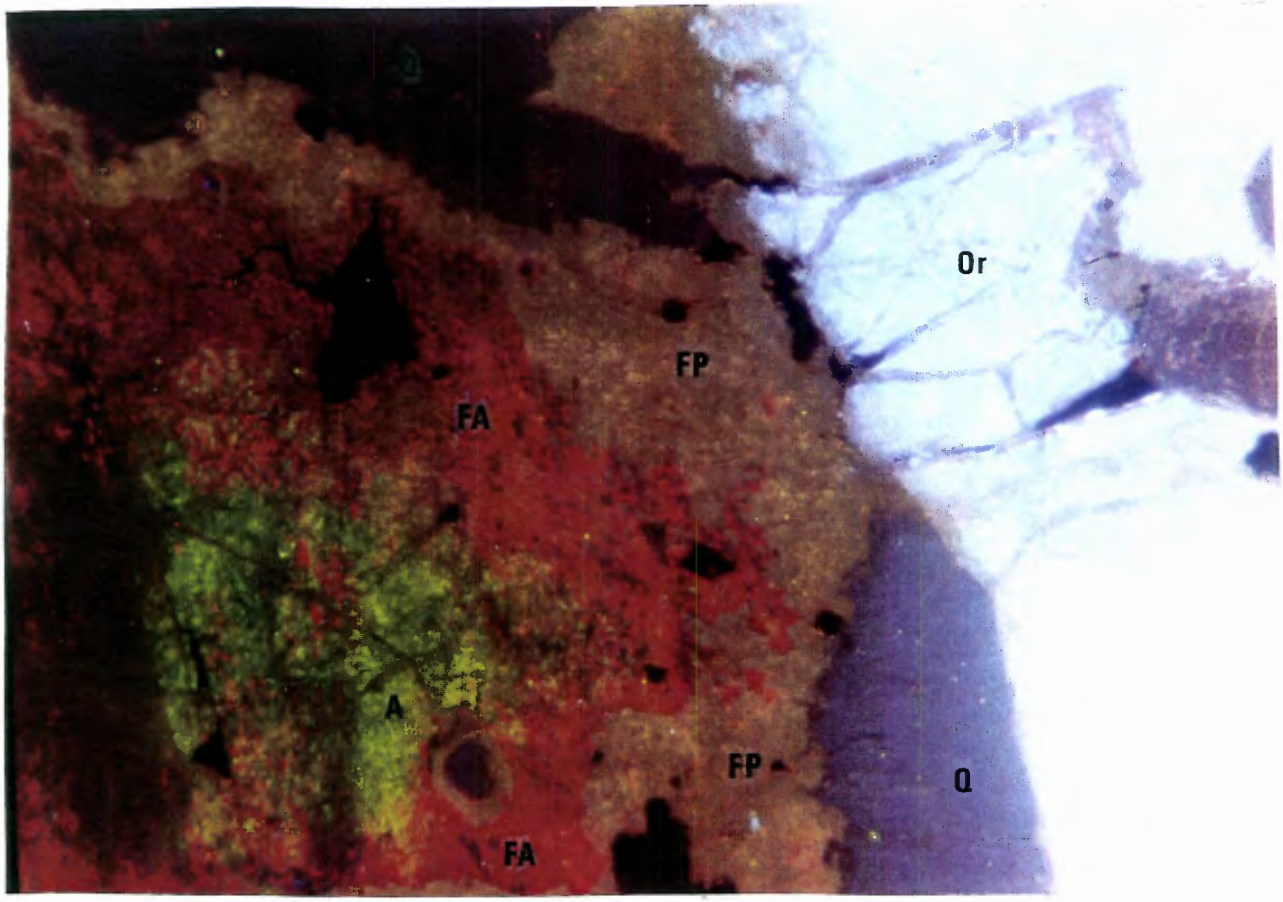

Figure 5. Cathodoluminescence photomicrograph of polished thin section from fenitized granitic clast at sample site 73 in intrusive breccia at the M and E No. 13 Prospect, Red Cloud mining district, Lincoln County, N. Mex., Magnification X 90, showing early replacement of original yellowish green-luminescing albite (A) with Mn^{2+} and/or Fe^{2+} activation by brilliant red-luminescing fenite albite (FA) with Fe^{3+} activation and late replacement of brilliant red-luminescing fenite albite, blue-luminescing orthoclase (Or) with Ti^{4+} activation, and bluish gray-luminescing quartz (Q) by tan-luminescing fenite potassium feldspar (FP) with Fe^{3+} activation. Photographic conditions: Kodak Ektapress Gold 400, 400 ASA, 363 seconds, 20 kV.

potassium feldspar commonly occurs as fine (as much as 0.05 mm in diameter), clear euhedral crystals rimming the clasts, where it has completely replaced the original feldspar. SEM back-scattered electron mode images could not differentiate between the replacing fenite albite and the original albite or the replacing fenite potassium feldspar and the original potassium feldspar, and no difference was detected in analysis. The fenite potassium feldspar also replaces the fenite albite feldspar indicating that the potassic fenitization was the latest event. Barite occurs as anhedral blebs, 1-20 microns in diameter, in the turbid areas where fenite feldspars have replaced original feldspars. Pyrite is commonly found with the fenite feldspar. The original albite crystals are also partially altered to sericite. Kaolinite fills some cavities in the matrix.

Observation under CL of the polished thin sections of samples 76 and 80 showed trachyte clasts with rims, patches, and veinlets of brilliant red-luminescing fenite albite and tan to tannish gray-luminescing fenite potassium feldspar in a matrix of dull orange-luminescing calcite and pale purple-luminescing fluorite (fig. 6). Most trachyte clasts are strongly fenitized, and tan-luminescing fenite potassium feldspar is dominant in some while in others red luminescing albite is the main fenite feldspar. The original albite luminesces a dark brown and the original potassium feldspar luminesces tan, slightly lighter in color than the invading fenite potassium feldspar. Some strongly fenitized trachyte clasts contain yellow-luminescing apatite with an overgrowth of LREE enriched, violet-luminescing apatite. Pale purple-luminescing fluorite occurs as scattered anhedral crystals replacing a few clasts. Trachyte clasts commonly contain fine, bright yellow-luminescing zircon crystals.

Late potassic fenitization of the breccia pipe is indicated by the K_2O concentrations of 8.70% to 14.88% at sample sites 72-74 and 84. Na_2O concentrations ranged from 0.54% to 4.9% and show an inverse relationship with potassium. Samples of the fenitized trachyte country rocks (sample sites 83 and 85) contain lower potassium concentrations and higher sodium concentrations. The higher potassium and lower sodium contents in samples from within the pipe indicate that the intensity of potassic fenitization was greater within the pipes

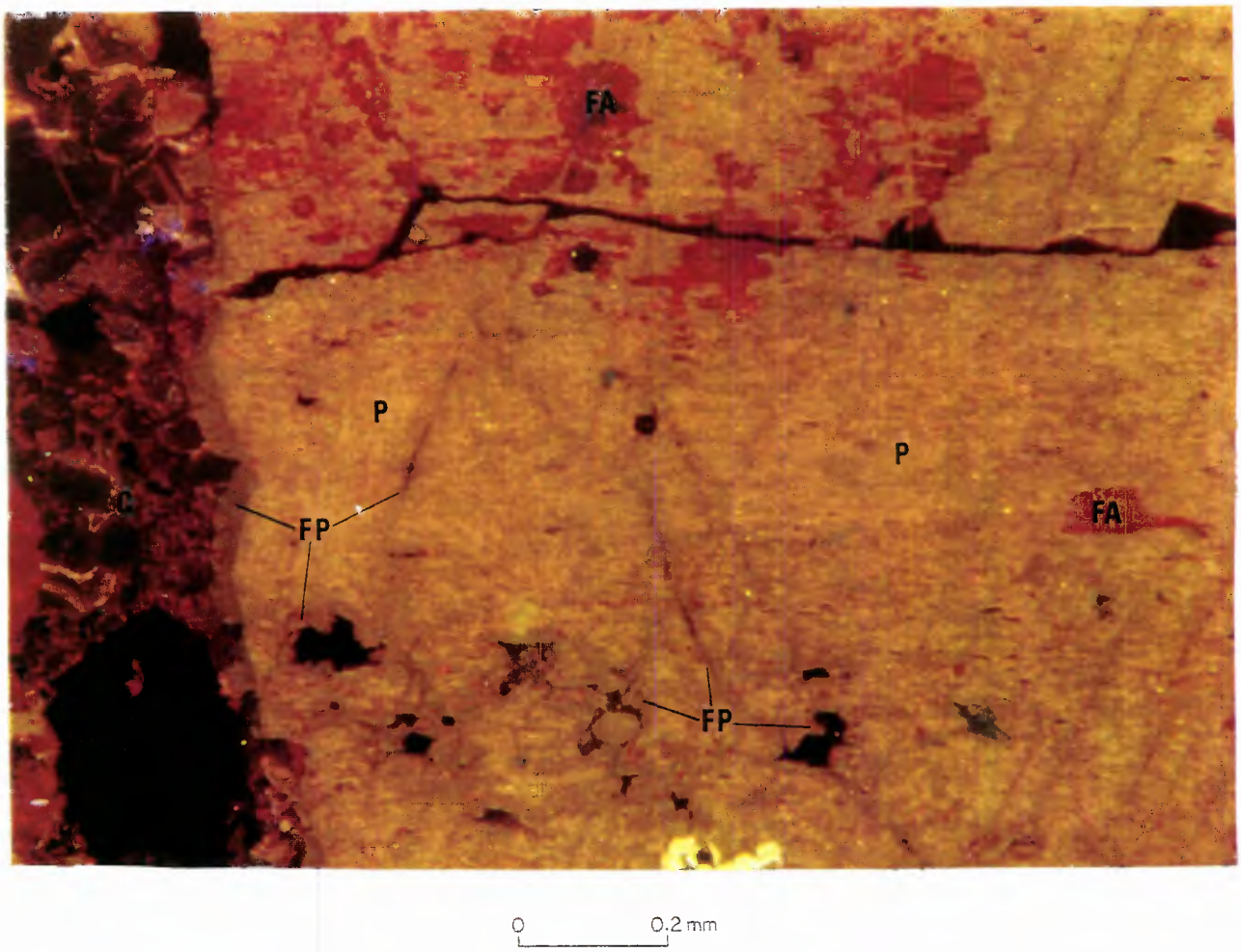

Figure 6. Cathodoluminescence photomicrograph of polished thin section from fenitized potassium feldspar phenocryst in trachyte clast at sample site 76 in intrusive breccia at the M and E No. 13 Prospect, Red Cloud mining district, Lincoln County, N. Mex., Magnification X 90, showing replacement of tan-luminescing potassium feldspar (P) phenocryst by patches of red-luminescing fenite albite (FA) with Fe^{3+} activation and later replacement by tan-luminescing fenite potassium feldspar (FP) with Fe^{3+} activation as rims and veinlets. The fenite potassium feldspar is a darker shade of tan than the original potassium feldspar phenocryst. The dull orange-luminescing mineral on the left-hand side of the picture is calcite (C) that has filled the matrix in this part of the intrusive breccia pipe. Photographic conditions: Kodak Ektapress Gold 400, 400 ASA, 457 seconds, 18 kV.

and that the process resulted in the removal of sodium as well as the addition of potassium.

A polished thin section of sample 78 from the center of the carbonatized trachyte block within the intrusive breccia contains abundant anhedral to euhedral calcite, averaging 0.05 mm in diameter, with hematite-limonite replacing parts of the trachytic groundmass. The groundmass consists of albite and potassium feldspar. The phenocrysts appear to have been primarily albite. The feldspars, especially the phenocrysts, are altered to sericite. Some vugs contain clumps of sericite. The mafic phenocrysts, probably originally hornblende as determined by the hexagonal crystal outlines, are totally altered and have been replaced by calcite, hematite-limonite pseudomorphs after pyrite, potassium feldspar, sericite, barite, and apatite. Vugs contained rims of subhedral to euhedral potassium feldspars with overgrowths of clear anhedral to subhedral calcite as much as 0.3 mm in diameter.

Sample 78 examined under CL, showed anhedral bright orange-luminescing calcite scattered throughout the tannish gray to gray-luminescing groundmass. Vugs containing coarse-grained calcite crystals show cyclic zoning of nonluminescing and orange-luminescing calcite. Abundant subhedral to euhedral violet-luminescing apatite, as long as 1.5 mm, is associated with the carbonatization (fig. 7) indicating LREE enrichment. The fenite potassium feldspar rimming vugs luminesces gray. No brilliant red-luminescing feldspars were observed, suggesting that sodic fenitizing solutions did not invade this part of the trachyte or that it has been replaced by the later potassic fenitization. Sample 78 contained concentrations of 8.16% calcium oxide (CaO) and 9.79% K_2O, and 2.07% Na_2O. The high potassium concentration in sample 78 suggests that the replacement of the trachyte is primarily by potassic fenitization.

Trachyte

In most exposures the trachyte host rock around the pipes has a bleached white to pinkish color due to weak to moderate incipient fenitization.

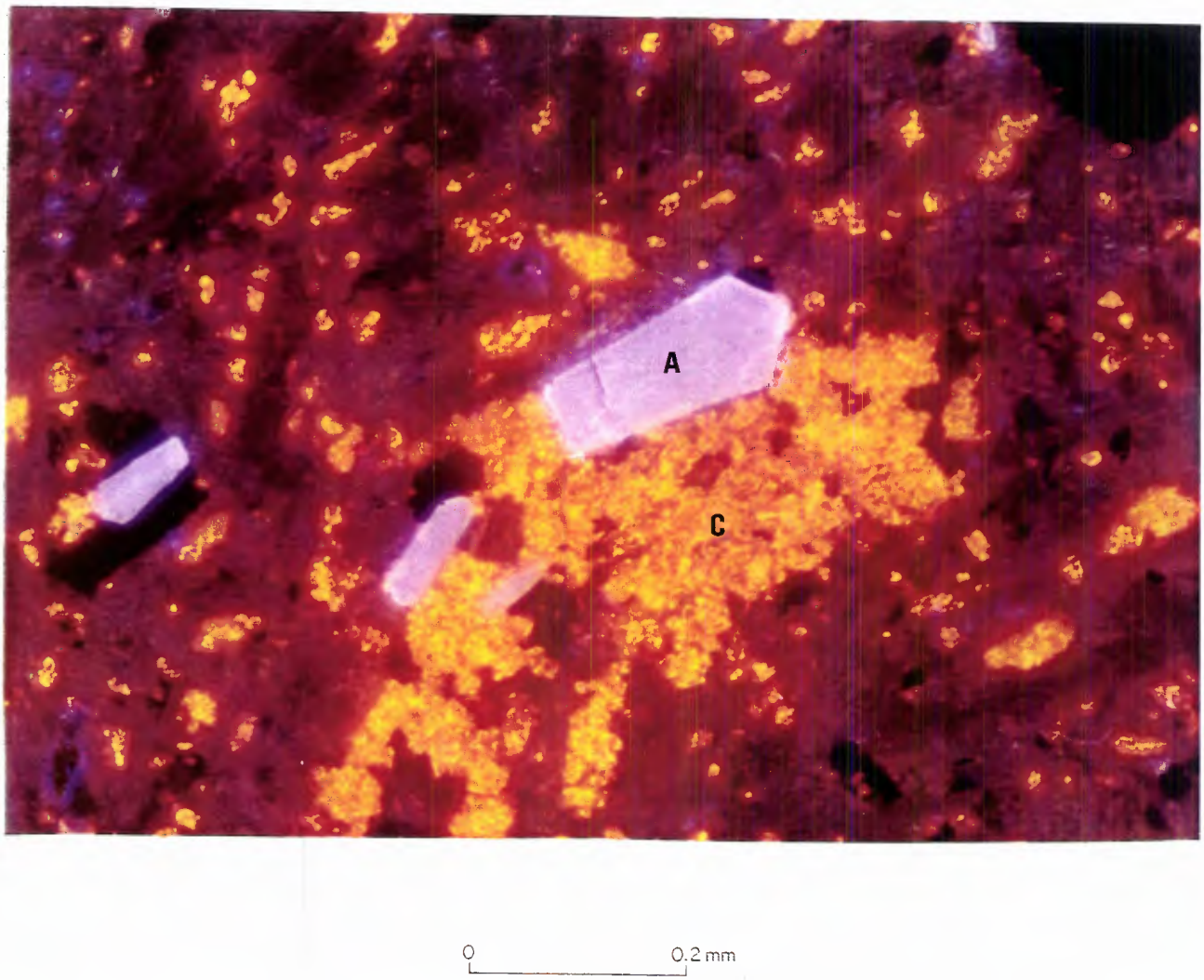

Figure 7. Cathodoluminescence photomicrograph of polished thin section from fenitized and carbonatized trachyte block at sample site 78 in intrusive breccia at the M and E No. 13 Prospect, Red Cloud mining district, Lincoln County, N. Mex., Magnification X 180, showing replacement of trachyte by brilliant orange-luminescing calcite (C) with Mn^{2+} activation and associated blue-luminescing apatite (A) with light-rare-earth-element activation. Photographic conditions: Kodak Ektar 125, 125 ASA, 188 seconds, 20 kV.

Two polished thin sections of sample 85 contained clear fine-grained fenite feldspar in veinlets and vugs, with hematite-limonite pseudomorphs after pyrite that cut both the groundmass and phenocrysts. The fenite feldspar is albite in some veinlets and potassium feldspar in others. The groundmass consists of albite and potassium feldspar. The phenocrysts are primarily albite and subordinate alkali feldspar. SEM-EDX analysis of one of the alkali feldspars showed it to be a barium-rich alkali feldspar, probably hyalophane (Or_{61} Ab_{29} Cn_6 An_4). The twinned albite phenocrysts (Ab_{96} Or_3 An_1) are rimmed by turbid potassium feldspar (Or_{93} Ab_7). The twinned albite core is commonly partially altered to sericite. Some phenocrysts contain cores or patches of fine aggregates of kaolinite. Quartz occurs as interstitial anhedral crystals ranging from 0.05 to 0.1 mm in diameter. Quartz is also present in vugs and veinlets as anhedral to euhedral crystals as long as 0.5 mm, containing abundant inclusions and at least some of the quartz has been introduced. Sample 85 plots as a quartz trachyte on the De La Roche R_1R_2 grid classification plot (Appendix C).

Observation under CL of polished thin sections from sample 85 shows incipient fenitization. Brilliant red-luminescing fenite albite and tan luminescing fenite potassium feldspar veinlets cut both the phenocrysts and the groundmass (fig. 8). The tan-luminescing fenite potassium feldspar completely replaces the red-luminescing fenite albite in the central part of the veinlets. The feldspars are intergrown on the edges of the veinlets, where the fenite potassium feldspar partially replaced the fenite albite. The phenocrysts consist of a dark brown to gray-luminescing albite core and a rim of tan-luminescing potassium feldspar, and in some phenocrysts the feldspars are intergrown. No color difference between the original tan-luminescing potassium feldspar and the replacing fenite potassium feldspar was observed. The barium-rich alkali feldspar luminesces blue. It was difficult to separate out the groundmass feldspars, but they appear to consist of dark brown-luminescing albite, light blue-luminescing potassium feldspar, and possibly tan-luminescing potassium feldspar that is partially replaced by tan-luminescing fenite potassium feldspar and red-luminescing fenite albite. Interstitial quartz luminesces

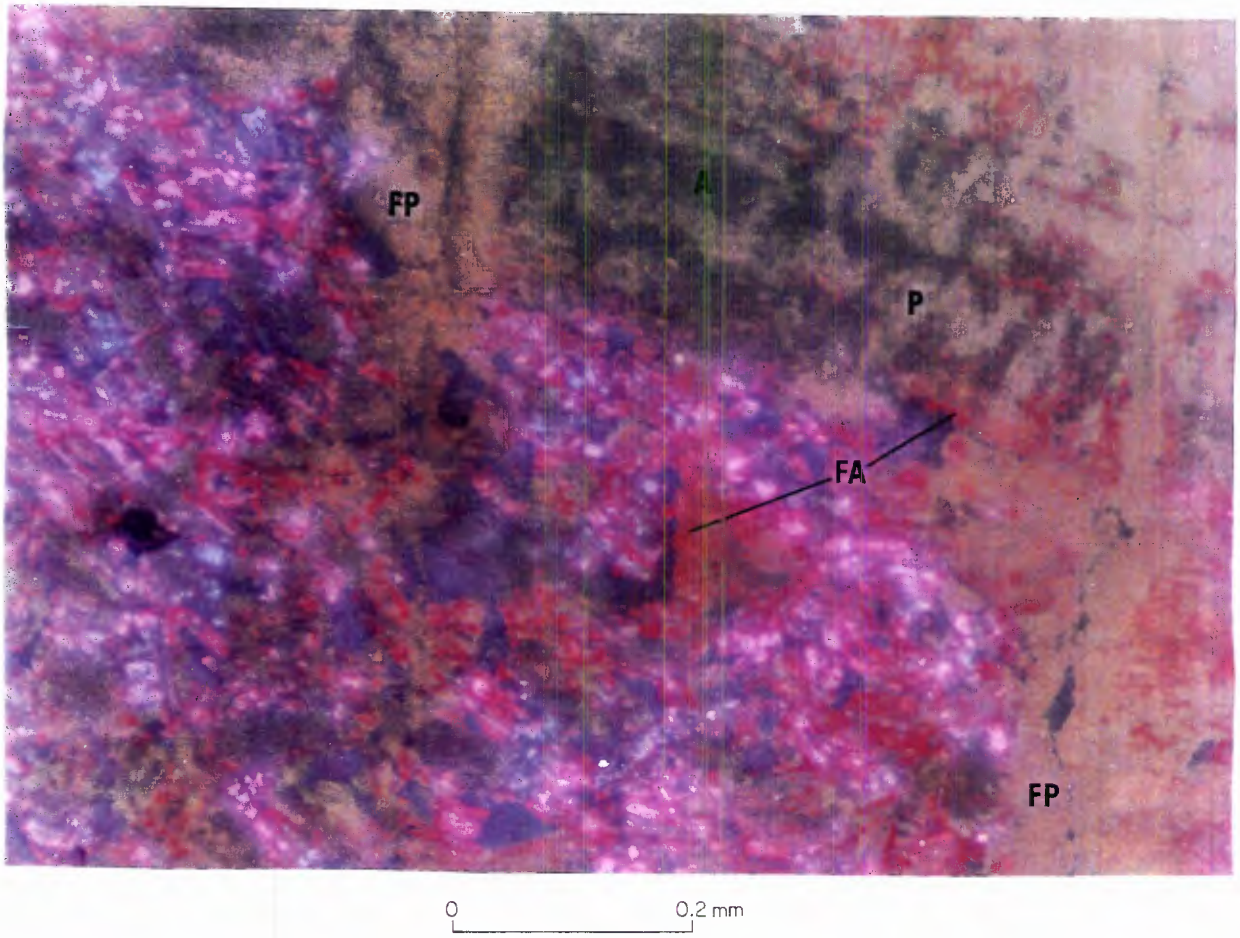

Figure 8. Cathodoluminescence photomicrograph of polished thin section from fenitized trachyte at sample site 85 near intrusive breccia at the M and E No. 13 Prospect, Red Cloud mining district, Lincoln County, N. Mex., Magnification X 180, showing replacement by patches of red-luminescing fenite albite (FA) with Fe^{3+} activation and later replacement by tan-luminescing fenite potassium feldspar (FP) with Fe^{3+} activation in veinlets that cut the groundmass and the rim of a phenocryst in the trachyte. The rim of the phenocryst is an intergrowth of tan-luminescing potassium feldspar (P) and dark brown or gray luminescing albite (A). No difference in color was detected between the fenite and original tan-luminescing potassium feldspars. The fine groundmass made it difficult to sort out the specific colors of each feldspar phase, but they appear to be tan-luminescing potassium feldspar, bluish white luminescing-potassium feldspar, and dark brown-luminescing albite. The bluish gray-luminescing mineral is interstitial quartz. Photographic conditions: Kodak Ektapress Gold 400, 400 ASA, 562 seconds, 15 kV.

bluish gray. The kaolinite patches in the phenocrysts luminesce dark blue. Samples 83 and 85 from the fenitized trachyte around the pipe contained 3.76% K_2O and 7.76% Na_2O, and 4.03% K_2O and 6.62% Na_2O, respectively.

Analytical Data

Thirteen samples (71-82, and 84) were taken from the large intrusive breccia pipe and 2 samples (83 and 85) from the fenitized trachyte country rock. Samples taken from the intrusive breccia contained erratic concentrations of REO's, ranging from 0.08% to 5.67% and averaging 1.57%. Y_2O_3 concentrations were also erratic ranging from 71 to 921 ppm, and averaging 331 ppm. Gold, silver, and base metal concentrations were present in trace amounts. The fenitized trachyte contained REO concentrations of 0.05% and 0.07%. Eight samples (71, 75, 76, 77, 79-82) from the highly mineralized zones in the large intrusive breccia pipe contained REO concentrations ranging from 0.27% to 5.67%, averaging 2.45%. Yttrium oxide concentrations ranged from 140 to 921 ppm and averaging 427 ppm. Fluorite concentrations ranged from 4.4% to 48.3%, averaged 19.06%.

Two samples (86 and 87) from the smaller pipe contained 0.17% and 2.8% REO, respectively. They also contained significant concentrations of Y_2O_3, 696 and 843 ppm.

Intrusive breccia north of the All American Prospect

Description

The area has been prospected by four small pits, one dug in hematite-stained sandstone and three dug on calcite and/or quartz veins in an oval shaped intrusive breccia, approximately 350 ft long and 200 ft wide (pl 2, sample sites 26-42). The intrusive breccia cuts through the center of an upfaulted block of Precambrian gneiss approximately 550 ft in diameter, that lies along the west side of the fault in Red Cloud Canyon (pl. 1). The faulting has placed the gneiss in contact with sandstone. The intrusive breccia pipe may connect to another oval-shaped 190 ft by 130 ft pipe that intrudes sandstone on the edge of

a block of gneiss, approximately 100 ft to the northwest; the intrusive breccia could not be traced due to soil cover. Mapping of the area was done mostly by float because outcrops are small and scattered, therefore contacts are approximate.

The intrusive breccia consists of angular to rounded clasts of gneiss, schist, sandstone, and trachyte in a brownish gray aphanitic matrix with crystal fragments. The clasts are primarily gneiss and range from 1/4 to 6 in. in diameter. Most of the intrusive breccia has been partially replaced by calcite (sample sites 36-39), and only the outside edges of the intrusive breccia in contact with the gneiss (sample sites 35 and 40) are not carbonatized. Fine-grained calcite replaces both the aphanitic matrix and rock clasts. White coarse-grained calcite has been deposited in fractures in the intrusive breccia, forming short discontinuous veinlets as wide as 1/4 in. that cut both the aphanitic matrix and rock clasts. At sample site 40, the dump of a caved pit contains fragments of intrusive breccia and fragments from a 6-in.-wide vein of vuggy botryoidal chalcedony.

The smaller intrusive breccia pipe that intrudes sandstone at sample site 31, is not carbonatized. The intrusive breccia consists primarily of angular to rounded, white to tan trachytic and gray andesitic clasts, subordinate sandstone and gneiss clasts in a bleached, tan to gray aphanitic matrix with fine crystal fragments. The gneiss clasts are as much as 2 ft in diameter, but the more common trachytic and andesitic clasts average 1/4 to 1 in. in diameter.

Scintillometer readings over outcrops of the intrusive breccia ranged from 75 to 80 cps, while readings over outcrops of the gneiss ranged from 45 to 85 cps. Scintillometer readings dropped to 35 to 45 cps over a few sandstone outcrops outside the block of gneiss. Scintillometer readings over the intrusive breccia pipe on the edge of the block of gneiss averaged 45 cps. The trachyte dike 100 ft north of the block of gneiss was the most radioactive rock; scintillometer readings ranged from 75 to 170 cps.

Mineralogy

Calcite, barite, quartz, and hematite-limonite pseudomorphs after pyrite occur in fractures and as cavity fillings in the intrusive breccia. A 2-micron chalcopyrite crystal was found as an inclusion within a quartz crystal of the original gneiss and is the only sulfide identified other than pyrite. One skeletal crystal of bastnaesite was identified in a vug that appears to have been 0.8 mm in length. One 30-micron xenotime crystal was found in a gneiss clast, but it could not be determined if it was introduced or part of the original rock.

Barite occurs as subhedral to euhedral tabular and prismatic crystals as long as 0.01 mm. The barite was found filling a narrow cavity lined with quartz crystals that rim fenitized rock clasts. The barite occurs mainly as overgrowths on quartz. A few prismatic barite crystals penetrate into the edges of euhedral quartz crystals, suggesting that barite crystallized at approximately the same time as some of the late crystallizing quartz as well as afterwards.

Quartz occurs as subhedral to euhedral zoned crystals, as long as 0.2 mm, commonly rimming the walls of fractures and cavities. The zoning in the quartz crystals is due to the presence of turbid bands that contain abundant inclusions. Euhedral zoned quartz crystals occur as overgrowths on fenite feldspar rimmed rock fragments, an indication that the crystallization of some quartz postdates the fenitization.

Calcite occurs as anhedral to euhedral, clear crystals, as much as 0.4 mm in diameter, in veinlets and cavities. The calcite commonly rims quartz crystals and occupies the central portion of the veinlets and cavities indicating it was the last mineral deposited. The calcite was generally nonluminescing or bluish gray under CL in the larger veinlets. A few dull orange-luminescing crystals were visible. Most of the calcite in the vugs and narrow veinlets was dull orange-luminescing.

Hematite-limonite pyritohedron and cubic pseudomorphs after pyrite, averaging 0.2 mm in diameter, are abundant in some calcite veinlets along with some manganese-iron oxides.

Alteration

The intrusive breccia, as well as adjacent gneiss, sandstone, and a trachyte dike have been altered by two episodes of incipient fenitization. The rocks have been altered by sodic fenitization followed by a later period of potassic fenitization. The fenitization can be traced over an area 700 ft by 550 ft and appears to be centered in the intrusive breccias and along faults. The central part of the intrusive breccia has also been carbonatized.

Intrusive Breccia

In outcrops of the intrusive breccia at sample sites 35-40, feldspar phenocrysts in rock clasts and crystal fragments in the matrix are commonly bleached white or pinkish in color. The mafic minerals are altered to hematite and limonite. The central part of the intrusive breccia at sample sites 36-39, is also carbonatized, and the aphanitic matrix has a brown color.

In a polished thin section taken from a gneiss rock clast from sample site 35 from the noncarbonatized part of the intrusive breccia, fine-grained, turbid fenite feldspar occurs along grain boundaries in sinuous veinlets replacing both feldspars and quartz (fig. 9). The fenite feldspars are albite and potassium feldspar and in most areas the fenite feldspars appear to be intergrown. Aegirine and crocidolite, a fibrous alkali amphibole, occur in the veinlets. The aegirine occurs as pleochroic, pale green to green, acicular to prismatic crystals. The crocidolite has variable pleochroic colors. It consists of fibrous clumps of pleochroic greenish yellow to yellowish brown crystals that are commonly pale blue-green on the edges. Individual needles are colorless to pale blue-green. The crystals have yellow and anomalous blue interference colors. It is similar to the amphibole seen at sample site 32 described in the next section. The yellowish brown color in the pleochroic scheme suggests it is an alkali amphibole of the eckermannite-arfvedsonite group. Hematite-limonite pseudomorphs after pyrite, zircon, and apatite also occur in the veinlets.

Observation under CL of the polished thin section from sample site 35 shows brilliant red-luminescing fenite albite and reddish tan to red to bluish gray-luminescing fenite potassium feldspar replacing blue-luminescing orthoclase,

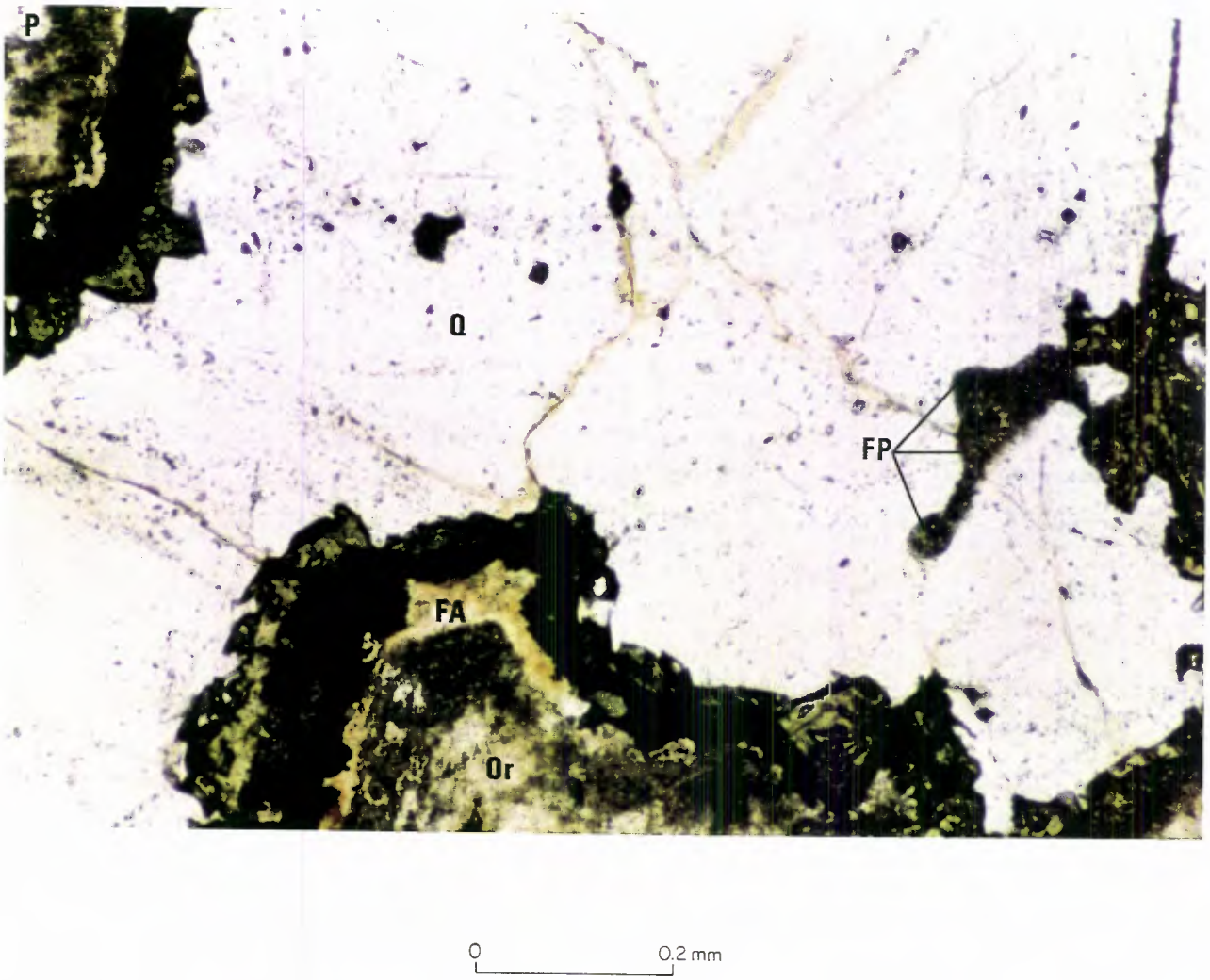

Figure 9. Photomicrograph of fenitized gneiss clast at sample site 35 in intrusive breccia at intrusive breccia north of All American Prospect, Red Cloud mining district, Lincoln County, N. Mex., Magnification X 112.5 plane-polarized light, showing sinuous turbid fenite veinlets along crystal boundaries, containing green aegirine, albite (FA), and potassium feldspar (FP). The crystal in the upper left hand corner is plagioclase (P), the clear crystal in the center is quartz (Q), and the crystal at the bottom of the picture is orthoclase (Or).

greenish yellow-luminescing oligoclase, and bluish gray- or gray-luminescing quartz (fig. 10). The fenite feldspars are commonly intergrown. In parts of the veinlets with a brilliant red-luminescence, fenite albite is the dominant fenite feldspar, and in parts of the veinlets with a duller red or reddish tan or bluish gray-luminescence, fenite potassium feldspar is the dominant fenite feldspar. Apatite luminesces yellow to orangish yellow and zircon, bright yellow.

In four polished thin sections made from sample sites 36, 38, and 39, from the carbonatized part of the pipe, no sodic pyroxene or amphibole was identified. All of the mafic minerals are altered to hematite-limonite, probably as a result of the carbonatization. Calcite occurs as anhedral to euhedral crystals that have replaced the mafic minerals, as well as in fractures and cavities described above. The fenite feldspar is both albite and potassium feldspar. A polished thin section from sample site 39, shows the sample is strongly fenitized and appears to be dominantly sodic. The cores of orthoclase crystals in the gneiss clasts are turbid where partially replaced by fenite feldspar. SEM-EDX analysis shows the turbid core consists of extremely fine patches and veinlets of albite replacing original orthoclase. The rims are commonly replaced by clear twinned albite. Turbid original twinned albite crystals were commonly replaced and rimmed by clear twinned fenite albite. SEM back-scattered electron mode images could not differentiate between the rimming albite and the original albite, and no difference was detected by SEM-EDX analysis. In polished thin sections from sample sites 36 and 38, both fenite albite and potassium feldspar were identified in veinlets. Fenite potassium feldspar commonly occurs as clear rims, patches, and veinlets in original feldspars and occurs as rims in vugs. The fenite potassium feldspar also replaces the fenite albite and indicates that the potassic fenitization was the latest event. Some vugs contain abundant plates of sericite. Quartz in the clasts is usually not veined by fenite feldspar, but is replaced by feldspar along the grain boundaries. Hematite-limonite pyritohedron pseudomorphs after pyrite are commonly found in veinlets of fenite feldspar. Anhedral to subhedral rutile crystals, as much as 80 microns in diameter, and anhedral to euhedral barite and celestite, 1 to 25 microns in

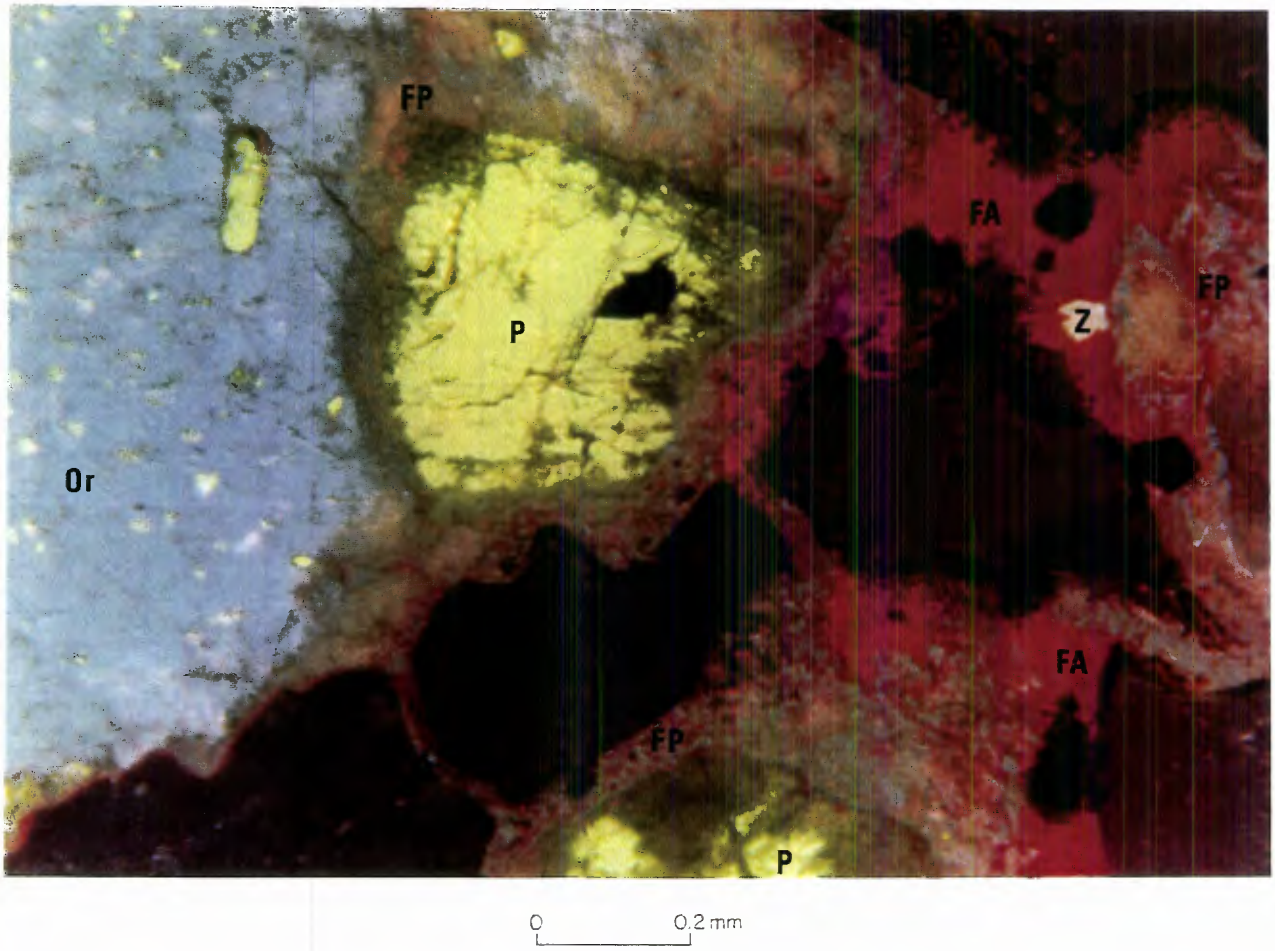

Figure 10. Cathodoluminescence photomicrograph of polished thin section from fenitized gneiss clast in intrusive breccia at sample site 35 at the intrusive breccia north of the All American Prospect, Red Cloud mining district, Lincoln County, N. Mex., Magnification X 90, showing sinuous fenite veinlets along crystal boundaries, containing brilliant red-luminescing fenite albite (FA) with Fe^{3+} activation, tan to reddish tan to red to bluish gray-luminescing fenite potassium feldspar (FP) with Fe^{3+} activation replacing greenish yellow-luminescing plagioclase (P) with Mn^{2+} and/or Fe^{2+} activation, blue-luminescing orthoclase (Or) with Ti^{4+} activation (area on left side of picture is microperthite-orthoclase with blebs of plagioclase), and bluish gray to gray-luminescing quartz (Q). The nonluminescing or black crystals are aegirine rimming and replacing the quartz. The black cubic or euhedral shaped crystals in the sinuous veinlets are hematite-limonite pseudomorphs after pyrite. The bright yellowish white crystal in the fenite veinlet is zircon (Z). Photographic conditions: Kodak Ektapress Gold 400, 400 ASA, 240 seconds, 18 kV.

diameter, occur as tabular crystals commonly found with fenite feldspar. Monazite occurs as scattered prismatic crystals as long as 30 microns. Apatite occurs as anhedral to euhedral scattered crystals in rock clasts and as clumps as much as 1.8 mm in diameter in some cavities in a matrix of quartz. A few clumps of sericite crystals were found filling vugs or cavities.

Observation under CL of the polished thin sections from sample sites 36, 38, and 39 showed that brilliant red-luminescing fenite albite and tan to pinkish tan or gray-luminescing fenite potassium feldspar has replaced the matrix and the clasts. Spectrum scans by Anthony Mariano indicate that the brilliant red-luminescence of the albite is due to ferric iron activation. Spectrum scans of the unusual tan-luminescing fenite potassium feldspar also showed activation due to ferric iron but that the spectrum also contains a broad intrinsic band that is probably due to a defect in the crystal structure of the feldspar (Anthony Mariano, consultant, Carlisle, Mass., oral commun., March 1992). Tan-luminescing fenite potassium feldspar commonly rims and veins early brilliant red-luminescing fenite albite and the original albite and orthoclase. Red-luminescing fenite potassium feldspar replaces original albite and orthoclase (fig. 11). One vug contained a rim of gray-luminescing fenite potassium feldspar. Feldspars in gneiss clasts were most commonly blue-luminescing potassium feldspar. Only a few yellowish green-luminescing plagioclase feldspar crystals were present in the aphanitic matrix; most were highly altered. In areas of weak fenitization, most apatite crystals luminesce yellow. In areas of strong fenitization, most of the apatite were lavender- or violet-luminescing prismatic crystals, averaging 0.3 mm in length, occurring in clumps and enclosing smaller, yellow-luminescing apatite. The lavender or violet luminescence of the late forming apatite indicates that it is enriched in LREE's. CL emission spectrum scans done by Anthony N. Mariano on the yellow-luminescing apatite showed the luminescence to be due to the dominance of dysprosium activation (HREE). Prismatic zircon crystals, averaging 0.06 mm in length, commonly luminesced bright yellow, although in some areas they were dull blue with yellow rims. Most of the calcite

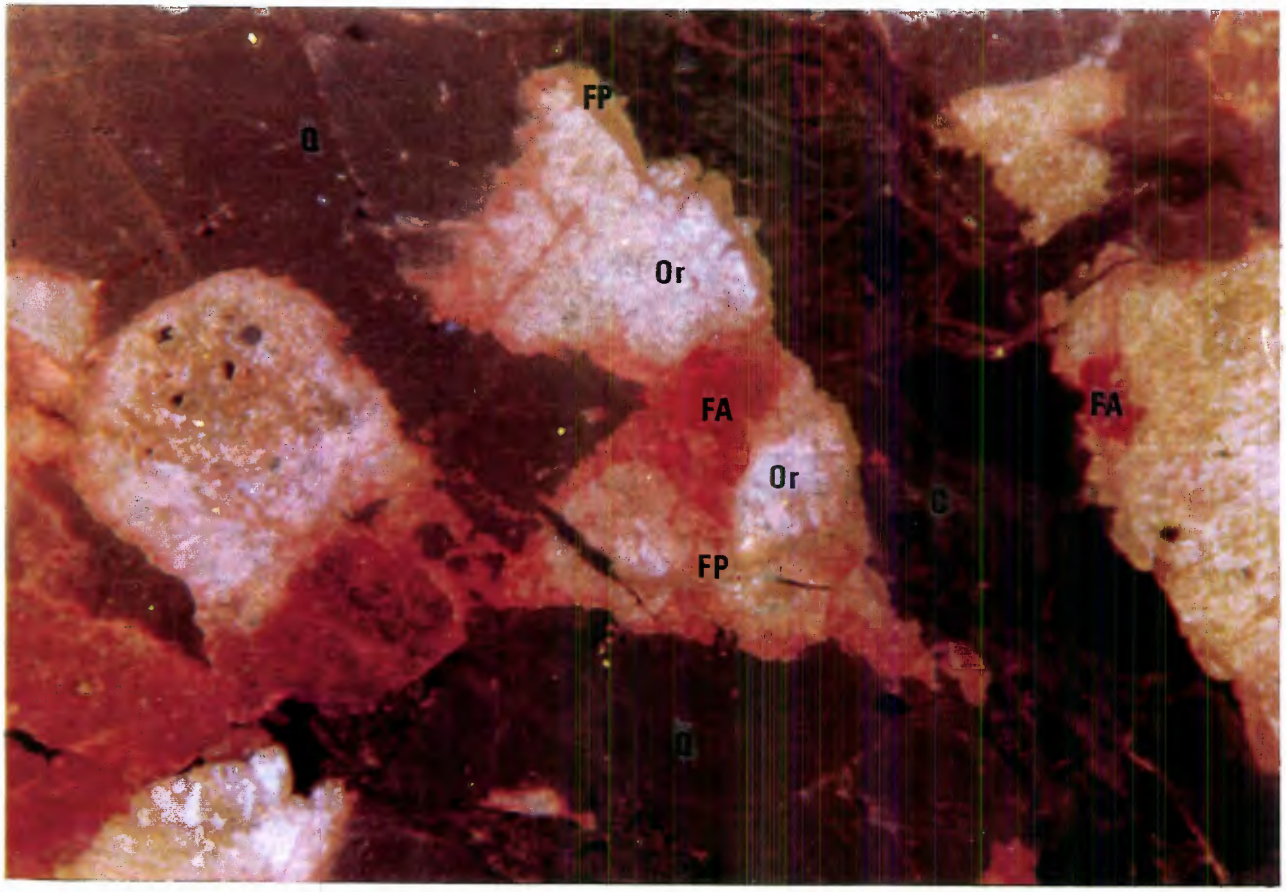

Figure 11. Cathodoluminescence photomicrograph of polished thin section from fenitized gneiss clast in intrusive breccia at sample site 36 at the intrusive breccia north of the All American Prospect, Red Cloud mining district, Lincoln County, N. Mex., Magnification X 90, showing early replacement of blue-luminescing orthoclase (Or) with Ti^{4+} activation by brilliant red-luminescing fenite albite (FA) with Fe^{3+} activation in patches and veinlets and later replacement by tan-luminescing fenite potassium feldspar (FP) with Fe^{3+} activation in rims and veinlets. The bluish gray-luminescing mineral in the clast is quartz (Q). The bluish gray-luminescing mineral in the veinlet is calcite (C) and quartz. Photographic conditions: Kodak Ektapress 400 gold, 400 ASA, 269 seconds, 20 kV.

luminesced dull orange or a bluish gray. A few small blebs of bright orange-luminescing calcite were observed.

The heterogeneous nature of the intrusive breccia makes it impossible to identify any specific trends or changes due to the fenitization, except to suggest that it has been altered primarily by sodic or potassic fenitization. Sample 35-40 ranged from 4.31% to 6.57% K_2O and 3.86% to 6.31% Na_2O. In samples 36-39 from the carbonatized part of the intrusive breccia, calcium oxide concentrations ranged from 1.72% to 9.42%.

The intrusive breccia at sample site 31 is strongly fenitized. A rock slab examined under CL contains abundant red-luminescing fenite feldspar veining and replacing both matrix and the rock clasts. Sample 31 contained 5.82% K_2O and 4.38% Na_2O.

Gneiss

The surrounding gneiss (sample sites 29, 30, 32, 33, 34, and 41) has been altered by incipient potassic and sodic fenitization. In outcrop, the weakly fenitized schistose parts of the gneiss (sample site 32) have a greenish cast, while the strongly fenitized parts are vuggy and bluish green in color with the feldspars commonly bleached white. Some of the vugs contain radiating clusters of greenish black prismatic aegirine crystals as long as 1.5 cm and a few prismatic quartz crystals as long as 3 mm. A stockwork of veinlets as wide as 3 mm were visible in some fragments, contain greenish black aegirine and feldspar cutting through and replacing the gneiss. Fractured surfaces commonly have a coating of blue crocidolite that appears to cut the fenitized gneiss. The crocidolite, examined in crushed grain mounts, is pleochroic pale bluish green to bluish green with anomalous blue to violet to brownish interference colors. The optical properties suggest the mineral is probably a fibrous variety of riebeckite, rather than arfvedsonite which usually has a brown color in its pleochroic scheme.

A polished thin section of sample 32, from the weakly fenitized schistose part of the gneiss, contained veinlets of fenite feldspar, aegirine, crocidolite,

rutile, barite, hematite-limonite pyritohedron pseudomorphs after pyrite, apatite, and monazite. The veinlets occur along crystal boundaries and rarely cut across crystals. The fenite feldspars are potassium feldspar and albite which occur as turbid, fine-grained masses replacing feldspars and quartz, commonly in sinuous veinlets with sharp walls. Some sericite formed from alteration of plagioclase feldspar and is best developed on the edges of the fenite veinlets. Crocidolite occurs as fibrous bundles in the veinlets commonly from alteration of biotite. The crocidolite is variable in color and occurs as pleochroic greenish yellow to yellowish brown, fibrous crystals that are pale bluish green on the edges. The crystals have yellow and anomalous blue interference colors. Individual needles are colorless to pale bluish green and are as long as 0.05 mm. The crocidolite replacing the biotite is commonly a dark yellowish brown. The chemical composition of the crocidolite was difficult to obtain by SEM-EDX analysis due to its fine fibrous habit. The optical properties and SEM-EDX analysis (Appendix D) suggest that it is a fibrous variety of the eckermannite-arfvedsonite group, according to the International Mineralogical Association (IMA) classification (Leake, 1978). Monazite occurs as small, 2-7 micron, prismatic crystals in the veinlets. Aegirine occurs as pale green to yellowish green pleochroic, acicular and prismatic crystals commonly found penetrating quartz. Rutile is found as anhedral to euhedral crystals as much as 2 mm in diameter in the veinlets. SEM-EDX analysis of the rutile crystals detected titanium with a few percent iron. One rutile crystal was found to contain appreciable tungsten; the concentration in the crystal increases from 0.3% WO_3 in the core to 9.4% WO_3 toward the edge of the crystal. Barite-celestite occurs as anhedral crystals 2-6 microns in diameter. Apatite, zircon, and sphene crystals in contact with the fenite veinlets are commonly ovoid in shape while those not in contact with the fenite veinlets are subhedral to euhedral suggesting that the ovoid crystals have been partially dissolved.

Observation under CL of the polished thin sections from sample 32 from the weakly fenitized schistose part of the gneiss shows brilliant red-luminescing fenite albite and reddish tan to red-luminescing fenite potassium feldspar

replacing both blue-luminescing orthoclase, greenish yellow-luminescing plagioclase, and bluish gray to gray-luminescing quartz. The CL emission spectra indicate that the red-luminescence in fenite feldspar is due to ferric iron activation (Fe^{3+}), the blue-luminescence in orthoclase is probably due to titanium (Ti^{4+}) activation, and the greenish yellow luminescence in plagioclase is due to ferrous iron (Fe^{2+}) or manganese (Mn^{2+}) activation (Appendix F). Apatites are yellow to orange yellow-luminescing and zircons are bright yellow-luminescing.

In contrast, a polished thin section from the strongly fenitized rock at the same location (sample site 32), contained few original minerals. The rock consists of a turbid mass of fenite potassium feldspar and albite, abundant crocidolite, and fine acicular aegirine. The fenite feldspars are intergrown, but in some areas fenite potassium feldspar is dominant, while in others the dominant feldspar is fenite albite. Biotite is altered to crocidolite. Only cores of andesine (Ab_{55} An_{37} Or_8) remain surrounded by turbid fenite feldspar. Some sericite is also developed within the andesine crystals at the contacts with the replacing fenite feldspar.

Observation under CL of the polished thin section (sample 32) from the strongly fenitized schistose part of the gneiss shows brilliant red-luminescing fenite albite and bluish gray to dull grayish red to red-luminescing fenite potassium feldspar has replaced much of the original orthoclase and quartz, with only cores of original yellowish green-luminescing andesine remaining (fig. 12). The fenite albite luminesces a brighter red than the fenite potassium feldspar. Zircon crystals luminesce bright yellow.

In outcrop, the weakly fenitized quartzofeldspathic parts of the gneiss may have a slight greenish tint, while the strongly fenitized parts are commonly vuggy and bleached white. Gray feldspars are commonly rimmed by white fenite feldspar. Greenish black aegirine or aegirine-augite crystals, as large as 2.5 mm, are scattered throughout the rock (fig. 13). Vugs contain euhedral, white fenite feldspar and euhedral, greenish black aegirine or aegirine-augite.

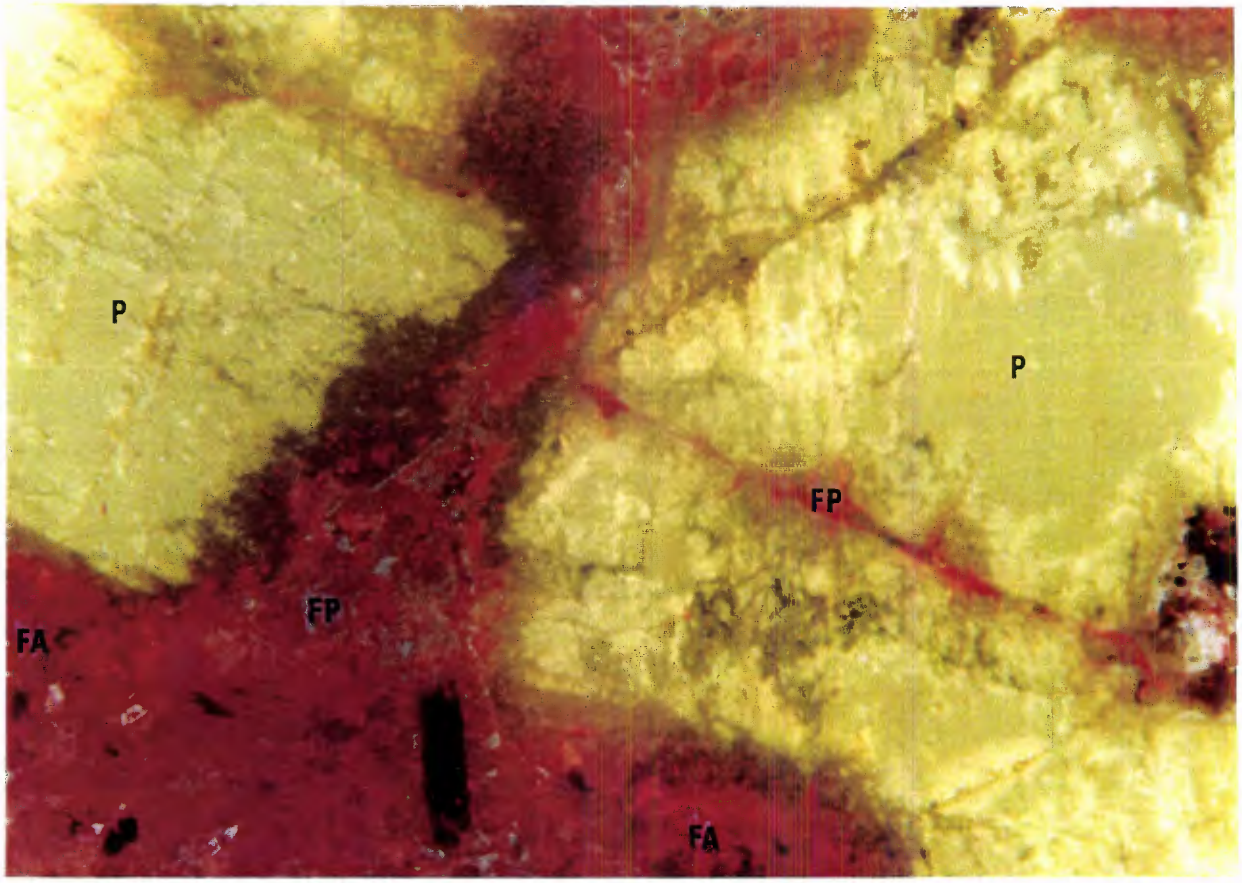

Figure 12. Cathodoluminescence photomicrograph of polished thin section from fenitized gneiss clast at sample site 32 near the intrusive breccia north of the All American Prospect, Red Cloud mining district, Lincoln County, N. Mex., Magnification X 90, showing remnants of original greenish yellow-luminescing plagioclase (P) crystals with Mn^{2+} and/or Fe^{2+} activation in a mass of brilliant red-luminescing fenite albite (FA) with Fe^{3+} activation and bluish gray to dull grayish red to red-luminescing potassium feldspar (FP) with Fe^{3+} activation. Photographic conditions: Kodak Ektapress Gold 400, 400 ASA, 158 seconds, 20 kV.

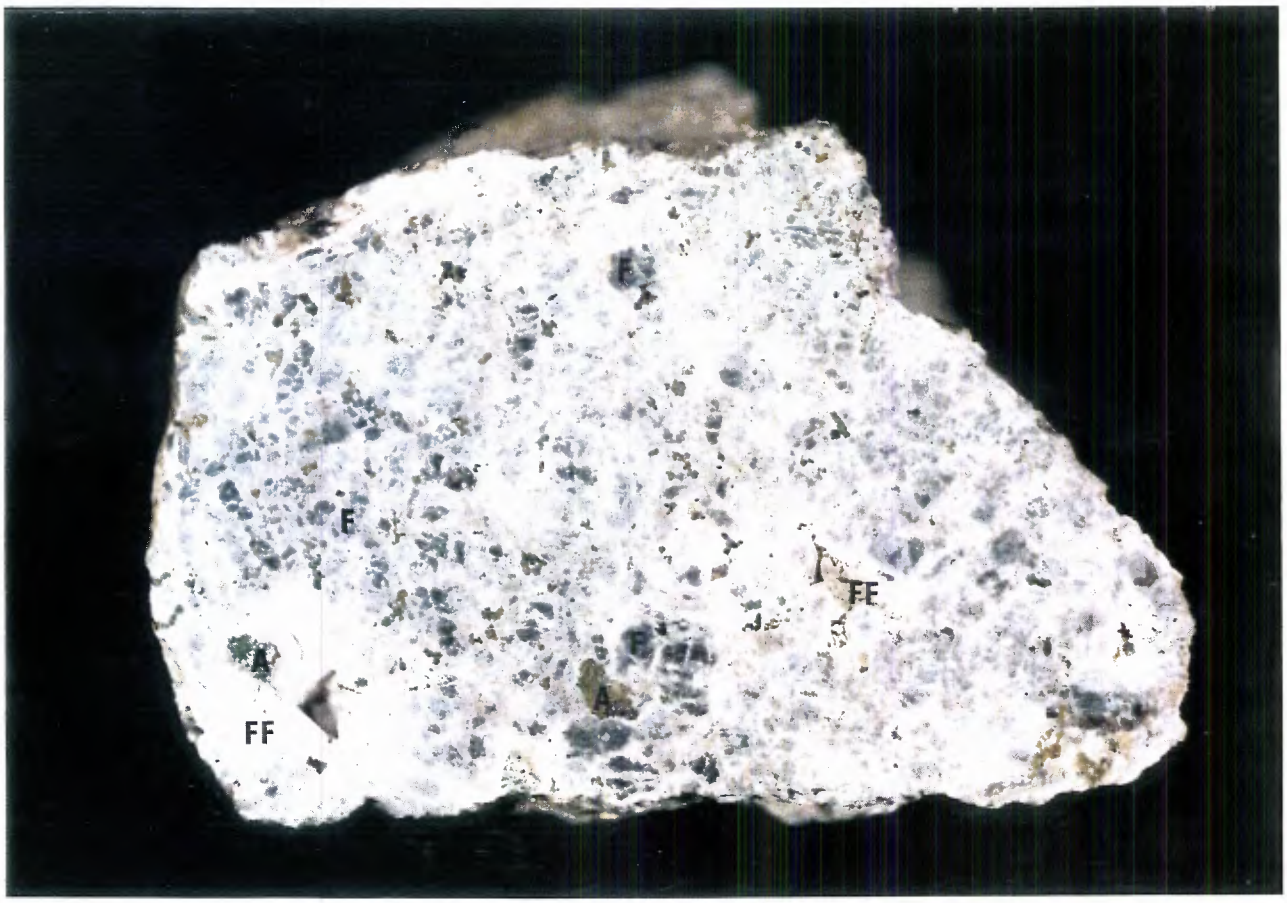

Figure 13. Photograph of fenitized gneiss float fragment found near sample site 32 near intrusive breccia north of the All American Prospect, Red Cloud mining district, Lincoln County, N. Mex., showing replacement of original gray feldspars (F) by white fenite feldspar (FF) (dominantly albite) and scattered crystals of green aegirine-augite (A). The fenite albite crystals are euhedral in the vug in the lower left of the picture.

Four polished thin sections were made from sample 29 and from three float fragments collected within 150 ft of sample site 32. These samples consist of moderately to strongly fenitized quartzofeldspathic gneiss. The gneiss is cut by sinuous veinlets of fenite feldspar. In the more strongly fenitized samples most of the original minerals have been replaced. Some quartz is always present but no biotite was found. One polished thin section has a mortar texture, in which small crystals are present along grain boundaries of the larger ones. The original feldspars (orthoclase and albite) consist of a partially replaced turbid core with completely replaced rims of fenite feldspar. The fenite feldspar is primarily albite in the polished thin sections examined. Clear twinned albite occurs in euhedral crystals as long as 0.1 mm rimming the original feldspars. Some of the sinuous fenite veinlets contain an intergrowth of fenite albite and fenite potassium feldspar. The fenite veinlets contain scattered light green to green pleochroic aegirine and deep green to yellowish green pleochroic aegirine-augite, ranging from 0.02 to 1.5 mm in length. The fenite veinlets also contain subhedral to euhedral sphene, zircon, hematite-limonite pseudomorphs after pyrite, and apatite. A few scattered clumps of 2- to 10-micron monazite crystals, as well as scattered thorite crystals, as much as 0.06 mm in diameter are found in the polished thin section from sample 29.

Subhedral to euhedral pyrochlore crystals ranging from 0.1 to 0.75 mm in diameter were found in fenite veinlets in a float fragment found near sample site 32 (fig. 14). The pyrochlore is estimated to make up 2% to 4% of the polished thin section. Most of the pyrochlore is pale yellowish brown, but some have reddish brown altered cores. SEM-EDX analysis of the yellowish brown pyrochlore detected 5.1% SiO2, 2.1% K_2O, 3.8% CaO, 23.4% TiO_2, 3.1% Fe_2O_3, 62.5% Nb_2O_5 and analysis of the reddish brown core detected 10.9% SiO_2, 4.4% K_2O, 4.6% CaO, 15.0% TiO_2, 2.1% Fe2O3, 36.8% Nb_2O_5, and 27.2% U_3O_8. The SEM-EDX analysis indicates that the pyrochlore group minerals are part of the betafite subgroup and appear to be two different species of potassium-rich betafite according to the IMA classification (Hogarth, 1977). Kalipyrochlore, a potassium-rich pyrochlore, has only been reported from the Lueshe carbonatite in Zaire. The potassic pyrochlore

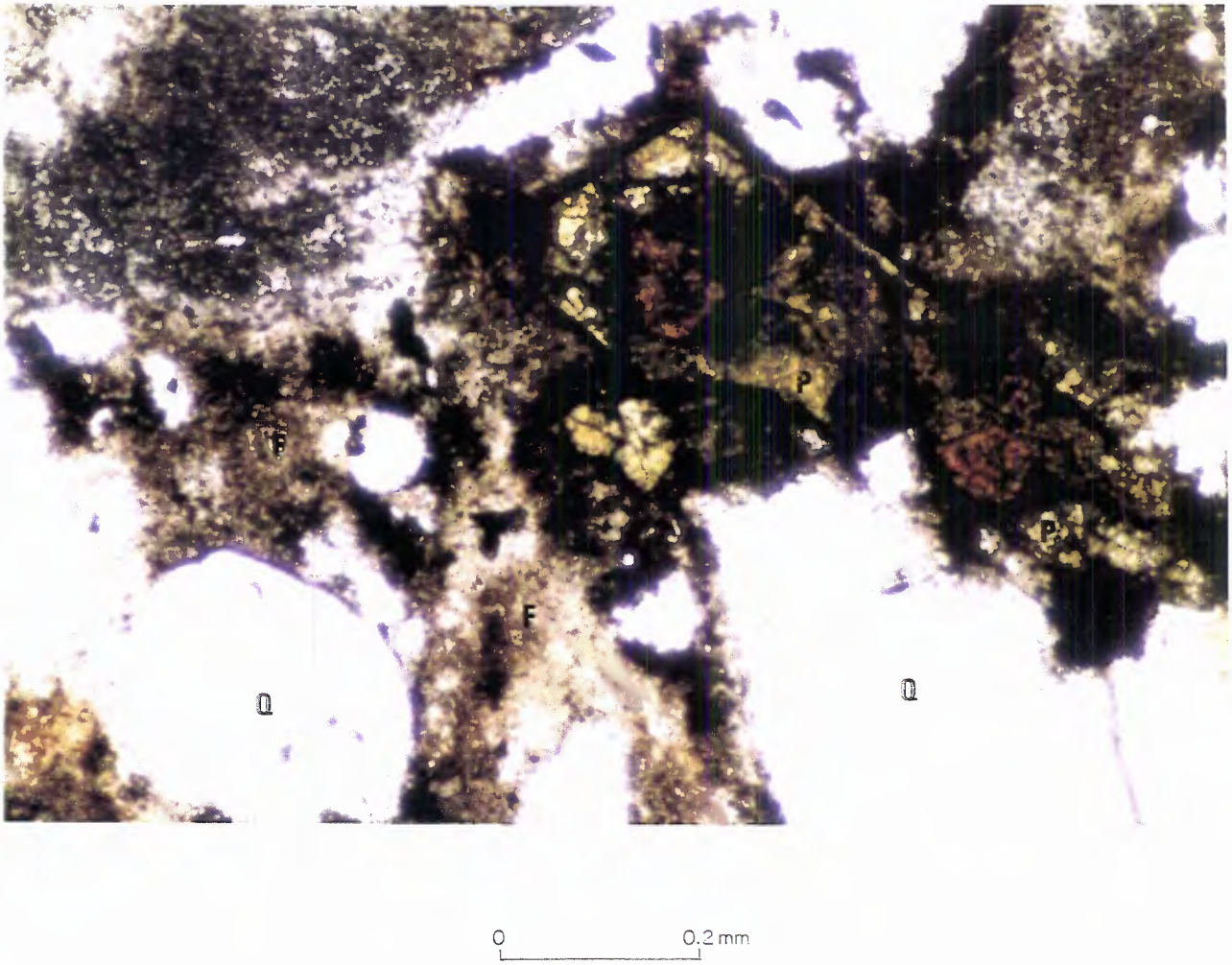

Figure 14. Photomicrograph of strongly fenitized gneiss float fragment found near sample site 32 near intrusive breccia north of the All American Prospect, Red Cloud mining district, Lincoln County, N. Mex., Magnification X 112.5, plane-polarized light, showing subhedral yellowish brown pyrochlore (P) with reddish brown uranium-rich cores in turbid fenite feldspar (F) veinlets in clear quartz (Q).

occurs in alluvial deposits and residual soils of the deposit. It is reportedly derived from normal pyrochlore by leaching of sodium, calcium, and fluorine and enrichment in potassium and water due to weathering (Wambeke, 1978). A few subhedral crystals of niobian rutile, as much as 0.5 mm in diameter, were also present in the fenite veinlets. SEM-EDX analysis of the niobian rutile detected 79.4% TiO_2, 5.3% FeO, and 15.3% Nb_2O_5. Unfortunately the original location of the fragment in outcrop is not known.

Observation under CL of the four polished thin sections showed mostly red-luminescing fenite feldspar veining and replacing most of the feldspar and quartz. Most apatite crystals are lavender- or violet-luminescing, commonly prismatic, as long as 0.3 mm, and occurred in clumps, enclosing smaller anhedral to euhedral, yellow-luminescing apatite. The CL emission spectra indicate that the violet color of the apatite is due to the dominance of europium and samarium activation (Appendix G). Subhedral to euhedral zircon crystals, as long as 0.06 mm, are bright yellow luminescing. In one area of the slide a rounded prismatic yellow-luminescing apatite crystal is partly enclosed by a brilliant yellow-luminescing euhedral zircon crystal. Both are totally enclosed by a euhedral prismatic lavender-luminescing apatite crystal (fig. 15). This feature suggests a sequence in which the original apatite of the gneiss, formed in an environment enriched in HREE, was subsequently partially enveloped by zircon and then LREE enriched lavender-luminescing apatite that crystallized from the invading fenite solutions. A few very small crystals of bright orange-luminescing calcite were visible.

The heterogeneous nature of the gneiss makes it difficult to identify changes due to fenitization from the chemical analysis, except to suggest that some areas may be dominated by potassic or sodic fenitization. Samples contained 5.19% to 9.35% K_2O and 3.49% to 7.48% Na_2O. Sample 29 plots as a quartz syenite on the De La Roche R_1R_2 grid classification plot (Appendix C).

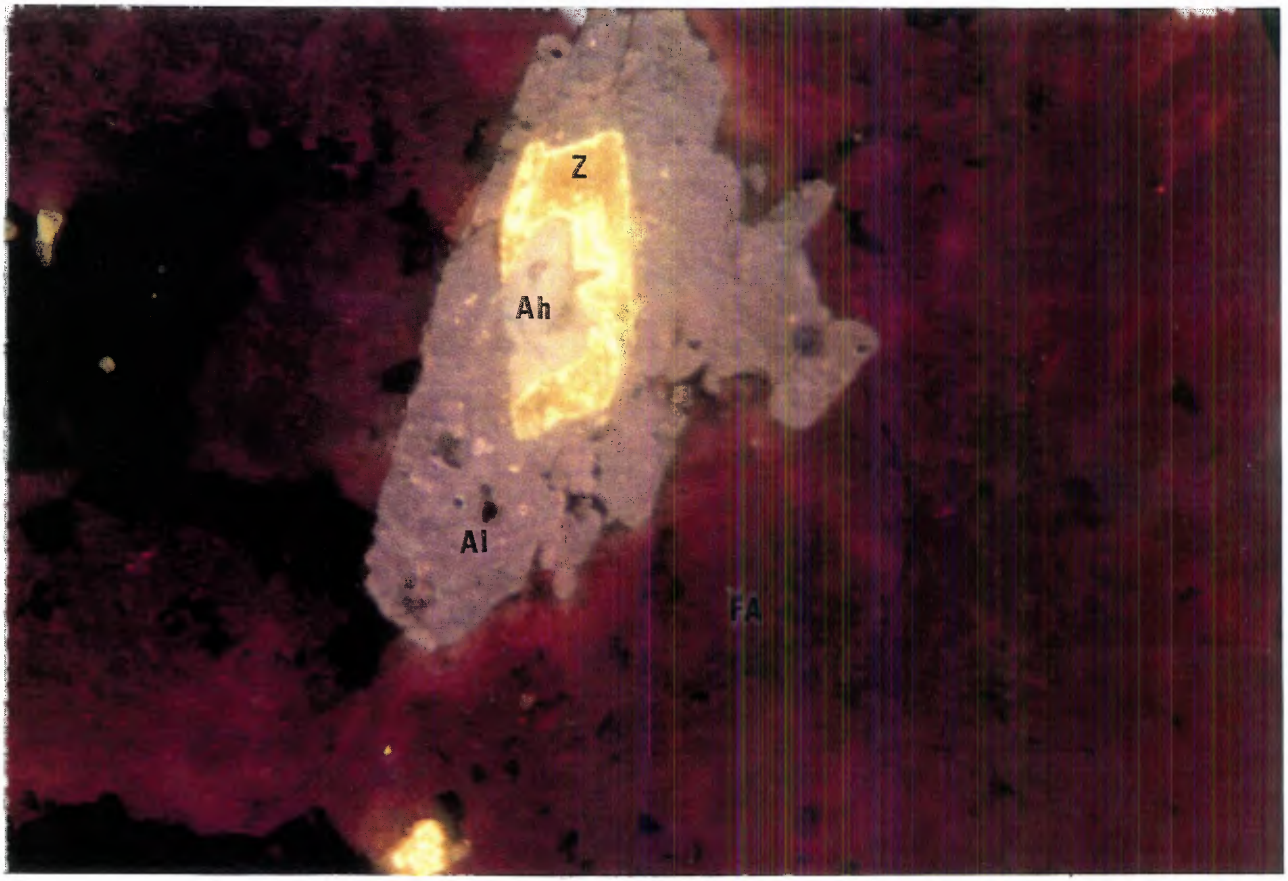

Figure 15. Cathodoluminescence photomicrograph of polished thin section from fenitized gneiss float fragment found near sample site 32 near the intrusive breccia north of the All American Prospect, Red Cloud mining district, Lincoln County, N. Mex., Magnification X 72, showing two dull yellow-luminescing apatite (Ah) crystals with heavy-rare-earth-element activation with an overgrowth of brilliant yellow-luminescing zircon (Z), that are both enveloped by lavender-luminescing apatite (Al) with light-rare-earth-element activation in red luminescing mass of fenite albite (FA) with Fe^{3+} activation. Photographic conditions, Kodak Ektapress Gold 400, 400 ASA, 36 seconds, 20 kV.

Sandstone

Fenitization was observed in the surrounding sandstones at sample sites 30 and 42. At sample site 30, on the northern edge of the gneiss, sandstone fragments in tree roots and in a caved pit are visibly altered. The sandstone fragments are vuggy and contain cubic hematite-limonite pseudomorphs after pyrite. In a polished thin section of the sample, fine-grained (less than 0.05 mm) fenite feldspar and abundant fine (0.02 to 0.2 mm) cubic hematite-limonite pseudomorphs after pyrite occurs in veinlets cutting the sandstone, commonly in the matrix between the grains. The sandstone contains original grains of quartz, plagioclase, and potassium feldspar. The veinlets also contain some fluorite and 2- to 7-micron-long prismatic monazite crystals.

Observation under CL showed brilliant red-luminescing fenite feldspar veining the sandstone and, more commonly, found replacing the matrix between the clastic grains. Some deep violet-luminescing fluorite and a few blebs of orange-luminescing calcite were visible. A few crystals of blue-luminescing apatite and bright yellow-luminescing zircon were also visible. The potassium felspar grains luminesce blue and the plagioclase grains luminesce a dull yellowish green. Quartz luminesces a bluish gray or gray.

At sample site 42, on the southeastern edge of the gneiss, the sandstone float and a small outcrop on the road are visibly altered. The sandstone contains clots and streaks of crocidolite (fig. 16). Small (as much as 0.5 mm in diameter) cubic hematite-limonite pseudomorphs after pyrite are present in some areas surrounding the crocidolite. Some float fragments contain brecciated material with feldspar fragments and prismatic greenish black aegirine crystals, as long as 5 mm. In a polished thin section of the sample, crocidolite needles occur between and penetrate the edges of the quartz grains. The crocidolite occurs as colorless to pale bluish green and greenish yellow to yellowish brown pleochroic clumps of needles as long as 0.05 mm. It has white to yellow to blue interference colors. The chemical composition of the crocidolite was difficult to obtain by SEM-EDX due to the fine fibrous habit, but it is more calcium- and magnesium-rich than the crocidolite analyzed from the fenitized gneiss at sample

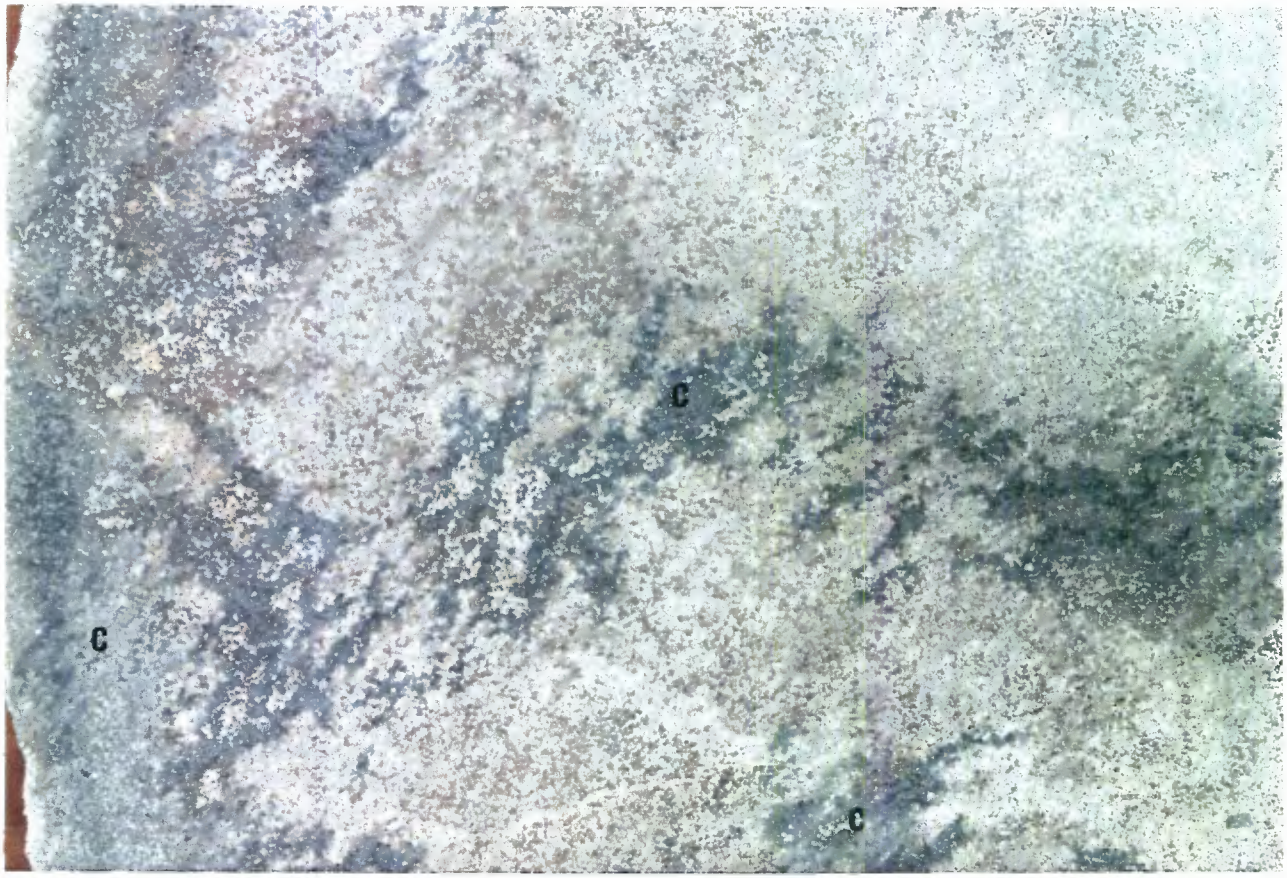

Figure 16. Photograph of fenitized sandstone from sample site 42 near intrusive breccia north of All American Prospect, Red Cloud mining district, Lincoln County, N. Mex., showing clots and streaks of blue crocidolite (C) replacing sandstone.

site 32 (Appendix D). SEM-EDX analysis indicate that it is probably a fibrous variety of a calcian alkali or sodic-calcic amphibole (Leake, 1978).

Observation under CL shows minor amounts of fine brilliant red-luminescing fenite feldspar associated with the nonluminescing amphibole between bluish gray-luminescing quartz grains and a few scattered blue-luminescing feldspar grains. Chemical analysis of the sandstone at sample site 42 indicates that sodium was introduced. It contained 4.16% Na_2O and 0.89% K_2O.

Trachyte

A 45-ft-wide trachyte dike, sample sites 26-28, is cut by the road and exposed for a length of 100 ft, about 100 ft north of the gneiss-sandstone contact. The dike is bleached white and cut by a stockwork of feldspar veinlets, as wide as 1 mm, that are stained by hematite-limonite.

In a polished thin section of sample 26, the original rock appears to have consisted primarily of fine albite groundmass and scattered albite phenocrysts. The dike is cut by numerous veinlets containing potassium feldspar, niobian rutile, a niobium-bearing mineral that compositionally approximates columbite, xenotime, galena, jarosite, and hematite-limonite spherulites and coatings. The potassium feldspar occurs as fine masses replacing albite and is found as euhedral crystals as large as 0.1 mm on the walls of fractures and in vugs. One xenotime and one galena crystal (less than 10 microns in size) were identified. The rutile and "columbite" occur intergrown in fine masses, as large as 0.1 mm; some of the "columbite" occurs in prismatic crystals as long as 5 microns. SEM-EDX analysis of three crystals of "columbite" detected an average of 69.4% Nb_2O_5, 17.8% MnO, 3.9% TiO_2, 3.3% FeO, and 5.6% SiO_2. SEM-EDX analysis of two crystals of niobian rutile crystals detected an average of 76.0% TiO_2, 16.2% Nb_2O_5, 2.4% FeO, 2.2% MnO, and 2.8% SiO_2. In addition some late quartz was deposited on some of the euhedral potassium feldspar crystals lining the walls of the veinlets where it is found mixed in with limonite. Samples 26 and 28 contained 9.37% and 10.20% Na_2O and 2.26% and 1.12% K_2O, respectively.

Observation under CL showed early replacement of the dike by sparse patches of brilliant red-luminescing fenite albite veinlets that are cut by later dull pinkish or reddish tan-luminescing luminescing fenite potassium feldspar veinlets. The groundmass consists primarily of dull yellowish green to gray-luminescing albite.

Float fragments found in the drainage 150 ft north of sample site 32 contained pinkish trachyte intruding the whitish gray gneiss. Highly weathered fragments contain some sericite in the vugs.

In a polished thin section, the trachyte consists of anhedral to subhedral albite crystals, ranging from 0.2 to 1 mm in length, averaging 0.5 mm in length. The albite crystals were commonly turbid. Minor amounts of aegirine are partially weathered out and altered to hematite-limonite. Zircon crystals ranging from 0.1 to 0.5 mm in length, and hematite-limonite pseudomorphs after pyrite, 0.4 mm in diameter are present.

Observation under CL shows brilliant red-luminescing fenite feldspar veinlets cutting both the trachyte and gneiss. Bright yellow-luminescing zircon crystals and a few small rose to orangish yellow-luminescing apatites were present.

Analytical Data

Analytical data from 6 samples (35-40) of the intrusive breccia showed anomalous concentrations of REO, gold, copper, zinc, fluorine, barium, and strontium in comparison to the altered host rocks. REO concentrations averaged 683 ppm in the intrusive breccia and 237 ppm in fenitized gneiss (sample sites 29, 30, 32-34, and 41). Gold concentrations averaged 47 ppb in the intrusive breccia and 6 ppb in fenitized host rocks (samples 29-34, 41, and 42). Copper and zinc concentrations averaged 67 ppm copper and 113 ppm zinc in the intrusive breccia and 15 ppm copper and 32 ppm zinc in the fenitized host rocks. Fluorine concentrations averaged 633 ppm in the intrusive breccia and 298 ppm in the fenitized host rocks. Barium and strontium concentrations in the intrusive breccia were as much as 6,000 ppm and 1,368 ppm, respectively. Manganese

concentrations as much as 0.3% were present in the intrusive breccia. The thorium concentration of 274 ppm in sample 29 was the highest found in all samples taken during this investigation.

The highest concentration of niobium in the fenitized gneiss was 150 ppm, but the sample with abundant pyrochlore was not analyzed. In only a few carbonatite complexes (e.g. Panda Hill, Tanzania and Lueshe, Zaire) are significant niobium concentrations found in the adjacent fenites but niobium is still more abundant at these deposits in the carbonatites (Deans, 1966, p. 395). Three samples (26-28) taken from the trachyte dike contained 251 to 286 ppm niobium.

Sky High Prospect

Description

The Sky High (Big Ben) Prospect (fig. 17, sample sites 1-20) consists of two groups of workings. The northern group (sample sites 1-8) consists of a 25-ft-deep shaft, a shaft caved at 10 ft deep, a 30- by 35-ft pit, two road cuts, and 2 small pits. The southern group (sample sites 10-20), approximately 200 ft to the south, consists of a 25-ft-long trench connecting to a caved adit, that is inferred to be 100 ft long, and a connecting shaft, caved at 19 ft deep, 260 ft of bulldozer trenches, a road cut, and 3 pits. The northern group of workings is cut on an elliptical-shaped intrusive breccia pipe exposed over a distance of 350 ft and ranging from 50 to 100 ft wide. The pipe intrudes sandstone and a trachyte dike or sill. The southern group of workings is cut on a tabular intrusive breccia zone exposed over a distance of 150 ft and ranging from 25 to 50 ft wide, and a few narrow zones, including one where a 3-ft-wide limestone bed is brecciated. The two intrusive breccias may be connected under the soil cover.

The northern intrusive breccia appears to be the main vent and consists of angular to subrounded fragments of trachyte, sandstone, and less common granitic clasts. At sample sites 2, 7, and 8, it is matrix-supported and contains a brown aphanitic matrix with crystal fragments. The trachyte clasts are variable and, although identification is difficult due to the alteration, consist mainly of a

coarser grained type with abundant, large feldspar phenocrysts, 3 mm to 1.2 cm in length, in a brown fine-grained groundmass and others that are finer grained consisting of feldspar phenocrysts less than 3 mm in length in a white to tan aphanitic groundmass. Calcite is abundant, as well as fluorite in some areas, and has filled cavities and fractures and partially replaced both the aphanitic matrix and rock fragments. At sample sites 1, and 3-6, no aphanitic matrix was visible in outcrop and the intrusive breccia appears to be clast-supported with calcite and fluorite filled cavities.

The southern intrusive breccia exposures consist of angular to subrounded sandstone, limestone, and a few trachyte clasts in a matrix of brown calcite and purple fluorite. No aphanitic matrix was evident in outcrop.

Scintillometer readings ranged from 140 to 170 cps in the workings in the northern pipe and 45 to 110 cps in the southern intrusive breccia. Scintillometer readings in the sandstones and trachyte outside the pipe were 45 cps, although some areas of brecciated trachyte were as high as 120 cps.

Mineralogy

The breccias contain calcite, fluorite, barite, quartz, and hematite-limonite pseudomorphs after pyrite. The minerals occur as replacements of the matrix and rock clasts and as open-space fillings forming drusy crystals and coatings on fractures and in cavities. Chrysocolla, malachite, azurite, wulfenite, mimetite, and manganese-oxide coatings occur in some areas.

Alteration

In outcrop, the altered trachyte and intrusive breccia are bleached white due to incipient fenitization. In the carbonatized parts of the intrusive breccia the matrix has a brown color. The feldspar crystal fragments and some of the trachyte clasts are bleached white.

Although no thin sections were made from samples taken at the Sky High Prospect, two slabs from sample sites 2 and 8 in the intrusive breccia consisting of sandstone and trachyte clasts in an aphanitic matrix were examined under CL.

The sandstone fragments contain bluish gray-luminescing quartz with few grains of blue-luminescing feldspar partially replaced by patches of anhedral orange-luminescing calcite and patches of pale purple-luminescing fluorite. Most trachyte clasts and the aphanitic matrix luminesced a dull yellowish gray to tan and were partially replaced by anhedral orange-luminescing calcite and pale purple-luminescing fluorite. A few scattered trachyte clasts were replaced by brilliant red-luminescing fenite feldspar veinlets. A few lavender- or violet-luminescing, prismatic crystals that are probably apatite are associated with the calcite. Fine yellow- and white- luminescing crystals that appear to be zircon are in the aphanitic matrix.

The northern intrusive breccia appears to have been subjected to three episodes of alteration, similar to the sequence present at the M and E No. 13 Prospect. Only a few red-luminescing fenite feldspar replaced clasts were found in examination by CL, and much of the intrusive breccia appears to have been replaced by gray- or tan-luminescing potassium fenite feldspar followed by carbonatization. Sample sites 2, 3, 8, and 9 contained from 3.51% to 12.01% K_2O, from 0.28% to 3.19% Na_2O, and 4.70% to 29.09 % CaO in the northern intrusive breccia. Sodium shows an inverse relationship to potassium. A late period of potassic fenitization, similar to the alteration found at the M and E no. 13 Prospect, in which potassium was introduced and sodium was removed is indicated by the chemical analysis.

Sample 18 from the southern intrusive breccia contained 4.49% CaO and only 0.75% K_2O and 0.05% Na_2O suggesting weak or no fenitization has occurred at this sample site.

Analytical Data

Twenty samples (1-20), taken from the Sky High Prospect, contained low concentrations of REO's, ranging from 0.08% to 1.04%, averaging 0.52%. Y_2O_3 concentrations were low, less than 254 ppm; however, some X-ray fluorescence analyses are suspect due to interference by lead. Gold, silver, and base metal concentrations were erratic over most of the breccia pipes. Gold concentrations

ranged from 30 to 610 ppb, averaging 134 ppb. Silver concentrations ranged from less than 0.2 to 27.3 ppm, averaging 2.6 ppm. Trace amounts of base metals were present, with some scattered concentrations as high as 3.3% lead, 0.6% copper, and 0.1% zinc.

Samples 1-6, taken over a width of 80 ft in the eastern part of the northern intrusive breccia, contained the most consistent gold and silver concentrations found in any of the breccia pipes. Gold concentrations ranged from 117 to 222 ppb, averaging 143 ppb, and silver concentrations ranged from 0.2 to 3.7 ppm, averaging 2.9 ppm.

Fault Breccia Deposits

Most of the fluorite-barite-quartz deposits in the Red Cloud district are of the fault-breccia type and are REE-rich. These deposits contain relatively high concentrations of REE'S but only minor amounts of lead, copper, silver, and arsenic. The Red Cloud Copper, Buckhorn, and Rio Tinto Mines are lead-copper-silver-arsenic-rich deposits and contain only low amounts of REE's. Nine of the larger deposits or prospects are discussed in the text below and shown on figures 18-24. Fifteen of the smaller or inaccessible deposits, mines, or prospects are summarized in table 3, and other occurrences are noted on plate 1 and in Appendix A.

Eagles Nest Prospect

Description

The Eagles Nest Prospect (fig. 18, sample sites 110-134) consists of a 220-ft-long adit with 80 ft of side drifts and eleven pits. The workings are on a steeply dipping, tabular zone, which trends approximately N. 45° W. and can be traced over a distance of 1,220 ft, of brecciated sandstone in a matrix of fluorite. The breccia zone appears to range from 10 to 55 ft wide, but an average is difficult to determine because of soil cover. The best exposure of the whole zone is in the adit where it is 55 ft wide. A conservative average width of 20 ft is estimated. The fractured sandstone outside the main zone

contains numerous fluorite veinlets. Parts of the breccia zone appear to be offset; it could not be determined if this was due to later faulting or just the irregular trend of the original fault zone.

Scintillometer readings ranged from 40 to 80 cps over outcrops and pits and trenches. Scintillometer readings in the main mineralized zone in the adit ranged from 100 to 175 cps, and were only 70 cps outside of the main zone in the fractured sandstone exposed in the side drifts.

Mineralogy

The Eagles Nest Prospect consists of fluorite, barite, bastnaesite, hematite-limonite pseudomorphs after pyrite, manganese oxide, and minor calcite deposited as open space fillings between angular sandstone clasts. Greenish yellow, tabular bastnaesite crystals, as long as 5 mm, in a matrix of purple fluorite were visible at some sample sites. Barite commonly occurs as translucent, bluish green crystals, as much as 2 cm in diameter. Chrysocolla and malachite occur as scattered blebs and coatings.

Alteration

The formation of minor pyrite and some replacement by fluorite was the only alteration observed in sandstone fragments and in the wallrocks. A rock slab containing brecciated sandstone fragments showed no evidence of fenitization.

Analytical Data

Twenty-five samples, 110-134, were taken at the prospect. Twenty-three samples (sample sites 110-126, 128, 130-134) from the main breccia zone ranged from 0.02% to 2.65% REO, averaging 1.27% REO. Samples 110-114 were taken from weathered outcrops, while all others were taken from the workings; lower REO concentrations may be due to leaching. Excluding these five samples, the REO concentrations averaged 1.37%. Y_2O_3 concentrations were low, averaging 107 ppm. In twenty-three samples (sample 110-126, 128, 130-134) from the main breccia zone, fluorite concentrations ranged from 12.84% to 65.24%, averaging 38.82%.

Two samples (sample 127 and 129) taken outside of the main zone in fractured sandstone contained 9.82% or less fluorite and 0.05% or less REO. Gold concentrations ranged from less than 5 to 755 ppb, averaging 83 ppb. Trace amounts of silver, lead, copper, and zinc also were present. Twenty-seven samples taken by the Bureau in 1943 contained from 0.0% to 34.32% barite, averaging 11.6% (Soule, 1946, p. 15).

Assuming a 20-ft-wide and 1,220-ft-long zone at least 200 ft deep, and using a tonnage factor of 14 ft^3/st, an inferred resource of 348,000 st was estimated, containing 1.3% REO and 39% fluorite.

Buckhorn Mine and Last Chance Prospect

Description

The Last Chance Prospect (fig. 19, sample sites 135-144) consists of a 260-ft-long adit, a 45-ft-deep shaft that connects at the bottom to the adit at a distance of 65 ft from the portal, and 6 pits or trenches.

The Buckhorn (Little Wonder) Mine (fig. 19, sample sites 145-151) consists of an 18-ft-long adit that connects to an inaccessible 135-ft-deep shaft, an inaccessible 20-ft-deep shaft and a 45-ft-deep shaft connected by a 30-ft-long drift; a 55-ft-long adit (Little Wonder adit) that connects to an inaccessible 35-ft-deep winze at the face, and seven pits or trenches.

The Buckhorn Mine and Last Chance Prospect appear to be on the same N. 30° W. trending, fault breccia zone in sandstone. At the Buckhorn Mine brecciated limestone fragments were found on the dumps. The main breccia zone, where visible, ranges from 5 to 15 ft wide and is steeply dipping. The mineralization occurs in a number of splays or horsetails, and intersects bedding planes and minor fractures along the fault, as well as in the main fault zone. At the Last Chance Prospect, the fault zone ranges from about 10 ft wide at the portal to 15 ft wide in the adit. The fault zone curves and narrows in the last 60 ft of the adit to 1 ft wide at the face, but it appears as if the adit was driven on a splay trending S. 55° E. off the main fault. The Little Wonder adit at the

Buckhorn Mine also appears to be on a splay trending S. 26°E. and curving to S 24° W off the main fault zone. At the Last Chance Prospect, the breccia zone consists primarily of fluorite, while at the Buckhorn Mine the zone consists of fluorite and abundant lead and copper sulfides that are almost totally oxidized to various secondary copper and lead minerals. The sulfide-mineralized rock appears to form a 500-ft-long shoot along the fault.

Scintillometer readings at the Last Chance Prospect ranged from 50 to 150 cps. Scintillometer readings at the Buckhorn Mine workings ranged from 40 to 140 cps.

Mineralogy

The Last Chance Prospect consists of fluorite, barite, bastnaesite, hematite-limonite pseudomorphs after pyrite, manganese oxide and minor calcite deposited as open space fillings in brecciated sandstone.

At the Buckhorn Mine, galena, tennantite, freibergite, proustite, xenotime, zircon, fluorite, quartz, minor calcite, and a few hematite-limonite pseudomorphs after pyrite were deposited as open-space fillings in brecciated sandstone and limestone. Two polished thin sections were examined, sample 147 from a sulfide-rich pocket in the middle of the breccia zone and another of a sulfide-rich veinlet from a fragment on the dump. The extremely oxidized condition made it difficult to determine the paragenesis of the minerals.

Tennantite is largely replaced by secondary copper and lead minerals. The secondary minerals commonly occur as rims surrounding the unreplaced tennantite core, leaving original crystal outlines still visible. The tennantite crystals range from 0.2 to 1.5 mm, and average 0.3 mm in diameter. SEM-EDX analysis of three tennantite crystals detected 43.5% to 45.3% copper, 17.8% to 19.3% arsenic, 7.8% to 9.2% zinc, 0 to 4.4% antimony, and 24.1% to 26.8% sulfur. The tennantite is rimmed and replaced by malachite, azurite, chrysocolla, digenite, covellite and a copper-lead carbonate. SEM-EDX analysis also identified fibrous masses of secondary minerals that appear to be the copper silicate shattuckite ($Cu_5 (SiO_3)_4 (OH)_2$); the arsenates, cuprian austinite (Ca (Cu,Zn) (AsO_4) (OH)), adamite

($(Zn,Cu)_2$ (AsO_4) (OH)), cornubite ($(Cu,Zn)_5$ (AsO_4) $(OH)_4$); and fine crystals (as much as 5 microns in diameter) of a silver-mercury-sulfide-halide (Ag-Hg-S-I), possibly perroudite or capgaronnite. Perroudite and capgaronite are two new minerals that occur as an alteration product of mercury-silver-bearing tennantite by halide-bearing solutions of marine origin at the Cap-Garonne sandstone-hosted copper-lead mine, Var, France (Sarp and others, 1987; Mason and others, 1992). At sample site 147, a sulfide pocket contained euhedral tennantite crystals in a mass of subhedral to euhedral quartz crystals that appear to have formed at the same time. Tennantite crystals were found crystallized directly on a sandstone clast with a mass of azurite and other secondary-copper minerals completely rimming the clast, which is in turn enclosed by fine-grained purple fluorite, in a dump fragment.

A freibergite crystal was identified in sample 147. The original euhedral crystal was 0.3 mm in diameter and occurs in a mass of subhedral to euhedral quartz crystals. It is rimmed by malachite, cerussite, and a lead arsenate. SEM-EDX analysis of three points on the crystal detected an average of 31.7% silver, 20.9% copper, 17.5% arsenic, 7.2% zinc, and 22.8% sulfur.

A few proustite crystals were identified in the polished thin section from the dump fragment. One occurs as a triangular-shaped crystal, originally euhedral and 0.3 mm in diameter (fig. 20). SEM-EDX analysis of one point on the crystal detected 55.0% silver, 15.6% arsenic, 6.2% zinc, 3.1% copper, and 20.1% sulfur. It is rimmed by the fibrous copper silicates, chrysocolla and shattuckite with clusters of fine (as long as 30 microns) prismatic crystals of iodargyrite (AgI) around the proustite crystal and along the boundary between the two copper silicates.

Galena is found with tennantite in the adit. In a polished thin section, it was seen only as blebs within the tennantite crystals, but cerussite was abundant in both samples. In sample 147, the cerussite occurs as anhedral to subhedral crystals between quartz crystals. The cerussite luminesces a pale bluish white under CL.

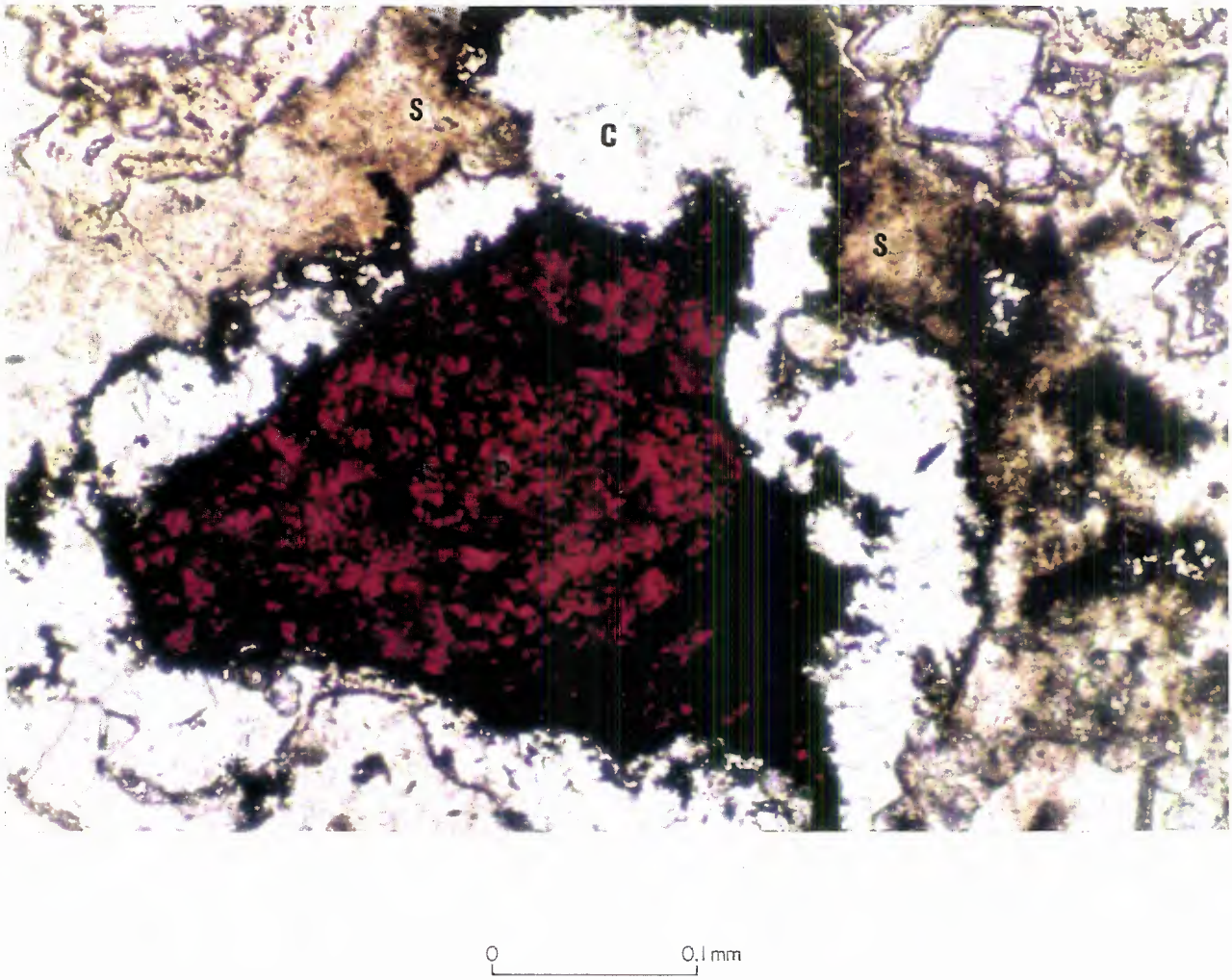

Figure 20. Photomicrograph of polished thin section from dump fragment from the Little Wonder adit, Buckhorn Mine, Red Cloud mining district, Lincoln County, NM, Magnification X 225, plane-polarized light, showing triangular shaped red proustite (P) crystal replaced by an inner rim of chrysocolla (C) and an outer rim of shattuckite (S). Black crystals rimming proustite and the chrysocolla and shattuckite boundary are iodargyrite.

One crystal of xenotime was identified in sample 147. It occurs as a euhedral crystal, 0.025 mm in diameter, between euhedral quartz crystals, and appears to have crystallized at approximately the same time as the tennantite, zircon, and larger quartz crystals. The xenotime crystal luminesces yellow under CL.

A few prismatic crystals of zircon, as much as 0.05 mm in diameter, are scattered throughout the polished thin section taken from sample 147 between euhedral quartz crystals. The zircon appears to have crystallized with the tennantite, xenotime, and larger quartz crystals. The zircon crystals luminesces yellow under CL.

Quartz is present in both polished thin sections and in hand specimens from the dump and appears to be of three separate generations. In the polished thin section from the sulfide pocket at sample site 147, quartz occurs as a mass of subhedral to euhedral prismatic crystals, as long as 0.3 mm. The quartz crystals are commonly corroded on crystal faces and have been broken from the walls of the vein by subsequent movement along the fault. In a hand sample and a polished thin section from dump fragments, the quartz is associated with tennantite and occurs as subhedral to euhedral prismatic crystals ranging from 0.1 mm to 2 mm in length. Finer quartz crystals, 0.01 to 0.05 mm in length, were deposited later and occur as scattered, subhedral to euhedral, corroded, prismatic crystals in a mass of fine fluorite cubes. In addition a third generation of quartz fills vugs as anhedral crystals, 0.05 mm to cryptocrystalline in size.

Potassium feldspar occurs as rhombic crystals with barite and quartz associated with the tennantite. Feldspar crystals range from 0.05 to 0.1 mm in length and appear to have formed early with the tennantite, barite, and larger quartz crystals. The potassium feldspar was nonluminescing or a dull brown under CL.

Barite, which occurs as anhedral crystals averaging 0.03 mm in length associated with quartz, and potassium feldspar, appears to have formed early with the tennantite, potassium feldspar, and larger quartz crystals.

Calcite occurs as scattered anhedral crystals in the matrix of the breccia and as white veinlets as wide as 5 mm cutting through both the matrix and sandstone and limestone clasts. Calcite appears to have been the last mineral deposited, not including those of supergene origin and some minor late quartz filling vugs. The calcite luminesces orange under CL.

Fluorite occurs as fine masses of purple, cubic crystals, ranging from 0.01 to 0.2 mm and averaging 0.05 mm in diameter. It is commonly replaced completely or rimmed by fibrous chrysocolla near tennantite crystals. At least some of the fluorite appears to have formed after the deposition of the tennantite, as it is seen rimming tennantite crystals that have been deposited directly on sandstone fragments. The fluorite luminesces pale purple under CL.

Pyritohedron and cubic hematite-limonite pseudomorphs after pyrite are found as scattered crystals as much as 2 mm in diameter.

A clay mineral, a brownish aluminum-silicate with intermixed copper was found between the quartz crystals in sample 147. Bright yellow mimetite crystals were found in the vugs of weathered fragments on the dumps. Paul Hlava (technical staff member, Sandia Laboratories, Albuquerque, N. Mex.) identified secondary anglesite, brochantite, celestite, cyanotrichite, duftite, linarite, mottramite, olivenite, and vanadinite by electron microprobe at the Buckhorn Mine (Peter Modreski, Geologist, U.S. Geological Survey, Denver, Colo., oral commun., March 1992).

Alteration

The only alteration observed in sandstone clasts and wallrocks was some replacement by fluorite and minor pyrite. Secondary copper and lead minerals have partially replaced some of the rock clasts. Polished thin sections observed under CL showed no evidence of fenitization.

Analytical Data

Seventeen samples, 135-151, were taken. Ten samples (135-144) taken at the Last Chance Prospect contained moderate amounts of REO. Samples contained from

0.09% to 1.88% REO, averaging 0.79% REO. Y_2O_3 concentrations in nine samples from the adit ranged from 217 to 528 ppm, averaging 406 ppm. Fluorite (CaF_2) concentrations ranged from 2.8% to 52.0%, averaging 25.0%. Gold concentrations ranged from 72 to 378 ppb, averaging 186 ppb. Trace amounts of silver, lead, copper, and zinc were present.

An inferred resource of 37,000 st containing 0.8% REO and 25.0% CaF_2 was calculated at the Last Chance Prospect. The tonnage calculation was made assuming a mineralized zone with an average width of 10 ft, a length of 260 ft, extending to a depth of 200 ft and using a tonnage factor of 14 ft^3/st.

Seven samples (145-151) taken from the Buckhorn Mine contained low amounts of REO. REO concentrations ranged from .06% to 0.80%, averaging 0.27%. Y_2O_3 concentrations appear to be comparable, but the concentrations are suspect due to interference from high lead concentrations in X-ray fluorescence analysis. Gold concentrations were the highest found at any mine or prospect in the district, ranging from 264 to 1,707 ppb (0.050 oz/st), averaging 762 ppb (0.022 oz/st). Silver concentrations ranged from 14.3 to 346.3 ppm (10.1 oz/st), averaging 105.8 ppm (3.1 oz/st). Lead concentrations ranged from 0.2% to 37.1% and averaged 10.8%. Copper concentrations ranged from 0.7% to 8.9%, averaging 3.9%. Zinc concentrations ranged from 0.04% to 0.4%, averaging 0.2%. Mercury concentrations ranged from 12 to 121 ppm, averaging 51 ppm. Uranium concentrations were as much as 34 ppm and the Buckhorn Mine is one of the few deposits where uranium is dominant over thorium. No resource estimates could be determined because most of the mineralized zone is inaccessible.

Old Hickory and Hoosier Girl North Prospects

Description

The Old Hickory Prospect (fig. 21, sample sites 165-171) consists of a 65-ft-long adit with an inaccessible winze at the face that curves at the bottom and connects to an inaccessible 200-ft-deep shaft 45 ft below the shaft collar, an inaccessible 70-ft-deep shaft, and 9 pits or trenches. The 200-ft-deep shaft

connects to 60 ft of drifts at the 100-ft level and 350 ft of drifts at the 200-ft level (Soule, 1946, p. 7).

The Old Hickory Prospect is on a mineralized fault breccia zone that trends approximately N. 20° E in sandstone. The mineralized zone is best exposed in the end of the adit, where it is at least 18 ft wide, and the face is still in mineralized rock. The length and width of the breccia zone could not be determined because of colluvial cover and caving of the trenches. Soule (1946, p. 9) and Rothrock and others (1946, pl. 14) reported that at the surface a steeply dipping elliptical-shaped zone of mineralized, brecciated sandstone and a brecciated trachyte dike is approximately 215 ft long and averages 30 ft wide. The zone is reported to pinch to 65 ft long and 3 ft wide at the 200-ft level (Rothrock and others, 1946, p. 119).

The Hoosier Girl North Prospect (fig. 21, sample sites 161-164) is 250 ft to the west and up slope from the Old Hickory Prospect. It consists of a 22-ft-deep shaft, an 18-ft-deep shaft, and 8 pits or trenches. A steeply dipping zone of mineralized, brecciated sandstone trends N. 5° W. and is at least 80 ft long and averages 3 ft wide. Another zone is exposed around the 22-ft-deep shaft and appears to be at least 9 ft wide.

Scintillometer readings ranged from 60 to 130 cps over outcrops and in the pits and trenches. Scintillometer readings over the mineralized zone in the adit ranged from 320 to 400 cps.

Mineralogy

Fluorite, celestite, quartz, bastnaesite, galena, tennantite, sphalerite, and sparse chalcopyrite were identified in a polished thin section from sample 169 from the Old Hickory adit examined by SEM. The minerals occur as open-space fillings between angular fragments of sandstone and some trachyte.

The bastnaesite occurs as tabular crystals as long as 0.3 mm within fluorite. SEM-EDX analysis of a tabular bastnaesite crystal detected 25.3% La_2O_3, 34.7% Ce_2O_3, 4.4% Pr_2O_3, 11.3% Nd_2O_3, 0.8% Sm_2O_3, 16.9% CO_3, 4.6% F, and 2.1% CaO. A REE-bearing mineral (containing more calcium and slightly lower REO content

than bastnaesite) occurs as fine granular masses commonly rimming calcite and found between the fluorite crystals. SEM-EDX analysis of five crystals detected an average of 21.8% La_2O_3, 34.8% Ce_2O_3, 4.8% Pr_2O_3, 12.3% Nd_2O_3, 0.8% Sm_2O_3, 17.4% CO_3, 4.8% F, and 2.9% CaO. The mineral appears to be a secondary REE-fluorocarbonate.

The sulfides commonly occur as blebs as much as 1.3 cm in diameter, with individual crystals as much as 0.4 mm in diameter. The sulfides occur totally enclosed in the larger fluorite crystals, as well as between the fluorite crystals. They appear to have crystallized at approximately the same time as the fluorite. Galena and tennantite are commonly surrounded and replaced by digenite (fig. 22). SEM-EDX analysis of the sphalerite crystals showed no detectable iron. Anglesite, chrysocolla, conichalcite, covellite, malachite, and a lead arsenate were found between the primary sulfides. The few chalcopyrite crystals were found partially altered to bornite. SEM-EDX analysis of two points on one of the tennantite crystals detected an average of 43.8% Cu, 0.2% Fe, 8.6% Zn, 18.2% As, and 29.1% S.

Purple fluorite occurs as large anhedral to subhedral broken cubic crystals, as much as 0.75 mm in diameter and as fine 0.5 mm subhedral to euhedral cubic crystals. Most of the fluorite crystals are corroded on the edges.

Quartz occurs as euhedral crystals on rock fragments and as anhedral masses and euhedral corroded crystals as long as 0.4 mm within the fluorite matrix.

Celestite, a strontium sulfate containing as much as 23% barium , occurs as corroded anhedral to bladed euhedral crystals, 0.01 to 0.2 mm in length. The anhedral crystals are found between, as well as enclosed by larger fluorite crystals. The euhedral crystals were found only in vugs and were commonly associated with sulfides.

A few fine calcite crystals are present between fluorite and celestite crystals. The calcite is anhedral and commonly rimmed by the anhedral REE-bearing aggregates.

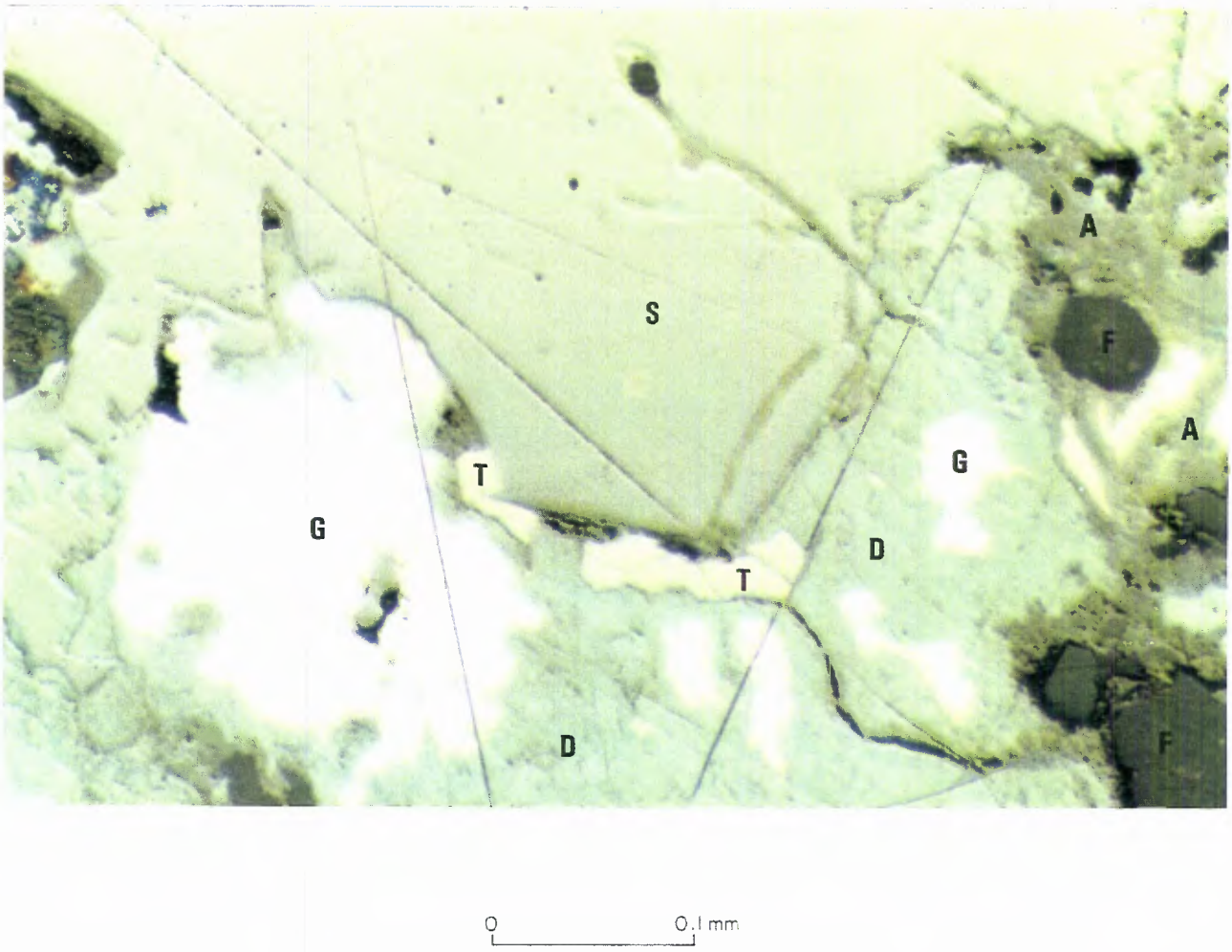

Figure 22. Photomicrograph of polished thin section from breccia at sample site 169 from adit at the Old Hickory Prospect, Red Cloud mining district, Lincoln County, N. Mex., Magnification X 225, reflected light, showing greenish gray-white tennantite (T) , white galena (G), and brownish gray sphalerite (S) replaced by blue digenite (D). Some galena is replaced by gray anglesite (A) on the right center part of the picture. The dark gray mineral is fluorite (F).

Alteration

Minor replacement by fluorite and pyrite, and some minor silicification of sandstone fragments and wallrock was the only alteration observed. A polished thin section of sample 163 and a slab containing angular sandstone fragments examined by CL showed no evidence of fenitization. The angular sandstone fragments consist of gray-luminescing quartz, scattered grains of blue-luminescing feldspar, and nonluminescing limonite-hematite pseudomorphs after pyrite. A few small bright red-luminescing patches were present in the slab but no distinct veinlets were visible. The sandstone clasts are in a matrix of greenish to pale purple-luminescing fluorite. Small amounts of a brilliant green-luminescing mineral were found coating vugs in fluorite crystals. The luminescence is probably due to HREE activation, and the mineral may be yttrofluorite (Anthony Mariano, consultant, Carlisle, Mass., oral commun., 1991).

Analytical Data

Seven samples from the Old Hickory Prospect (164-170) contained 0.54% to 3.33% REO and averaged 2.31% REO. Yttrium oxide concentrations could not be determined by XRF due to interference from lead. A significant concentration (300 to 500 ppm yttrium oxide) is suggested by high concentrations of associated HREE and by comparison to two samples from the Hoosier Girl North Prospect. Fluorite (CaF_2) content ranged from 26.96% to 65.43% and averaged 49.27%. In addition, samples averaged 390 ppb gold, 4.4 ppm silver, 0.6% lead, 0.4% copper, and 0.3% zinc. This is one of the few prospects where significant amounts of precious and base metals occur with high REE's.

Samples 161 and 162 from the Hoosier Girl North Prospect contained 0.65% and 2.26% REO. Yttrium oxide concentrations were 488 and 507 ppm. Trace amounts of gold, silver, lead, copper, and zinc were detected.

An inferred resource of 32,000 st containing 2.3% REO, 49.3% fluorite, 390 ppb gold, 0.6% lead, 0.4% copper, and 0.3% zinc was calculated at the Old Hickory Prospect. The tonnage calculation was made by assuming the mineralized zone has

an average width of 16 ft, an average length of 140 ft, extends to a depth of 200 ft and using a tonnage factor of 14 ft^3/st.

Conqueror No. 4 and Hilltop Prospects

Description

The Conqueror No. 4 and Hilltop Prospects (fig. 23, sample sites 189-204) consist of a 70-ft-long adit and 19 pits or trenches. The workings are on an irregular steeply dipping tabular zone of brecciated sandstone with a fluorite matrix that trends approximately N. 45 E. and can be traced for a distance of 850 ft. The breccia zone curves and splits, but some of the offsets may be due to later faulting. The main breccia zone ranges from 5 to 25 ft wide, but its average width is difficult to determine due to soil cover. Fractured sandstone outside of the main zone contains numerous fluorite veinlets. A conservative average width of 10 ft is estimated.

Scintillometer readings ranged from 40 to 90 cps over outcrops and in the pits and trenches. Scintillometer readings in the adit ranged from 65 to 110 cps.

Mineralogy

The Conqueror No. 4 and Hilltop Prospects contain fluorite, barite, bastnaesite, hematite-limonite pseudomorphs after pyrite, manganese oxide, and minor calcite deposited as open-space fillings between angular sandstone clasts. Malachite and chrysocolla were found as blebs and coatings at some sample sites.

Alteration

Minor replacement by fluorite and pyrite in sandstone fragments and in the wallrocks was the only alteration observed.

Analytical Data

Sixteen samples, 189-204, taken along the breccia zone contained 0.07% to 2.75% REO, averaging 1.17% REO. Yttrium oxide concentrations were low, averaging 120 ppm. Fluorite concentrations ranged from 7.81% to 79.12%, averaging 38.36%. Gold concentrations were 53 ppb or less; only trace amounts of silver, lead, copper, and zinc were present. In 39 samples taken by the Bureau in 1943, barite concentrations ranged from 0.0% to 36.9%, averaging 11.8% (Soule, 1946, p. 16).

An inferred resource of 120,000 st, containing 1.2% REO and 38% fluorite was calculated. The tonnage calculation was made assuming a 10-ft-wide and 850-ft-long mineralized zone that extends to a depth of at least 200 ft and using a tonnage factor of 14 ft^3/st.

Red Cloud Copper and Red Cloud Fluorite Mines

Description

The Red Cloud Copper (Corona Queen, Deadwood) Mine (fig. 24, sample sites 226-232) consists of an inaccessible shaft (Red Cloud shaft) over 100 ft deep, a 65-ft by 40-ft pit that is 30 ft deep, a 14-ft-diameter pit and the inaccessible Deadwood shaft approximately 300 ft to the southwest (pl. 1). The Deadwood shaft is reported to be 70 ft deep with four drifts connecting to open stopes; the dump appears to have been removed (Homer Milford, Environmental Coordinator, Abandoned Mine Land Bureau, Santa Fe, New Mexico, oral commun., October 1991). The Red Cloud shaft was reported to be at least 200 ft deep with drifting on the 200 ft level toward the Red Cloud Fluorite deposit (Rothrock and others, 1946, p. 111). The drifts in the Deadwood and Red Cloud shafts may connect, however maps of the workings have not been published. Little is known about the extent of the mineralization at the Red Cloud Copper Mine, although it was the largest producer of base and precious metals in the district. The only mineralized zone exposed is 16 ft wide in the east wall of a large pit and trends N. 65° E., narrowing to 10 ft wide in a small pit 56 ft away. A fault in Red

Cloud Canyon striking N. 24° W. and dipping 50° SW. cuts through the large pit, and no mineralization is visible on the west wall.

The Red Cloud Fluorite (Conqueror No. 9) Mine (fig. 24, sample sites 233-237) is approximately 250 ft southeast of the Red Cloud Copper Mine and is possibly associated with the base metal mineralization at the Red Cloud Copper Mine. The Red Cloud Fluorite Mine was developed on mineralized brecciated sandstone that is exposed in the walls of a large pit, 140 ft long, as wide as 65 ft, and 50 ft deep.

The Bureau of Mines performed most of the exploratory work in 1943. They developed an adit with 280 ft of drifts that connect to a 20-ft-deep winze and 40-ft-high raise, an inclined 110-ft-deep shaft, collared at the same level as the adit, with 340 ft of drifts on the 35-ft level, and 40 ft of drift on the 100-ft level (Soule, 1946, p. 7). The upper part of the deposit, at and above the adit level was mined out and the inclined shaft and drifts are now covered by rubble. Perhac and Heinrich (1964, p. 228) reported that the major ore shoot contained about 11,000 tons of 50% fluorite, of which nearly 6,500 tons was mined. Only small zones of the high-grade fluorite were found below the main deposit in the inclined shaft and connecting drifts (Rothrock and others, 1946, pl. 13).

The deposit is situated between three faults. A N. 24° W. striking fault in Red Cloud Canyon, on the west, that separates olivine basalt from sandstone, and a northwest-striking fault and northeast-striking fault intersect at an angle of 55° on the east, just beyond the pit wall, that places Precambrian granite in contact with sandstone. (See Rothrock and others, 1946, pl. 13).

Scintillometer readings ranged from 55 to 500 cps over the tabular zone at the Red Cloud Copper Mine and from 60 to 175 cps at the Red Cloud Fluorite Mine.

Mineralogy

The only mineralized rock exposed at the Red Cloud Copper Mine is a tabular breccia zone in sandstone. The breccia zone consists of angular sandstone fragments in a matrix of fluorite, calcite, and masses of fine-grained secondary

copper and lead minerals. Chrysocolla, malachite, azurite, bornite, chalcocite, anglesite, and cerussite are visible. Perhac (1960, P. 166-169) reported primary galena in a polished thin section. DeMark (1980) reported on the identification of mimetite, conichalcite, wulfenite, vanadinite, and mottramite. Modreski (1983) identified agardite associated with the other secondary minerals.

At the Red Cloud Fluorite Mine, the mineralized breccia is exposed in the walls of the large pit. The breccia consists of angular sandstone fragments, commonly 1/2 to 2 in. in diameter in a matrix of massive purple fluorite with pink barite, greenish yellow bastnaesite, and limonite pseudomorphs after pyrite that occur as open-space fillings. A thin section of sample 237 contained subhedral tabular bastnaesite crystals that are commonly broken, ranging from 0.1 to 2 mm in length in a fluorite matrix. Some of the bastnaesite crystals are surrounded by rims of dark purple fluorite. Subhedral to anhedral quartz crystals as long as 1 mm and anhedral corroded barite crystals were scattered throughout the fluorite matrix. Agardite, a secondary hydrous REE-bearing copper arsenate occurring as yellow-green to dull green tufts of acicular prismatic crystals less than 0.1 mm in length, was identified by DeMark (1980). Modreski (1979, 1983) conducted microprobe analysis of agardite specimens and found them to be enriched in LREE with a REE distribution similar to the bastnaesite. A few fragments contained minor chrysocolla and malachite lining vugs.

Alteration

The replacement by fluorite and minor pyrite in sandstone fragments and wallrocks was the only alteration observed. At the Red Cloud Copper Mine, the wallrock is replaced by fluorite and hematite-limonite pseudomorphs after pyrite a few inches away from the breccia zone, and the blebs of hematite-limonite are visible for a few additional inches.

At the Red Cloud Fluorite Mine, a rock slab cut from brecciated sandstone at sample site 237 examined by CL showed no evidence of fenitization. Angular sandstone clasts of the breccia show dull orangish brown to gray-luminescing quartz grains, scattered grains of blue-luminescing feldspar, and nonluminescing

hematite-limonite pseudomorphs after pyrite in a matrix of pale purple-luminescing fluorite.

Analytical Data

Six samples (226-232) taken at the Red Cloud Copper Mine contained 0.27% REO or less. Five samples (226-230) taken from the tabular breccia zone average 35 ppb gold, 1.2 oz/st silver, 0.7% copper, 6.4% lead, and 0.3% zinc. Mercury concentrations are as much as 54 ppm. Uranium concentrations were as much as 195 ppm. The Red Cloud Copper Mine is one of the few deposits in the district where uranium is predominant over thorium. No resources were calculated because most of the mineralized zone is inaccessible.

Four samples (233-236) taken from the walls of Red Cloud Fluorite Mine contained 0.23% to 3.29% REO, and averaged 1.8% REO. A select grab of fragments in the bottom of the pit (sample 237) contained 1.4% REO. Only trace amounts of precious and base metals were present. No resources were calculated because most of the mineralized zone is not exposed and reported lower grade mineralization lies at depth below the Red Cloud Fluorite Mine pit (Rothrock and others, 1946, pl. 13).

Iron Replacement Deposits

Four small pyrometasomatic iron deposits occur within the Red Cloud district where trachyte has come into contact with limestone beds in the Yeso Formation. The American Mine and the Little Marie (Rare Metals) and Iron Lamp prospects occur in replaced limestone xenoliths, and the Red Cliff (Gallinas, Corona, Iron Chief) Mine occurs in a replaced limestone bed above a trachyte sill.

The American Mine (sample site 58) consists of an irregularly shaped magnetite-hematite body that was mined by opencuts and pits over a 300 ft by 200 ft area. A skarn consisting of diopside, tremolite, allanite, feldspar, and magnetite-hematite is present along the trachyte contact. Sample 58 taken along the skarn contact contained 34.2% Fe and 1,090 ppm REO. The REE-bearing mineral

is black tabular allanite as long as 4 mm that was identified by X-ray diffraction by Dave Allerton, U.S. Geological Survey.

The Little Marie Prospect (sample site 59) consists of two magnetite-hematite bodies, approximately 10 ft to 15 ft in width, in a 350-ft-long xenolith. The area was prospected by a 45-ft-deep shaft, a 60-ft-deep shaft, a 10-ft-long adit, and several pits and trenches. A few diopside-tremolite skarn fragments were found on the dump. Sample 59 of the magnetite-hematite fragments on the dump contained 47.1% Fe and 209 ppm REO.

The Iron Lamp Prospect (sample site 96) consists of an 18-ft-deep shaft and a few pits and trenches cut on a limestone xenolith over a distance of 130 ft. A magnetite-hematite body is exposed in the shaft where it is approximately 4 ft in width. Sample 96 of the magnetite-hematite fragments on the dump contained 50.3% Fe and 125 ppm REO.

The Red Cliff Mine (sample site 260) consists of two pits approximately 20 ft by 150 ft and 70 ft by 110 ft in which nearly horizontal 8-ft-thick magnetite-hematite bodies were mined. Sample 260 taken from a remaining part of the magnetite-hematite body, contained 44.8% Fe and 216 ppm REO.

In addition to the iron skarns mentioned above, one other small skarn was found (sample site 61) exposed in a small pit. Diopside and fibrous tremolite are abundant in the pit, and a few fragments of magnetite-hematite were found in float nearby. Sample 61 of the diopside-tremolite skarn contained 627 ppm REO.

SEQUENCE OF EVENTS AND ORIGIN

Iron Replacement Deposits

The iron deposits are pyrometasomatic replacements formed during the intrusion of the trachyte magma. The iron deposits occur where trachyte has come in contact with limestone beds in the Yeso Formation. The deposits are not related to the fluorite-barite-quartz deposits. Similar iron replacement deposits are found around other Tertiary intrusions in the Lincoln County

Porphyry Belt, such as the Capitan Mountains and Jicarilla Mountains (Kelley, 1949).

Faulting

A major period of faulting, apparently due to magmatic activity at depth, followed crystallization of the trachyte magma. Blocks of Precambrian gneissic granite and gneiss were upfaulted to their present position along the fault in Red Cloud Canyon. Blocks of sheared trachyte are visible in Red Cloud Canyon along the trace of the fault.

Intrusive Breccias

The intrusive breccia pipes formed after the period of faulting and are best seen where the pipe north of the All American Prospect cuts the upfaulted block of Precambrian gneiss. Other intrusive breccia pipes appear to be localized along the faults in Red Cloud Canyon; all of the pipes contain clasts of Precambrian gneiss or gneissic granite, Permian sandstone and Tertiary trachyte.

Fenitization

Incipient fenitization occurred after the formation of the intrusive breccia pipes and is evidenced by the rimming of the intrusive breccia clasts by fenite feldspar and by the greater intensity of the alteration within the pipes as opposed to the country rocks. Fenitization was identified in all rock slabs and polished thin sections made from samples taken from the intrusive breccia pipes and the adjacent country rocks. Fenitization was also identified in trachyte dikes and outcrops of syenite and gneissic granite along faults in Red Cloud Canyon. The presence of fenitization in a number of intrusive breccia pipes, trachyte dikes, and along some faults suggests that a large alkalic magma at depth is the source of fenite fluids that used the structures as channelways rather than from individual magma bodies intruding the pipes. Fenitization is one of the most characteristic features associated with carbonatites (Heinrich, 1966, p. 69-73). McKie (1966, p. 261) states that in alkaline intrusions with

associated fenites, in which no carbonatite has been recognized, the absence of carbonatite may imply that the volatile rich carbonate fraction was not fixed at the currently exposed level or that the carbonatite was not a sizeable body. Fenite aureoles have also been identified around peralkaline granites (e.g., Strange Lake, Quebec-Labrador, Canada (Currie, 1985) and agpaitic nepheline syenites (e.g., Lovozero, Kola Peninsula, USSR (Borodin and Pavlenko, 1979, p. 529)). At the M and E No. 13 Prospect and at the intrusive breccia north of the All American Prospect where the rocks were examined in detail, two distinct episodes of incipient fenitization were identified. An early period of sodic fenitization is indicated by the replacement of the original minerals by albite. Aegirine and crocidolite are also developed at the intrusive breccia north of the All American Prospect. A later period of potassic fenitization is indicated by the replacement of the original minerals and the fenite albite by potassium feldspar. Early sodic fenitization and a later period of potassic fenitization has also been reported at the Malawi carbonatites, Africa (Wooley, 1982, p.13-14) and the Amba Dongar carbonatite, India (Sukaheswala and Viladkar, 1981). SEM-EDX analysis of the fenite feldspars in the Red Cloud district indicate that they are pure potassium feldspar and pure albite (Appendix D). Le Bas (1987, p. 77) reports that syenitic fenite aureoles which develop around carbonatites usually contain almost pure orthoclase ($Or_{>85}$) or almost pure albite ($Ab_{>90}$), while aureoles which develop around ijolites and syenites usually contain alkali feldspar ($Ab_{60-40}Or_{40-60}$). Some authors have proposed that these solutions reflect a different source rock while others have suggested that in carbonatite complexes, potassic fenitization is dominant in the upper level of the system while sodic fenitization is dominant in the lower levels (Gold, 1991; Wooley, 1982).

The brilliant red luminescence of fenite feldspars observed under CL, results from ferric iron activation and is characteristic of feldspars formed by the invading fenite solutions that crystallize under conditions of high alkalinity and moderate to high temperatures (Mariano, 1988, p. 112-113). All fenite albite examined in this study luminesced a brilliant red and spectrum

scans had a band with a peak wavelength at 700 nanometers indicating that it is due to ferric iron activation (Appendix F). The unusual and variable CL of the late fenite potassium feldspar, dominantly tan although varying from gray to bluish gray to tan to red, is probably due to a defect in the crystal structure of the feldspar (Anthony N. Mariano, consultant, Carlisle, Mass., oral commun., March, 1992). Broad intrinsic spectral bands are found characteristically in examination of synthetic materials with structural defects. Spectrum scans done by Anthony N. Mariano on the fenite potassium feldspars from the intrusive breccia north of the All American Prospect (sample 36) and the intrusive breccia at the M and E No. 13 Prospect (sample 73)(Appendix F), showed them to be dominated by ferric iron activation. Two bands were identified, one very broad intrinsic band with a peak wavelength at 590 nanometers in the yellow part of the CL spectrum and another band of higher intensity with a peak wavelength at 690 nanometers that corresponds to ferric iron.

The presence of blue-violet-lavender-luminescing apatite in the fenitized rocks indicates LREE enrichment. This luminescence is most commonly found in primary apatite from carbonatites and associated rocks (Mariano, 1988, p. 101). CL emission spectra of a blue luminescing apatite in a fenite veinlet indicate that the blue CL is due to the dominance of europium and samarium activation (Appendix G). The strong LREE enrichment of the invading fenite solutions is also indicated by the presence of monazite within the fenite veinlets.

The extent of the fenitization was not determined during this study, but it is present in the intrusive breccia pipes and adjacent country rocks, and along faults in Red Cloud Canyon, covering an area of approximately 5 mi^2. Fenitized aureoles surrounding alkaline complexes range from a few inches to 3 mi in thickness. A thinner aureole is characteristic in host rocks adjacent to the alkaline intrusions and a thick aureole is characteristic in host rocks above the alkaline intrusions (Kapustin, 1980, p. 43).

High to moderate temperatures (400°C to 700°C) are estimated for fenitization by most studies (Eckermann, 1966, p. 26; Kresten and Morgan, 1986, p. 36-38; Haggerty and Mariano, 1983, p. 379). Le Bas (1987, p.77) reports that

the pure compositions of the albite and potassium feldspar reflect a temperature of less than 550°C for carbonatite fenitization, while the alkali feldspar composition reflects the higher temperature of silicate fenitization of more than 700°C.

Mineralization

REE-bearing fluorite-barite-quartz mineralization formed after the fenitization and is indicated by crystals deposited as open-space fillings on fenitized rock clasts in the intrusive breccias. REE-bearing fluorite-barite-quartz deposits are commonly found associated with carbonatite complexes and are believed to have formed from hydrothermal fluids derived from the final volatile stage of carbonatite formation (Heinrich, 1966, 251-252). Bastnaesite is the major REE-bearing mineral in the deposits and is enriched in LREE. Carbonatites and their associated deposits are usually LREE dominant, while the mineral deposits associated with peralkaline granite (e.g., Strange Lake, Quebec-Labrador, Canada) and quartz syenites complexes (e.g., Pajarito Mountain, N. Mex.), and agpaitic nepheline syenite complexes (e.g., Lovozero, Kola Peninsula, USSR and Ilimaussaq, Greenland) are usually HREE dominant (Mariano, 1989, p. 317, 331, and 335). In almost all of the deposits investigated in the Red Cloud district, early coarse-grained minerals are broken or bent followed by later deposition of fine-grained minerals indicating a period of movement followed by the release of pressure and lower temperatures. A geothermometric fluid inclusion study of bastnaesite crystals indicated temperatures of formation of 175°C to 185° C (Perhac and Heinrich, 1964, p. 226). Preliminary results from fluid inclusion studies on over 40 fluid inclusions in bastnaesite crystals from the Red Cloud district gave homogenization temperatures of 230°C to 255°C and salinities of 16 to 21 weight % NaCl equivalent (Anthony E. Williams-Jones, McGill University, Canada, oral commun., September, 1992).

In addition to the REE-bearing fluorite-barite-quartz deposits with minor amounts of precious and base metals, deposits at the Red Cloud Copper, Buckhorn, and Rio Tinto Mines are lead-copper-silver-arsenic-rich fluorite-barite-quartz

deposits that contain only low amounts of LREE'S. The sulfide mineral assemblage consists of low-Fe tennantite, galena, low-Fe-sphalerite, and proustite, and is most similar to the "iron poor copper-arsenic veins" of the Butte-Tsumeb-Chuquicamata type (Ramdohr, 1980, p. 570, 785). The Buckhorn Mine deposit appears to be a small shoot along the same fault as the Last Chance Prospect which contains typical REE-bearing fluorite-barite-quartz mineralization. The absence of LREE'S, the dominance of uranium over thorium, the low iron contents of the tennantite and sphalerite, and the absence of pyrite suggest that some form of segregation has taken place. Sulfides are common in carbonatites and are typical of late stage carbonatites and related hydrothermal veins (Kapustin, 1980, p. 104-114).

Carbonatization

Carbonatization followed fenitization and mineralization in the intrusive breccias and is indicated by calcite replacement of and calcite overgrowths on fluorite, barite, quartz, and fenite feldspar. The carbonatized areas of the pipes commonly contain abundant blue to violet luminescing apatite, indicating LREE enrichment, a feature commonly found in carbonatite and associated rocks (Mariano, 1988, p. 101). Carbonatization is a common feature found in carbonatite complexes (Heinrich, 1966, p. 133). The carbonatization of some of these intrusive breccias suggests the presence of carbonatite at depth and that a carbonatite body may be closer to the surface within these pipes.

Silica Deposition

In most of the deposits, deposition of minor amounts of fine-grained quartz and chalcedony in vugs and along some fractures appears to have been the last event aside from supergene processes.

PROCESSING

Examination of polished thin sections from the deposits indicates that the bastnaesite crystals should be easy to liberate during grinding because of the

coarse size of the crystals (greater than 0.1 mm in diameter). The liberation of the xenotime would require fine grinding because of the fine size of the crystals, (10-250 microns).

In 1946, the Bureau conducted processing tests on bulk samples for the recovery of fluorite and bastnaesite (Soule, 1946, p. 18-25). Samples from the Red Cloud Mine, All American and Hoosier Group Prospects were ground to -200 mesh and floated. An excellent recovery (85.9% to 89.9%) of high-grade metallurgical fluorite (91.4% to 96.2%) was obtained in three samples. However, acid-grade fluorspar was not attained in these tests. A sample from the Red Cloud Fluorite Mine was ground to -20 mesh and by a combination of tabling and flotation, high grade bastnaesite and metallurgical-grade fluorite were recovered. The tests produced a 70.8% and 72.0% REO concentrate with a recovery of 59.6% and 78.1% of the REO and a 92.9% and 95.5% fluorite concentrate with a recovery of 55.0% and 67.3% of the fluorite. The fluorite was separable from silica in flotation tests to produce acid grade material but a satisfactory separation from the bastnaesite was not obtained.

ECONOMIC CONSIDERATIONS

Although no economic resources were identified from the current data in the Red Cloud district, significant concentrations of REE, fluorite, and precious and base metals are present. Economic concentrations may occur in the hydrothermal breccia deposits or in a carbonatite body at depth; however, the depth to a carbonatite body may be economically prohibitive. Future development would probably involve the coproduction or byproduction of some of these commodities.

Rare-Earth-Elements

Present data indicate that the REE-bearing fluorite-barite-quartz fault breccia deposits exposed at the surface are too low grade and lack sufficient tonnage to support a commercial mining operation. The REO concentrations, as much as 2.3%, are lower in comparison to the bastnaesite-bearing carbonatite ore mined by open-pit method at Mountain Pass, Calif., where resources total 31

million st averaging 8.6% REO with a cutoff grade of 5% (Unocal Corp., 1988, p. 53).

The best targets for economic resources of REE are in the intrusive breccia pipes, where sufficient tonnages may be found. The hydrothermal mineralization in the intrusive breccia at the M and E No. 13 Prospect appears to hold the greatest potential for REE. The moderate REO concentrations, as much as 5.67% and an average of 2.45%, also include a significant amount of yttrium oxide, one of the higher value REE. Samples contained as much as 0.09% Y_2O_3, with an average 0.04%. Although there are no primary yttrium-producing deposits in the U.S., evaluation of the Pajarito yttrium-zirconium deposit, N. Mex. which contains a reported 2.4 million st averaging 0.18% Y_2O_3 is currently in progress (Scherer, 1990).

The high REO concentrations and carbonatization in the intrusive breccia pipes, especially the M and E. No. 13 Prospect, suggest that a carbonatite body is present at depth which may contain higher concentrations of REE.

Fluorite

Inferred resources of fluorite identified at the Eagles Nest, Conqueror No. 4 and Hilltop, and Old Hickory Prospects, while of sufficient grade (38% to 49% CaF_2), are of small tonnage (32,000 to 348,000 st), and are not of sufficient size to justify the cost of several million dollars for a mill.

As of 1992, the only major operator producing fluorite in the U.S. was the Ozark-Mahoning Company, from the Cave-in-Rock district in southern Illinois. Production has come from bedded replacement deposits containing more than 0.5 million st with an approximate cutoff grade of 30% CaF_2. The deposits have been mined by shafts sunk as deep as 1,000 ft, from which drifts have followed fluorite mineralization down dip to depths of 1,500 ft. Production of acid grade fluorite (not less than 97% CaF_2) from these mines from 1989 to 1991 was 70,000 st per year and accounts for almost all of the U.S. production. In addition to fluorite, the deposits contain a few percent lead and zinc, and some barite, which add significant components to the profitability of the operation.

Vein-type deposits in the district have been mined in the past to a depth of 600 ft. (Eric Livingston, Geologist, Ozark-Mahoning Company, Rosiclare, Illinois, oral commun., January 1992).

The fluorite deposits in the Red Cloud district have not been adequately delineated. Inferred resources identified by the Bureau are estimates from the limited exposures of the mineralized zones but additional work may identify sufficient tonnages to justify the cost of a mill. Future development will probably require production from a number of the fluorite deposits and probably the coproduction of REE's and barite.

Precious and Base Metals

Present data indicate that the precious- and base-metal-rich fluorite-barite-quartz breccia deposits exposed at the surface are too small or too low in grade to support a commercial mining operation. Although high concentrations of precious and base metals were identified in some of the fault breccia deposits (e. g. Buckhorn Mine containing an average of 0.022 oz/st gold, 3.1 oz/st silver, 10.8% lead, 3.9% copper, and 0.2% zinc), the deposits are small and lack sufficient tonnage to support a commercial mining operation.

The carbonatized intrusive breccias in the Red Cloud district appear to be the best exploration targets for economic gold deposits. Gold concentrations as high as 610 ppb and 165 ppb were present at the Sky High Prospect and at the intrusive breccia north of the All American Prospect, respectively. Six samples from part of the intrusive breccia at the Sky High Prospect contained 117-222 ppb gold, and were the most consistent group of gold concentrations in intrusive breccias.

Gold deposits are not usually associated with carbonatites. The only known carbonatite with gold production is the unique Phalaborwa copper-bearing-carbonatite deposit in South Africa, where the gold is recovered as a byproduct with silver and platinum from anode slimes (Eriksson, 1989, p. 222). However, fluorite-barite-quartz fault and intrusive breccia deposits and fenitized rocks in the Red Cloud district contain anomalous concentrations of gold. Anomalous gold concentrations are also present in carbonatites, breccias, and veins in the

upper hydrothermal level of the carbonatite systems exposed in the Laughlin Peak area, N. Mex. and the Bear Lodge Mountains, Wyo. Bureau of Mines samples from carbonatite dikes or small plugs in the Bear Lodge Mountains and the Laughlin Peak area contained gold concentrations as high as 344 ppb and 62 ppb, respectively. Samples from intrusive breccias and veins in the Bear Lodge Mountains and the Laughlin Peak area contained gold concentrations as high as 19,000 ppb (0.554 oz/st) and 75 ppb, respectively. In the Bear Lodge Mountains drilling by FMC corporation and International Curator Resources Limited identified a subeconomic gold resource of 2 million st containing 0.021 oz/st in a brecciated phonolitic trachyte dike (Joseph Kapler, consultant International Curator Resources Limited, Englewood, Colo., oral commun., May 1990). At the Rocky Boy's alkaline stock on the Rocky Boy's Indian Reservation, Bearpaw Mountains, Mont., where iron-, copper-, and lead-sulfide-rich carbonatite dikes have been identified, stream sediment and rock chip samples collected by the U.S. Geological Survey contained greater than 5,000 ppb (0.146 oz/st) gold (Armbrustmacher and others, 1992). Peter Modreski also reports anomalous gold (greater than 5 ppb) in some of the fenitized rocks (Peter Modreski, Geologist, U.S. Geological Survey, Denver, Colo., oral commun., March 1992). Although no rich bonanza-type deposits may be expected, because none have been found associated with carbonatites, large low-grade deposits such as the Zortman-Landusky Mine in the Little Rocky Mountains, Mont. (36 million st with an average grade of 0.019 oz/st (651 ppb) Au and 0.13 oz/st Ag (Wilson and Kyser, 1988, p. 1,332)), may be possible. Carbonatite systems such as the Bear Lodge Mountains have only recently been explored for gold and little analytical data has been published.

Anomalous concentrations of precious and base metals within the carbonatized intrusive breccia pipes, especially at the Sky High Prospect, suggest that a carbonatite body is present at depth which may contain significant concentrations of base metals. Iron-, copper-, lead-, and zinc-sulfides have been found in carbonatites. Some are richer in sulfides than others, but none

approaches the concentrations (315 million st containing 0.69% copper) found in the Phalaborwa carbonatite, Republic of South Africa (Deans, 1966, p. 393-394).

FUTURE EXPLORATION AND DEVELOPMENT

Gold exploration in the Gallinas Mountains is expected to continue over the next several years. Several companies currently have exploration programs for gold associated with alkaline rocks. Exploration, including geophysical and geochemical surveys, trenching, and drilling, is expected to continue at the current level.

REE exploration is not expected in the immediate future. Current production of REE's, especially the LREE's, is expected to meet the demand. China is producing large amounts of REE's and current REE prices are lower than in past years (James Hedrick, Mineral Commodity Specialist, Bureau of Mines, Washington, DC, oral commun., March 1992).

Product (oxide)	Percent/ purity	Price per pound
Cerium	99.00	$8.75
Dysprosium	96.00	60.00
Erbium	98.00	65.00
Europium	99.99	745.00
Gadolinium	99.99	65.00
Lanthanum	99.99	8.75
Neodymium	96.00	6.75
Do	99.90	40.00
Praseodymium	96.00	16.80
Samarium	96.00	65.00
Terbium	99.90	375.00
Yttrium	99.99	52.50

(Molycorp Inc. rare-earth oxide prices as of year-end 1990; purity expressed as percent of total rare-earth oxides.)

In the future, increased demand for REE's may lead to significant exploration in the Red Cloud district.

CONCLUSIONS

The presence of LREE-bearing fluorite-barite-quartz deposits and associated fenitization and carbonatization suggest that this is the upper hydrothermal

level of a carbonatite system. Although no economic resources were identified from the current data, significant concentrations of REE's, fluorite, gold, silver, lead, copper, and zinc are present at the surface. The intrusive breccia pipes have not been fully explored and appear to be the best targets for REE's, and precious and base metals. No carbonatites were identified on the surface, however, they are inferred to be present at depth. A carbonatite body may contain increased concentrations of REE's and base metals.

RECOMMENDATIONS

The known mineralized intrusive breccia pipes in the district have not been adequately explored. Trenching and additional sampling are required to determine the true size and shape of the pipes and to better define metal concentrations and their extent within the pipes. Drilling is required to test these pipes at depth. Carbonatites are inferred to be present at depth and drilling in the intrusive breccia pipes may penetrate carbonatite bodies that may be near the surface. Detailed magnetic and gravity surveys may help delineate a carbonatite body at depth. A late stage REE-rich carbonatite should be represented by a magnetic low and a gravity high.

The trachyte laccolith is generally poorly exposed and heavily forested, and additional breccia pipes are probably present. The mineralized and carbonatized intrusive breccia pipes are also poorly exposed in comparison to the noncarbonatized pipes. Additional exploration will probably identify other pipes and geochemical surveys may help find intrusive breccia pipes that are mineralized.

REFERENCES

Adams, J. W., 1965, Rare Earths; in Mineral and water resources of New Mexico: New Mexico Bureau of Mines and Mineral Resources, Bulletin 87, p. 234-237.

Armbrustmacher, T. J., King, H. D., and Modreski, P. J., 1992, Mineral resource investigation, Black Mountain-Miners Gulch area, Southern Rocky Boy Indian Reservation, Bearpaw Mountains, Montana: A preliminary report, in 1992 Indian Minerals Conference: U.S. Department of the Interior, Bureau of Indian Affairs, Division of Energy and Mineral Resources, p. 74-76.

Bates, R. L., and Jackson, J. A., eds., 1980, Glossary of geology (2nd ed.): Falls Church Virginia, American Geological Institute, 751 p.

Borodin, L. S., and Pavlenko, A. S., 1979, The role of metasomatic processes in the formation of alkaline rocks, in Sorensen, H., ed., The alkaline rocks: John Wiley and Sons, p. 515-534.

Clark, K. F., and Foster, C. T., and Damon, P. E., 1982, Cenozoic mineral deposits and subduction-related magmatic arcs in Mexico: Geological Society America Bulletin, v. 93, p. 533-544.

Currie, K. L., 1985, An unusual peralkaline granite near Lac Brisson, Quebec-Labrador: Geological Survey of Canada, Paper 85-1A, p. 73-80.

Deans, T., 1966, Economic mineralogy of African carbonatites, in Tuttle, O. F. and Gittins, J., eds., Carbonatites: New York, John Wiley and Sons, p. 385-413.

De La Roche, H., Leterrier, J., Grandeclaude, P., and Marchal, M., 1980, A classification of volcanic and plutonic rocks using R_1R_2-diagram and major element analyses-Its relationship with current normenclature: Chemical Geology, v. 29, p. 183-210.

DeMark, R. S., 1980, The Red Cloud Mines, Gallinas Mountains, New Mexico: Mineralogical Record, v. 11, p. 69-72.

Eckermann, H. V., 1966, Progress of research on the Alno carbonatite, in Tuttle, O. F. and Gittins, J., eds., Carbonatites: New York, John Wiley and Sons, p. 3-31.

Eriksson, S. C., 1989, Phalaborwa: a saga of magmatism, metasomatism and miscibility: in Bell, Keith, ed., Carbonatites genesis and evolution: Unwyn Hyman Ltd., p. 221-254.

Geake, J. E., Walker, G., Telfer, D. J., Mills, A. A., and Garlick, G. F. J., 1973, Luminescence of lunar terrestrial and synthesized plagioclase caused by MN^{2+} and FE^{3+} in Proceedings of the Fourth Lunar Science Conference, Supplement 4: Geochimica et Cosmochimica Acta, v. 3, p. 3181-3189.

Glass, J. J., and Smalley, R. G., 1945, Bastnaesite (Gallinas Mountains, New Mexico): American Mineralogist, v. 30, p. 601-615.

Gold, D. P., 1991, Carbonatites: An important source for space-age materials: Society For Mining, Metallurgy, and Exploration, Inc., Preprint Number 91-139, 9 p.

Griswold, G. B., 1959, Mineral deposits of Lincoln County, New Mexico: New Mexico Bureau of Mines and Mineral Resources, Bulletin 67, p. 64-71.

Haggerty, S. E., and Mariano, A. N., 1983, Strontian-loparite and strontio-chevkinite: Two new minerals in rheomorphic fenites from the Parana Basin carbonatites, South America: Contributions to Mineralogy and Petrology, Springer Verlag, v. 84, p. 365-381.

Harrer, C. M., and Kelly, F. J., 1963, Reconnaissance of iron resources in New Mexico: U. S. Bureau of Mines Information Circular 8190, p. 46-48.

Heinrich, E. W., 1966, The geology of carbonatites: Chicago, Rand McNally and Co., 555 p.

Hogarth, D. D., 1977, Classification and nomenclature of the pyrochlore group: American Mineralogist, v. 62, p. 403-410.

Kapustin, Y. L., 1980, Mineralogy of carbonatites: New Delhi, India, Amerind Publishing Company Pvt. Ltd., 259 p.

Kelley, V. C., 1949, Geology and economics of New Mexico iron ore deposits: University of New Mexico Publications in Geology, No. 2, p. 171-178.

Kelley, V. C., Rothrock, H. E., and Smalley, R. G., 1946, Geology and mineral deposits of the Gallinas District, Lincoln County, New Mexico: U. S. Geological Survey Strategic Minerals Investigation Preliminary Map 3-211, scale.

Kresten, P., and Morgan, V., 1986, Fenitization at the Fen Complex, Southern Norway: Lithos, v. 19, p. 27-42.

Leake, B. E., 1978, Nomenclature of amphiboles: Canadian Mineralogist, v. 16, p. 501-520.

Le Bas, M. J., 1987, Nephelinites and carbonatites, in Fitton, J. G., and Upton, B. G. J., eds., Alkaline Igneous Rocks: Geological Society Special Publication no. 30, p. 53-83.

Mason, B., Mumme, W. G., and Sarp, H., 1992, Capgaronnite, HgS.Ag(Cl,Br,I), a new sulfide-halide mineral from Var, France: American Mineralogist, v. 77, p.197-200.

Mariano, A. N., Ito, J., and Ring, P. J., 1973, Cathodoluminescence of plagioclase feldspars: Geological Society of America, Abstracts with Programs 5, p. 726.

Mariano, A. N., 1978, The application of cathodoluminescence for carbonatite exploration and characterization, in Braga, C. J., ed., Proceedings of the First International Symposium on Carbonatites, Pocos de Caldas, Minas Gerais, Brasil: Brasilia Departmento National da Producao Mineral, p. 39-57.

_____1988, Some further geological applications of cathodoluminescence, in Marshall, D. J., Cathodoluminescence of geological materials: Boston, Unwin Hyman, p. 94-123.

_____1989, Economic geology of rare-earth elements, in Lipin, B. R., and McKay, G. A., eds., Geochemistry and mineralogy of rare-earth elements: Mineralogical Society Of America, Reviews in Mineralogy, v. 21, p. 309-337.

Marshall, D. J., 1988, Cathodoluminescence of geological materials, Boston, Unwin Hyman, 146 p.

McAnulty, W. N., 1978, Fluorspar in New Mexico: New Mexico Bureau of Mines and Mineral Resources, Memoir 34, 64 p.

McCallum, M. E., 1985, Experimental evidence for fluidization processes in breccia pipe formation: Economic Geology, v. 80, no. 6, p. 1523-1543.

McKie, D., 1962, Goyazite and florencite from two African carbonatites: Mineralogical Magazine, v. 33, p. 281-297.

_____1966, Fenitization, in Tuttle, O. F. and Gittins, J., eds, Carbonatites: New York, John Wiley and Sons, P. 261-294.

McLemore, V. T., North, R. M., and Leppert, S., 1988a, REE, Niobium, and thorium districts and occurrences in New Mexico: New Mexico Bureau of Mines and Mineral Resources, Open File Report 324, 27 p.

_____1988b, Rare-earth elements in New Mexico: New Mexico Geology, v. 10, no. 2, p. 33-38.

McLemore, V. T., 1991, Gallinas Mountain mining district, New Mexico in New Mexico Geological Society Guidebook: 42nd Field Conference, Sierra Blanca, Sacramento, Capitan Ranges, p. 63-64.

Modreski, P. J., 1979, Abstract-Rare earth elements in agardite and in other minerals from the Red Cloud district, New Mexico: New Mexico Minerals Symposium, University of New Mexico, Albuquerque, New Mexico.

_____1983, Abstract-Agardite-(La), A chemically complex rare-earth arsenate from the Gallinas district, Lincoln County, New Mexico, in Oxidation mineralogy of base metal deposits: Fifth Joint Mineralogical Society of America-Friends of Mineralogy Symposium, Tucson, Arizona.

North, R. M., and McLemore, V. T., 1988, A classification of precious metal deposits of New Mexico, in Schafer, R. W., Cooper, J. J., and Vikre, P. G., eds. Bulk mineable precious metal deposits of the western United States: Geological Society of Nevada, Reno, p. 625-659.

Perhac, R. M., 1960, Geology and mineral deposits of the Gallinas Mountains, New Mexico: University of Michigan, unpublished Ph. D. dissertation, 224 p.

_____1970, Geology and mineral deposits of the Gallinas Mountains, Lincoln and Torrance Counties, New Mexico: New Mexico Bureau of Mines and Mineral Resources Bulletin 95, 51 p.

Perhac, R. M., and Heinrich, E. W., 1964, Fluorite-bastnaesite deposits of the Gallinas Mountains, New Mexico, and bastnaesite paragenesis: Economic Geology, v. 59, p. 226-239.

Ramdohr, P., 1980, The ore minerals and their intergrowths, v. 2 (2nd ed.): Elmsford, New York, Pergamon Press Inc., International series in earth sciences , v. 35, 1,207 p.

Roeder, P. L., MacArthur, D., Ma, X. P., Palmer, G. R., and Mariano, A. N., 1987, Cathodoluminescence and microprobe study of rare-earth elements in apatite: American Mineralogist, v. 72, p. 801-811.

Rothrock, H. E., Johnson, C. H., and Hahn, A. D., 1946, Fluorspar resources of New Mexico: New Mexico Bureau of Mines and Mineral Resources Bulletin 21, p. 108-122.

Sarp, H., Birch, W. D., Hlava, P. F., Pring, A., Sewell, D. K. B., and Nickel, E. H., 1987, Perroudite, a new sulfide-halide of Hg and Ag from Cap-Garronne, Var, France, and from Broken Hill, New South Wales, and Coppin Pool, Western Australia: American Mineralogist, v. 72, p. 1251-1256.

Scherer, R. L., 1990, Pajarito yttrium-zirconium deposit, Otero County, New Mexico: New Mexico Geology v. 12, no. 2.

Soule, J. H., 1943, Gallinas fluorspar deposits, Lincoln County, New Mexico: U. S. Bureau of Mines War Minerals Report 125, 14 p.

_____1946, Exploration of the Gallinas Fluorspar deposits, Lincoln County, New Mexico: U.S. Bureau of Mines Report of Investigations 3854, 25 p.

Sukheswala, R. N., and Viladkar, S. G., 1981, Fenitized sandstones in Amba Dongar Carbonatites, Gujarat, India: Journal Geological Society of India, v. 22, p. 368-374.

Unocal Corporation, 1988, Annual Report: P.O. Box 7600, Los Angeles, CA, 90051, 58 p.

Wambeke, L. V., 1978, Kalipyrochlore, a new mineral of the pyrochlore group: American Mineralogist, v. 63, p. 528-530.

Williams, F. E., 1963, Fluorspar deposits of New Mexico: Bureau of Mines Information Circular 8307, 143 p.

Wilson, M. R., and Kaiser, T. K., 1988, Geochemistry of porphyry hosted Au-Ag deposits in the Little Rocky Mountains, Montana: Economic Geology, v. 83, no. 7, p. 1329-1346.

Wooley, A. R., 1982, A discussion of carbonatite evolution and nomenclature, and the generation of sodic and potassic fenites: Mineralogical Magazine, v. 46, p. 13-17.

Woodward, L. A., and Fulp, M. S., 1991, Gold mineralization associated with alkali trachyte breccia in the Gallinas mining district, Lincoln County, New Mexico in New Mexico Geological Society Guidebook: 42nd Field Conference, Sierra Blanca, Sacramento, Capitan Ranges, p. 323-325.

Table 3.-- Summary of miscellaneous mines, prospects, and mineralized areas in the Red Cloud mining district, Gallinas Mountains, Lincoln County, N. Mex.

Property name	Summary	Sample Data
Unprospected area (pl. 1, sample sites 22 and 23)	An unprospected area containing a 15 ft wide fenitized trachyte dike (sample site 22) and a mass of fenitized syenite (sample site 23) exposed for a distance of approximately 450 ft. Fluorite and sericite are visible in the vugs and scintillometer readings were as high as 110 cps. The fenitized rocks may lie along a NE trending fault as mapped by Kelley (1946) that extends to the Sky High Prospect but no fault zone was evident in outcrop. A polished thin section from sample site 22 consisted of a vuggy mass of subhedral to euhedral tabular feldspar crystals averaging 0.4 mm with remnants of scattered phenocrysts. The feldspars are turbid and contain clear rims of fenite potassium feldspar and fenite albite. Purple fluorite occurs in the vugs with abundant plates of sericite. One bastnaesite crystal 0.15 mm in diameter was found in a vug. Observation under CL shows incipient fenitization, brilliant red to pink to orange-luminescing fenite albite and tan-luminescing fenite potassium feldspar as veinlets, patches, and rims. A few scattered zircon crystals luminesced yellow. A polished thin section from sample site 23 consisted of a vuggy mass of subhedral tabular crystals ranging from 0.9 to 4 mm long, averaging 2 mm. The original feldspars appear to have been mainly potassium feldspar with subordinate plagioclase that are largely altered to sericite. The original feldspars are turbid and replaced by veinlets, patches, and rims of fenite albite and fenite potassium feldspar. The fenite albite is twinned. A few crystals of biotite are mostly altered to hematite-limonite. A few scattered hematite-limonite pseudomorphs after pyrite averaging 0.2 mm in diameter and zircon crystals were present. Apatite commonly occurs as prismatic crystals associated with the biotite as long as 0.2 mm. Sericite occurs in the vugs in hexagonal plates averaging 0.2 mm in diameter. Rhombic crystals ranging from 0.4 to 1.8 mm in length that have been totally altered to an extremely fine-grained (less than 20 microns in diameter) mass of various minerals. Potassium feldspar, apatite, monazite, a titanium oxide, a titanium-iron oxide, a calcium-titanium-REE-bearing carbonate, a titanium-REE-bearing phosphate, and a calcium-REE-fluorocarbonate were detected by SEM-EDX analysis. Observation under CL showed incipient fenitization, brilliant red-luminescing fenite albite and tan-luminescing fenite potassium feldspar as veinlets, patches, and rims. The fenite feldspars replace blue-luminescing feldspar and a few yellowish green-luminescing plagioclase crystals. Anhedral to euhedral crystals of lavender to rose-luminescing apatite. Sericite luminesced a dark red or reddish black. Fluorite luminesced a pale purple to violet. The zircon crystals luminesced yellow. A few scattered patches of orange-luminescing calcite were present. Sample 23 contained 8.46% potassium oxide and 4.60% sodium oxide.	Sample 22 and 23 contained low REO concentrations of 0.02% and 0.07%, respectively. The samples also contained as much as 71 ppb gold, 1,435 ppm fluorine, and 118 ppm niobium.

Table 3.-- Summary of miscellaneous mines, prospects, and mineralized areas in the Red Cloud mining district, Gallinas Mountains, Lincoln County, N. Mex.--continued

All American Prospect (pl. 1, sample sites 48-52)	All American Prospect consists of an inaccessible shaft at least 57 ft deep, a 11-ft-deep shaft, and several pits and trenches that are mostly caved. The main shaft is reported to be 85 ft deep with 175 ft of drifting at the bottom of the shaft (Griswold, 1959, p. 69). The prospect lies between the intersection of the major fault in Red Cloud Canyon, striking N. 30° W. on the east and a northern fault with Precambrian gneiss striking approximately east-west, and a southern fault striking approximately N. 80° W. was mapped by Kelley and others (1946) and Perhac (1960, p. 201). Only a few small bedrock exposures and dump fragments from the workings containing brecciated sandstone and trachyte with fluorite, barite, and some calcite filling in open spaces. Griswold (1959, p. 68) reported that highly fractured and brecciated limestone and sandstone with erratically distributed fluorite, barite, calcite and minor amounts of copper oxides in the matrix occur in the drifts at the bottom of the 85-ft-deep shaft.	Samples 48-52 contained 0.03% to 0.33% REO. Only trace amounts of precious and base metals were present.
Pride No. 2 Prospect (fig. 25, sample sites 89 and 90)	Pride No. 2 Prospect consists of timbered and partially caved 15-ft-deep shaft, 2 pits, and a 220-ft-long trench. The workings expose a small breccia and fracture zone in trachyte for a distance of 80 ft and approximately 4 ft in width, striking N. 10° E. and dipping vertically. Fluorite with galena, malachite, and chrysocolla occur in the matrix of the breccia and in fractures.	A select grab sample (90) of breccia fragments from the shaft dump and a chip sample (89) from the pit contained 2.14% and 0.66% REO, respectively. Sample 90 also contained 6.2% lead and 0.5% copper. Gold and silver concentrations were as much as 71 ppb and 2.9 ppm, respectively.
17 No. 2 Prospect (pl. 1, sample sites 97 and 98)	The 17 No. 2 prospect consists of a 30-ft-long adit in an fenitized and carbonatized intrusive breccia. The intrusive breccia appears to be a small pipe at least 50 ft in diameter. It consists of angular to rounded clasts of sandstone, siltstone, granite, trachyte and limestone in an aphanitic matrix. A polished thin section from sample site 98 showed anhedral to euhedral quartz crystals as long as 0.1 mm, commonly containing needle-shaped inclusions that line the walls of some cavities. Anhedral and subhedral calcite crystals averaging 0.12 mm in diameter fills some cavities occupying the central part indicating that it was deposited after the quartz and also replaces some sandstone fragments. Examination by CL showed incipient fenitization, brilliant red-luminescing fenite feldspar veinlets cutting both the matrix and rock clasts. Apatites in nonfenitized areas were commonly yellow-luminescing. Blue-, lavender-, and orange-yellow luminescing apatites were present in areas of brilliant red-luminescing feldspar. Zircon luminesces a bright yellow. Calcite in cavities is nonluminescing while limestone clasts contain orange-luminescing calcite.	Two chip samples (97 and 98) of the intrusive breccia contained 0.05% and 0.06% REO. Low concentrations of gold, 17 and 23 ppb, and trace amounts of base metals were present.
Park Prospect (fig. 26 , sample sites 99-103)	The Park Prospect consists of a 19-ft-deep shaft and 4 pits. The shaft and three of the pits are in fractured and brecciated sandstone containing calcite and minor fluorite. No trend was apparent. One pit (sample site 100) is in an intrusive breccia.	Sample 102 contained 1.76% REO, but samples 99-101 and 103 contained only 0.03% to 0.21% REO. Gold and silver concentrations were as much as 16 ppb and 0.2 ppm, respectively.

Table 3.-- Summary of miscellaneous mines, prospects, and mineralized areas in the Red Cloud mining district, Gallinas Mountains, Lincoln County, N. Mex.--continued

Helen S Prospect (pl. 1, sample sites 105-107)	The Helen S Prospect consists of a 120 ft by 100 ft bulldozed area and 2 pits. The workings were cut on small irregular breccia and fracture zones as wide as 2 ft in trachyte and at brecciated trachyte-sandstone contact. No trend was apparent. Fluorite occurs in the matrix of the breccia.	Samples 105-107 contained 0.04% to 0.98% REO. Gold concentrations were 116 ppb or less.
Congress Prospect (fig. 27, sample sites 154-156)	The Congress Prospect consists of a shaft caved at 11 ft, a 16-ft-deep shaft, and 5 pits that cut two approximately 3-ft-wide brecciated zones along dolomitic limestone-sandstone contacts and one 4.5-ft-wide zone of brecciated sandstone. Calcite and fluorite occur in the matrix of the breccias.	Samples 154-156 contained 0.10% to 3.92% REO. Gold concentrations were 45 ppb or less.
Bottleneck Prospect (fig. 28, sample sites 157-160)	The Bottleneck Prospect consists of a 37-ft-deep shaft, a caved adit, and two pits. The caved adit was reported to be 55 ft long (Soule, 1946, p. 17). The workings are along a irregular brecciated zone in sandstone and limestone. Soule (1946, p. 17) mapped an irregular breccia zone 110 ft long that is 5 ft wide at the ends and swells to 43 ft wide in the middle, trending north-south. Calcite, fluorite, barite, hematite-limonite pseudomorphs after pyrite, manganese oxide and minor sphalerite occur in the matrix of the breccia.	Samples 157-160 contained 1.55% to 2.57% REO. Samples contained as much as 289 ppb gold.
Eureka Prospect (fig. 29, sample sites 172-177)	The Eureka Prospect consists of a caved adit, an 18-ft-deep shaft, two 16-ft-deep shafts, an inclined 16-ft-deep shaft, 5 pits and a trench. The adit appears to connect with the shafts and was 240 ft long (Perhac, 1960, p. 191) The workings cut irregular zones of brecciated sandstone as wide as 10 ft. Fluorite and some quartz occur in the matrix of the breccias.	Samples 172-177 contained 0.07% to 1.06% REO. Sample 172 contained 596 ppb gold but all others contained 99 ppb or less. Samples 172-177 contained 1.3 to 36.2 ppm silver, 365 to 18,267 ppm (1.8%) copper, and 301 to 21,400 ppm (2.1%) lead.
Hoosier Boy Prospect (fig. 30, sample sites 178-182)	The Hoosier Boy Prospect consists of a 17-ft-long adit, and 10 pits or short trenches. The workings expose brecciated zones in sandstone and one in limestone as wide as 8 ft. Fluorite, barite, calcite, and pyrite occur in the matrix of the breccias.	Samples 178-182 contained 0.12% to 5.19% REO. Sample 178 contained 1.4% lead. Samples contained as much as 150 ppb gold and 0.9 ppm silver.
Hoosier Girl South Prospect (fig. 31, sample sites 183-186)	The Hoosier Girl South Prospect consist of a 15-ft-deep inclined shaft, a 70-ft-long bulldozer trench, and 5 pits. The shaft and an adjoining pit cut a zone of brecciated sandstone at least 5 ft wide. Fluorite and barite occur in the matrix of the breccias.	Samples 183-186 contained 0.18% to 2.16% REO. Samples 183 and 184 from the shaft and adjoining pit contained as much as 1.4% lead and 0.7% copper. Gold concentrations ranged from 107 to 920 ppb. Silver concentrations were 9.4 ppm or less.
Hilltop Prospect (fig. 32, sample sites 187 and 188)	The Hilltop Prospect consists of 18-ft-deep shaft, and 5 pits. Two pits expose brecciated sandstone and the shaft exposes a brecciated dolomitic limestone-sandstone contact. Fluorite, calcite, barite, and pyrite occur in the matrix of the breccias.	Samples 187 and 188 of brecciated sandstone in the pits contained 1.43% and 3.38% REO, respectively. Gold concentrations were 57 ppb or less.

Table 3.-- Summary of miscellaneous mines, prospects, and mineralized areas in the Red Cloud mining district, Gallinas Mountains, Lincoln County, N. Mex.--continued

Conqueror Apex Prospect (fig. 33, sample sites 205-207)	The Conqueror Apex Prospect consists of a 14-ft-deep shaft, 4 trenches, and 2 pits. The workings are on irregular brecciated zones in sandstone, conglomeratic sandstone, and trachyte dike.	Samples 205-207 contained 0.10% to 5.15% REO. Gold concentrations were 48 ppb or less.
Summit Prospect (fig. 34, sample sites 208-211)	The Summit Prospect consists of a 22-ft-deep shaft and 6 pits. The workings are cut on 1.5 to 2.6 ft wide breccia zones in sandstone or along dolomitic limestone-sandstone contacts. Most trend approximately northeast. Fluorite, barite, calcite, pyrite, and minor malachite occur in the matrix of the breccias.	Samples 208-211 contained 0.47% to 1.78% REO. Gold and silver concentrations were as much as 107 ppb and 6.0 ppm, respectively.
White Oaks Prospect (fig. 35, sample sites 213-220)	The White Oaks Prospect consists of a 38-ft-long adit, a 25-ft-deep shaft, 10 pits and a 30-ft-long trench. The workings expose brecciated zones in sandstone and along limestone-sandstone contacts as wide as 7.5 ft, trending approximately north-south. Fluorite, barite, and calcite occur in the matrix of the breccias.	Samples 213-220 contained 0.02% to 1.14% REO. Concentrations of as much as 81.6 ppm silver, 3.7% copper, and 1.7% lead were present in some samples. Gold concentrations were 73 ppb or less.
Little Jack Prospect (fig. 36, sample sites 243-245)	The Little Jack Prospect consists of a 13-ft-deep shaft, 7 pits and 2 trenches. The workings expose a breccia zone 110 ft long and approximately 2 ft in width containing fluorite and quartz.	Three samples (243-245) contained only 0.02% to 0.06% REO. Gold concentrations were 36 ppb or less.
Conqueror No. 10 Mine (fig. 37, sample sites 247-251)	The Conqueror No. 10 Mine consists of 30-ft-long adit and an approximately 50 ft by 50 ft pit where bastnaesite-fluorite ore was mined. The adit is driven in a breccia zone 45 ft wide and 65 ft long that appears to trend about N. 15° W. in sandstone and conglomeratic sandstone. The pit appears to have been cut on a breccia zone due to the intersection of few faults in sandstone, dolomitic limestone, and a trachyte dike.	Samples 247-251 contained concentrations of 0.31% to 3.04% REO. Gold concentrations were 80 ppb or less.

Table 3.-- Summary of miscellaneous mines, prospects, and mineralized areas in the Red Cloud mining district, Gallinas Mountains, Lincoln County, N. Mex.--continued

Rio Tinto Mine (fig. 38, sample sites 245-257)	The Rio Tinto Mine consists of a main shaft at least 100 ft deep, a shaft caved at 16 ft deep, and 8 trenches. The workings cut breccia and fracture zones in sandstone, limestone, and a trachyte dike. The shafts are inaccessible and the bedrock is exposed only in a few trenches. Perhac (1960, p. 195) and Griswold (1959, p. 67) contain maps of the 130-ft level of the 230-ft-deep main shaft. The maps are different but Griswold's appears to be more accurate and shows approximately 200 ft of drifting. The 16-ft-deep caved shaft was reported to be 30 ft deep (Perhac, 1960, p. 195) and a raise at this spot on the 130-ft level was reported by Griswold (1959, p. 67). Fluorite, barite, galena, chalcocite, malachite, chrysocolla, azurite, and hematite-limonite are found in the matrix of breccia fragments on the dumps. A fenitized radioactive trachyte dike is exposed in the western most trench. A polished thin section of the trachyte from sample site 253 examined by SEM-EDX consists of scattered subhedral 1-2 mm long mainly albite phenocrysts in a trachytic groundmass, containing albite and subordinate potassium feldspar crystals averaging 0.25 mm in length. The dike is cut by a stockwork of potassium feldspar, barite, hematite-limonite veinlets as wide as 1/8 in. Sericitic alteration of feldspar is present along the veinlets. Examination under CL showed faint reddish tan-luminescencing potassium feldspar veinlets. One very small vug contains a brilliant red-luminescing rim, that is probably fenite albite. The dominantly albite groundmass luminesces a dull yellowish green to gray.	Assay data obtained by Perhac from the New Mexico Copper Corporation from twenty-seven samples on the 130 ft level averaged 0.8 oz/st silver, 2.8% lead, 1.0% copper, and 42% fluorite (Perhac, 1960, p. 197). In addition, a few samples contained molybdenum (as much as 0.68%) and uranium (as much as 0.11% U_3O_8). The mineralization is mainly precious- and base-metal-rich with only low amounts of REO's. Bureau's samples 254-257 contained as much as 170 ppb gold, 21 ppm silver, 2.3% copper, and 1.3% lead. REO concentrations ranged from 0.02% to 0.17%. Samples 252 and 253 from the trachyte dike contained as much as 0.06% REO, 183 ppm niobium, 98 ppm thorium, and 17 ppb gold.

EXPLANATION OF SYMBOLS FOR FIGURES 17-19, 21, 23-38

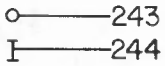

SAMPLE LOCALITY -- Showing sample number

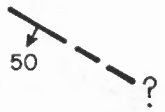

FAULT -- Showing strike and dip; dashed where approximate; queried where uncertain

VEIN OR NARROW BRECCIA ZONE -- Showing strike and dip; dashed where approximate

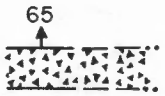

BRECCIA ZONE -- Showing strike and dip; dashed where approximate; dotted where projected

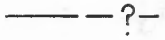

CONTACT -- Dashed where approximate; queried where uncertain

STOCKPILE

DUMP

INTERMITTENT STREAM

U.S. BUREAU OF MINES DRILL HOLE -- Showing direction

DRILL HOLE

EXPLANATION OF SYMBOLS FOR FIGURES 17-19, 21, 23-38 -- Continued

Ba - Barite

Ca - Calcite

F - Fluorite

Qtz - Quartz

SURFACE OPENINGS

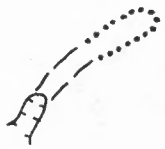

PORTAL OF ADIT WITH OPENCUT -- Underground workings dashed on figures that show both surface and subsurface workings; dotted where projected

OPENCUT

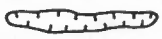

TRENCH

PIT

SHAFT

INCLINED SHAFT -- Showing degree of inclination of underground workings; chevrons pointing down

BOTTOM OF SHAFT, RAISE, OR WINZE

WINZE

EXPLANATION OF SYMBOLS FOR FIGURES 17-19, 21, 23-38 -- Continued

LITHOLOGY

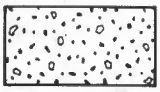

INTRUSIVE BRECCIA

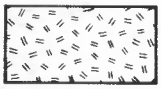

TRACHYTE

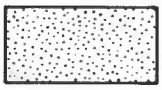

SANDSTONE

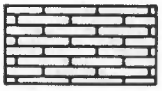

LIMESTONE / DOLOMITIC LIMESTONE / CALCAREOUS SHALE

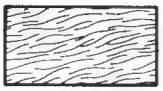

GNEISS

Sample		Analytical Data									
No.	Length (ft)	REO (%)	Y_2O_3 (PPM)	Au (PPB)	Ag (PPM)	Cu (PPM)	Pb (PPM)	Zn (PPM)	K_2O (%)	Na_2O (%)	CaO (%)
1	6.0	0.63	56	174	0.2	1266	559	309	na	na	na
2	9.5	0.39	138	139	0.5	301	141	398	3.51	0.28	29.09
3	5.0	0.33	75	222	1.0	223	318	1330	12.01	0.70	4.70
4	7.5	0.50	68	175	3.5	3121	367	232	na	na	na
5	5.0	0.38	86	117	2.5	559	278	698	na	na	na
6	3.0	0.52	74	170	3.7	7220	337	411	na	na	na
7	5.0	0.36	144	37	<0.2	14	68	279	na	na	na
8	5.0	0.23	79	31	<0.2	17	22	57	7.86	3.19	7.24
9	2.0	0.52	94	54	<0.2	11	47	323	10.51	1.10	8.59
10	3.0	0.64	94	30	<0.2	81	584	89	na	na	na
11	3.0	0.08	36	35	0.6	62	350	100	na	na	na
12	1.0	0.64	<203	496	27.3	4250	29700	182	na	na	na
13	5.0	0.78	84	135	<0.2	415	1869	911	na	na	na
14	10.0	0.78	170	28	<0.2	158	205	529	na	na	na
15	4.0	0.65	135	19	<0.2	263	181	297	na	na	na
16	2.0	0.24	117	32	0.2	19	81	103	na	na	na
17	1.0	0.21	77	63	0.9	108	799	547	na	na	na
18	2.0	0.64	100	33	<0.2	32	321	239	0.75	0.05	4.49
19	2.0	0.95	160	80	<0.2	63	519	201	na	na	na
20	Grab select	1.04	<254	610	11.2	5823	33400	933	na	na	na

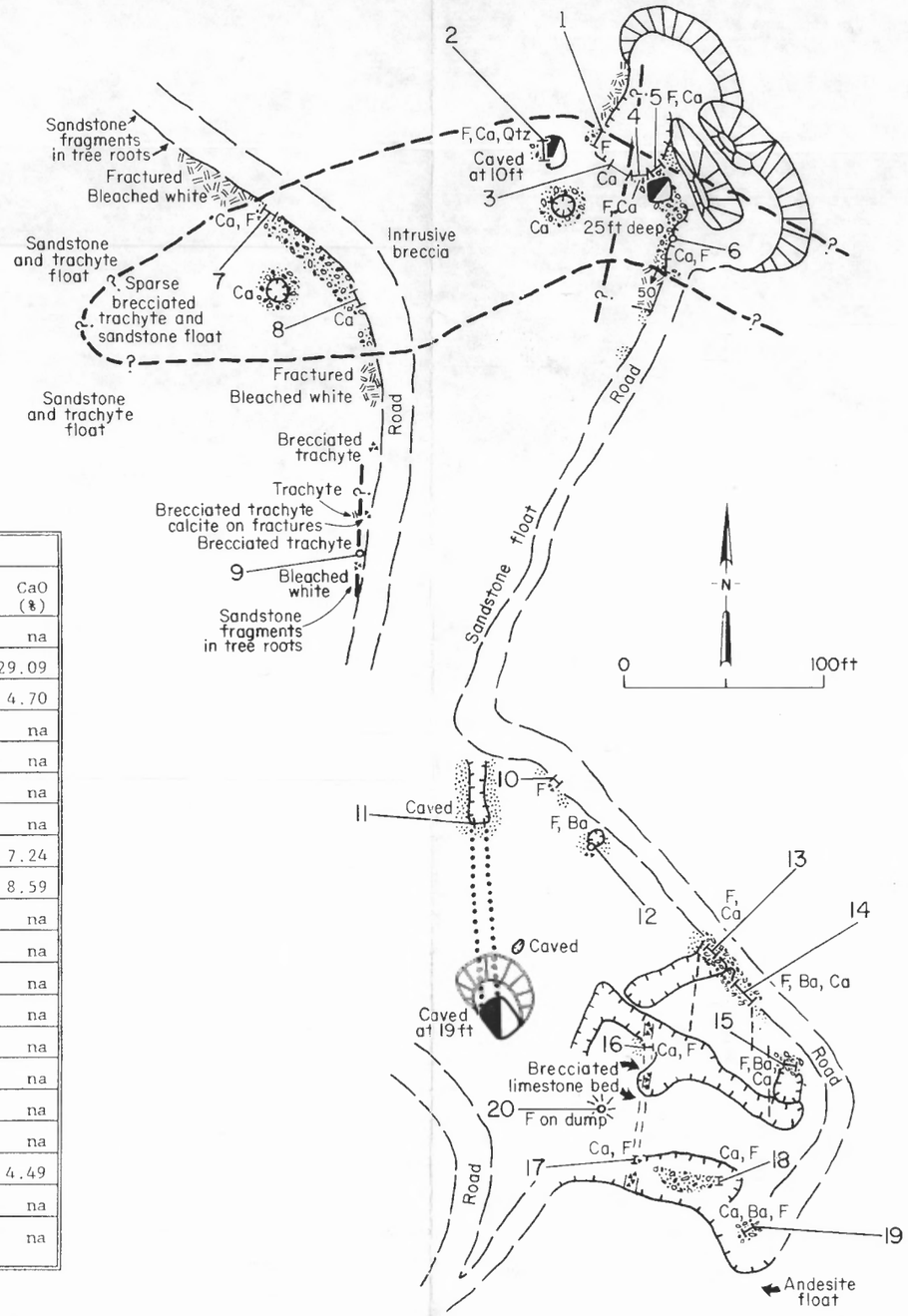

Figure 17. Map of the Sky High Prospect, showing sample sites 1-20 and analytical data.

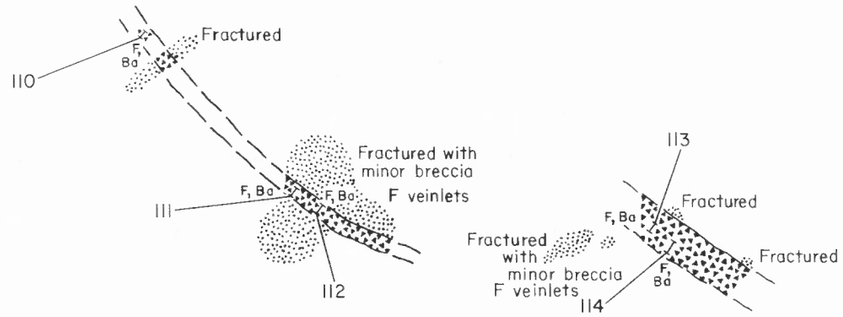

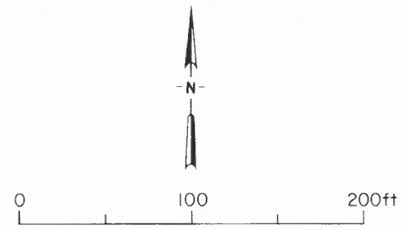

Sample		Analytical Data							
No.	Length (ft)	REO (%)	Y_2O_3 (PPM)	CaF_2 (%)	Au (PPB)	Ag (PPM)	Cu (PPM)	Pb (PPM)	Zn (PPM)
110	7.0	0.02	72	49.32	30	0.5	8	18	52
111	6.0	0.35	100	12.84	<5	<0.2	109	42	26
112	6.5	0.84	164	27.74	6	<0.2	26	59	54
113	6.5	0.68	81	28.84	7	<0.2	16	32	109
114	9.0	0.39	95	29.80	<5	<0.2	12	21	99
115	2.5	2.21	105	50.35	12	<0.2	65	80	51
116	5.5	2.35	113	41.61	29	<0.2	87	113	117
117	4.5	0.50	84	22.09	51	<0.2	32	76	93
118	5.0	2.65	142	54.15	45	<0.2	196	236	175
119	4.0	0.66	57	16.23	28	<0.2	126	53	166
120	3.5	1.43	101	37.98	49	<0.2	9	47	125
121	4.0	2.32	137	62.99	94	<0.2	166	168	182
122	4.0	1.51	118	60.62	22	<0.2	31	95	90
123	5.0	0.95	68	34.63	404	0.2	758	84	858
124	4.0	2.28	95	45.00	66	<0.2	39	228	268
125	3.0	0.55	133	34.63	78	<0.2	17	35	96
126	3.0	0.20	108	17.57	98	0.5	16	27	182
128	3.5	1.40	94	32.47	755	<0.2	299	66	130
130	4.0	1.68	122	45.00	75	<0.2	22	62	75
131	5.0	0.54	114	33.70	28	<0.2	5	50	183
132	6.0	1.49	142	65.25	<5	<0.2	108	154	110
133	4.0	3.02	112	37.98	10	<0.2	19	58	2
134	7.0	1.30	107	52.20	21	<0.2	138	74	90

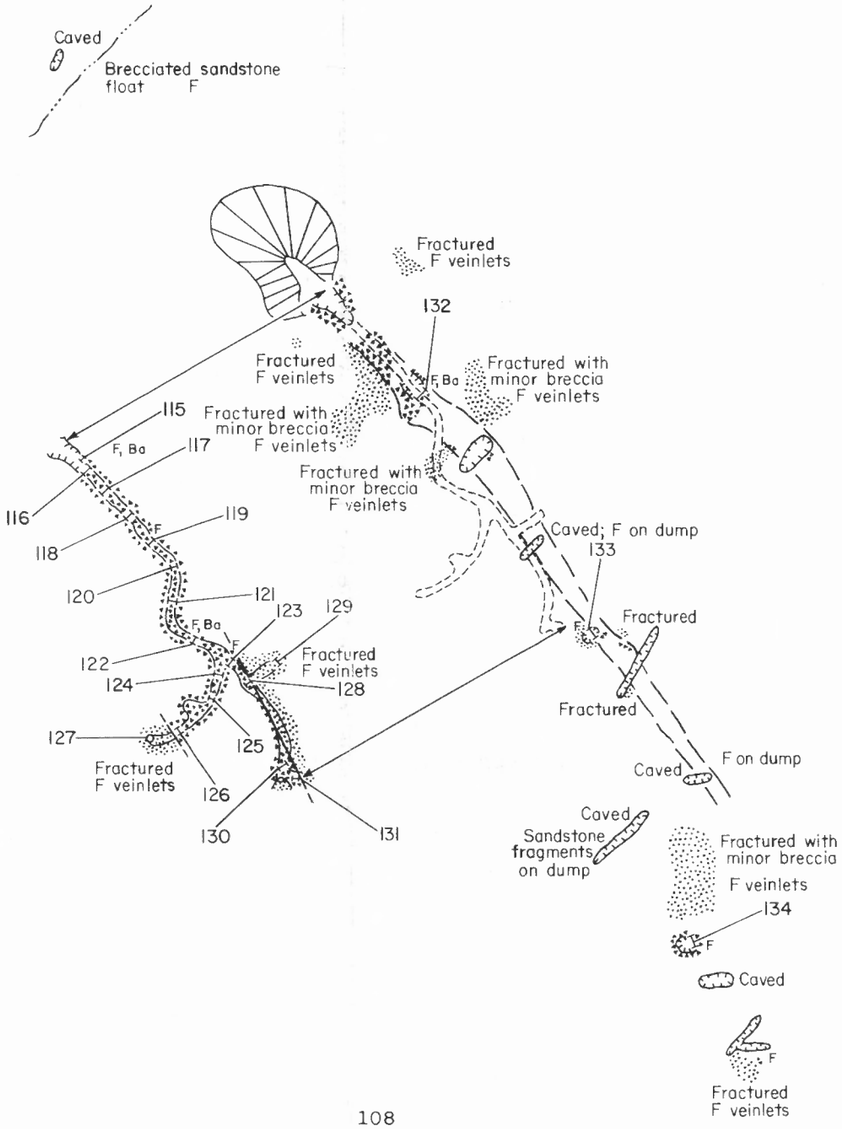

Figure 18. Map of Eagles Nest Prospect, showing sample sites 110-134 and analytical data.

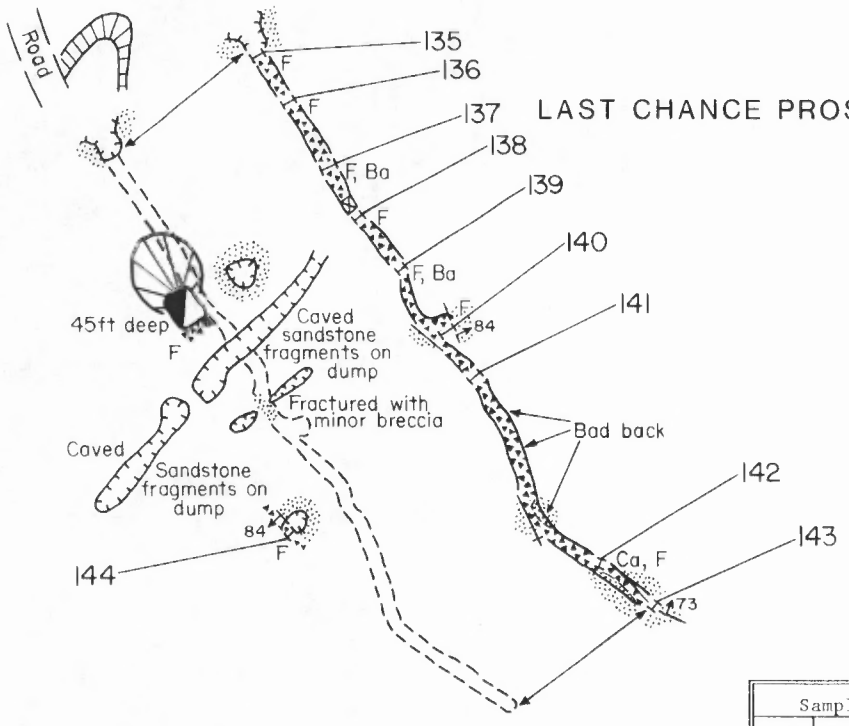

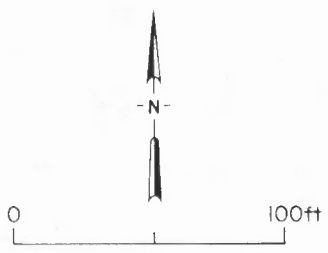

Sample		Analytical Data							
No.	Length (ft)	REO (%)	Y_2O_3 (PPM)	CaF_2 (%)	Au (PPB)	Ag (PPM)	Cu (PPM)	Pb (PPM)	Zn (PPM)
135	3.8	1.88	495	32.88	72	<0.2	270	127	360
136	3.0	0.50	423	17.59	85	<0.2	405	71	369
137	3.0	1.27	384	42.74	131	0.7	1482	129	668
138	3.0	0.59	420	30.25	157	1.1	435	112	579
139	3.0	0.78	443	51.95	378	<0.2	1240	157	355
140	5.0	0.24	291	36.82	367	1.2	824	112	247
141	3.0	0.13	217	24.99	329	1.0	423	129	192
142	3.0	0.76	452	7.32	96	<0.2	64	405	410
143	1.0	1.67	528	2.77	118	<0.2	186	1711	423
144	1.7	0.09	<203	5.34	130	1.4	727	2151	180
145	4.0	0.80	<762	na	615	22.2	10409	24500	1578
146	1.0	0.15	<292	na	307	52.1	24400	228700	4342
147	1.7	0.06	<228	na	264	364.3	89200	370900	3424
148	0.6	0.28	76	na	770	14.3	10627	1578	433
149	Grab select	0.38	<279	na	1707	68.6	45300	29300	2750
150	Grab select	0.21	<228	na	531	197.1	88000	98500	3541
151	5.0	0.04	<343	na	1137	39.7	6648	4094	670

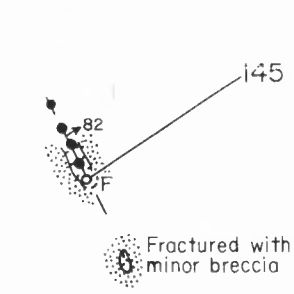

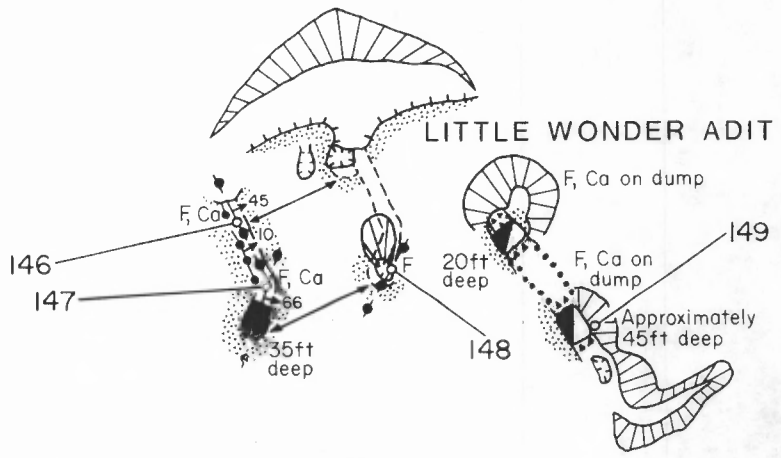

BUCKHORN MINE

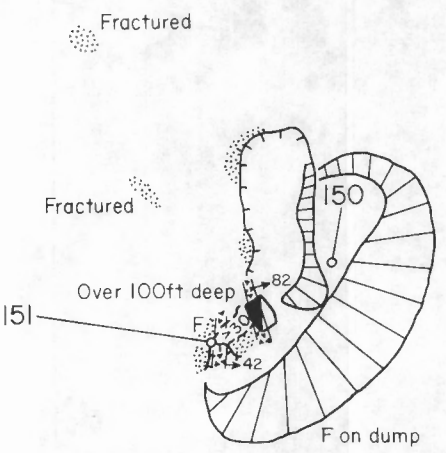

Figure 19. Map of Buckhorn Mine and Last Chance Prospect, showing sample sites 135-151 and analytical data.

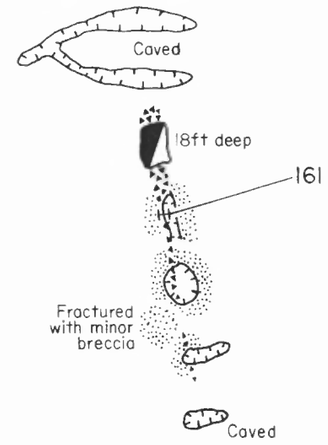

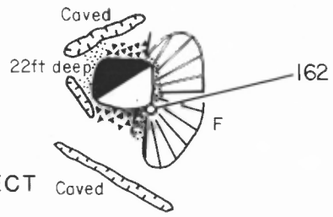

HOOSIER GIRL NORTH PROSPECT

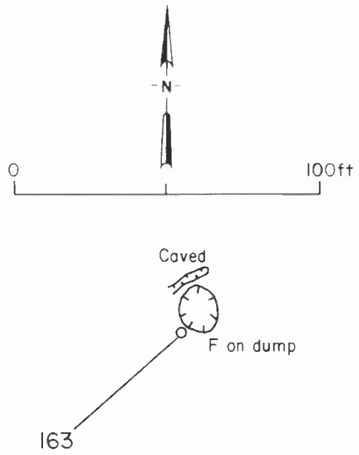

Sample		Analytical Data							
No.	Length (ft)	REO (%)	Y_2O_3 (PPM)	CaF_2 (%)	Au (PPB)	Ag (PPM)	Cu (PPM)	Pb (PPM)	Zn (PPM)
161	3.0	2.26	488	na	74	<0.2	216	409	328
162	Grab select	0.65	507	na	29	<0.2	575	294	234
163	Grab select	0.43	269	na	74	<0.2	448	1680	400
164	5.0	0.54	152	26.96	163	<0.2	127	348	74
165	7.0	2.36	<89	46.36	293	3.2	3818	8284	453
166	3.0	1.60	<114	36.82	594	13.8	8774	4288	986
167	5.0	1.96	121	60.83	246	4.6	4240	3260	2670
168	5.0	3.21	<89	54.25	600	<0.2	2577	5429	3337
169	5.0	3.33	<127	54.25	526	6.9	5174	8144	9726
170	3.0	3.17	<76	65.43	307	2.5	2800	4219	1935
171	4.0	0.17	178	na	208	0.5	219	115	161

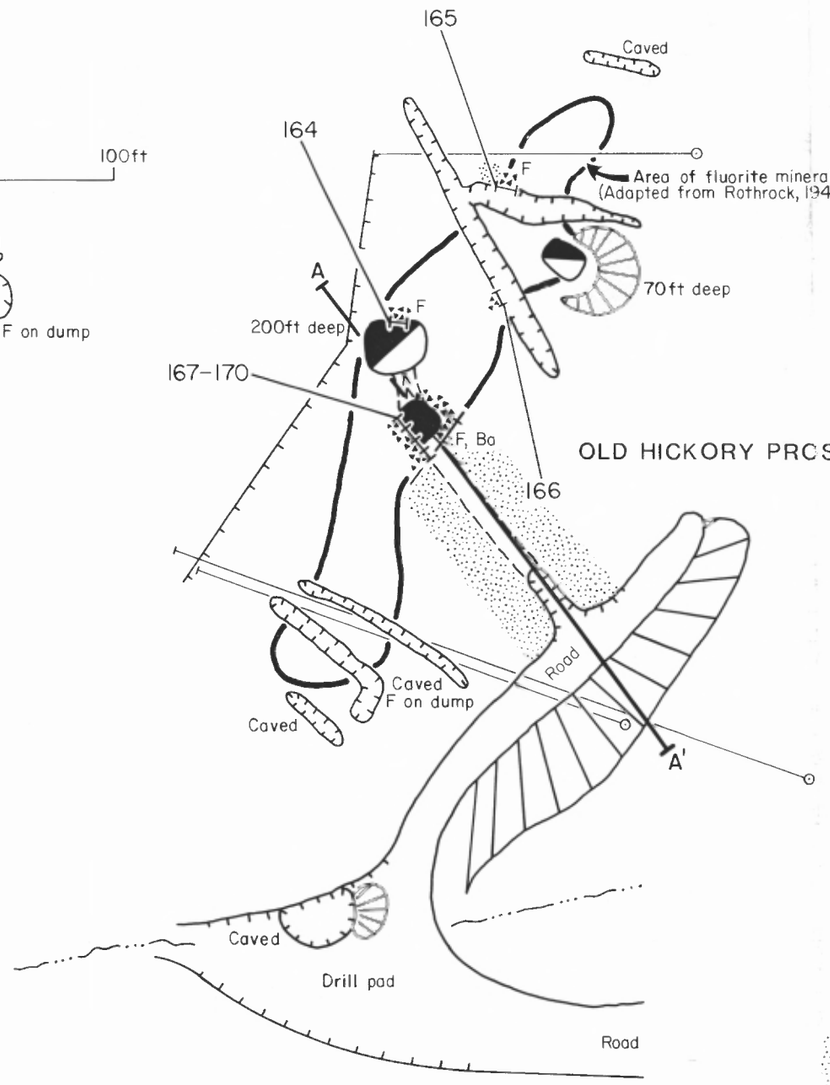

OLD HICKORY PROSPECT

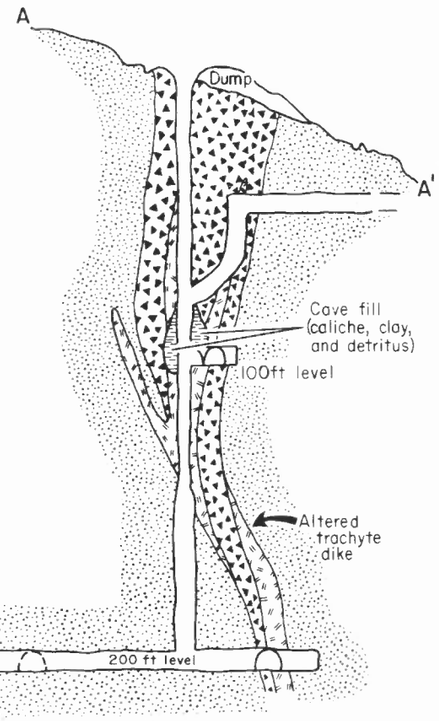

Cross-section sketch (adapted from Rothrock, 1946, plate 14)

Figure 21. Map of Old Hickory and Hoosier Girl Prospects, showing sample sites 161-171 and analytical data.

Sample		Analytical Data							
No.	Length (ft)	REO (%)	Y_2O_3 (PPM)	CaF_2 (%)	Au (PPB)	Ag (PPM)	Cu (PPM)	Pb (PPM)	Zn (PPM)
189	5.0	2.75	123	23.84	<5	<0.2	42	86	103
190	5.0	2.66	126	32.16	<5	<0.2	30	93	85
191	8.0	0.59	94	21.27	13	<0.2	21	29	100
192	8.0	0.19	95	9.45	9	<0.2	52	52	235
193	1.7	1.42	165	79.12	<5	<0.2	7	78	38
194	4.5	1.37	166	72.95	<5	<0.2	14	80	156
195	3.0	0.80	147	48.29	<5	<0.2	10	48	34
196	2.5	0.12	88	12.84	14	<0.2	42	43	86
197	4.5	1.53	162	50.35	23	<0.2	17	84	61
198	3.5	0.07	98	18.97	53	0.3	18	31	97
199	Grab	1.14	170	76.04	6	<0.2	4	64	41
200	Grab	0.86	108	32.78	20	<0.2	7	34	43
201	5.0	2.31	135	46.65	<5	<0.2	19	99	25
202	3.0	2.18	117	62.99	8	<0.2	7	57	9
203	4.0	0.15	43	7.81	<5	<0.2	13	23	34
204	2.0	0.70	79	18.19	15	<0.2	13	41	39

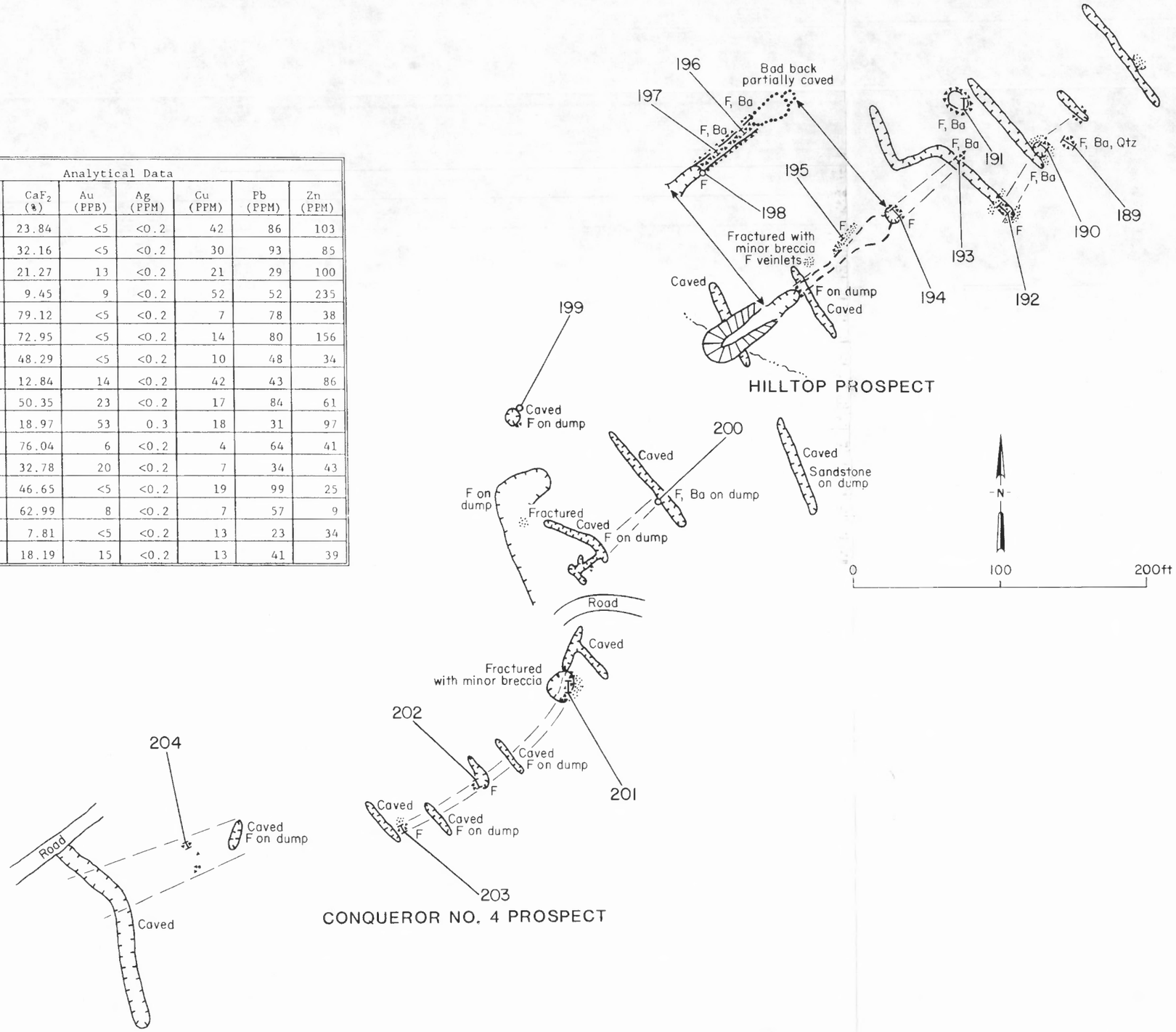

Figure 23. Map of Conqueror No. 4 and Hilltop Prospects, showing sample sites 189-204 and analytical data.

Sample		Analytical Data						
No.	Length (ft)	REO (%)	Y_2O_3 (PPM)	Au (PPB)	Ag (PPM)	Cu (PPM)	Pb (PPM)	Zn (PPM)
226	5.0	0.04	68	7	0.7	270	796	588
227	5.0	0.24	<190	27	13.1	5962	9815	2778
228	1.0	0.11	<190	67	102.8	13067	210600	2128
229	5.0	0.05	<152	14	4.5	1876	5012	4716
230	4.0	0.20	68	<58	83.6	15173	93400	2954
231	3.0	0.03	75	30	2.6	728	747	397
232	Grab 20-ft grid	0.27	<140	31	9.4	3798	27600	6914
233	5.0	0.93	152	24	<0.2	150	115	174
234	4.5	2.65	220	<19	0.6	73	131	462
235	5.0	0.23	117	7	1.3	201	378	303
236	5.0	3.29	344	5	<0.2	29	125	481
237	Grab select	1.41	194	<12	<0.2	135	753	65

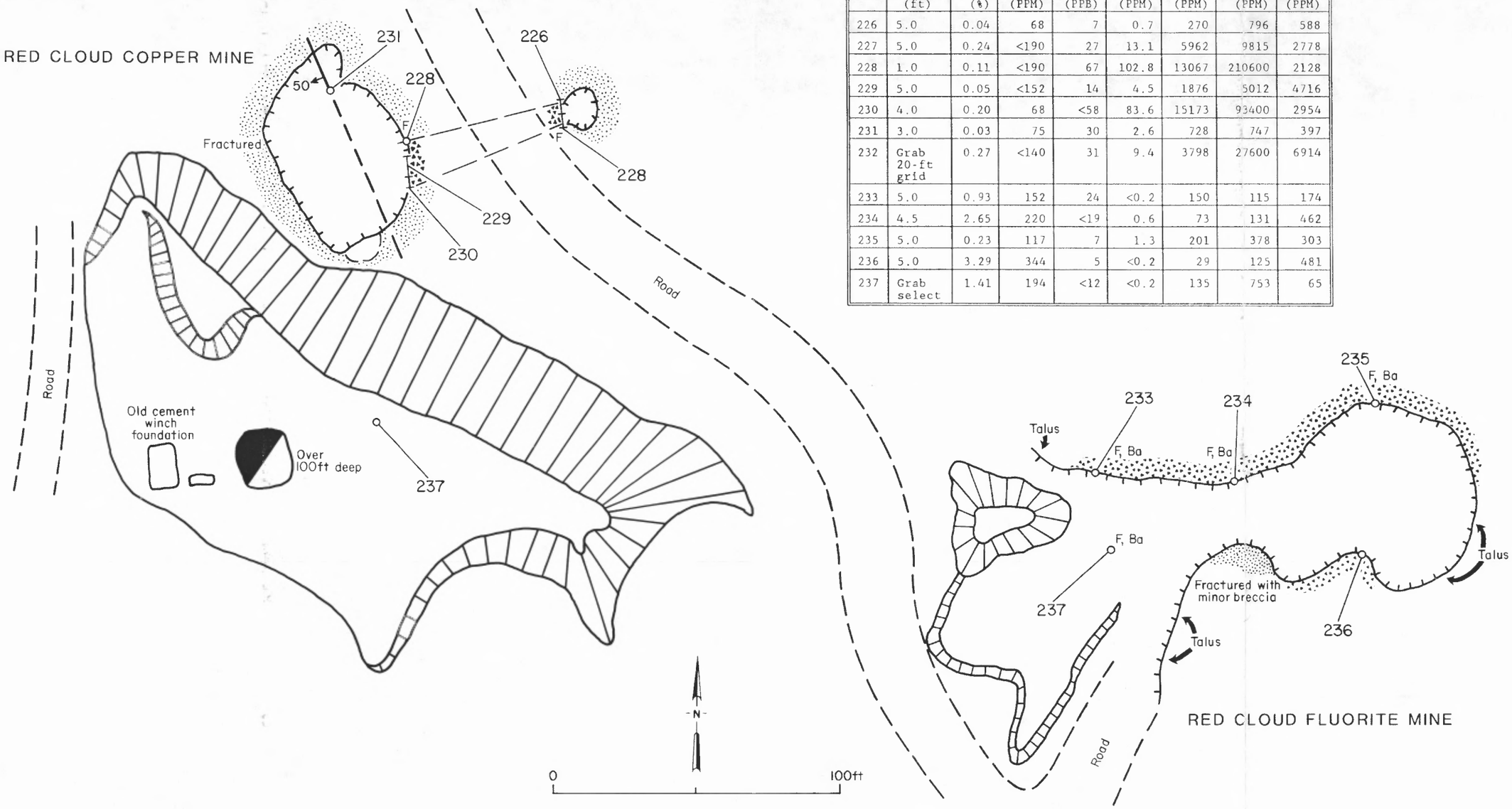

Figure 24. Map of Red Cloud Copper and Fluorite Mines, showing sample sites 226-237 and analytical data.

Sample		Analytical Data						
No.	Length (ft)	REO (%)	Y_2O_3 (PPM)	Au (PPB)	Ag (PPM)	Cu (PPM)	Pb (PPM)	Zn (PPM)
89	4.0	0.66	<470	18	<0.2	206	3441	174
90	Grab select	2.14	<444	71	2.9	5254	61800	554

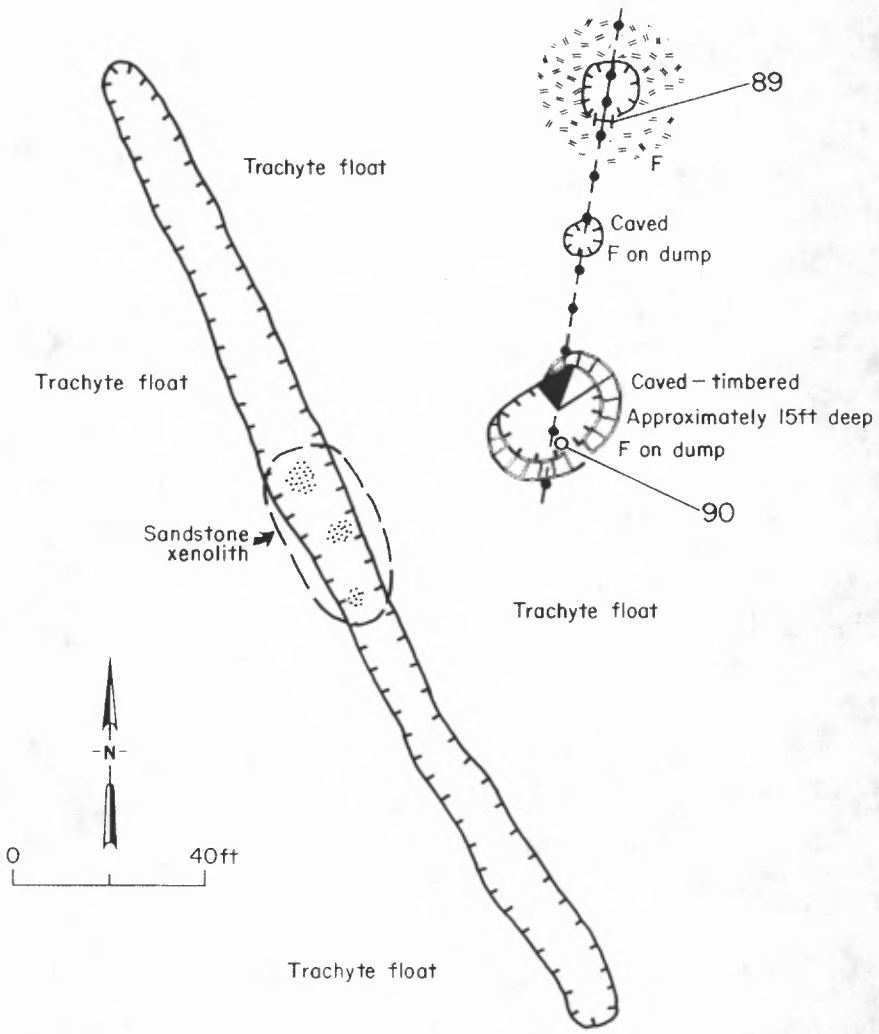

Figure 25. Map of Pride No. 2 Prospect, showing sample sites 89 and 90 and analytical data.

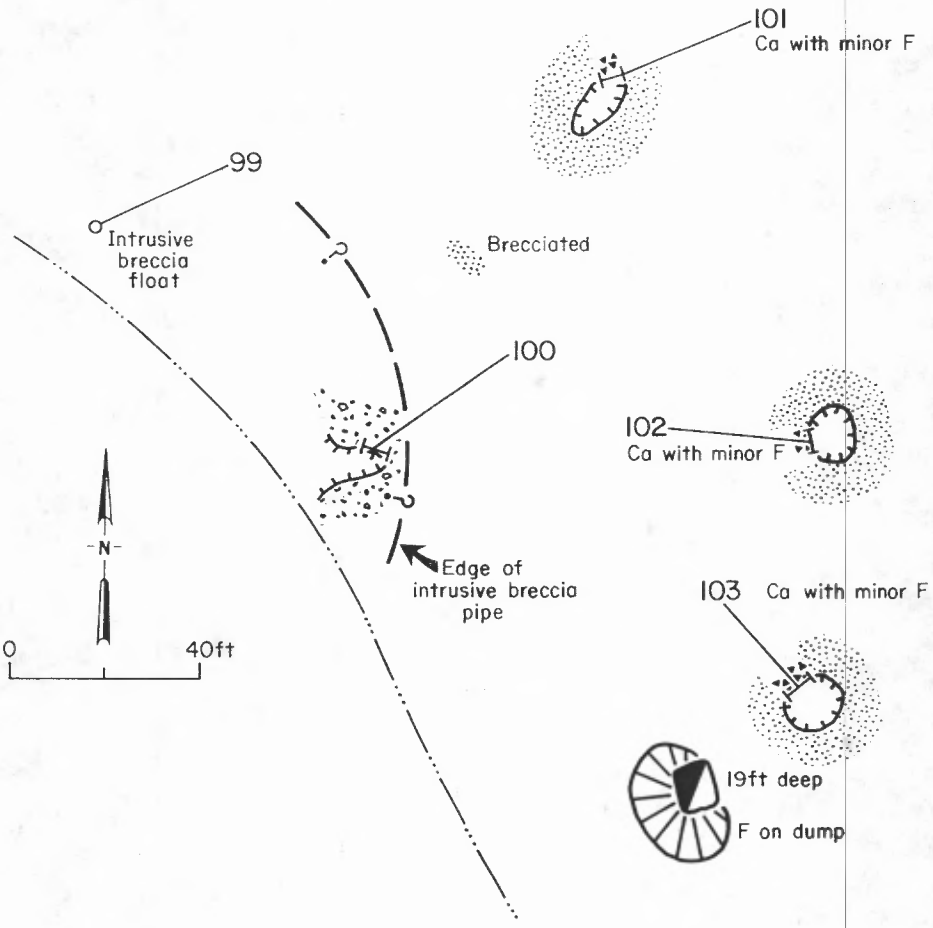

Sample		Analytical Data						
No.	Length (ft)	REO (%)	Y_2O_3 (PPM)	Au (PPB)	Ag (PPM)	Cu (PPM)	Pb (PPM)	Zn (PPM)
99	Grab	0.08	128	<5	<0.2	11	25	56
100	3.0	0.11	108	16	<0.2	10	22	56
101	2.0	0.03	38	11	0.2	5	6	11
102	3.0	1.76	161	7	<0.2	15	255	52
103	4.0	0.21	142	<5	<0.2	75	11	67

Figure 26. Map of Park Prospect, showing sample sites 99-103 and analytical data.

Sample		Analytical Data						
No.	Length (ft)	REO (%)	Y_2O_3 (PPM)	Au (PPB)	Ag (PPM)	Cu (PPM)	Pb (PPM)	Zn (PPM)
154	4.0	3.92	197	29	<0.2	99	406	152
155	3.3	0.10	133	45	0.3	73	236	87
156	4.5	0.29	389	21	<0.2	228	52	225

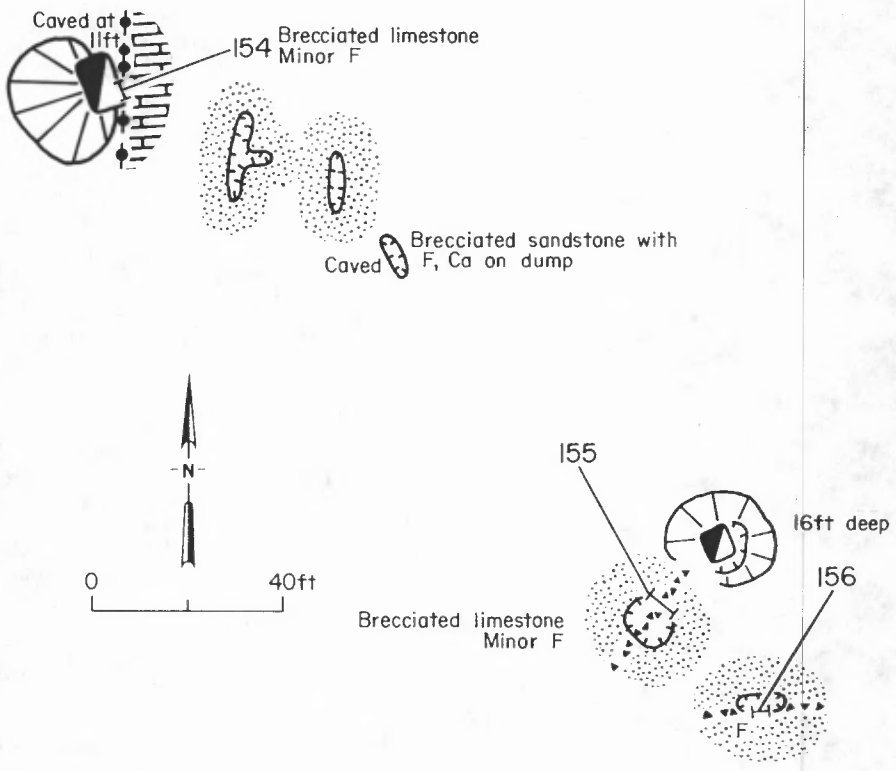

Figure 27. Map of Congress Prospect, showing sample sites 154-156 and analytical data.

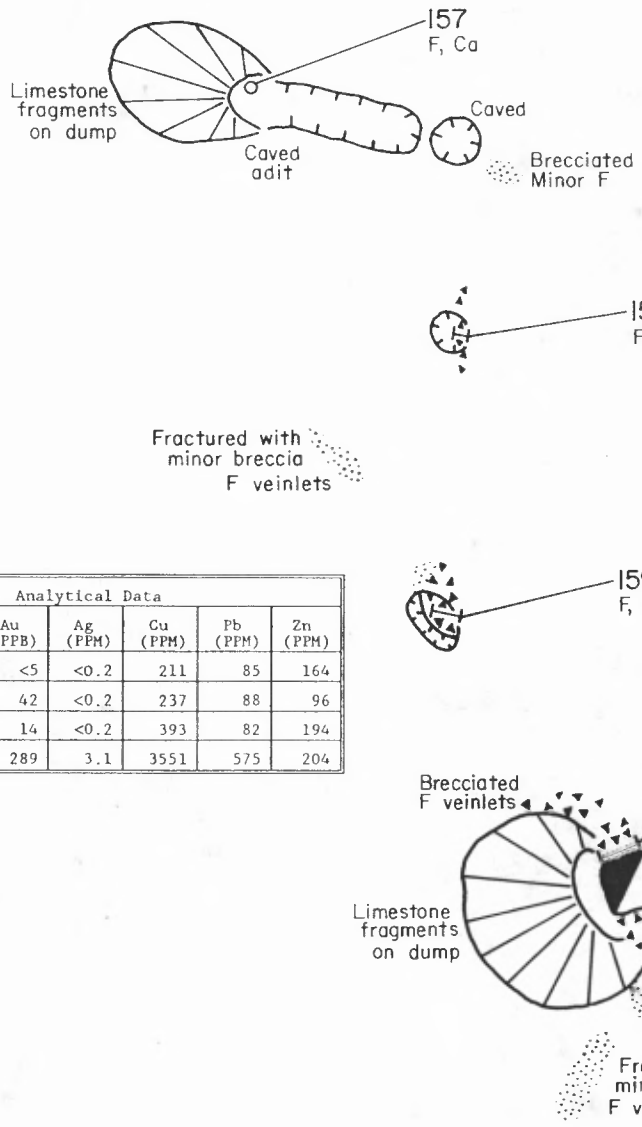

Sample		Analytical Data						
No.	Length (ft)	REO (%)	Y_2O_3 (PPM)	Au (PPB)	Ag (PPM)	Cu (PPM)	Pb (PPM)	Zn (PPM)
157	Grab	1.55	114	<5	<0.2	211	85	164
158	3.0	2.54	144	42	<0.2	237	88	96
159	4.0	2.57	123	14	<0.2	393	82	194
160	6.0	1.85	164	289	3.1	3551	575	204

Figure 28. Map of Bottleneck Prospect, showing sample sites 157-160 and analytical data.

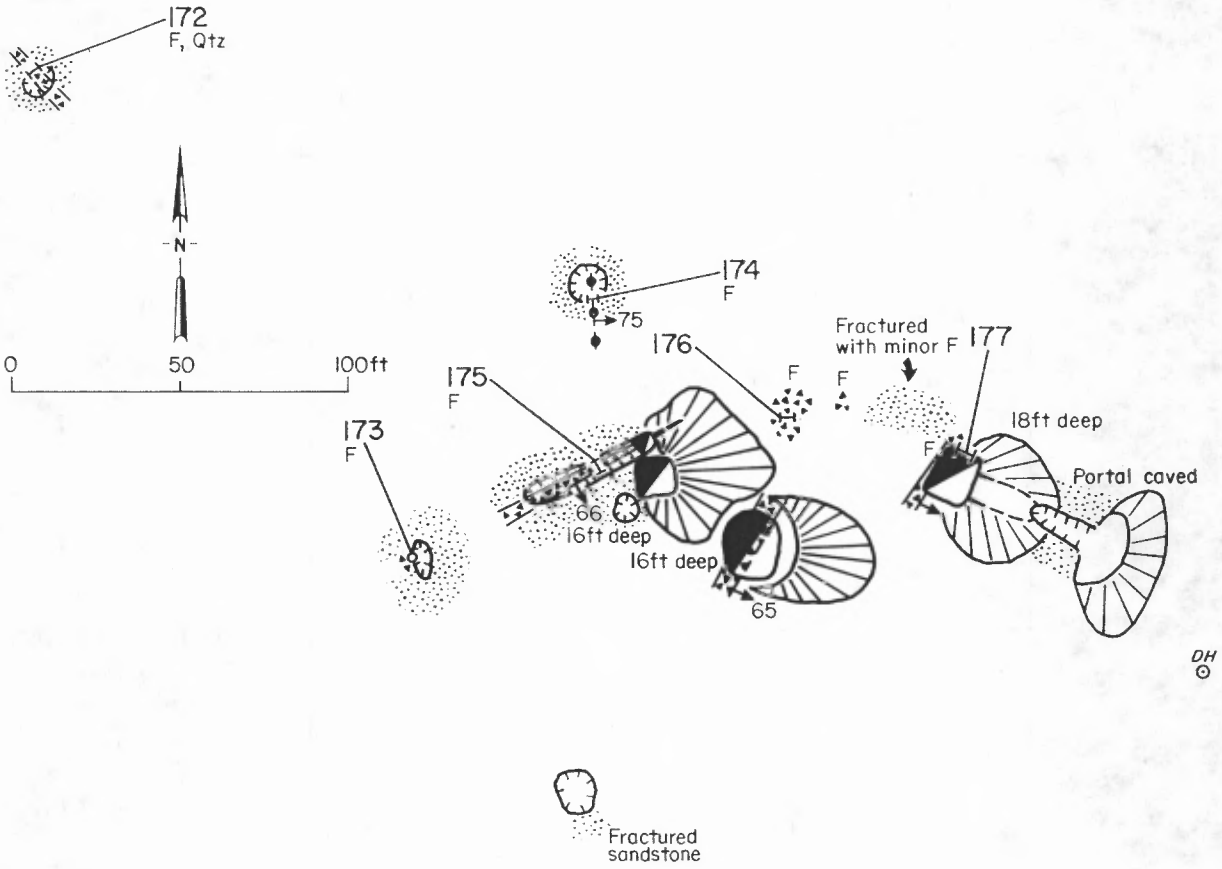

Sample		Analytical Data						
No.	Length (ft)	REO (%)	Y_2O_3 (PPM)	Au (PPB)	Ag (PPM)	Cu (PPM)	Pb (PPM)	Zn (PPM)
172	5.0	0.07	<140	596	36.2	18267	17100	3853
173	2.5	0.08	104	25	2.6	365	301	154
174	3.0	0.09	151	11	1.3	540	296	1115
175	4.0	0.27	133	99	25.8	19600	1094	2001
176	5.0	1.06	178	67	13.6	18118	21400	189
177	4.0	0.25	148	20	6.0	1297	446	317

Figure 29. Map of Eureka Prospect, showing sample sites 172-177 and analytical data.

Sample		Analytical Data						
No.	Length (ft)	REO (%)	Y_2O_3 (PPM)	Au (PPB)	Ag (PPM)	Cu (PPM)	Pb (PPM)	Zn (PPM)
178	5.0	2.14	53	150	<0.2	660	13800	726
179	5.0	1.37	390	76	0.9	1749	266	300
180	5.0	5.19	302	66	<0.2	423	220	80
181	5.0	0.12	121	25	<0.2	314	247	48
182	Grab select	1.18	338	23	0.5	313	125	160

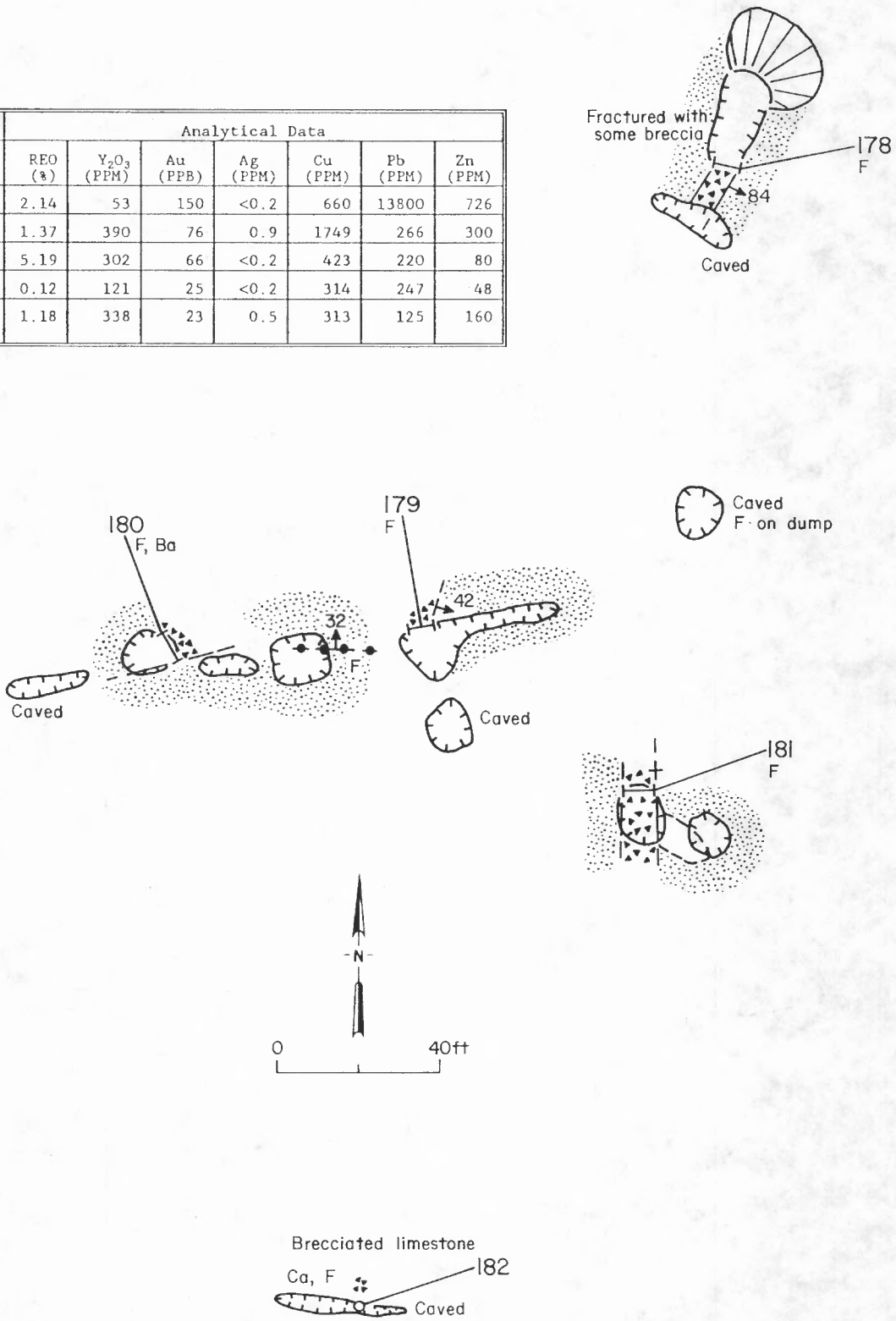

Figure 30. Map of Hoosier Boy Prospect, showing sample sites 178-182 and analytical data.

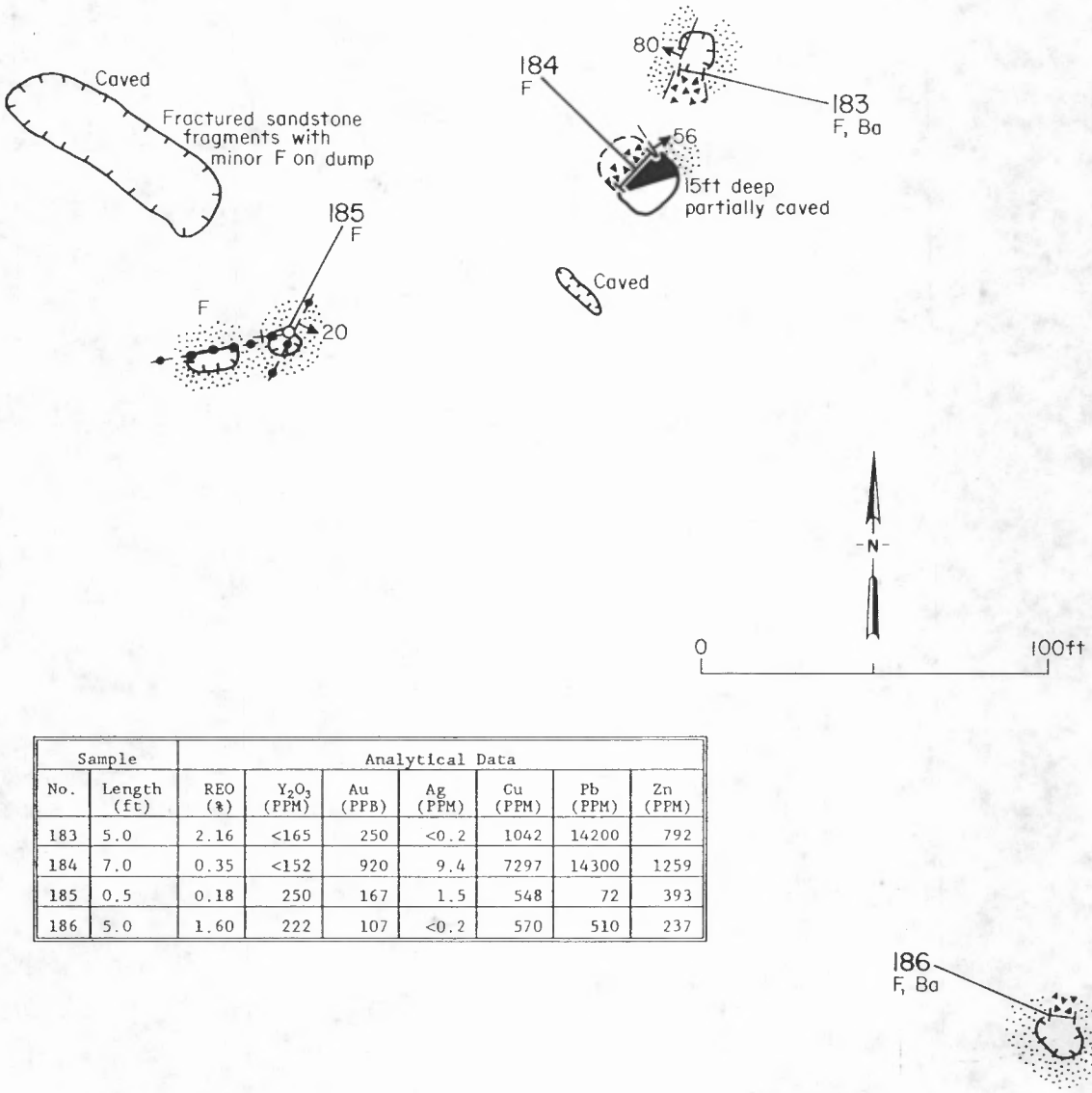

Sample		Analytical Data						
No.	Length (ft)	REO (%)	Y_2O_3 (PPM)	Au (PPB)	Ag (PPM)	Cu (PPM)	Pb (PPM)	Zn (PPM)
183	5.0	2.16	<165	250	<0.2	1042	14200	792
184	7.0	0.35	<152	920	9.4	7297	14300	1259
185	0.5	0.18	250	167	1.5	548	72	393
186	5.0	1.60	222	107	<0.2	570	510	237

Figure 31. Map of Hoosier Girl South Prospect, showing sample sites 183-186 and analytical data.

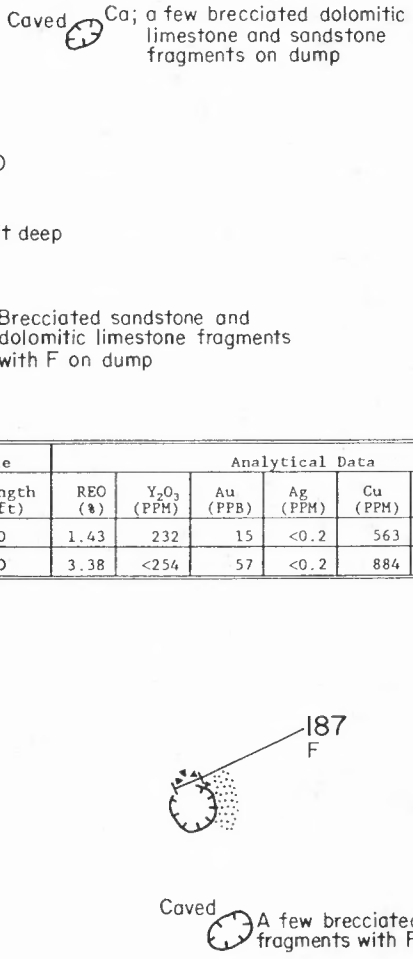

Sample		Analytical Data						
No.	Length (ft)	REO (%)	Y_2O_3 (PPM)	Au (PPB)	Ag (PPM)	Cu (PPM)	Pb (PPM)	Zn (PPM)
187	2.0	1.43	232	15	<0.2	563	1546	42
188	3.0	3.38	<254	57	<0.2	884	6457	324

Figure 32. Map of Hilltop Prospect, showing sample sites 187 and 188 and analytical data.

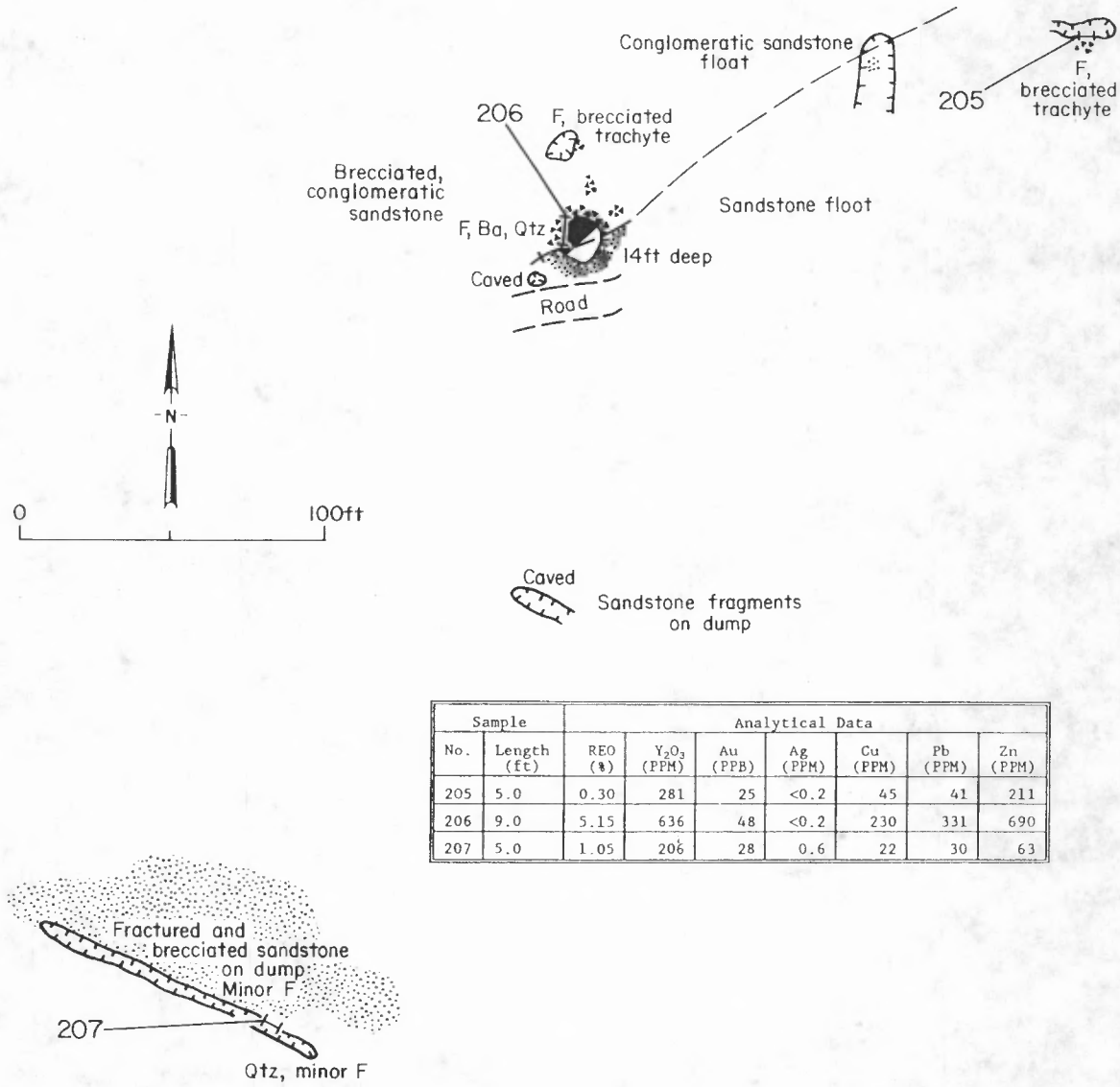

Sample		Analytical Data						
No.	Length (ft)	REO (%)	Y_2O_3 (PPM)	Au (PPB)	Ag (PPM)	Cu (PPM)	Pb (PPM)	Zn (PPM)
205	5.0	0.30	281	25	<0.2	45	41	211
206	9.0	5.15	636	48	<0.2	230	331	690
207	5.0	1.05	206	28	0.6	22	30	63

Figure 33. Map of Conqueror Apex Prospect, showing sample sites 205-207 and analytical data.

Sandstone fragments with minor breccia on dump

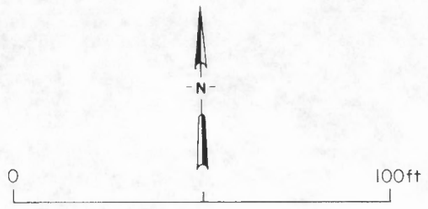

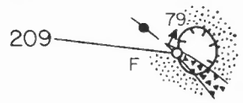

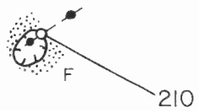

Sample		Analytical Data						
No.	Length (ft)	REO (%)	Y_2O_3 (PPM)	Au (PPB)	Ag (PPM)	Cu (PPM)	Pb (PPM)	Zn (PPM)
208	Grab	1.24	188	107	<0.2	196	411	40
209	2.6	1.78	265	102	<0.2	875	506	827
210	1.5	0.50	149	31	6.0	376	322	113
211	2.5	0.47	196	25	<0.2	222	190	105

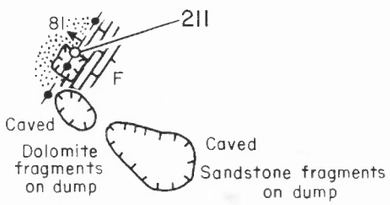

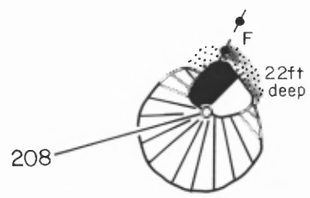

Figure 34. Map of Summit Prospect, showing sample sites 208-211 and analytical data.

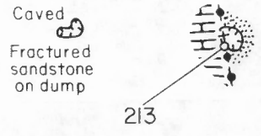

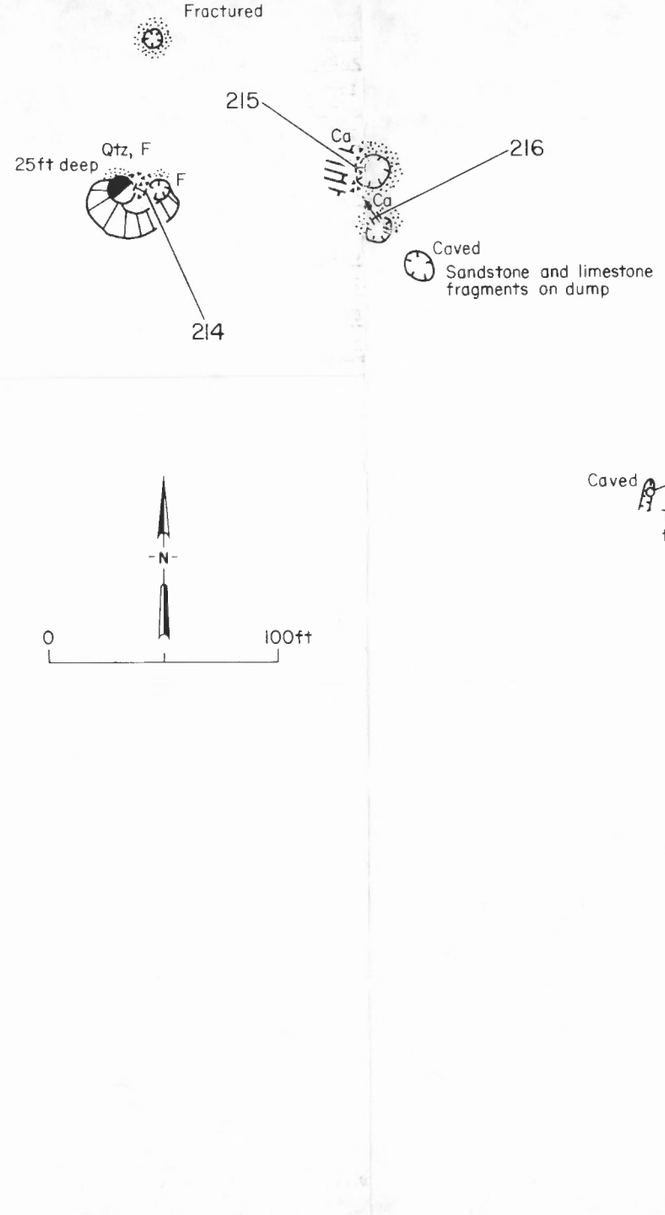

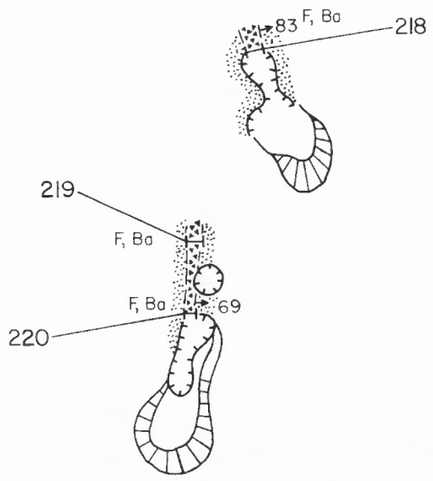

Sample		Analytical Data						
No.	Length (ft)	REO (%)	Y_2O_3 (PPM)	Au (PPB)	Ag (PPM)	Cu (PPM)	Pb (PPM)	Zn (PPM)
213	7.0	0.06	146	23	0.7	186	93	126
214	4.0	0.02	25.4	60	81.6	37000	1062	5717
215	4.0	0.02	90.2	19	36.8	10471	28	841
216	3.5	0.02	94.0	12	9.2	4387	23	549
217	Grab	0.04	53.3	15	<0.2	110	18	61
218	7.5	1.14	257.8	34	1.9	606	158	578
219	6.0	0.65	<190	40	1.9	606	16800	241
220	3.0	0.12	<140	73	4.1	957	3561	166

Figure 35. Map of White Oak Prospect, showing sample sites 213-220 and analytical data.

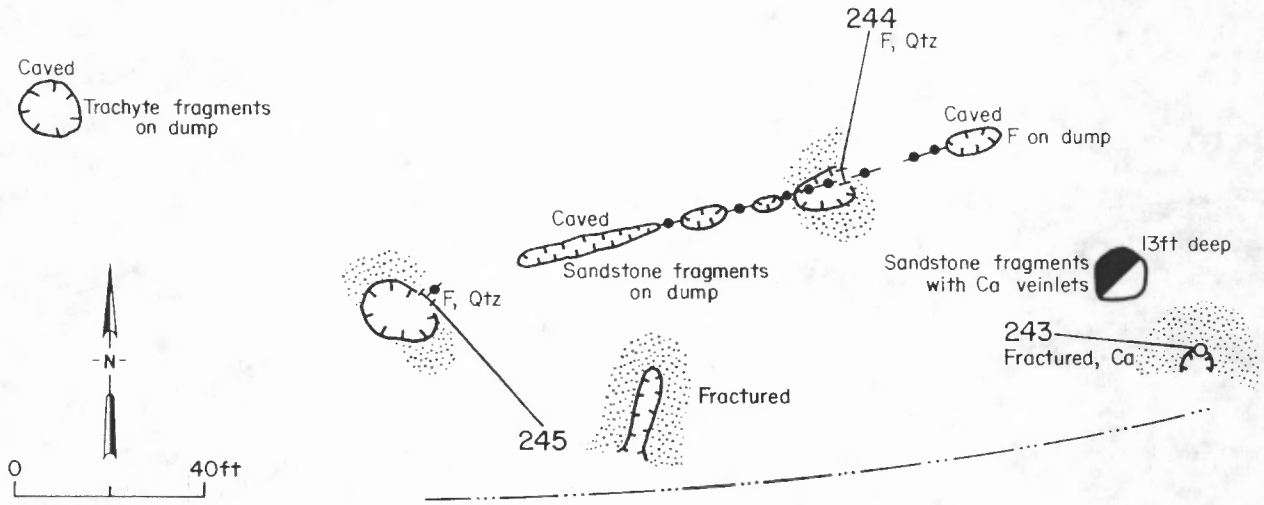

Sample		Analytical Data						
No.	Length (ft)	REO (%)	Y_2O_3 (PPM)	Au (PPB)	Ag (PPM)	Cu (PPM)	Pb (PPM)	Zn (PPM)
243	1.0	0.06	64	36	1.9	543	241	181
244	2.0	0.02	62	10	0.7	173	12	44
245	3.0	0.03	57	7	0.9	171	26	24

Figure 36. Map of Little Jack Prospect, showing sample sites 243-245 and analytical data.

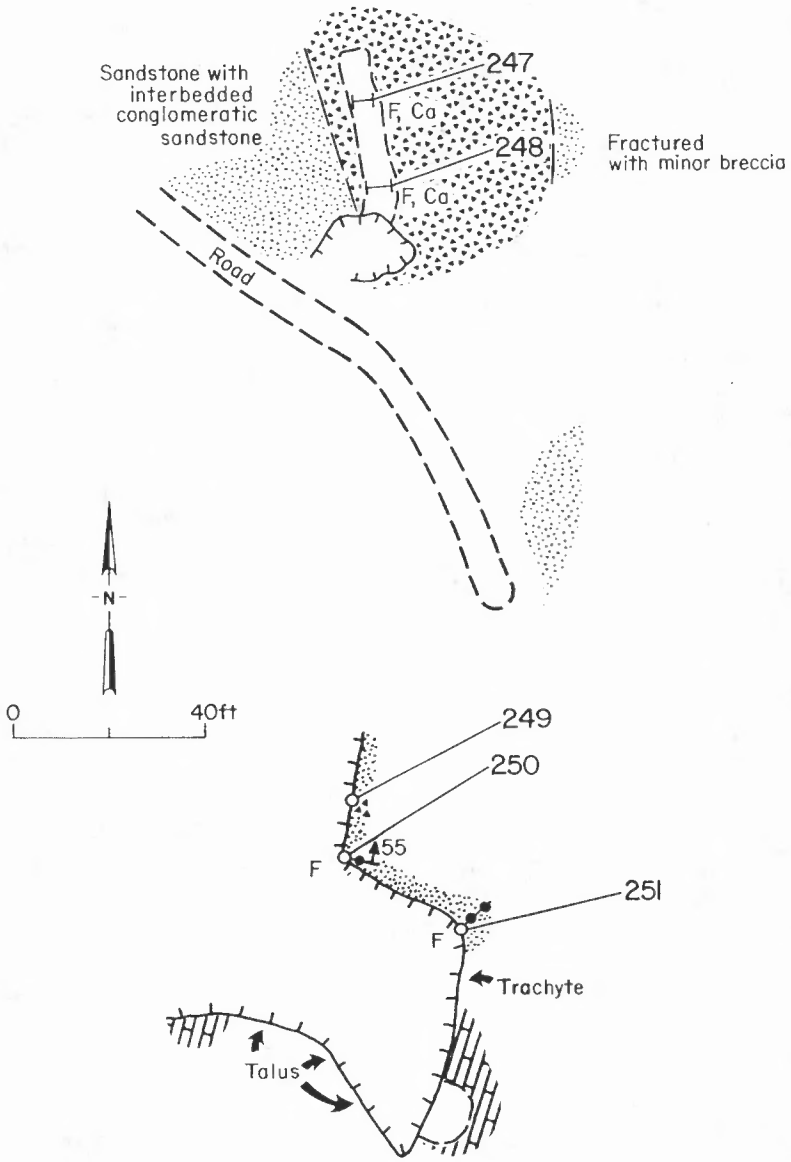

Sample		Analytical Data						
No.	Length (ft)	REO (%)	Y_2O_3 (PPM)	Au (PPB)	Ag (PPM)	Cu (PPM)	Pb (PPM)	Zn (PPM)
247	5.0	1.31	102	41	<0.2	311	440	182
248	5.0	0.31	121	30	<0.2	148	99	231
249	3.0	2.32	180	80	<0.2	678	148	624
250	2.3	1.64	103	29	<0.2	594	171	1463
251	1.0	3.04	96	63	<0.2	529	200	766

Figure 37. Map of Conqueror No. 10 Mine, showing sample sites 247-251 and analytical data.

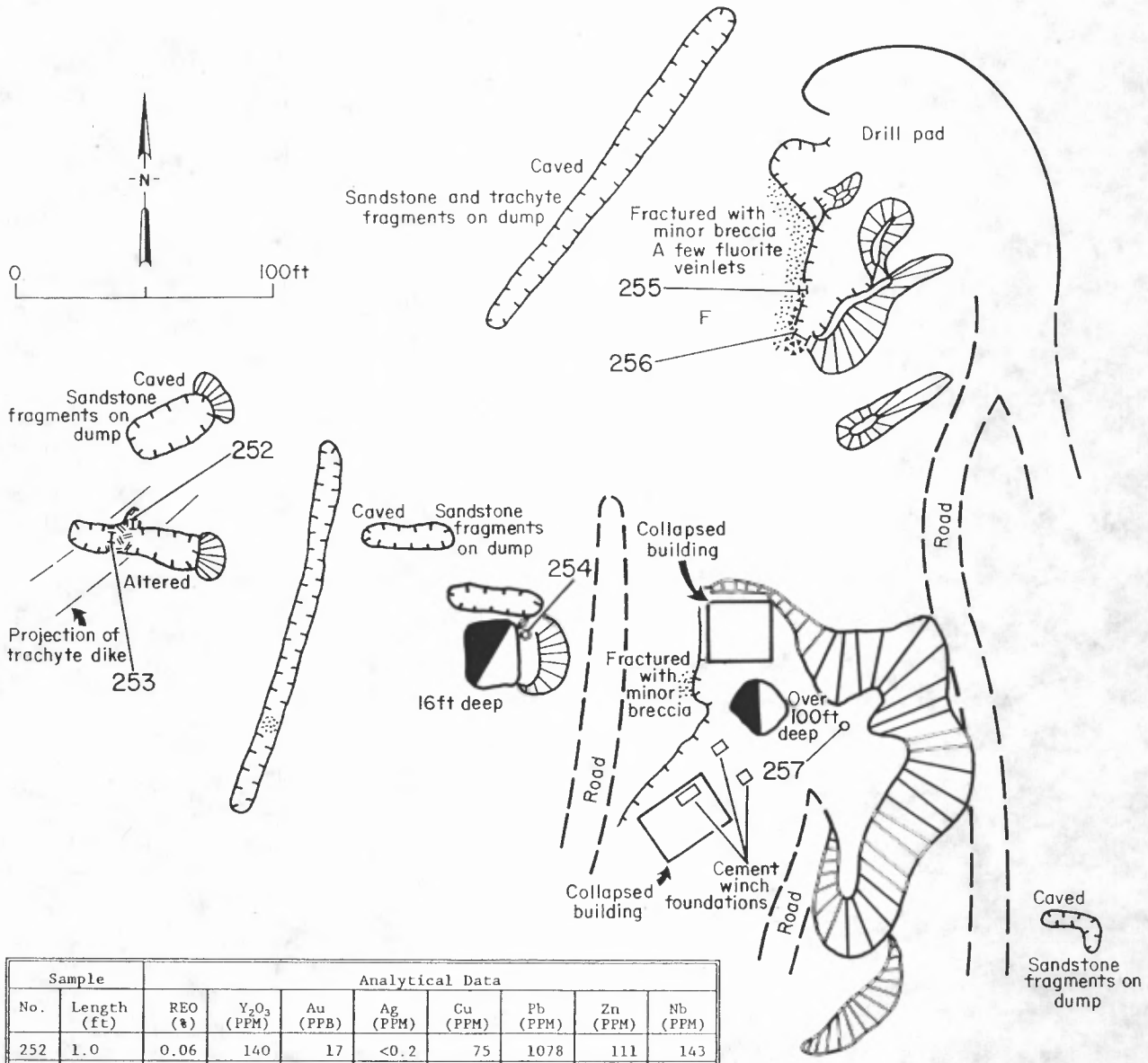

Sample		Analytical Data							
No.	Length (ft)	REO (%)	Y_2O_3 (PPM)	Au (PPB)	Ag (PPM)	Cu (PPM)	Pb (PPM)	Zn (PPM)	Nb (PPM)
252	1.0	0.06	140	17	<0.2	75	1078	111	143
253	1.0	0.02	52	8	0.2	158	764	116	183
254	Grab select	0.04	<114	93	21.0	23200	12900	1782	na
255	1.0	0.09	100	170	13.0	4727	30000	249	15
256	5.0	0.04	<178	149	9.0	1305	9077	416	na
257	Grab 10-ft grid	0.17	105	94	3.1	903	1987	194	26

Figure 38. Map of Rio Tinto Mine, showing sample sites 252-257 and analytical data.

Appendix A.-- Analytical results and sample descriptions for samples from the Red Cloud mining district, Lincoln County, N. Mex.

[INA, instrumental neutron activation analysis performed three times; INA*, instrumental neutron activation analysis; AA, atomic absorption spectroscopy; ICP, inductively coupled plasma - emmision spectroscopy; FA-AA, fire assay with atomic absorption spectroscopy finish; XRF, X-ray fluorescence; SI, specific ion method; CVAA, cold vapor atomic absorption spectroscopy; DIST, distillation; Fe analysis with asterisk by titrametric method; <, less than; >, greater than; na, not analyzed; xx, not applicable; opt, ounces per short ton; %, percent; PPB, parts per billion; PPM, parts per million; REO, rare-earth-element-oxides; Hg analysis with asterisk in PPB; Mn analysis with asterisk in PPM]

Sample Number	La PPM (INA)	Ce PPM (INA)	Pr PPM (INA)	Nd PPM (INA)	Sm PPM (INA)	Eu PPM (INA)	Gd PPM (INA)	Light Group REO	Tb PPM (INA)	Dy PPM (INA)	Ho PPM (INA)	Er PPM (INA)	Tm PPM (INA)	Yb PPM (INA)	Lu PPM (INA)	Y PPM (XRF)	Heavy Group REO	Total REO
1	2320.0	2550	<80	362	50.50	11.7	<200	6202	3.6	17.8	3.7	<100	<2	6.9	0.82	59	113	6314
2	1230.0	1570	na	340	41.70	9	na	3726	2.9	na	na	na	2.4	8.8	1.10	109	156	3882
3	1190.0	1290	<90	215	27.30	4.2	<200	3194	1.8	9.1	2.3	<100	<2	6.4	0.85	44	79	3273
4	1830.0	1990	<130	291	42.20	9.5	<300	4876	2.9	12.2	2.9	<100	<2	5.2	0.68	54	96	4972
5	1430.0	1480	<160	225	27.80	6.1	<300	3712	1.9	8.7	2.2	<100	<2	6.5	0.85	68	109	3822
6	1920.0	2020	107	265	35.70	7.3	<200	5102	2.4	12.5	2.8	<100	<2	6.2	0.70	58	102	5204
7	1160.0	1410	na	330	43.00	8.1	na	3453	2.9	na	na	na	<2	8.1	1.00	113	157	3610
8	754.0	912	na	180	26.30	5.2	na	2201	1.8	na	na	na	<2	5.6	0.59	62	88	2289
9	2100.0	1960	na	290	32.40	6.8	na	5134	2.7	na	na	na	<2	8.9	1.00	74	108	5243
10	2620.0	2350	<80	315	35.20	7.8	<200	6242	2.0	11.6	3.6	<100	<2	5.6	0.61	74	121	6363
11	283.0	300	<50	44	7.11	1.4	<200	744	<1.0	2.0	<1.0	<100	<2	2.6	0.31	28	41	786
12	2570.0	2440	65	323	54.00	12.1	<200	6401	4.3	26.4	4.9	<100	<2	9.5	1.07	<160	53	6454
13	2840.0	2990	180	438	66.80	14.2	<200	7648	4.3	23.9	4.1	<100	<2	7.7	0.85	66	131	7779
14	2800.0	2970	200	422	63.50	12.4	<600	7577	4.4	21.8	5.5	<100	<2	13.4	1.75	134	224	7801
15	2450.0	2410	155	324	45.30	9.5	<700	6319	3.4	17.7	4.1	<100	<2	7.2	0.81	106	173	6492
16	902.0	871	50	116	18.40	3.9	<200	2298	1.7	8.0	2.6	<100	<2	10.9	1.68	92	145	2443
17	780.0	796	<50	118	18.90	4.1	<200	2011	1.6	5.6	1.6	<100	<2	4.2	0.52	61	93	2104

Appendix A.-- Analytical results and sample descriptions for samples from the Red Cloud mining district, Lincoln County, New Mexico.--continued

Sample Number	La PPM (INA)	Ce PPM (INA)	Pr PPM (INA)	Nd PPM (INA)	Sm PPM (INA)	Eu PPM (INA)	Gd PPM (INA)	Light Group REO	Tb PPM (INA)	Dy PPM (INA)	Ho PPM (INA)	Er PPM (INA)	Tm PPM (INA)	Yb PPM (INA)	Lu PPM (INA)	Y PPM (XRF)	Heavy Group REO	Total REO
18	2650.0	2370	<180	284	37.30	7.9	<400	6267	2.5	8.0	2.3	<100	<2	7.2	0.93	79	124	6392
19	3660.0	3580	<500	627	77.70	16.0	<600	9326	4.6	20.9	5.0	<100	3	14.3	1.70	126	217	9542
20	4210.0	3940	<150	565	86.30	18.8	<200	10333	6.4	31.0	6.8	<100	<2	13.4	1.47	<200	68	10401
21	155.0	200	na	67	12.10	3	na	509	<1	na	na	na	<2	3.1	0.41	33	46	555
22	65.4	76	na	16	2.80	0.6	na	191	<1	na	na	na	<2	2.2	0.27	27	37	228
23	217.0	280	na	69	10.00	2.5	na	680	<1	na	na	na	<2	2.5	0.33	30	41	722
24	237.0	390	na	120	22.20	5.1	na	932	2.3	na	na	na	<2	8.0	1.00	101	141	1073
25	1000.0	1540	na	470	105.00	27	na	3647	11.0	na	na	na	<2	28.0	3.20	418	579	4226
26	159.0	250	<50	48	8.68	1.7	<200	547	<1.0	6.5	1.8	<100	<2	5.9	0.90	59	92	640
27	110.0	193	<50	50	7.11	1.1	<200	423	<1.0	3.7	1.7	<100	<2	6.5	1.08	57	87	510
28	96.0	178	<50	56	7.64	1.4	<200	397	<1.0	5.8	2.2	<100	<2	7.5	1.13	76	116	512
29	76.4	120	na	47	7.00	1.6	na	294	<1	na	na	na	<2	2.4	0.27	27	37	332
30	75.2	120	na	35	4.70	1.1	na	275	<1	na	na	na	<2	2.1	0.28	14	20	296
31	149.0	232	<50	82	13.50	3.1	<200	561	1.2	4.2	<1.0	<100	<2	3.7	0.50	51	76	637
32	35.0	49	na	17	3.60	1.3	na	124	<1	na	na	na	<2	1.3	0.17	15	21	145
33	86.5	120	na	37	5.90	1.2	na	293	<1	na	na	na	<2	3.9	0.65	33	47	340
34	29.0	47	na	14	3.20	1	na	111	<1	na	na	na	<2	1.9	0.22	11	16	128
35	60.7	120	na	43	7.50	1.9	na	274	<1	na	na	na	<2	3.1	0.47	27	38	312
36	283.0	310	na	64	13.40	2.7	na	789	1.4	na	na	na	<2	4.2	0.50	57	79	868
37	106.0	180	na	63	12.80	3.2	na	427	<1	na	na	na	<2	2.7	0.34	26	36	464

Appendix A.-- Analytical results and sample descriptions for samples from the Red Cloud mining district, Lincoln County, New Mexico.--continued

Sample Number	La PPM (INA)	Ce PPM (INA)	Pr PPM (INA)	Nd PPM (INA)	Sm PPM (INA)	Eu PPM (INA)	Gd PPM (INA)	Light Group REO	Tb PPM (INA)	Dy PPM (INA)	Ho PPM (INA)	Er PPM (INA)	Tm PPM (INA)	Yb PPM (INA)	Lu PPM (INA)	Y PPM (XRF)	Heavy Group REO	Total REO
38	310.0	340	na	86	14.60	3.3	na	883	1.4	na	na	na	<2	3.5	0.39	39	56	939
39	139.0	210	na	81	14.90	3.7	na	525	1.2	na	na	na	<2	3.0	0.39	31	45	570
40	281.0	340	na	110	19.00	4	na	879	1.6	na	na	na	<2	4.2	0.49	55	77	956
41	49.0	68	na	21	3.50	1	na	167	<1	na	na	na	<2	1.8	0.24	9	14	180
42	34.0	58	na	19	4.50	0.9	na	139	<1	na	na	na	<2	1.7	0.26	20	28	167
43	127.0	210	na	71	14.10	3.4	na	494	1.1	na	na	na	<2	3.1	0.43	36	51	545
44	200.0	311	<100	94	15.50	3.5	<200	730	1.0	4.8	1.6	<100	<2	3.9	0.55	55	83	814
45	205.0	327	<90	79	16.00	3.8	<200	739	1.3	4.1	1.2	<100	<2	3.7	0.55	53	80	818
46	1500.0	1570	110	250	43.30	10.2	<200	4080	3.2	11.5	2.1	<100	<2	7.4	0.93	106	163	4244
47	297.0	285	<50	54	9.79	2.5	<200	759	1.4	7.6	1.7	<100	<2	5.6	0.74	78	119	878
48	91.4	98	na	24	4.20	0.8	na	255	<1	na	na	na	<2	2.7	0.37	37	50	305
49	522.0	520	67	86	15.2	3	<200	1421	2	10	<1	<100	<1.0	7.3	1.0	64	105	1526
50	780.0	793	<50	120	20.00	4.9	<200	2012	2.0	8.5	2.9	<100	<2	7.3	0.93	87	135	2148
51	956.0	1300	<100	297	37.40	10.0	<200	3045	4.3	20.7	5.0	<100	<2	13.2	1.70	162	257	3302
52	512.0	534	na	110	16.70	3.8	na	1374	1.6	na	na	na	<2	4.6	0.59	57	80	1454
53	1970.0	2080	160	295	42.10	8.1	<200	5336	3.0	12.7	3.1	<100	<2	6.3	0.70	117	178	5514
54	91.1	170	na	45	7.40	1.7	na	370	<1	na	na	na	<2	4.6	0.62	42	59	429
55	79.5	130	na	50	10.50	2.4	na	319	1.0	na	na	na	<2	3.7	0.50	46	64	383
56	113.0	189	<50	57	13.90	3.3	<200	440	1.2	<4.0	<1.0	<100	<2	3.8	0.45	44	62	502
57	101.0	171	<50	48	11.80	2.8	<200	392	1.0	3.3	<1.0	<100	<2	3.1	0.44	42	62	454

Appendix A.-- Analytical results and sample descriptions for samples from the Red Cloud mining district, Lincoln County, New Mexico.--continued

Sample Number	La PPM (INA)	Ce PPM (INA)	Pr PPM (INA)	Nd PPM (INA)	Sm PPM (INA)	Eu PPM (INA)	Gd PPM (INA)	Light Group REO	Tb PPM (INA)	Dy PPM (INA)	Ho PPM (INA)	Er PPM (INA)	Tm PPM (INA)	Yb PPM (INA)	Lu PPM (INA)	Y PPM (XRF)	Heavy Group REO	Total RED
58	436.0	410	<50	53	5.8	1	<200	1061	<1	2	<1	<100	<1.0	4.1	1.2	16	29	1090
59	62.9	89	<50	13	2.05	0.6	<200	196	<1.0	1.6	<1.0	<100	<2	0.9	0.13	8	13	209
60	100.0	182	<50	46	10.20	2.5	<200	399	<1.0	5.9	1.5	<100	<2	2.9	0.43	32	53	452
61	177.0	251	<50	54	8.84	1.7	<200	577	<1.0	3.5	1.5	<100	<2	6.5	1.51	28	50	627
62	193.0	278	<70	66	13.60	2.9	<200	648	<1.0	6.5	<1.0	<100	<2	3.8	0.59	40	63	711
63	159.0	245	<80	64	13.40	3.3	<200	567	1.2	7.0	2.0	<100	<2	3.9	0.50	48	78	645
64	813.0	966	83	161	27.80	6.5	<200	2410	2.7	18.3	3.6	<100	<2	7.8	0.95	144	221	2631
65	107.0	162	<50	41	9.01	2.1	<200	376	<1.0	7.4	1.6	<100	<2	3.3	0.46	38	63	439
66	123.0	180	na	53	10.00	2	na	429	<1	na	na	na	<2	3.8	0.51	37	52	480
67	131.0	198	<50	43	8.76	1.9	<200	448	<1.0	6.1	<1.0	<100	<2	4.0	0.58	38	60	509
68	112.0	180	<50	37	8.66	1.7	<200	397	<1.0	2.8	<1.0	<100	<2	3.6	0.52	35	52	450
69	118.0	183	<50	57	8.65	1.8	<200	431	<1.0	4.4	<1.0	<100	<2	3.7	0.54	41	62	493
70	153.0	231	<50	48	8.92	1.8	<200	518	<1.0	6.1	1.6	<100	<2	4.4	0.64	39	64	583
71	9000.0	13400	880	2900	200.00	67.8	180	31102	22.0	92	17	31	3.4	20.9	1.80	458	797	31899
72	1290.0	1960	180	412	54.30	10.2	<200	4575	4.1	18.0	5.5	<100	3	16.0	2.36	187	293	4868
73	698.0	899	na	190	32.00	7.1	na	2136	3.0	na	na	na	2.3	16.0	2.20	125	186	2322
74	358.0	470	na	130	22.70	4.9	na	1148	2.1	na	na	na	2.6	13.0	1.70	168	235	1384
75	18900.0	22100	1340	4360	514.00	109.0	200	55427	33.4	160.0	34.0	<100	10	60.6	6.97	725	1270	56697
76	4500.0	4930	359	732	85.40	14.6	<200	12442	4.7	12.2	2.3	<100	<2	11.1	1.43	110	176	12618
77	4240.0	5010	362	785	103.00	17.6	<200	12320	5.7	16.7	4.6	<100	2	21.4	2.60	177	285	12605

Appendix A.-- Analytical results and sample descriptions for samples from the Red Cloud mining district, Lincoln County, New Mexico.--continued

Sample Number	La PPM (INA)	Ce PPM (INA)	Pr PPM (INA)	Nd PPM (INA)	Sm PPM (INA)	Eu PPM (INA)	Gd PPM (INA)	Light Group REO	Tb PPM (INA)	Dy PPM (INA)	Ho PPM (INA)	Er PPM (INA)	Tm PPM (INA)	Yb PPM (INA)	Lu PPM (INA)	Y PPM (XRF)	Heavy Group REO	Total REO
78	466.0	572	na	130	18.90	4.1	na	1390	1.4	na	na	na	<2	5.2	0.66	56	79	1469
79	8560.0	9560	1270	1440	169.00	28.3	<200	24631	8.5	33.8	7.4	<100	3	26.2	3.71	221	375	25006
80	11900.0	15600	1220	2630	337.00	58.8	<200	37182	19.1	59.2	17.9	<100	9	55.0	5.97	696	1074	38256
81	880.0	1130	<130	197	28.70	5.4	<200	2625	1.9	4.4	1.3	<100	<2	6.7	1.01	66	101	2726
82	5860.0	7260	400	1170	156.00	27.7	<200	17422	8.1	24.8	7.2	<100	3	19.3	2.64	235	373	17795
83	183.0	230	na	64	12.10	2.9	na	577	1.4	na	na	na	<2	8.0	1.00	93	130	707
84	158.0	220	na	67	14.40	3.4	na	540	2.3	na	na	na	2	12.0	1.50	160	223	764
85	83.2	130	na	42	8.40	1.9	na	314	<1	na	na	na	<2	4.3	0.63	54	74	388
86	306.0	380	na	83	19.50	4.7	na	923	5.5	na	na	na	6.4	40.0	5.00	548	761	1684
87	8860.0	11000	750	2480	330.00	67.7	<200	27506	24.0	89.0	19.3	<100	7	43.2	5.26	664	1058	28565
88	190.0	299	<50	87	14.00	3.4	<200	695	1.0	5.3	1.8	<100	<2	5.8	0.83	82	121	816
89	7690.0	8790	<700	1390	231.00	48.4	<1600	21259	14.6	53.6	14.7	<100	10	32.2	3.76	<350	148	21407
90	2290.0	2500	270	390	68.70	13.9	<500	6481	6.3	29.8	8.9	<100	4	27.3	3.50	<370	91	6572
91	177.0	277	<90	62	13.10	2.8	<200	623	1.1	5.4	1.4	<100	<2	4.1	0.60	56	86	708
92	458.0	514	<100	97	17.50	3.7	<200	1277	1.6	6.0	2.2	<100	<2	6.8	0.99	97	143	1420
93	671.0	796	<130	125	21.00	4.4	<200	1895	1.6	6.2	2.6	<100	<2	7.7	1.19	80	124	2018
94	523.0	546	<50	92	16.00	3.7	<200	1383	1.3	5.5	2.4	<100	<2	5.2	0.75	68	104	1487
95	297.0	422	<70	91	16.10	2.9	<200	971	1.0	5.4	2.2	<100	<2	4.3	0.58	52	81	1052
96	41.4	47	<50	10	1.90	<0.5	<200	117	<1.0	<1.0	<1.0	<100	<2	0.6	0.10	5	7	125
97	157.0	226	<50	64	11.30	2.5	<200	539	<1.0	4.7	<2.0	<100	<2	3.8	0.51	52	76	616

Appendix A.-- Analytical results and sample descriptions for samples from the Red Cloud mining district, Lincoln County, New Mexico.--continued

Sample Number	La PPM (INA)	Ce PPM (INA)	Pr PPM (INA)	Nd PPM (INA)	Sm PPM (INA)	Eu PPM (INA)	Gd PPM (INA)	Light Group REO	Tb PPM (INA)	Dy PPM (INA)	Ho PPM (INA)	Er PPM (INA)	Tm PPM (INA)	Yb PPM (INA)	Lu PPM (INA)	Y PPM (XRF)	Heavy Group REO	Total REO
98	113.0	175	<50	41	9.34	2.1	<200	399	1.0	4.1	<2.0	<100	<2	4.0	0.61	52	77	476
99	190.0	264	<80	62	12.00	2.9	<200	622	1.2	4.1	<1.0	<100	<2	3.3	0.49	101	139	760
100	344.0	391	<60	68	12.10	2.4	<200	958	1.4	6.7	2.7	<100	<2	5.3	0.65	85	127	1085
101	96.0	112	<50	24	5.14	1.0	<200	279	<1.0	2.9	1.2	<100	<2	2.1	0.30	30	46	324
102	6280.0	7280	<300	1180	122.00	21.7	<200	17435	5.4	15.7	4.1	<100	3	7.6	1.07	127	204	17638
103	720.0	755	<200	117	18.70	3.7	<200	1891	1.9	8.5	3.6	<100	<2	8.0	1.06	112	169	2060
104	88.8	118	<50	36	6.52	1.4	<200	294	<1.0	3.1	1.5	<100	<2	3.2	0.47	47	69	363
105	2340.0	3940	320	1060	190.00	45.3	<200	9243	12.0	42.0	8.3	<100	3	12.9	1.73	402	602	9845
106	242.0	380	<50	108	16.80	3.4	<200	878	1.8	8.8	2.7	<100	<2	8.2	1.22	122	181	1059
107	63.3	97	<50	35	7.73	1.8	<200	240	1.4	6.6	1.7	<100	<2	5.2	0.68	79	118	358
108	2370.0	3410	na	780	107.00	20	na	7819	7.1	na	na	na	<2	17.0	2.10	315	430	8249
109	2890.0	3200	na	650	61.70	10	na	7970	3.2	na	na	na	<2	7.1	0.83	95	133	8104
110	35.0	58	na	25	8.40	2.7	na	157	1.7	na	na	na	<2	5.0	0.64	57	81	238
111	997.0	1480	na	360	46.90	7.8	na	3396	2.3	na	na	na	<2	3.9	0.51	79	108	3504
112	2540.0	3550	na	840	97.80	16	na	8242	4.9	na	na	na	<2	6.1	0.82	129	177	8419
113	2330.0	2780	na	560	57.40	10	na	6717	2.2	na	na	na	<2	3.6	0.54	64	89	6805
114	1310.0	1570	na	320	37.90	7.1	na	3817	2.1	na	na	na	<2	5.3	0.63	75	104	3921
115	8880.0	8340	na	1450	107.00	21	na	22018	5.7	na	na	na	<2	7.5	1.00	83	122	22139
116	9000.0	9310	na	1500	119.00	17	na	23354	3.8	na	na	na	<2	5.2	0.93	89	124	23478
117	1910.0	1930	na	330	32.90	5.5	na	4953	2.3	na	na	na	<2	4.6	0.49	66	92	5045

Appendix A.-- Analytical results and sample descriptions for samples from the Red Cloud mining district, Lincoln County, New Mexico.--continued

Sample Number	La PPM (INA)	Ce PPM (INA)	Pr PPM (INA)	Nd PPM (INA)	Sm PPM (INA)	Eu PPM (INA)	Gd PPM (INA)	Light Group REO	Tb PPM (INA)	Dy PPM (INA)	Ho PPM (INA)	Er PPM (INA)	Tm PPM (INA)	Yb PPM (INA)	Lu PPM (INA)	Y PPM (XRF)	Heavy Group REO	Total REO
118	9000.0	11400	740	1930	155.00	25	55	27274	8.5	25	6	<10	2.4	11.0	1.30	112	204	27478
119	2660.0	2480	na	400	33.40	5	na	6544	1.8	na	na	na	<2	5.2	0.60	45	66	6609
120	5910.0	5320	na	840	63.80	12	na	14243	4.0	na	na	na	<2	7.0	1.00	80	115	14358
121	9000.0	9130	na	1360	120.00	23	na	22992	3.7	na	na	na	2.2	21.0	1.80	108	170	23161
122	5970.0	5740	na	950	82.20	15	na	14940	4.6	na	na	na	<2	8.4	0.92	93	134	15074
123	3790.0	3590	na	620	52.40	10	na	9459	3.5	na	na	na	<2	4.9	0.83	54	79	9538
124	9000.0	8780	na	1460	112.00	22	na	22679	4.2	na	na	na	5.5	13.0	1.40	75	123	22802
125	2140.0	2030	na	370	33.90	6.3	na	5362	2.6	na	na	na	<2	8.3	0.94	105	147	5509
126	739.0	742	na	140	17.40	3.3	na	1922	1.8	na	na	na	<2	5.5	0.67	85	117	2039
127	80.0	110	na	40	8.90	2.1	na	294	1.5	na	na	na	<2	5.9	0.75	88	121	415
128	5670.0	5260	na	860	69.90	12	na	13897	3.8	na	na	na	<2	8.2	0.74	74	109	14005
129	142.0	160	na	48	8.30	1.9	na	435	<1	na	na	na	<2	3.7	0.51	30	43	477
130	6750.0	6320	na	1090	86.50	13	na	16699	4.3	na	na	na	<2	10.4	1.00	96	140	16839
131	2130.0	2010	na	350	32.70	7.3	na	5318	2.6	na	na	na	<2	6.7	0.85	90	126	5444
132	5680.0	5760	na	1060	92.80	17	na	14773	4.6	na	na	na	<2	10.0	1.10	112	160	14934
133	9000.0	14400	800	2160	132.00	18.6	46	31069	4.9	17	3.9	<17	<2	9.4	1.29	88	154	31249
134	5410.0	4760	na	780	65.70	11	na	12906	3.7	na	na	na	<2	7.1	1.00	84	120	13026
135	4950.0	8000	650	1570	282.00	54.2	<200	18157	14.0	59.4	12.4	<100	6	24.7	2.81	390	632	18789
136	1190.0	1980	200	410	79.80	16.6	<200	4539	6.1	34.9	6.0	<100	<2	16.1	2.17	333	498	5036
137	3330.0	5440	330	1100	200.00	39.8	<200	12224	11.5	47.6	8.2	<100	3	18.1	2.27	302	487	12712

Appendix A.-- Analytical results and sample descriptions for samples from the Red Cloud mining district, Lincoln County, New Mexico.--continued

Sample Number	La PPM (INA)	Ce PPM (INA)	Pr PPM (INA)	Nd PPM (INA)	Sm PPM (INA)	Eu PPM (INA)	Gd PPM (INA)	Light Group REO	Tb PPM (INA)	Dy PPM (INA)	Ho PPM (INA)	Er PPM (INA)	Tm PPM (INA)	Yb PPM (INA)	Lu PPM (INA)	Y PPM (XRF)	Heavy Group REO	Total REO
138	1550.0	2450	<300	486	92.40	19.9	<200	5385	7.0	40.6	8.9	<100	<2	17.6	2.18	331	508	5892
139	1860.0	3140	250	780	130.00	27.8	<200	7245	9.1	46.0	9.4	<100	3	18.6	2.22	349	544	7789
140	526.0	900	<100	260	45.00	10.9	<200	2039	4.7	28.7	6.6	<100	<2	12.5	1.53	229	353	2392
141	270.0	470	<100	150	28.50	7.0	<200	1083	3.6	22.0	4.1	<100	<2	10.7	1.32	171	265	1348
142	1900.0	3280	<300	704	141.00	29.0	<200	7088	8.5	24.8	9.6	<120	<2	11.8	1.37	356	516	7605
143	4370.0	7470	<600	1580	304.00	60.0	200	16070	17.3	34.1	13.5	<140	3	23.5	3.04	416	636	16706
144	226.0	383	<50	85	20.00	4.9	<200	842	2.4	16.7	3.0	<100	<2	8.4	1.04	<160	36	878
145	1870.0	3590	240	770	184.00	41.1	<200	7838	15.4	82.4	16.9	<100	6	34.3	4.02	<600	182	8020
146	333.0	697	<50	160	30.00	9.4	<200	1439	3.4	16.7	4.0	<100	<2	10.0	1.25	<230	40	1480
147	169.0	270	<90	62	13.80	4.4	<200	608	1.5	6.4	<3.0	<100	<2	5.0	0.70	<180	16	623
148	847.0	1110	70	197	45.30	10.4	<200	2670	2.8	15.3	3.3	<100	<2	7.5	0.83	60	110	2780
149	799.0	1720	<100	510	98.90	22.2	<300	3687	7.2	32.0	5.6	<100	4	13.9	1.74	<220	74	3761
150	469.0	934	<200	260	51.00	12.9	<200	2021	4.0	17.0	3.0	<100	<2	8.9	1.18	<180	39	2060
151	72.0	153	<50	52	18.10	6.1	<200	352	4.2	35.8	6.7	<100	<2	24.2	3.12	<270	85	437
152	203.0	385	<50	140	27.20	6.5	<200	891	2.4	14.9	3.6	<100	<2	9.8	1.25	110	176	1068
153	450.0	755	<50	179	25.50	4.4	<200	1656	1.5	5.1	1.6	<100	<2	4.2	0.54	68	101	1757
154	9000.0	20000	na	4150	200.00	48	na	39057	10.0	na	na	na	<3	31.0	1.60	84	155	39212
155	283.0	350	na	89	15.60	3.5	na	876	1.7	na	na	na	<2	6.0	0.73	75	105	981
156	784.0	1100	na	280	50.20	11	na	2610	4.7	na	na	na	3	16.0	1.90	218	306	2916
157	6180.0	5840	na	1000	90.20	15	na	15398	4.0	na	na	na	2	12.0	0.89	90	136	15534

Appendix A.-- Analytical results and sample descriptions for samples from the Red Cloud mining district, Lincoln County, New Mexico.--continued

Sample Number	La PPM (INA)	Ce PPM (INA)	Pr PPM (INA)	Nd PPM (INA)	Sm PPM (INA)	Eu PPM (INA)	Gd PPM (INA)	Light Group REO	Tb PPM (INA)	Dy PPM (INA)	Ho PPM (INA)	Er PPM (INA)	Tm PPM (INA)	Yb PPM (INA)	Lu PPM (INA)	Y PPM (XRF)	Heavy Group REO	Total REO
158	9000.0	10500	na	1780	168.00	34	na	25170	7.7	na	na	na	5.4	19.0	1.60	113	182	25352
159	9000.0	10500	na	2050	200.00	39	na	25529	9.2	na	na	na	2	19.0	1.60	97	160	25688
160	5670.0	7940	na	1800	200.00	45	na	18281	10.0	na	na	na	2.2	11.0	0.94	129	191	18473
161	5080.0	9860	820	2410	489.00	102.0	<200	21963	20.5	49.4	9.8	<100	4	15.9	1.93	384	604	22567
162	1290.0	2600	240	670	161.00	40.0	<200	5854	11.3	45.0	9.3	<100	3	18.6	2.11	399	609	6463
163	943.0	1750	130	486	74.60	15.7	<200	3979	3.0	10.0	1.7	<100	<2	2.2	0.28	212	289	4268
164	1380.0	2230	166	567	76.80	16.8	<200	5195	4.3	17.2	4.4	<100	<2	6.2	0.78	120	190	5385
165	7380.0	10000	530	1900	254.00	48.1	<200	23555	8.5	21.9	4.0	<100	2	9.4	1.05	<70	54	23608
166	5100.0	6570	540	1200	152.00	27.8	<200	15917	6.9	28.0	6.3	<100	2	8.3	0.87	<90	60	15977
167	6130.0	8020	678	1520	200.00	40.1	<700	19428	8.6	32.0	3.9	<100	<2	8.2	0.99	95	182	19610
168	10300.0	13400	700	2570	315.00	58.0	<200	32024	12.2	38.0	7.7	<100	3	10.0	0.94	<70	82	32106
169	10800.0	13600	1160	2490	291.00	52.5	<200	33256	11.8	31.8	5.9	<100	3	11.2	1.17	<100	74	33330
170	10500.0	12800	1160	2260	260.00	49.5	<200	31659	9.3	22.6	5.2	<100	2	9.1	1.07	<60	56	31715
171	312.0	672	53	208	43.00	10.0	<200	1519	3.3	15.6	3.1	<100	<2	7.1	0.89	140	212	1731
172	130.0	273	<50	115	25.80	8.2	<200	646	3.2	14.0	3.3	<100	<2	5.7	0.73	<110	31	677
173	156.0	306	<50	100	21.50	5.6	<200	689	1.9	11.0	2.4	<100	<2	4.4	0.51	82	127	817
174	166.0	304	<50	100	23.80	6.0	<200	702	2.6	13.4	4.1	<100	<2	8.7	1.08	119	185	887
175	600.0	1170	<50	320	53.90	13.4	<200	2525	3.5	17.0	3.5	<100	<2	6.7	0.71	105	169	2695
176	3400.0	4450	240	818	119.00	24.0	<200	10600	6.3	27.0	5.8	<100	3	8.0	1.18	<140	59	10659
177	549.0	952	100	320	57.60	13.9	<200	2332	4.1	18.0	4.8	<100	<2	8.9	1.03	117	191	2523

Appendix A.-- Analytical results and sample descriptions for samples from the Red Cloud mining district, Lincoln County, New Mexico.--continued

Sample Number	La PPM (INA)	Ce PPM (INA)	Pr PPM (INA)	Nd PPM (INA)	Sm PPM (INA)	Eu PPM (INA)	Gd PPM (INA)	Light Group REO	Tb PPM (INA)	Dy PPM (INA)	Ho PPM (INA)	Er PPM (INA)	Tm PPM (INA)	Yb PPM (INA)	Lu PPM (INA)	Y PPM (XRF)	Heavy Group REO	Total REO
178	5880.0	9570	550	1940	303.00	59.3	<200	21432	9.4	19.5	2.8	<100	<2	4.5	0.52	<100	42	21474
179	3720.0	5870	538	1400	173.00	33.0	<200	13740	6.5	28.8	6.1	<100	2	12.6	1.49	190	307	14047
180	15700.0	22700	1200	4100	539.00	100.0	<200	51928	13.7	24.9	2.9	<100	<2	5.5	0.89	144	238	52166
181	3460.0	5090	340	1000	150.00	30.8	<200	11794	7.0	21.7	4.8	<100	2	9.6	1.10	168	266	12060
182	330.0	511	58	107	22.90	5.4	<200	1211	1.8	9.3	2.9	<100	<2	5.2	0.62	57	95	1306
183	6040.0	9450	600	1960	317.00	63.8	<200	21582	11.6	32.8	6.3	<100	<2	6.5	0.77	<130	66	21649
184	847.0	1460	110	420	79.60	21.7	<200	3439	6.8	28.0	7.3	<100	3	9.2	1.03	<120	63	3503
185	344.0	653	<90	200	45.60	11.8	<200	1468	4.6	20.1	6.5	<100	<2	12.3	1.47	197	302	1770
186	5020.0	6640	410	1160	149.00	29.8	<200	15705	7.3	23.3	5.9	<100	2	10.3	1.23	175	280	15984
187	3700.0	6200	480	1300	221.00	46.3	<200	13989	11.6	51.5	7.4	<100	4	15.2	1.83	183	337	14327
188	9720.0	14200	1500	2700	389.00	71.8	230	33736	15.7	58.4	7.0	<100	3	8.7	1.47	<200	108	33844
189	9000.0	12000	na	2180	167.00	26	na	27379	5.4	na	na	na	<2	5.9	0.78	97	137	27516
190	9000.0	11400	na	2030	162.00	28	na	26470	6.6	na	na	na	2.5	6.9	0.65	99	145	26614
191	2500.0	2100	na	360	27.30	5.6	na	5847	1.7	na	na	na	<2	4.8	0.64	74	102	5949
192	591.0	744	na	140	17.90	3.3	na	1767	1.7	na	na	na	<2	5.9	0.70	75	105	1872
193	5720.0	5310	na	860	79.90	16	na	14048	7.0	na	na	na	<2	9.5	1.40	130	186	14233
194	4630.0	5200	na	1030	104.00	21	na	12861	6.4	na	na	na	2.4	94.0	1.10	131	285	13146
195	2700.0	3210	na	680	81.00	16	na	7817	4.8	na	na	na	3.6	8.9	0.82	116	168	7985
196	383.0	400	na	96	13.20	2.8	na	1067	1.4	na	na	na	<2	4.9	0.65	69	96	1163
197	6030.0	5720	na	1050	94.50	19	na	15109	5.4	na	na	na	2.7	9.1	1.00	128	183	15292

Appendix A.-- Analytical results and sample descriptions for samples from the Red Cloud mining district, Lincoln County, New Mexico.--continued

Sample Number	La PPM (INA)	Ce PPM (INA)	Pr PPM (INA)	Nd PPM (INA)	Sm PPM (INA)	Eu PPM (INA)	Gd PPM (INA)	Light Group REO	Tb PPM (INA)	Dy PPM (INA)	Ho PPM (INA)	Er PPM (INA)	Tm PPM (INA)	Yb PPM (INA)	Lu PPM (INA)	Y PPM (XRF)	Heavy Group REO	Total REO
198	223.0	230	na	62	10.40	2.5	na	634	1.3	na	na	na	<2	4.7	0.62	77	105	739
199	4350.0	4290	na	810	82.40	16	na	11178	6.0	na	na	na	<2	12.0	1.10	134	192	11370
200	3420.0	3240	na	560	50.90	10	na	8538	3.6	na	na	na	<2	5.8	0.72	85	120	8657
201	9000.0	9040	na	1410	102.00	17	na	22929	4.9	na	na	na	3.1	11.0	1.70	106	158	23088
202	8970.0	8130	na	1320	107.00	20	na	21709	4.6	na	na	na	2.2	7.4	1.00	92	134	21843
203	520.0	561	na	110	12.30	2.2	na	1418	<1	na	na	na	<2	2.5	0.32	34	46	1465
204	2630.0	2720	na	480	44.90	7.5	na	6882	2.5	na	na	na	<2	5.7	0.70	62	89	6971
205	887.0	1130	<70	238	33.30	7.2	<200	2688	3.6	19.0	5.1	<100	<2	17.4	2.47	221	335	3023
206	19100.0	19300	920	3520	390.00	66.8	<200	50718	23.4	70.0	16.0	<100	7	35.4	4.55	501	815	51533
207	250.0	335	<50	85	17.00	4.5	<200	810	2.4	14.0	3.0	<100	<2	8.0	1.05	162	238	1048
208	3440.0	5260	370	1060	173.00	35.9	<200	12107	9.0	40.0	5.9	<100	<2	9.9	1.16	148	264	12370
209	4070.0	7560	700	2100	357.00	75.3	<200	17398	16.7	53.2	9.7	<100	<2	11.7	1.49	209	372	17770
210	1310.0	2110	157	430	80.00	17.3	<200	4806	4.8	20.7	4.0	<100	<2	6.7	0.84	117	191	4997
211	1060.0	1940	180	510	91.60	21.1	<200	4452	6.0	29.3	4.7	<100	<2	9.1	1.09	154	253	4705
212	3130.0	5630	530	1340	282.00	65.0	<200	12851	15.8	53.3	10.2	<100	3	16.0	1.75	250	432	13283
213	92.7	186	<50	77	18.90	5.4	<200	445	2.5	12.0	3.1	<100	<2	7.5	0.95	115	176	620
214	54.7	77	<60	24	6.76	2.1	<200	193	1.1	6.6	<3.0	<100	<2	2.4	0.16	20	37	230
215	14.0	36	<50	20	6.80	2.5	<200	93	1.6	8.3	2.0	<100	<2	3.6	0.44	71	108	201
216	20.0	33	<50	18	5.32	2.0	<200	92	1.1	4.9	<1.0	<100	<2	3.1	0.41	74	105	196
217	95.8	160	<50	61	11.10	2.5	<200	387	<1.0	4.9	1.2	<100	<2	3.5	0.55	42	65	452

Appendix A.-- Analytical results and sample descriptions for samples from the Red Cloud mining district, Lincoln County, New Mexico.--continued

Sample Number	La PPM (INA)	Ce PPM (INA)	Pr PPM (INA)	Nd PPM (INA)	Sm PPM (INA)	Eu PPM (INA)	Gd PPM (INA)	Light Group REO	Tb PPM (INA)	Dy PPM (INA)	Ho PPM (INA)	Er PPM (INA)	Tm PPM (INA)	Yb PPM (INA)	Lu PPM (INA)	Y PPM (XRF)	Heavy Group REO	Total REO
218	2830.0	4900	320	1250	178.00	37.7	<200	11141	8.0	29.0	4.4	<100	<2	9.2	1.06	203	317	11458
219	1570.0	2780	260	760	106.00	28.7	<200	6444	6.2	19.2	3.9	<100	<2	7.4	0.65	<150	43	6487
220	280.0	533	<50	160	29.20	7.3	<200	1182	2.5	10.7	2.5	<100	<2	5.5	0.70	<110	25	1207
221	7230.0	9970	800	1780	261.0	53	<200	23533	10	38	<3	<100	<1.0	12.0	0.6	149	259	23792
222	278.0	780	<50	140	23.90	5.9	<200	1437	2.5	11.0	3.0	<100	<2	12.0	1.83	155	232	1669
223	102.0	172	<50	56	9.96	2.8	<200	401	1.6	6.9	2.5	<100	<2	7.7	1.15	96	145	546
224	617.0	1520	120	580	148.00	37.7	<200	3536	11.0	42.6	5.5	<100	<2	14.8	1.86	263	421	3957
225	950.0	1180	130	209	38.50	8.5	<200	2947	3.6	19.1	3.3	<100	<2	8.5	1.03	179	268	3215
226	81.7	126	<50	50	7.69	1.9	<200	313	1.1	6.8	1.4	<100	<2	4.2	0.55	54	85	397
227	701.0	1030	71	205	42.60	9.1	<200	2411	3.6	18.8	2.4	<100	<2	9.9	1.13	<150	41	2452
228	354.0	416	<180	119	27.70	7.3	<200	1082	2.3	14.0	4.0	<100	<2	5.2	0.87	<150	30	1112
229	113.0	199	<50	53	15.80	3.9	<200	450	1.9	10.8	2.4	<100	<2	6.0	0.75	<120	25	475
230	625.0	783	<50	190	36.9	9	<200	1925	2	13	<9	<100	<1.0	5.5	0.8	54	93	2018
231	44.7	78	<50	40	7.23	1.5	<200	201	1.2	5.9	1.2	<100	<2	4.2	0.53	59	88	289
232	822.0	1120	70	204	35.90	7.0	<200	2645	2.3	9.6	3.0	<100	2	7.8	0.92	<110	26	2671
233	3110.0	3690	224	615	92.60	17.8	<200	9077	4.1	16.9	4.3	<100	<2	7.6	0.81	120	191	9268
234	9610.0	10200	800	1490	201.0	40	<200	26171	9	36	<4	<100	<1.0	17.0	1.1	173	292	26463
235	734.0	822	58	185	25.30	5.1	<200	2143	1.9	9.2	2.3	<100	<2	6.3	0.80	92	140	2283
236	11700.0	12800	837	2040	254.00	43.2	<200	32417	12.9	35.0	10.0	<100	3	25.2	2.60	271	446	32863
237	4760.0	5590	450	890	124.0	24	<200	13866	6	28	<2	<100	<1.0	11.0	0.9	153	247	14113

Appendix A.-- Analytical results and sample descriptions for samples from the Red Cloud mining district, Lincoln County, New Mexico.--continued

Sample Number	La PPM (INA)	Ce PPM (INA)	Pr PPM (INA)	Nd PPM (INA)	Sm PPM (INA)	Eu PPM (INA)	Gd PPM (INA)	Light Group REO	Tb PPM (INA)	Dy PPM (INA)	Ho PPM (INA)	Er PPM (INA)	Tm PPM (INA)	Yb PPM (INA)	Lu PPM (INA)	Y PPM (XRF)	Heavy Group REO	Total REO
238	11600.0	12900	430	1920	216.00	41.1	<200	31755	8.5	21.2	2.9	<100	<2	8.3	0.95	79	148	31903
239	264.0	350	<50	70	15.40	3.8	<200	823	1.8	11.1	3.7	<100	<2	9.4	1.20	90	145	969
240	374.0	502	<80	107	22.70	4.3	<200	1183	2.1	12.2	2.9	<100	<2	8.0	1.10	75	125	1308
241	2.7	<5	<50	<10	0.27	<0.1	<200	3	<1.0	<1.0	<1.0	<100	<2	<0.5	<0.10	3	4	7
242	16.0	21	<50	10	2.19	0.6	<200	58	<1.0	1.0	<1.0	<100	<2	0.7	0.12	15	21	79
243	174.0	205	<50	49	7.87	1.8	<200	513	<1.0	3.4	1.0	<100	<2	3.5	0.46	50	73	586
244	26.0	43	<50	18	4.37	1.2	<200	108	<1.0	4.1	<1.0	<100	<2	3.0	0.42	49	71	179
245	47.0	78	<50	36	6.30	1.6	<200	198	<1.0	4.1	<1.0	<100	<2	2.6	0.38	45	65	263
246	255.0	360	<50	87	17.70	4.4	<200	848	2.3	13.0	2.9	<100	<2	9.6	1.30	154	229	1077
247	4320.0	5980	<300	658	77.70	13.6	<200	12944	2.9	18.2	6.0	<100	<2	7.3	1.09	80	142	13086
248	831.0	1320	147	164	26.90	5.4	<200	2921	1.8	15.2	4.0	<100	<2	10.3	1.40	95	158	3080
249	8630.0	9080	400	1340	149.00	27.4	<200	22992	6.7	28.3	4.8	<100	3	12.0	1.42	142	245	23237
250	6480.0	6430	<500	880	94.90	17.0	<200	16287	4.4	11.1	2.6	<100	<2	9.1	1.03	81	135	16422
251	10800.0	12300	570	1900	220.00	39.1	<200	30256	8.6	24.3	4.2	<100	<2	9.0	0.96	76	150	30407
252	120.0	209	<50	63	12.80	3.1	<200	477	1.7	14.0	2.8	<100	<2	9.4	1.42	110	170	647
253	38.8	74	<50	25	5.05	1.1	<200	168	<1.0	4.1	1.2	<100	<2	4.8	0.80	41	65	233
254	92.4	146	<50	60	12.20	3.6	<200	368	1.7	10.7	2.8	<100	<2	4.2	0.45	<90	23	390
255	249.0	370	<50	85	20.7	5	<200	854	2	11	1	<100	<1.0	6.3	0.9	43	79	933
256	84.0	175	<50	67	15.30	4.2	<200	404	2.3	12.0	1.9	<100	<2	8.4	1.02	<140	29	434
257	467.0	692	50	140	26.0	6	<200	1617	2	10	<1	<100	<1.0	5.4	0.8	49	83	1700

Appendix A.-- Analytical results and sample descriptions for samples from the Red Cloud mining district, Lincoln County, New Mexico.--continued

Sample Number	La PPM (INA)	Ce PPM (INA)	Pr PPM (INA)	Nd PPM (INA)	Sm PPM (INA)	Eu PPM (INA)	Gd PPM (INA)	Light Group REO	Tb PPM (INA)	Dy PPM (INA)	Ho PPM (INA)	Er PPM (INA)	Tm PPM (INA)	Yb PPM (INA)	Lu PPM (INA)	Y PPM (XRF)	Heavy Group REO	Total REO
258	120.0	224	<50	76	12.80	3.4	<200	511	1.0	4.1	<1.0	<100	<2	3.7	0.56	47	70	581
259	41.1	74	<50	27	6.90	1.6	<200	176	<1.0	5.5	1.4	<100	<2	3.9	0.52	52	79	255
260	64.4	86	<50	23	2.9	<1	<200	206	<1	<1	<1	<100	<1.0	0.8	<0.1	7	10	216

Appendix A.-- Analytical results and sample descriptions for samples from the Red Cloud mining district, Lincoln County, N. Mex.--continued

Sample Number	LREO/ HREO	% LREO	Sc PPM (INA)	Th PPM (INA)	U PPM (INA)	Th/U RATIO	Au PPB (FA-AA)	Ag PPM (ICP)	Cu PPM (ICP)	Pb PPM (ICP)	Zn PPM (ICP)	Mo PPM (ICP)	Nb PPM (XRF)	Ni PPM (ICP)	Co PPM (ICP)	Bi PPM (ICP)	As PPM (ICP)	Sb PPM (ICP)
1	55	98.2	4.13	28.1	26.5	1.1	174	0.2	1266	559	309	6	na	3	3	39	50	7
2	24	96.0	4.20	22.0	6.5	3.4	139	0.5	301	141	398	7	na	9	4	<5	121	<5
3	40	97.6	4.22	38.2	9.2	4.2	222	1.0	223	318	1330	8	na	6	6	<5	123	9
4	51	98.1	3.45	25.8	18.9	1.4	175	3.5	3121	367	232	11	na	3	3	24	70	10
5	34	97.1	4.39	29.1	11.7	2.5	117	2.5	559	278	698	6	na	7	4	<5	97	<5
6	50	98.0	8.65	32.4	27.2	1.2	170	3.7	7220	337	411	9	na	5	6	25	124	12
7	22	95.6	2.50	67.5	14.0	4.8	37	<0.2	14	68	279	8	na	5	5	<5	94	<5
8	25	96.2	2.80	38.0	7.9	4.8	31	<0.2	17	22	57	5	na	7	7	<5	42	<5
9	47	97.9	4.50	45.0	8.0	5.6	54	<0.2	11	47	323	5	na	6	8	<5	44	<5
10	52	98.1	1.82	5.5	4.5	1.2	30	<0.2	81	584	89	194	na	6	2	5	34	9
11	18	94.8	3.21	4.8	2.4	2.0	35	0.6	62	350	100	22	na	10	4	<5	21	5
12	121	99.2	2.09	24.1	10.9	2.2	496	27.3	4250	2.97%	182	618	na	<1	2	16	985	206
13	59	98.3	3.75	6.4	10.5	0.6	135	<0.2	415	1869	911	364	na	5	3	7	42	10
14	34	97.1	7.34	9.2	10.2	0.9	28	<0.2	158	205	529	44	na	10	4	<5	40	8
15	37	97.3	3.96	5.9	13.3	0.4	19	<0.2	263	181	297	11	na	6	8	<5	19	<5
16	16	94.1	2.11	5.9	4.0	1.5	32	0.2	19	81	103	37	na	5	2	<5	8	<5
17	22	95.6	3.10	20.5	7.7	2.7	63	0.9	108	799	547	93	na	14	14	12	116	17
18	50	98.1	4.75	3.2	5.9	0.5	33	<0.2	32	321	239	22	na	5	3	<5	20	<5
19	43	97.7	6.66	14.4	10.0	1.4	80	<0.2	63	519	201	24	na	9	5	<5	16	<5
20	153	99.3	3.76	19.3	42.7	0.5	610	11.2	5823	3.34%	933	1316	na	2	4	23	1039	224

Appendix A.-- Analytical results and sample descriptions for samples from the Red Cloud mining district, Lincoln County, New Mexico.--continued

Sample Number	LREO/ HREO	% LREO	Sc PPM (INA)	Th PPM (INA)	U PPM (INA)	Th/U RATIO	Au PPB (FA-AA)	Ag PPM (ICP)	Cu PPM (ICP)	Pb PPM (ICP)	Zn PPM (ICP)	Mo PPM (ICP)	Nb PPM (XRF)	Ni PPM (ICP)	Co PPM (ICP)	Bi PPM (ICP)	As PPM (ICP)	Sb PPM (ICP)
21	11	91.7	14.90	30.0	6.8	4.4	<5	<0.2	50	32	83	2	na	14	18	<5	<5	<5
22	5	83.7	0.55	23.0	8.7	2.6	71	<0.2	10	52	43	2	118	1	1	<5	<5	<5
23	16	94.3	1.00	71.3	6.4	11.1	12	<0.2	17	17	51	<1	118	1	4	<5	<5	<5
24	7	86.8	1.00	49.0	14.0	3.5	41	<0.2	18	503	123	41	na	3	2	<5	16	6
25	6	86.3	2.80	20.0	20.0	1.0	19	<0.2	29	711	321	81	na	10	6	6	23	17
26	6	85.6	0.97	120.0	23.6	5.1	<5	<0.2	14	178	7	6	na	2	<1	<5	13	<5
27	5	82.9	0.53	120.0	19.0	6.3	45	<0.2	6	26	8	2	na	1	<1	<5	<5	<5
28	3	77.5	0.52	130.0	23.0	5.7	19	<0.2	5	52	10	1	na	3	<1	<5	<5	<5
29	8	88.7	0.62	274.0	8.8	31.1	<5	<0.2	9	10	15	1	na	3	2	<5	<5	<5
30	13	93.1	0.80	34.0	4.5	7.6	<5	<0.2	6	17	21	1	89	4	2	<5	<5	<5
31	7	88.1	17.00	24.0	5.0	4.8	5	<0.2	26	19	62	3	na	22	15	<5	<5	<5
32	6	85.7	4.60	5.1	1.2	4.3	25	<0.2	18	10	20	2	3	4	5	<5	<5	<5
33	6	86.2	1.50	36.0	4.1	8.8	12	<0.2	30	102	62	4	55	11	5	<5	<5	<5
34	7	87.2	0.38	56.6	13.0	4.4	<5	<0.2	8	23	20	1	150	5	2	<5	<5	<5
35	7	87.7	3.90	33.0	5.2	6.3	<5	<0.2	25	71	62	2	na	14	7	<5	<5	<5
36	10	90.9	4.50	23.0	3.1	7.4	165	<0.2	193	16	108	7	na	19	10	<5	<5	<5
37	12	92.1	20.10	23.0	5.0	4.6	18	<0.2	54	18	120	3	57	22	23	<5	5	<5
38	16	94.1	17.70	25.0	4.7	5.3	73	<0.2	47	28	144	3	52	21	16	<5	<5	<5
39	12	92.2	19.00	31.0	4.9	6.3	11	<0.2	53	20	133	5	74	24	19	<5	<5	<5
40	11	91.9	18.20	23.0	5.5	4.2	15	<0.2	30	20	113	6	61	25	20	<5	<5	<5

Appendix A.-- Analytical results and sample descriptions for samples from the Red Cloud mining district, Lincoln County, New Mexico.--continued

Sample Number	LREO/ HREO	% LREO	Sc PPM (INA)	Th PPM (INA)	U PPM (INA)	Th/U RATIO	Au PPB (FA-AA)	Ag PPM (ICP)	Cu PPM (ICP)	Pb PPM (ICP)	Zn PPM (ICP)	Mo PPM (ICP)	Nb PPM (XRF)	Ni PPM (ICP)	Co PPM (ICP)	Bi PPM (ICP)	As PPM (ICP)	Sb PPM (ICP)
41	12	92.4	0.37	60.7	6.6	9.2	<5	<0.2	10	17	42	<1	102	3	2	<5	<5	<5
42	5	83.4	5.40	5.3	<1	xx	7	<0.2	12	5	15	<1	9	5	2	<5	<5	<5
43	10	90.6	10.20	27.0	6.2	4.4	<5	<0.2	56	12	71	4	na	17	16	<5	10	<5
44	9	89.8	10.40	27.8	3.9	7.1	20	<0.2	34	18	69	3	na	18	14	<5	<5	<5
45	9	90.3	10.70	32.5	5.7	5.7	12	<0.2	10	19	45	<1	na	27	12	<5	7	<5
46	25	96.2	6.15	27.8	14.0	2.0	21	<0.2	18	63	53	13	na	4	2	<5	9	<5
47	6	86.5	6.81	7.1	2.4	3.0	<5	0.4	11	51	41	3	na	6	3	8	24	6
48	5	83.5	5.70	6.3	1.7	3.7	<5	<0.2	2	21	29	4	na	12	3	<5	<5	<5
49	14	93.1	4.90	18.0	7	2.6	5	<0.5	22	64	156	14	na	14	<5	<5	3.8	2.7
50	15	93.7	6.70	10.3	9.3	1.1	<5	<0.2	27	63	87	7	na	6	4	<5	14	<5
51	12	92.2	6.40	16.0	18.0	0.9	<5	<0.2	9	84	35	6	na	4	2	<5	<5	<5
52	17	94.5	3.70	19.0	6.9	2.8	<5	<0.2	9	33	88	5	na	4	5	<5	10	<5
53	30	96.8	5.25	12.4	14.7	0.8	14	<0.2	20	70	20	7	na	4	3	<5	11	<5
54	6	86.2	0.63	63.4	10.0	6.3	9	<0.2	4	8	30	3	181	2	2	<5	<5	<5
55	5	83.2	8.40	18.0	3.9	4.6	<5	<0.2	14	8	25	<1	na	19	16	<5	<5	<5
56	7	87.6	6.11	20.5	5.8	3.5	12	0.4	48	233	66	9	na	22	6	<5	34	8
57	6	86.3	8.30	22.7	3.4	6.7	7	0.2	64	52	65	3	na	19	9	<5	18	5
58	37	97.4	2.50	8.0	20	0.4	8	0.7	12	13	30	24	na	11	120	<5	7.0	2.1
59	15	93.7	0.50	13.8	18.9	0.7	<5	<0.2	88	31	41	6	na	11	34	26	<5	14
60	8	88.3	7.41	20.9	3.2	6.5	<5	0.2	22	55	39	2	na	17	10	<5	16	<5

Appendix A.-- Analytical results and sample descriptions for samples from the Red Cloud mining district, Lincoln County, New Mexico.--continued

Sample Number	LREO/ HREO	% LREO	Sc PPM (INA)	Th PPM (INA)	U PPM (INA)	Th/U RATIO	Au PPB (FA-AA)	Ag PPM (ICP)	Cu PPM (ICP)	Pb PPM (ICP)	Zn PPM (ICP)	Mo PPM (ICP)	Nb PPM (XRF)	Ni PPM (ICP)	Co PPM (ICP)	Bi PPM (ICP)	As PPM (ICP)	Sb PPM (ICP)
61	11	92.0	4.97	3.6	<1.0	xx	<5	<0.2	70	340	53	<1	na	6	7	6	<5	<5
62	10	91.1	8.59	28.0	5.5	5.1	15	<0.2	28	88	45	12	na	16	12	<5	<5	5
63	7	88.0	6.57	31.3	6.2	5.0	<5	<0.2	12	26	57	11	na	15	11	<5	12	<5
64	11	91.6	1.30	56.4	4.5	12.5	30	<0.2	86	109	19	10	na	4	2	<5	39	75
65	6	85.7	8.82	19.6	4.2	4.7	<5	0.5	11	23	32	3	na	14	11	<5	<5	<5
66	8	89.2	5.70	43.0	9.5	4.5	<5	<0.2	7	5	33	3	na	15	11	<5	5	<5
67	7	88.1	4.82	59.7	11.2	5.3	<5	<0.2	41	19	32	1	na	13	11	<5	16	6
68	8	88.4	5.14	54.0	12.0	4.5	<5	<0.2	23	81	78	5	na	13	8	<5	14	<5
69	7	87.4	4.50	56.0	11.5	4.9	<5	<0.2	5	18	39	2	na	9	6	<5	8	<5
70	8	89.0	4.45	67.9	12.8	5.3	<5	<0.2	16	55	31	2	na	16	12	<5	<5	<5
71	39	97.5	2.20	20.0	7.6	2.6	141	<0.2	6	72	16	20	<1	5	2	<5	<5	<5
72	16	94.0	1.90	49.0	9.8	5.0	27	<0.2	9	36	37	20	na	5	3	<5	<5	<5
73	12	92.0	1.60	38.0	10.0	3.8	58	<0.2	25	1244	52	41	72	3	2	<5	7	<5
74	5	83.0	1.60	38.0	7.8	4.9	35	<0.2	8	180	24	6	93	5	3	<5	<5	<5
75	44	97.8	2.52	30.0	13.0	2.3	116	<0.2	108	1353	17	72	na	3	2	<5	46	<5
76	71	98.6	4.29	47.6	6.0	7.9	19	<0.2	30	402	47	63	na	6	3	<5	26	11
77	43	97.7	3.64	36.3	6.8	5.3	24	<0.2	15	685	58	33	na	5	5	<5	<5	<5
78	18	94.6	2.20	42.0	5.3	7.9	<5	<0.2	9	78	150	10	148	2	8	<5	7	<5
79	66	98.5	6.30	52.0	9.2	5.7	29	<0.2	34	1701	82	54	na	7	3	<5	<5	<5
80	35	97.2	3.00	130.0	84.0	1.5	17	<0.2	95	64	43	34	na	3	4	<5	<5	<5

Appendix A.-- Analytical results and sample descriptions for samples from the Red Cloud mining district, Lincoln County, New Mexico.--continued

Sample Number	LREO/ HREO	% LREO	Sc PPM (INA)	Th PPM (INA)	U PPM (INA)	Th/U RATIO	Au PPB (FA-AA)	Ag PPM (ICP)	Cu PPM (ICP)	Pb PPM (ICP)	Zn PPM (ICP)	Mo PPM (ICP)	Nb PPM (XRF)	Ni PPM (ICP)	Co PPM (ICP)	Bi PPM (ICP)	As PPM (ICP)	Sb PPM (ICP)
81	26	96.3	2.55	47.7	4.1	11.6	18	<0.2	178	2124	79	232	na	4	3	<5	49	22
82	47	97.9	4.43	42.5	7.2	5.9	24	<0.2	14	968	113	20	na	4	2	<5	<5	<5
83	4	81.6	0.68	56.4	7.8	7.2	11	<0.2	12	389	43	9	132	3	2	<5	9	<5
84	2	70.7	2.00	43.0	7.5	5.7	<5	<0.2	4	148	24	6	102	5	4	<5	<5	<5
85	4	80.9	0.94	50.5	3.8	13.3	<5	<0.2	2	3	11	2	135	3	2	<5	<5	<5
86	1	54.8	1.50	40.0	13.0	3.1	27	<0.2	6	44	6	46	69	4	2	<5	18	<5
87	26	96.3	1.93	100.0	17.0	5.9	32	<0.2	11	75	53	150	na	4	3	<5	<5	<5
88	6	85.2	1.50	41.6	6.2	6.7	48	<0.2	9	7	58	3	na	3	3	<5	<5	<5
89	144	99.3	4.06	122.0	26.0	4.7	71	2.9	5254	6.18%	554	134	na	8	5	7	>2000	893
90	71	98.6	2.21	69.7	13.0	5.4	18	<0.2	206	3441	174	25	na	7	3	<5	83	42
91	7	87.9	8.14	37.2	5.7	6.5	<5	<0.2	19	79	21	<1	na	15	4	<5	6	<5
92	9	89.9	0.82	47.3	6.2	7.6	13	<0.2	10	29	23	4	na	2	<1	<5	<5	<5
93	15	93.9	2.00	37.3	7.6	4.9	55	<0.2	21	67	77	4	na	2	4	<5	8	<5
94	13	93.0	2.40	45.4	7.4	6.1	15	<0.2	17	43	115	26	na	4	3	<5	<5	<5
95	12	92.3	1.44	43.1	3.7	11.6	10	<0.2	29	28	35	1	na	3	2	<5	<5	<5
96	16	94.3	0.56	2.1	8.4	0.3	6	<0.2	104	56	77	14	na	10	17	32	<5	14
97	7	87.6	6.62	29.0	5.7	5.1	23	<0.2	19	18	74	4	na	14	7	<5	24	<5
98	5	83.8	6.64	28.5	5.7	5.0	17	<0.2	11	13	80	6	na	15	8	<5	10	<5
99	4	81.8	9.09	28.4	5.2	5.5	<5	<0.2	11	25	56	3	na	18	10	<5	13	<5
100	8	88.3	6.90	9.6	4.1	2.3	16	<0.2	10	22	56	22	na	17	7	<5	11	5

Appendix A.-- Analytical results and sample descriptions for samples from the Red Cloud mining district, Lincoln County, New Mexico.--continued

Sample Number	LREO/ HREO	% LREO	Sc PPM (INA)	Th PPM (INA)	U PPM (INA)	Th/U RATIO	Au PPB (FA-AA)	Ag PPM (ICP)	Cu PPM (ICP)	Pb PPM (ICP)	Zn PPM (ICP)	Mo PPM (ICP)	Nb PPM (XRF)	Ni PPM (ICP)	Co PPM (ICP)	Bi PPM (ICP)	As PPM (ICP)	Sb PPM (ICP)
101	6	86.0	7.27	6.5	2.0	3.3	11	0.2	5	6	11	2	na	16	4	<5	14	<5
102	86	98.8	3.08	25.5	24.6	1.0	7	<0.2	15	255	52	17	na	5	5	<5	<5	<5
103	11	91.8	7.14	8.4	4.8	1.8	<5	<0.2	75	11	67	23	na	15	5	<5	<5	<5
104	4	80.9	6.86	8.7	2.8	3.1	15	<0.2	5	25	76	2	na	17	5	<5	<5	<5
105	15	93.9	1.50	110.0	14.0	7.9	49	<0.2	135	86	51	113	na	4	2	<5	13	17
106	5	82.9	0.93	63.6	8.1	7.9	32	<0.2	39	12	5	5	na	1	<1	<5	12	9
107	2	67.0	9.06	9.0	4.4	2.0	116	2.5	40	34	83	7	na	14	7	<5	<5	<5
108	18	94.8	4.80	40.0	5.7	7.0	145	<0.2	14	51	203	7	na	17	8	<5	<5	<5
109	60	98.4	4.80	23.0	4.9	4.7	43	<0.2	3	39	140	6	na	15	8	<5	7	<5
110	2	66.0	3.20	6.2	2.1	3.0	<5	0.5	8	18	52	3	na	8	5	<5	14	<5
111	31	96.9	1.40	20.0	5.5	3.6	<5	<0.2	109	42	26	11	na	7	5	<5	50	20
112	46	97.9	3.80	25.0	12.0	2.1	6	<0.2	26	59	54	14	na	9	4	<5	5	<5
113	76	98.7	4.30	21.0	4.9	4.3	7	<0.2	16	32	109	14	na	12	6	<5	12	<5
114	37	97.3	4.50	13.0	4.3	3.0	<5	<0.2	12	21	99	8	na	11	5	<5	<5	<5
115	181	99.5	2.40	26.0	5.6	4.6	12	<0.2	65	80	51	16	na	5	3	<5	15	7
116	188	99.5	3.70	28.0	18.0	1.6	29	<0.2	87	113	117	18	na	12	6	<5	7	<5
117	54	98.2	3.20	11.0	6.9	1.6	51	<0.2	32	76	93	8	na	14	7	<5	5	<5
118	133	99.3	3.40	38.0	19.0	2.0	45	<0.2	196	236	175	32	na	15	6	<5	27	18
119	99	99.0	4.70	18.0	5.5	3.3	28	<0.2	126	53	166	23	na	20	10	<5	12	<5
120	124	99.2	6.50	28.0	4.3	6.5	49	<0.2	9	47	125	9	na	20	11	<5	<5	<5

Appendix A.-- Analytical results and sample descriptions for samples from the Red Cloud mining district, Lincoln County, New Mexico.--continued

Sample Number	LREO/ HREO	% LREO	Sc PPM (INA)	Th PPM (INA)	U PPM (INA)	Th/U RATIO	Au PPB (FA-AA)	Ag PPM (ICP)	Cu PPM (ICP)	Pb PPM (ICP)	Zn PPM (ICP)	Mo PPM (ICP)	Nb PPM (XRF)	Ni PPM (ICP)	Co PPM (ICP)	Bi PPM (ICP)	As PPM (ICP)	Sb PPM (ICP)
121	135	99.3	4.90	39.0	7.1	5.5	94	<0.2	166	168	182	19	na	13	5	<5	14	<5
122	111	99.1	3.10	21.0	7.4	2.8	22	<0.2	31	95	90	7	na	9	5	<5	<5	<5
123	120	99.2	4.50	18.0	6.3	2.9	404	0.2	758	84	858	15	na	18	11	<5	328	158
124	185	99.5	4.90	30.0	12.0	2.5	66	<0.2	39	228	268	26	na	19	8	<5	17	<5
125	37	97.3	4.00	15.0	5.7	2.6	78	<0.2	17	35	96	8	na	12	5	<5	10	<5
126	16	94.3	6.70	12.0	4.2	2.9	98	0.5	16	27	182	10	na	19	10	6	44	13
127	2	70.8	5.90	8.6	3.2	2.7	17	0.5	18	27	74	6	na	18	5	<5	15	<5
128	128	99.2	3.40	24.0	7.2	3.3	755	<0.2	299	66	130	18	na	12	7	<5	189	30
129	10	91.0	9.00	10.0	3.1	3.2	30	0.2	11	9	241	1	na	29	8	<5	23	<5
130	119	99.2	4.00	30.0	13.0	2.3	75	<0.2	22	62	75	14	na	8	5	<5	17	<5
131	42	97.7	6.10	14.0	5.8	2.4	28	<0.2	5	50	183	9	na	14	6	<5	6	<5
132	92	98.9	2.70	23.0	12.0	1.9	<5	<0.2	108	154	110	29	na	7	4	<5	14	6
133	203	99.5	2.60	41.0	65.0	0.6	10	<0.2	19	58	2	4	na	5	3	<5	<5	<5
134	107	99.1	4.50	24.0	5.1	4.7	21	<0.2	138	74	90	15	na	7	3	<5	31	18
135	29	96.6	7.93	26.0	7.1	3.7	72	<0.2	270	127	360	7	na	27	10	5	77	8
136	9	90.1	8.20	13.0	4.9	2.7	85	<0.2	405	71	369	5	na	27	10	16	83	7
137	25	96.2	18.00	22.4	7.2	3.1	131	0.7	1482	166	668	7	na	34	9	10	276	37
138	11	91.4	8.35	11.7	3.1	3.8	157	1.1	435	95	579	5	na	26	10	<5	183	18
139	13	93.0	9.46	14.0	4.2	3.3	378	<0.2	1240	157	355	2	na	19	7	45	393	76
140	6	85.3	10.80	10.8	4.2	2.6	367	1.2	824	112	247	4	na	21	8	23	265	14

Appendix A.-- Analytical results and sample descriptions for samples from the Red Cloud mining district, Lincoln County, New Mexico.--continued

Sample Number	LREO/ HREO	% LREO	Sc PPM (INA)	Th PPM (INA)	U PPM (INA)	Th/U RATIO	Au PPB (FA-AA)	Ag PPM (ICP)	Cu PPM (ICP)	Pb PPM (ICP)	Zn PPM (ICP)	Mo PPM (ICP)	Nb PPM (XRF)	Ni PPM (ICP)	Co PPM (ICP)	Bi PPM (ICP)	As PPM (ICP)	Sb PPM (ICP)
141	4	80.3	11.00	10.0	3.0	3.3	329	1.0	423	129	192	3	na	23	9	10	210	25
142	14	93.2	21.40	12.5	18.2	0.7	96	<0.2	64	405	410	14	na	30	9	6	129	8
143	25	96.2	22.10	27.0	3.6	7.5	118	<0.2	186	1711	423	22	na	44	15	<5	50	7
144	23	95.9	4.00	6.7	4.1	1.6	130	1.4	727	2151	180	6	na	17	8	<5	638	43
145	43	97.7	9.65	16.2	14.0	1.2	615	22.2	10409	2.45%	1578	49	na	28	12	21	1852	312
146	36	97.3	6.81	6.0	25.0	0.2	307	1.52opt	2.44%	22.87%	4342	1194	na	5	5	30	>2000	645
147	39	97.5	1.48	2.2	16.0	0.1	264	10.10opt	8.92%	37.09%	3424	136	na	<1	2	94	>2000	1200
148	24	96.0	1.60	7.9	13.9	0.6	770	14.3	10627	1578	433	13	na	7	3	17	>2000	634
149	50	98.0	2.10	7.8	16.0	0.5	1707	2.05opt	4.53%	2.93%	2750	46	na	6	8	82	>2000	1190
150	52	98.1	2.00	8.7	34.0	0.3	531	5.75opt	8.80%	9.85%	3541	65	na	2	11	72	>2000	>2000
151	4	80.6	3.05	9.0	9.0	1.0	1137	39.7	6648	4094	670	12	na	2	2	23	>2000	714
152	5	83.5	4.16	47.4	12.3	3.9	79	2.5	282	55	30	69	na	3	2	<5	39	10
153	16	94.2	2.92	10.0	10.8	0.9	<5	<0.2	16	26	30	123	na	10	4	<5	<5	<5
154	251	99.6	6.30	68.0	6.7	10.1	29	<0.2	99	406	152	5	na	8	3	<5	<5	<5
155	8	89.3	9.00	6.9	4.2	1.6	45	0.3	73	236	87	6	na	15	6	<5	33	<5
156	9	89.5	5.50	10.0	6.9	1.4	21	<0.2	228	52	225	17	na	18	6	<5	47	8
157	113	99.1	5.20	21.0	4.6	4.6	<5	<0.2	211	85	164	7	na	10	5	<5	8	<5
158	138	99.3	3.80	27.0	2.9	9.3	42	<0.2	237	88	96	5	na	7	3	<5	17	10
159	160	99.4	4.90	49.0	7.1	6.9	14	<0.2	393	82	194	27	na	11	4	<5	46	16
160	95	99.0	4.10	63.3	19.0	3.3	289	3.1	3551	575	204	56	na	6	4	8	788	384

Appendix A.-- Analytical results and sample descriptions for samples from the Red Cloud mining district, Lincoln County, New Mexico.--continued

Sample Number	LREO/ HREO	% LREO	Sc PPM (INA)	Th PPM (INA)	U PPM (INA)	Th/U RATIO	Au PPB (FA-AA)	Ag PPM (ICP)	Cu PPM (ICP)	Pb PPM (ICP)	Zn PPM (ICP)	Mo PPM (ICP)	Nb PPM (XRF)	Ni PPM (ICP)	Co PPM (ICP)	Bi PPM (ICP)	As PPM (ICP)	Sb PPM (ICP)
161	36	97.3	5.49	123.0	8.9	13.8	74	<0.2	216	409	328	178	na	28	7	<5	7	8
162	10	90.6	2.66	19.0	1.6	11.9	29	<0.2	575	294	234	58	na	4	1	14	155	22
163	14	93.2	0.71	15.0	2.6	5.8	74	<0.2	448	1680	400	58	na	3	1	<5	420	213
164	27	96.5	4.56	19.0	8.1	2.3	163	<0.2	127	348	74	6	na	9	4	<5	69	12
165	439	99.8	4.65	90.6	17.0	5.3	293	3.2	3813	8284	453	246	na	7	6	<5	1999	401
166	265	99.6	7.18	52.7	14.0	3.8	594	13.8	8774	4288	986	50	na	7	8	<5	1877	438
167	107	99.1	5.42	47.8	33.6	1.4	246	4.6	4240	3260	2670	18	na	12	4	<5	713	240
168	389	99.7	3.84	69.0	65.0	1.1	600	<0.2	2577	5429	3337	10	na	14	7	<5	640	222
169	447	99.8	3.91	78.2	52.0	1.5	526	6.9	5174	8144	9726	35	na	6	5	<5	1377	273
170	561	99.8	3.26	89.0	36.5	2.4	307	2.5	2800	9219	1935	111	na	7	3	<5	742	118
171	7	87.7	4.70	13.0	7.9	1.6	208	0.5	219	115	161	20	na	18	6	<5	79	22
172	21	95.4	3.54	4.7	69.0	0.1	596	36.2	18267	1.71%	3853	51	na	17	4	28	>2000	1291
173	5	84.4	3.61	6.8	10.0	0.7	25	2.6	365	301	154	25	na	8	3	8	292	132
174	4	79.1	9.20	12.2	6.6	1.8	11	1.3	540	296	1115	35	na	44	10	9	232	45
175	15	93.7	7.48	16.4	26.8	0.6	99	25.8	1.96%	1094	2001	16	na	13	6	40	>2000	1179
176	180	99.4	2.64	60.6	78.9	0.8	67	13.6	18118	2.14%	189	262	na	2	2	27	>2000	>2000
177	12	92.4	9.26	24.7	15.0	1.6	20	6.0	1297	446	317	68	na	12	6	<5	660	172
178	509	99.8	2.75	77.3	37.6	2.1	150	<0.2	660	1.38%	726	246	na	6	4	<5	264	89
179	45	97.8	5.20	50.0	15.0	3.3	76	0.9	1749	266	300	76	na	23	8	<5	284	88
180	218	99.5	7.51	150.0	19.0	7.9	66	<0.2	423	220	80	7	na	5	3	<5	43	51

Appendix A.-- Analytical results and sample descriptions for samples from the Red Cloud mining district, Lincoln County, New Mexico.--continued

Sample Number	LREO/ HREO	% LREO	Sc PPM (INA)	Th PPM (INA)	U PPM (INA)	Th/U RATIO	Au PPB (FA-AA)	Ag PPM (ICP)	Cu PPM (ICP)	Pb PPM (ICP)	Zn PPM (ICP)	Mo PPM (ICP)	Nb PPM (XRF)	Ni PPM (ICP)	Co PPM (ICP)	Bi PPM (ICP)	As PPM (ICP)	Sb PPM (ICP)
181	44	97.8	2.55	48.8	16.0	3.1	25	<0.2	314	247	48	43	na	6	3	<5	80	18
182	13	92.7	8.51	7.3	5.0	1.5	23	0.5	313	125	160	6	na	8	5	<5	65	18
183	325	99.7	5.40	85.8	19.6	4.4	250	<0.2	1042	1.42%	792	78	na	4	3	<5	266	141
184	54	98.2	4.43	10.0	17.9	0.6	920	9.4	7297	1.43%	1259	32	na	6	5	14	>2000	1262
185	5	83.0	12.00	17.4	9.2	1.9	167	1.5	548	72	393	16	na	26	8	<5	162	55
186	56	98.3	3.72	55.0	10.9	5.0	107	<0.2	570	510	237	15	na	5	2	<5	180	88
187	41	97.6	1.80	40.0	10.0	4.0	15	<0.2	563	1546	42	3	na	2	2	<5	101	19
188	312	99.7	3.30	93.5	<20.0	xx	57	<0.2	884	6457	324	50	na	7	4	<5	385	33
189	200	99.5	2.40	53.1	4.4	12.1	<5	<0.2	42	86	103	12	na	6	2	<5	<5	<5
190	183	99.5	2.20	46.0	7.2	6.4	<5	<0.2	30	93	85	9	na	7	3	<5	<5	<5
191	57	98.3	2.80	12.0	3.4	3.5	13	<0.2	21	29	100	14	na	11	4	<5	15	<5
192	17	94.4	3.70	11.0	7.0	1.6	9	<0.2	52	52	235	20	na	23	15	<5	28	9
193	76	98.7	2.30	16.0	3.6	4.4	<5	<0.2	7	78	38	6	na	3	2	<5	<5	<5
194	45	97.8	3.30	29.0	6.4	4.5	<5	<0.2	14	80	156	22	na	8	3	<5	<5	<5
195	47	97.9	1.40	45.0	22.0	2.0	<5	<0.2	10	48	34	20	na	5	3	<5	<5	<5
196	11	91.8	4.50	8.5	3.7	2.3	14	<0.2	42	43	86	6	na	15	5	<5	16	<5
197	82	98.8	4.00	25.0	14.0	1.8	23	<0.2	17	84	61	9	na	8	4	<5	<5	<5
198	6	85.7	5.30	8.0	2.0	4.0	53	0.3	18	31	97	6	na	17	6	<5	24	<5
199	58	98.3	2.20	12.0	21.0	0.6	6	<0.2	4	64	41	6	na	3	2	<5	<5	<5
200	71	98.6	3.40	15.0	6.0	2.5	20	<0.2	7	34	43	7	na	6	4	<5	25	<5

Appendix A.-- Analytical results and sample descriptions for samples from the Red Cloud mining district, Lincoln County, New Mexico.--continued

Sample Number	LREO/ HREO	% LREO	Sc PPM (INA)	Th PPM (INA)	U PPM (INA)	Th/U RATIO	Au PPB (FA-AA)	Ag PPM (ICP)	Cu PPM (ICP)	Pb PPM (ICP)	Zn PPM (ICP)	Mo PPM (ICP)	Nb PPM (XRF)	Ni PPM (ICP)	Co PPM (ICP)	Bi PPM (ICP)	As PPM (ICP)	Sb PPM (ICP)
201	145	99.3	2.40	43.0	9.1	4.7	<5	<0.2	19	99	25	29	na	4	3	<5	<5	<5
202	162	99.4	2.50	28.0	10.0	2.8	8	<0.2	7	57	9	68	na	3	2	<5	<5	<5
203	31	96.8	2.50	8.0	3.8	2.1	<5	<0.2	13	23	34	13	na	11	5	<5	8	<5
204	77	98.7	2.60	19.0	6.7	2.8	15	<0.2	13	41	39	8	na	9	5	<5	7	<5
205	8	88.9	2.64	59.0	16.6	3.6	25	<0.2	45	41	211	24	na	7	3	7	<5	<5
206	62	98.4	10.00	30.0	38.0	0.8	48	<0.2	230	331	690	9	na	28	9	<5	22	18
207	3	77.3	4.30	6.2	3.7	1.7	28	0.6	22	30	63	16	na	10	3	<5	<5	<5
208	46	97.9	1.68	37.8	9.4	4.0	107	<0.2	196	411	40	14	na	3	2	<5	25	<5
209	47	97.9	13.00	93.0	10.9	8.5	102	<0.2	875	506	827	96	na	32	7	<5	206	58
210	25	96.2	3.30	22.1	9.8	2.3	31	6.0	376	322	113	19	na	12	4	<5	75	15
211	18	94.6	5.51	24.1	5.0	4.8	25	<0.2	222	190	105	13	na	9	5	<5	40	10
212	30	96.7	3.17	39.7	23.0	1.7	<5	<0.2	1073	731	128	5	na	8	6	<5	200	71
213	3	71.7	8.38	14.0	4.0	3.5	23	0.7	186	93	126	3	na	10	10	<5	54	10
214	5	83.8	3.88	8.5	75.0	0.1	61	2.38opt	3.70%	1062	5717	8	na	15	6	51	>2000	1467
215	1	46.1	8.16	2.9	5.4	0.5	19	36.8	10471	28	841	2	na	10	10	22	1261	408
216	1	46.6	6.36	3.1	3.0	1.0	12	9.2	4387	23	549	4	na	11	11	11	746	208
217	6	85.6	4.41	30.0	7.0	4.3	15	<0.2	110	18	61	2	na	9	3	<5	34	<5
218	35	97.2	3.13	52.4	7.7	6.8	34	1.9	606	158	578	74	na	7	3	<5	248	47
219	151	99.3	4.09	28.6	16.0	1.8	40	1.9	606	1.68%	241	511	na	5	3	<5	688	109
220	47	97.9	3.00	12.5	9.0	1.4	73	4.1	957	3561	166	30	na	7	9	6	434	162

Appendix A.-- Analytical results and sample descriptions for samples from the Red Cloud mining district, Lincoln County, New Mexico.--continued

Sample Number	LREO/ HREO	% LREO	Sc PPM (INA)	Th PPM (INA)	U PPM (INA)	Th/U RATIO	Au PPB (FA-AA)	Ag PPM (ICP)	Cu PPM (ICP)	Pb PPM (ICP)	Zn PPM (ICP)	Mo PPM (ICP)	Nb PPM (XRF)	Ni PPM (ICP)	Co PPM (ICP)	Bi PPM (ICP)	As PPM (ICP)	Sb PPM (ICP)
221	91	98.9	5.81	52.4	9	5.8	27	5.3	175	70	228	22	na	17	12	<5	80.5	22.9
222	6	86.1	1.33	77.5	18.0	4.3	18	<0.2	84	38	36	6	na	4	2	<5	12	<5
223	3	73.5	1.08	90.7	22.0	4.1	28	<0.2	12	86	42	2	na	2	<1	<5	<5	<5
224	8	89.4	9.34	27.7	8.6	3.2	47	0.7	533	116	694	30	na	42	8	6	94	35
225	11	91.7	3.05	17.6	4.4	4.0	7	<0.2	54	41	61	5	na	6	2	<5	<5	<5
226	4	78.7	4.75	6.9	3.8	1.8	7	0.9	270	796	588	16	na	14	5	<5	66	32
227	59	98.3	5.64	13.1	22.5	0.6	27	13.1	5962	9815	2778	73	na	13	9	17	1473	449
228	36	97.3	4.37	8.5	70.0	0.1	67	3.00opt	13067	21.06%	2128	1198	na	3	3	29	>2000	>2000
229	18	94.7	3.80	7.9	13.1	0.6	14	4.5	1876	5012	4716	41	na	14	6	11	461	94
230	21	95.4	5.87	12.0	195	0.1	<58	2.44opt	15173	9.34%	2954	298	na	8	<10	19	>9000.0	2950.0
231	2	69.4	13.40	10.3	4.5	2.3	30	2.6	728	747	397	10	na	26	29	8	184	59
232	102	99.0	8.32	14.7	17.0	0.9	31	9.4	3798	2.76%	6914	486	na	27	13	21	>2000	381
233	48	97.9	5.72	15.1	23.6	0.6	24	<0.2	150	115	174	13	na	18	5	<5	48	26
234	90	98.9	21.00	31.0	19	1.6	<19	0.6	73	131	462	26	na	17	26	8	35.0	9.5
235	15	93.9	7.00	10.0	6.2	1.6	7	1.3	201	378	303	5	na	20	8	<5	58	20
236	73	98.6	33.00	50.0	32.7	1.5	5	<0.2	29	125	481	29	na	20	7	<5	12	8
237	56	98.3	2.80	16.0	24	0.7	<12	<0.5	135	753	65	15	na	8	<5	7	143.0	46.8
238	214	99.5	7.03	68.5	28.5	2.4	15	<0.2	1832	752	158	11	na	10	4	<5	492	163
239	6	85.0	4.39	11.7	6.4	1.8	28	0.2	167	1057	148	5	na	12	4	<5	49	22
240	9	90.4	4.59	50.2	9.7	5.2	22	<0.2	156	178	133	9	na	10	6	<5	62	24

Appendix A.-- Analytical results and sample descriptions for samples from the Red Cloud mining district, Lincoln County, New Mexico.--continued

Sample Number	LREO/ HREO	% LREO	Sc PPM (INA)	Th PPM (INA)	U PPM (INA)	Th/U RATIO	Au PPB (FA-AA)	Ag PPM (ICP)	Cu PPM (ICP)	Pb PPM (ICP)	Zn PPM (ICP)	Mo PPM (ICP)	Nb PPM (XRF)	Ni PPM (ICP)	Co PPM (ICP)	Bi PPM (ICP)	As PPM (ICP)	Sb PPM (ICP)
241	1	47.7	0.13	<0.5	<1.0	ERR	<5	0.3	6	3	45	<1	na	1	1	<5	<5	<5
242	3	73.4	2.63	2.6	<1.0	ERR	9	0.4	8	5	8	<1	na	6	2	<5	<5	<5
243	7	87.5	6.81	3.8	2.4	1.6	36	1.9	543	241	181	5	na	19	19	9	225	74
244	2	60.5	4.26	7.8	2.0	3.9	10	0.7	173	12	44	2	na	9	4	<5	69	23
245	3	75.2	2.34	9.2	1.7	5.4	7	0.9	171	26	24	2	na	5	2	<5	54	21
246	4	78.7	6.90	16.0	3.0	5.3	61	0.9	222	69	208	5	na	17	3	<5	59	19
247	91	98.9	9.59	67.1	12.3	5.5	41	<0.2	311	440	182	33	na	31	23	<5	142	18
248	18	94.9	10.60	28.8	9.1	3.2	30	<0.2	148	99	231	35	na	32	14	<5	101	20
249	94	98.9	4.47	38.3	41.8	0.9	80	<0.2	678	148	624	27	na	10	6	<5	114	11
250	120	99.2	4.63	29.4	24.8	1.2	29	<0.2	594	171	1463	28	na	48	9	<5	106	16
251	201	99.5	4.61	52.9	50.7	1.0	63	<0.2	529	200	766	13	na	16	13	<5	54	16
252	3	73.7	1.45	97.6	16.6	5.9	17	<0.2	75	1078	111	153	na	3	<1	<5	37	18
253	3	72.3	0.45	77.0	19.0	4.1	8	0.2	158	764	116	8	na	2	<1	<5	71	13
254	16	94.2	5.92	4.2	36.4	0.1	93	21.0	2.32%	1.29%	1782	76	na	44	22	45	1571	484
255	11	91.5	2.70	10.0	19	0.5	170	13.0	4727	3.00%	249	34	na	6	<5	<5	1270.0	218.0
256	14	93.2	2.79	9.2	13.8	0.7	149	9.0	1305	9077	416	56	na	6	2	10	1688	304
257	19	95.1	4.10	17.0	7	2.4	94	3.1	903	1987	194	90	na	13	<5	<5	386.0	73.1
258	7	87.9	8.37	33.0	6.1	5.4	94	<0.2	10	6	30	2	na	7	8	<5	24	<5
259	2	69.1	10.50	9.4	2.6	3.6	24	<0.2	7	4	8	2	na	24	4	<5	9	<5
260	21	95.5	0.79	1.8	4	0.5	<2	<0.5	13	14	55	7	na	<1	78	<5	29.0	1.7

Appendix A.-- Analytical results and sample descriptions for samples from the Red Cloud mining district, Lincoln County, N. Mex.--continued

Sample Number	Hg PPM (CVAA)	Fe PCT (ICP)	Mn PCT (ICP)	Ba PPM (XRF)	Cr PPM (ICP)	W PPM (ICP)	Sr PPM (XRF)	F PPM (SI)	F % (DIST)	CaF2 %
1	0.298	1.41	D.D8	>20D00	11	<10	1126	na	na	xx
2	0.028	1.76	2190*	49D0	26	<20	467	na	na	xx
3	D.125	2.56	0.15	13000	19	<10	966	na	na	xx
4	0.100	1.65	0.13	15600	14	<10	1174	na	na	xx
5	0.096	1.60	0.23	10700	24	<10	987	na	na	xx
6	0.097	2.10	0.36	8400	10	<1D	>2000	na	na	xx
7	<0.010	2.56	3093*	6100	13	<20	943	na	na	xx
8	<0.010	2.54	1705*	4700	14	<20	1482	na	na	xx
9	0.016	2.04	2111*	8200	8	<20	876	na	na	xx
10	0.042	0.95	0.03	>20000	63	<10	>2000	na	na	xx
11	0.064	0.78	0.10	1700	97	<10	378	na	na	xx
12	1.403	1.10	<0.01	9000	14	<10	>2000	na	na	xx
13	0.130	2.74	0.09	18700	10	<10	1175	na	na	xx
14	0.087	2.10	0.38	>20000	16	<10	>2000	na	na	xx
15	0.052	1.00	0.22	17100	11	<10	>2000	na	na	xx
16	0.063	0.63	0.37	8200	11	<10	463	na	na	xx
17	0.121	3.15	0.70	7300	6	<10	1335	na	na	xx
18	0.038	0.74	0.27	14500	8	<10	683	na	na	xx
19	0.085	1.48	0.49	>20000	12	<10	973	na	na	xx
20	2.659	0.66	0.02	15800	11	<10	>2000	na	na	xx

Appendix A.-- Analytical results and sample descriptions for samples from the Red Cloud mining district, Lincoln County, New Mexico.--continued

Sample Number	Hg PPM (CVAA)	Fe PCT (ICP)	Mn PCT (ICP)	Ba PPM (XRF)	Cr PPM (ICP)	W PPM (ICP)	Sr PPM (XRF)	F PPM (SI)	F % (DIST)	CaF2 %
21	<0.010	4.86	957*	3700	16	<20	1431	na	na	xx
22	<0.010	0.52	727*	690	12	<20	63	907	na	xx
23	<0.010	2.09	1225*	1800	18	<20	749	1435	na	xx
24	0.051	1.74	138*	4000	12	<20	224	na	na	xx
25	0.087	1.17	2727*	16200	13	<20	380	na	na	xx
26	0.034	1.44	<0.01	1200	15	<10	168	na	na	xx
27	0.018	1.12	<0.01	110	22	<10	47	na	na	xx
28	<0.010	1.07	0.02	50	25	<10	27	na	na	xx
29	<0.010	0.86	216*	1800	28	<20	508	141	na	xx
30	<0.010	1.19	205*	2000	24	<20	77	317	na	xx
31	0.020	3.96	0.21	1900	59	<10	534	na	na	xx
32	<0.010	1.81	212*	1500	65	<20	350	94	na	xx
33	<0.010	1.74	1814*	1100	31	<20	298	79	na	xx
34	<0.010	1.21	351*	2400	17	<20	896	100	na	xx
35	<0.010	1.63	1892*	1600	37	<20	459	201	na	xx
36	<0.010	2.16	2534*	1600	44	<20	329	395	na	xx
37	<0.010	4.17	1441*	3000	55	<20	542	676	na	xx
38	<0.010	3.77	3066*	2800	41	<20	1104	867	na	xx
39	<0.010	4.31	1850*	3700	61	<20	1368	772	na	xx

Appendix A.-- Analytical results and sample descriptions for samples from the Red Cloud mining district, Lincoln County, New Mexico.--continued

Sample Number	Hg PPM (CVAA)	Fe PCT (ICP)	Mn PCT (ICP)	Ba PPM (XRF)	Cr PPM (ICP)	W PPM (ICP)	Sr PPM (XRF)	F PPM (SI)	F % (DIST)	CaF2 %
40	<0.010	4.59	2094*	6000	70	<20	515	889	na	xx
41	<0.010	1.60	405*	3200	22	<20	801	131	na	xx
42	0.014	0.44	264*	330	38	<20	453	1231	na	xx
43	0.018	4.40	1692*	2000	18	<20	1089	na	na	xx
44	0.044	4.58	0.20	1500	37	<10	1375	na	na	xx
45	<0.010	5.19	0.33	1400	33	<10	399	na	na	xx
46	0.026	1.26	0.05	>20000	22	<10	1369	na	na	xx
47	0.024	0.64	0.09	2200	54	<10	436	na	na	xx
48	<0.010	1.15	1253*	700	50	<20	640	na	na	xx
49	100*	2.1	782*	2900	62	<10	530	na	na	xx
50	0.033	1.59	0.09	14400	28	<10	848	na	na	xx
51	<0.010	0.51	0.02	11000	21	<10	861	na	na	xx
52	<0.010	1.18	316*	6200	18	<20	1797	na	na	xx
53	0.035	0.56	0.02	16900	49	<10	1316	na	na	xx
54	<0.010	1.65	707*	430	19	<20	107	140	na	xx
55	<0.010	3.36	823*	1100	37	<20	445	na	na	xx
56	0.066	5.13	0.21	1600	21	<10	68	na	na	xx
57	0.069	4.83	0.24	1500	27	<10	469	na	na	xx
58	40*	34.20*	2308*	280	29	<10	29	na	na	xx

Appendix A.-- Analytical results and sample descriptions for samples from the Red Cloud mining district, Lincoln County, New Mexico.--continued

Sample Number	Hg PPM (CVAA)	Fe PCT (ICP)	Mn PCT (ICP)	Ba PPM (XRF)	Cr PPM (ICP)	W PPM (ICP)	Sr PPM (XRF)	F PPM (SI)	F % (DIST)	CaF2 %
59	0.027	47.14*	0.13	950	56	<10	31	na	na	xx
60	0.024	4.31	0.12	1100	80	<10	646	na	na	xx
61	0.073	3.57	0.17	1000	14	<10	165	na	na	xx
62	0.054	4.75	0.15	2500	66	<10	393	na	na	xx
63	0.032	4.43	0.20	2600	24	<10	559	na	na	xx
64	0.040	0.72	0.01	8100	63	<10	735	na	na	xx
65	0.037	4.08	0.11	1100	39	<10	434	na	na	xx
66	0.028	3.25	1415*	1000	32	<20	295	na	na	xx
67	0.014	5.07	0.07	820	26	<10	236	na	na	xx
68	0.049	3.25	0.09	770	27	<10	309	na	na	xx
69	0.067	2.71	0.06	700	25	<10	205	na	na	xx
70	0.029	3.81	0.15	710	27	<10	332	na	na	xx
71	<0.010	1.54	2773*	>20000	28	<20	1325	>20000	na	xx
72	0.021	1.36	0.40	3300	28	<10	352	na	na	xx
73	0.013	4.43	233*	4000	34	<20	202	786	na	xx
74	<0.010	2.63	2214*	3300	16	<20	246	345	na	xx
75	0.027	2.51	0.06	>20000	44	<10	>2000	na	na	xx
76	0.052	0.93	0.17	11100	6	<10	428	na	5.480	11.26
77	0.041	0.69	0.16	9500	5	<10	439	na	5.600	11.51

Appendix A.-- Analytical results and sample descriptions for samples from the Red Cloud mining district, Lincoln County, New Mexico.--continued

Sample Number	Hg PPM (CVAA)	Fe PCT (ICP)	Mn PCT (ICP)	Ba PPM (XRF)	Cr PPM (ICP)	W PPM (ICP)	Sr PPM (XRF)	F PPM (SI)	F % (DIST)	CaF2 %
78	<0.010	3.39	1222*	4000	5	<20	639	10186	na	xx
79	0.050	1.23	0.32	9700	7	<10	496	na	11.680	24.00
80	0.044	1.00	0.22	12900	8	<10	839	na	23.520	48.33
81	0.055	0.78	0.12	3100	8	<10	566	na	2.150	4.42
82	0.052	0.86	0.47	10500	5	<10	405	na	16.480	33.87
83	<0.010	1.41	217*	1500	21	<20	188	187	na	xx
84	<0.010	1.50	746*	2000	29	<20	140	226	na	xx
85	<0.010	0.87	1105*	770	17	<20	247	602	na	xx
86	0.014	3.46	357*	2700	21	<20	90	363	na	xx
87	<0.010	1.53	0.35	>20000	23	<10	437	na	na	xx
88	0.012	1.94	0.21	3600	27	<10	168	na	na	xx
89	5.081	2.91	0.66	20000	14	<10	502	na	na	xx
90	0.198	2.12	0.14	6500	17	<10	524	na	na	xx
91	0.033	1.41	0.09	970	26	<10	534	na	na	xx
92	0.062	0.66	0.07	3300	13	<10	190	na	na	xx
93	0.031	1.26	0.14	2900	11	<10	309	na	na	xx
94	0.014	2.23	0.13	2800	19	<10	178	na	na	xx
95	0.036	0.58	0.13	1700	20	<10	802	na	na	xx
96	0.054	55.30*	0.01	230	74	<10	47	na	na	xx

Appendix A.-- Analytical results and sample descriptions for samples from the Red Cloud mining district, Lincoln County, New Mexico.--continued

Sample Number	Hg PPM (CVAA)	Fe PCT (ICP)	Mn PCT (ICP)	Ba PPM (XRF)	Cr PPM (ICP)	W PPM (ICP)	Sr PPM (XRF)	F PPM (SI)	F % (DIST)	CaF2 %
97	0.021	3.15	0.37	2200	28	<10	445	na	na	xx
98	0.016	3.32	0.49	1800	27	<10	417	na	na	xx
99	0.016	4.04	0.10	1900	33	<10	481	na	na	xx
100	<0.010	2.32	0.25	2500	41	<10	409	na	na	xx
101	0.018	1.92	0.08	1800	29	<10	85	na	na	xx
102	<0.010	0.93	0.18	18700	13	<10	591	na	na	xx
103	0.133	1.71	0.25	3000	25	<10	347	na	na	xx
104	<0.010	2.33	0.04	580	44	<10	117	na	na	xx
105	0.138	1.24	0.01	16000	43	<10	1036	na	na	xx
106	0.067	1.59	<0.01	2100	49	<10	366	na	na	xx
107	0.117	2.39	0.05	3100	124	<10	199	na	na	xx
108	0.045	1.96	2439*	>20000	28	<20	528	na	na	xx
109	<0.010	1.72	519*	19100	30	<20	384	na	na	xx
110	<0.010	0.68	476*	1800	33	<20	333	na	24.000	49.32
111	0.017	0.87	127*	10200	54	<20	430	na	6.250	12.84
112	0.012	0.91	960*	20000	45	<20	1056	na	13.500	27.74
113	<0.010	1.44	1374*	14900	48	<20	385	na	11.600	28.84
114	<0.010	1.34	718*	8700	31	<20	342	na	14.500	29.80
115	0.029	1.02	91*	>20000	21	<20	1836	na	24.500	50.35

Appendix A.-- Analytical results and sample descriptions for samples from the Red Cloud mining district, Lincoln County, New Mexico.--continued

Sample Number	Hg PPM (CVAA)	Fe PCT (ICP)	Mn PCT (ICP)	Ba PPM (XRF)	Cr PPM (ICP)	W PPM (ICP)	Sr PPM (XRF)	F PPM (SI)	F % (DIST)	CaF2 %
116	0.024	1.37	555*	>20000	26	<20	1900	na	20.250	41.61
117	0.020	1.18	974*	7100	43	<20	639	na	10.750	22.09
118	0.190	1.41	1417*	>20000	18	<20	>2000	na	26.350	54.15
119	0.024	2.00	814*	9200	47	<20	>2000	na	7.900	16.23
120	<0.010	1.69	786*	16100	27	<20	>2000	na	18.480	37.98
121	0.098	1.62	1355*	>20000	16	<20	>2000	na	30.650	62.99
122	0.018	0.89	543*	>20000	17	<20	1557	na	29.500	60.62
123	0.373	2.24	768*	13300	23	<20	>2000	na	16.850	34.63
124	0.039	2.00	1329*	>20000	23	<20	1653	na	21.900	45.00
125	<0.010	1.16	513*	11000	32	<20	795	na	16.850	34.63
126	<0.010	1.85	973*	3000	45	<20	365	na	8.550	17.57
127	0.012	1.55	1285*	740	48	<20	193	na	4.780	9.82
128	0.730	1.63	442*	>20000	26	<20	>2000	na	15.800	32.47
129	<0.010	2.42	872*	840	37	<20	>2000	na	4.450	9.14
130	<0.010	1.31	502*	>20000	23	<20	1758	na	21.900	45.00
131	<0.010	1.53	1117*	7800	32	<20	1080	na	16.400	33.70
132	0.090	1.14	651*	18800	17	<20	1947	na	31.750	65.25
133	0.011	0.41	67*	>20000	34	<20	1153	na	18.480	37.98
134	0.099	0.97	419*	>20000	27	<20	1222	na	25.400	52.20

Appendix A.-- Analytical results and sample descriptions for samples from the Red Cloud mining district, Lincoln County, New Mexico.--continued

Sample Number	Hg PPM (CVAA)	Fe PCT (ICP)	Mn PCT (ICP)	Ba PPM (XRF)	Cr PPM (ICP)	W PPM (ICP)	Sr PPM (XRF)	F PPM (SI)	F % (DIST)	CaF2 %
135	0.150	3.71	0.32	>20000	30	<10	911	na	16.000	32.88
136	0.179	3.16	0.46	11400	45	<10	436	na	8.560	17.59
137	0.868	6.98	0.76	>20000	51	<10	1009	na	20.800	42.74
138	0.972	3.16	0.59	11800	60	<10	631	na	14.720	30.25
139	1.653	3.40	0.24	>20000	60	<10	875	na	25.280	51.95
140	0.601	2.88	0.15	16000	73	<10	687	na	17.920	36.82
141	1.118	2.97	0.21	8900	91	<10	460	na	12.160	24.99
142	0.890	4.53	1.59	17400	38	<10	481	na	3.560	7.32
143	0.196	5.91	2.77	>20000	62	<10	553	na	1.350	2.77
144	0.535	1.78	0.23	4100	61	<10	377	na	2.600	5.34
145	12.174	4.84	0.39	>20000	86	<10	658	na	na	xx
146	28.000	1.08	0.08	5300	108	<10	235	na	na	xx
147	89.000	0.44	0.01	5100	37	<10	1564	na	na	xx
148	13.624	2.52	0.01	>20000	162	<10	1126	na	na	xx
149	53.000	2.62	0.03	18100	28	<10	505	na	na	xx
150	121.000	0.96	0.05	11300	22	<10	1487	na	na	xx
151	39.000	1.45	<0.01	2500	53	<10	1801	na	na	xx
152	0.166	>10.00	<0.01	5000	18	12	1827	na	na	xx
153	<0.010	1.70	0.01	4700	152	<10	213	na	na	xx

Appendix A.-- Analytical results and sample descriptions for samples from the Red Cloud mining district, Lincoln County, New Mexico.--continued

Sample Number	Hg PPM (CVAA)	Fe PCT (ICP)	Mn PCT (ICP)	Ba PPM (XRF)	Cr PPM (ICP)	W PPM (ICP)	Sr PPM (XRF)	F PPM (SI)	F % (DIST)	CaF2 %
154	0.081	1.07	2241*	>20000	11	<20	1483	na	na	xx
155	0.066	1.51	3621*	3300	57	<20	358	na	na	xx
156	0.092	2.01	1399*	13500	39	<20	510	na	na	xx
157	0.059	1.04	1220*	>20000	24	<20	1052	na	na	xx
158	0.133	0.87	1162*	>20000	19	<20	1036	na	na	xx
159	0.258	1.20	1297*	>20000	32	<20	1085	na	na	xx
160	5.523	1.06	289*	>20000	41	<20	>2000	na	na	xx
161	0.229	2.85	0.24	>20000	37	<10	1111	na	na	xx
162	0.192	0.66	<0.01	>20000	10	<10	980	na	na	xx
163	0.149	0.79	0.02	>20000	68	<10	941	na	na	xx
164	0.125	0.76	0.04	9400	116	<10	471	na	13.120	26.96
165	5.299	1.33	0.04	>20000	49	<10	1903	na	22.560	46.36
166	9.371	1.02	0.05	15500	61	<10	1285	na	17.920	36.82
167	4.113	0.60	0.04	>20000	35	<10	>2000	na	29.600	60.83
168	2.465	0.78	0.03	>20000	12	<10	>2000	na	26.400	54.25
169	4.845	0.65	0.02	>20000	14	<10	>2000	na	26.400	54.25
170	3.860	0.26	<0.01	>20000	11	<10	>2000	na	31.840	65.43
171	0.153	2.03	0.14	2400	149	<10	179	na	na	xx
172	22.000	1.32	<0.01	3300	69	<10	308	na	na	xx

Appendix A.-- Analytical results and sample descriptions for samples from the Red Cloud mining district, Lincoln County, New Mexico.--continued

Sample Number	Hg PPM (CVAA)	Fe PCT (ICP)	Mn PCT (ICP)	Ba PPM (XRF)	Cr PPM (ICP)	W PPM (ICP)	Sr PPM (XRF)	F PPM (SI)	F % (DIST)	CaF2 %
173	1.302	1.58	0.01	7000	61	<10	295	na	na	xx
174	2.052	3.88	0.26	2400	69	<10	225	na	na	xx
175	46.000	2.99	0.04	5300	79	<10	289	na	na	xx
176	14.555	1.37	0.02	12700	28	<10	794	na	na	xx
177	0.692	5.01	0.08	7500	31	<10	1003	na	na	xx
178	1.470	2.38	<0.01	>20000	60	<10	>2000	na	na	xx
179	1.215	3.94	0.13	18700	42	<10	1331	na	na	xx
180	0.418	1.45	0.07	>20000	12	<10	915	na	na	xx
181	0.266	1.28	<0.01	>20000	34	<10	>2000	na	na	xx
182	0.265	1.04	0.43	3300	7	<10	426	na	na	xx
183	1.139	0.86	0.01	>20000	18	<10	>2000	na	na	xx
184	3.958	1.40	0.02	>20000	14	<10	1140	na	na	xx
185	0.271	1.92	0.26	4000	20	<10	1541	na	na	xx
186	1.156	1.27	<0.01	>20000	31	<10	1141	na	na	xx
187	0.552	0.24	0.01	>20000	8	<10	>2000	na	na	xx
188	1.188	1.04	0.04	>20000	45	<10	>2000	na	na	xx
189	0.020	0.75	469*	>20000	48	<20	>2000	na	11.600	23.84
190	0.014	0.53	341*	>20000	39	<20	>2000	na	15.650	32.16
191	0.042	1.05	565*	9200	46	<20	634	na	10.350	21.27

Appendix A.-- Analytical results and sample descriptions for samples from the Red Cloud mining district, Lincoln County, New Mexico.--continued

Sample Number	Hg PPM (CVAA)	Fe PCT (ICP)	Mn PCT (ICP)	Ba PPM (XRF)	Cr PPM (ICP)	W PPM (ICP)	Sr PPM (XRF)	F PPM (SI)	F % (DIST)	CaF2 %
192	0.032	2.23	950*	6700	39	<20	777	na	4.600	9.45
193	<0.010	0.25	237*	>20000	4	<20	1579	na	38.500	79.12
194	0.049	0.67	566*	>20000	13	<20	1648	na	35.500	72.95
195	0.010	0.85	126*	15100	34	<20	737	na	23.500	48.29
196	0.029	1.24	979*	3100	59	<20	263	na	6.250	12.84
197	0.065	0.72	399*	>20000	24	<20	1437	na	24.500	50.35
198	0.071	1.28	235*	1500	36	<20	269	na	9.230	18.97
199	<0.010	0.32	358*	>20000	8	<20	1744	na	37.000	76.04
200	0.030	0.77	169*	11200	44	<20	1130	na	15.950	32.78
201	0.031	0.57	67*	>20000	23	<20	1232	na	22.700	46.65
202	<0.010	0.30	17*	>20000	13	<20	>2000	na	30.650	62.99
203	<0.010	1.14	443*	3000	70	<20	215	na	3.800	7.81
204	<0.010	1.48	200*	12700	42	<20	347	na	8.850	18.19
205	0.015	1.98	0.11	4500	43	<10	236	na	na	xx
206	0.186	4.40	0.87	>20000	82	<10	588	na	na	xx
207	0.033	1.17	0.15	3500	113	<10	168	na	na	xx
208	0.159	0.39	<0.01	>20000	17	<10	>2000	na	na	xx
209	0.540	4.42	0.41	>20000	54	<10	1657	na	na	xx
210	0.261	1.33	0.04	9400	100	<10	1461	na	na	xx

Appendix A.-- Analytical results and sample descriptions for samples from the Red Cloud mining district, Lincoln County, New Mexico.--continued

Sample Number	Hg PPM (CVAA)	Fe PCT (ICP)	Mn PCT (ICP)	Ba PPM (XRF)	Cr PPM (ICP)	W PPM (ICP)	Sr PPM (XRF)	F PPM (SI)	F % (DIST)	CaF2 %
211	0.243	1.22	0.03	10400	69	<10	1394	na	na	xx
212	1.412	0.59	0.03	>20000	17	<10	>2000	na	na	xx
213	0.646	2.14	0.16	1500	28	<10	592	na	na	xx
214	154.000	1.03	0.02	1600	81	<10	708	na	na	xx
215	27.000	1.16	0.08	250	34	<10	115	na	na	xx
216	9.040	1.18	0.09	140	28	<10	155	na	na	xx
217	0.453	1.65	0.06	800	32	<10	976	na	na	xx
218	1.317	1.06	<0.01	17300	36	<10	689	na	na	xx
219	19.000	0.65	0.03	14800	39	<10	1427	na	na	xx
220	1.077	1.02	0.02	2400	39	<10	357	na	na	xx
221	2000*	3.8	1820*	59100	280	12	>2000	na	na	xx
222	0.439	0.55	<0.01	2000	15	<10	153	na	na	xx
223	0.210	1.01	<0.01	690	10	<10	94	na	na	xx
224	0.398	4.38	0.51	16700	39	<10	1073	na	na	xx
225	0.032	0.76	0.02	5700	46	<10	410	na	na	xx
226	0.173	1.78	0.10	1300	82	<10	127	na	na	xx
227	2.024	2.10	0.38	5700	58	<10	324	na	na	xx
228	54.000	1.38	0.03	5600	36	<10	154	na	na	xx
229	1.052	1.38	0.06	800	62	<10	152	na	na	xx

Appendix A.-- Analytical results and sample descriptions for samples from the Red Cloud mining district, Lincoln County, New Mexico.--continued

Sample Number	Hg PPM (CVAA)	Fe PCT (ICP)	Mn PCT (ICP)	Ba PPM (XRF)	Cr PPM (ICP)	W PPM (ICP)	Sr PPM (XRF)	F PPM (SI)	F % (DIST)	CaF2 %
230	>5000*	3.1	333*	4400	<150	35	317	na	na	xx
231	0.432	3.58	0.16	690	49	<10	172	na	na	xx
232	3.281	2.98	0.29	5800	64	<10	318	na	na	xx
233	0.137	1.56	0.11	19400	53	<10	453	na	na	xx
234	175*	3.5	666*	79000	280	12	942	na	na	xx
235	0.225	2.22	0.09	5000	53	<10	230	na	na	xx
236	0.075	2.57	0.46	16100	45	<10	709	na	na	xx
237	395*	1.4	325*	26900	130	<10	750	na	na	xx
238	1.697	1.45	0.30	>20000	17	<10	>2000	na	na	xx
239	0.059	2.02	0.42	2600	40	<10	267	na	na	xx
240	0.153	3.48	0.14	3200	34	<10	341	na	na	xx
241	0.017	0.05	<0.01	<20	2	<10	608	na	na	xx
242	0.079	0.42	0.02	640	12	<10	131	na	na	xx
243	0.481	1.77	0.17	440	19	<10	282	na	na	xx
244	0.232	0.56	0.02	120	35	<10	13	na	na	xx
245	0.196	0.48	<0.01	180	43	<10	521	na	na	xx
246	0.105	2.61	0.04	2300	61	<10	177	na	na	xx
247	0.233	4.62	0.45	16700	46	<10	345	na	na	xx
248	0.211	4.15	0.86	3400	52	<10	331	na	na	xx

Appendix A.-- Analytical results and sample descriptions for samples from the Red Cloud mining district, Lincoln County, New Mexico.--continued

Sample Number	Hg PPM (CVAA)	Fe PCT (ICP)	Mn PCT (ICP)	Ba PPM (XRF)	Cr PPM (ICP)	W PPM (ICP)	Sr PPM (XRF)	F PPM (SI)	F % (DIST)	CaF2 %
249	0.275	3.14	0.02	18200	51	<10	708	na	na	xx
250	0.213	7.59	0.17	>20000	56	<10	1008	na	na	xx
251	0.149	1.60	0.10	>20000	23	<10	>2000	na	na	xx
252	0.081	1.41	<0.01	830	25	<10	76	na	na	xx
253	0.202	0.95	0.02	400	12	<10	59	na	na	xx
254	3.610	1.33	0.14	4500	52	<10	577	na	na	xx
255	2800*	1.0	77*	4100	<85	20	2091	na	na	xx
256	0.991	1.12	<0.01	1700	51	<10	287	na	na	xx
257	570*	2.0	937*	5130	74	15	378	na	na	xx
258	<0.010	4.43	0.10	1900	22	<10	96	na	na	xx
259	0.038	2.61	0.05	160	35	<10	116	na	na	xx
260	30*	44.80*	3222*	200	41	14	53	na	na	xx

Appendix A.-- Analytical results and sample descriptions for samples from the Red Cloud mining district, Lincoln County, N. Mex.--continued

Sample Number	Bi PPM (ICP)	Br PPM (INA*)	Cd PPM (ICP)	Ga PPM (ICP)	Hf PPM (INA*)	Rb PPM (INA*)	Se PPM (INA*)	Ta PPM (INA*)	Te PPM (AA)	V PPM (ICP)	W PPM (INA*)	Zr PPM (ICP)
46	<5	4.8	3	17	12	140	<5	0.9	0.4	24	17	194
47	<5	3.8	2	56	29	110	19	<0.5	0.6	46	15	228
48	19	<180.0	108	33	<6	93	<24	<0.5	0.6	72	29	2954
49	<5	16.0	4	18	<4	100	<14	<0.5	0.4	15	17	249
50	8	3.6	<1	80	39	86	29	<0.5	<0.2	73	<15	462
208	7	4.9	<1	<216	18	64	8	<0.5	<0.2	19	<9	65
209	<5	<0.5	3	19	3	78	<5	<0.5	<0.2	198	2	30
210	<5	<0.5	1	16	10	130	<5	1.0	<0.2	28	5	156
211	<5	0.8	2	17	<1	<5	<5	<0.5	<0.2	414	3	55

Appendix A.-- Analytical results and sample descriptions for samples from the Red Cloud mining district, Lincoln County, New Mexico.--continued

Sample No.	Length type	Description
1	6.0-ft chip	Fenitized intrusive breccia; mainly subangular trachyte clasts and a few sandstone clasts, fluorite, malachite, and chrysocolla in matrix; 140 cps.
2	9.5-ft chip	Carbonatized and fenitized intrusive breccia; mainly subangular to rounded sandstone with minor trachyte clasts in a brown aphanitic matrix with crystal fragments, some areas with vuggy matrix consisting of brown calcite and fluorite with botryoidal crusts of manganese oxide, hematite-limonite; 60 cps.
3	5.0-ft chip	Fenitized intrusive breccia; mainly trachyte clasts, one granite clast 1 ft in diameter, calcite coating cavities; 140 cps.
4	7.5-ft chip	Fenitized intrusive breccia; subangular to rounded trachyte and sandstone clasts, fluorite, chrysocolla, malachite, and calcite in matrix, hematite-limonite, manganese oxide; 170 cps.
5	5.0-ft chip	Fenitized intrusive breccia; mainly sandstone clasts, minor fluorite and calcite in matrix; 140 cps.
6	3.0-ft chip	Carbonatized and fenitized intrusive breccia; trachyte and sandstone clasts as much as 5 in. in diameter in brown calcite matrix, minor fluorite and chrysocolla, hematite-limonite; 140 cps.
7	5.0-ft chip	Fenitized intrusive breccia; trachyte and sandstone clasts, fluorite in matrix, minor calcite; 150 cps.
8	5.0-ft chip	Carbonatized and fenitized intrusive breccia; bleached trachyte, sandstone, and granite clasts in a brown aphanitic matrix with crystal fragments, hematite-limonite; 125 cps.
9	2.0-ft chip	Carbonatized and fenitized and brecciated trachyte; calcite, minor fluorite; 120 cps.
10	3.0-ft chip	Brecciated sandstone; fluorite, minor calcite; 50 cps.
11	3.0-ft chip	Fractured sandstone; hematite-limonite; 120-170 cps.
12	1.0-ft chip	Brecciated sandstone; fluorite, barite, chrysocolla, wulfenite, minor calcite, hematite-limonite, manganese oxide.
13	5.0-ft chip	Intrusive breccia; mainly sandstone clasts and a few trachyte clasts, fluorite and calcite in matrix; 50 cps.
14	10.0-ft chip	Intrusive breccia; sandstone and trachyte clasts, fluorite, barite, and calcite in matrix; 50 cps.
15	4.0-ft chip	Intrusive breccia; sandstone and limestone clasts, appears to have been brecciated along bedding plane, fluorite, barite, and calcite in matrix; 50 cps.
16	2.0-ft chip	Brecciated limestone bed, angular limestone clasts, calcite and minor fluorite in matrix; 40 cps.
17	1.0-ft chip	Brecciated limestone bed, angular limestone clasts, calcite and minor fluorite in matrix; 45 cps.

Appendix A.-- Analytical results and sample descriptions for samples from the Red Cloud mining district, Lincoln County, New Mexico.--continued

Sample No.	Length type	Description
18	2.0-ft chip	Intrusive breccia; angular to subrounded limestone and sandstone clasts, calcite matrix, hematite-limonite, manganese oxide; 45 cps.
19	2.0-ft chip	Intrusive breccia; limestone and sandstone clasts, calcite matrix, barite; 45 cps.
20	Grab select	Fragments of brecciated sandstone from stockpile, fluorite, chrysocolla, malachite, calcite coating open spaces, hematite-limonite.
21	Grab	Fragments of fenitized andesite porphyry dike, contains euhedral hornblende, augite and plagioclase phenocrysts in a aphanitic matrix.
22	3.0-ft chip	Fenitized trachyte dike 15 ft wide, vuggy aphanitic groundmass with a few remnants of feldspar phenocrysts; pink tabular feldspar crystals, fluorite cubes, and hexagonal plates of sericite crystals in vugs; 110 cps.
23	2.0-ft chip	Fenitized syenite, consisting of pink feldspar with minor biotite, altered brown acute rhombohedral shaped crystals, some areas vuggy with vugs containing tabular feldspar and euhedral hexagonal plates of muscovite; 160 cps.
24	3.0-ft chip	Shaft, 10 ft deep; brecciated trachyte dike in contact with brecciated limestone, calcite; 85 cps.
25	4.0-ft chip	Shaft, 10 ft deep; brecciated limestone in contact with brecciated sandstone and trachyte dike (sample 24), calcite; 85 cps.
26	1.0-ft chip	Fenitized and fractured trachyte dike, aphanitic groundmass with scattered albite phenocrysts cut by potassium feldspar veinlets with hematite-limonite; 90 cps.
27	3.0-ft chip	Fenitized trachyte dike, aphanitic groundmass with scattered feldspar phenocrysts cut by potassium feldspar veinlets much as 1/8 in. in width, hematite-limonite; 170 cps.
28	3.0-ft chip	Fenitized trachyte dike, aphanitic groundmass with scattered feldspar phenocrysts cut by potassium feldspar veinlets with hematite-limonite; 155 cps.
29	Composite chip 5-ft area	Fenitized gneiss, gray feldspars rimmed by white fenite feldspar, aegirine; 45 cps.
30	Grab	Fragments of fenitized gneiss in tree roots, gray feldspars rimmed by white fenite feldspar, aegirine; 45 cps.
31	Composite chip 5-ft area	Fenitized intrusive breccia; gneiss, sandstone, andesite, and trachyte clasts in a tan aphanitic matrix with crystal fragments, bleached; 20-50 cps.
32	Composite chip 5-ft area	Variably fenitized banded gneiss; gneiss has overall green color cast, gray feldspars rimmed by white fenite feldspar, aegirine, in places gneiss cut by veinlets as much as 1/2 in. wide containing green aegirine, blue sodic amphibole, fenite feldspar, hematite-limonite, and fluorite; vugs containing radiating clusters of green prismatic aegirine crystals as much as 1/2 in. long, blue sodic amphibole coating fractures; 50 cps.

Appendix A.-- Analytical results and sample descriptions for samples from the Red Cloud mining district, Lincoln County, New Mexico.--continued

Sample No.	Length type	Description
33	Grab	Fragments of fenitized gneiss in tree roots; gray feldspars rimmed by white fenite feldspar, aegirine; 50 cps.
34	1.0-ft chip	Fenitized gneiss, gray feldspars rimmed by white fenite feldspar, aegirine, 75 cps.
35	Grab	Fragments of fenitized gneiss and intrusive breccia in tree roots; aegirine; 75 cps.
36	Grab	Fenitized and carbonatized intrusive breccia; gneiss fragments in an aphanitic matrix, bleached, hematite-limonite; 60 cps.
37	Grab	Fragments of fenitized and carbonatized intrusive breccia in tree roots; angular to subrounded granite and gneiss clasts in a brown aphanitic matrix, hematite-limonite; 50 cps.
38	Grab	Fragments of fenitized and carbonatized intrusive breccia from dump; angular to subrounded sandstone, schist, granite, and gneiss clasts as much as 12 in. in diameter in a brown aphanitic matrix, 1/8 to 1/4 in. wide white calcite veinlets, hematite-limonite; 75 cps.
39	Grab	Fragments of fenitized and carbonatized intrusive breccia from dump; angular to subrounded granite, gneiss, trachyte clasts as much as 10 in. in diameter in a brown aphanitic matrix, 1/8 to 1/4 in. wide white calcite veinlets, hematite-limonite; 80 cps.
40	Grab	Fragments of silicified intrusive breccia from dump; chalcedony partially replacing and filling open space in intrusive breccia, silicified fragments as wide as 6 in., vuggy, hematite-limonite; 70 cps.
41	2.0-ft chip	Fenitized gneiss, gray feldspars rimmed by white fenite feldspars, aegirine, 85 cps.
42	Composite chip 10-ft area	Fenitized sandstone; sandstone with clots of blue crocidolite and hematite pseudomorphs after cubic pyrite; 45 cps.
43	1.0-ft chip	Carbonatized intrusive breccia; subangular granitic and sandstone clasts as much as 6 in. in diameter in a tan aphanitic matrix with crystal fragments; 80 cps.
44	Composite chip 10-ft area	Fenitized intrusive breccia; angular to subrounded granitic, trachyte, and sandstone clasts as much as 6 in. in diameter in a tan aphanitic matrix with crystal fragments, minor calcite, hematite-limonite; 40 cps.
45	Grab	Intrusive breccia; angular to subrounded granite, trachyte, and sandstone clasts as much as 6 in. in diameter in a tan aphanitic matrix with crystal fragments, minor calcite, hematite-limonite; 60 cps.
46	1.0-ft chip	Opencut, 12 ft by 15 ft; brecciated zone in trachyte, striking N. 45° W. and dipping 39° E.; abundant fluorite; 100 cps.
47	2.0-ft chip	Outcrop; brecciated sandstone, fluorite, minor calcite; 30 cps.
48	1.0-ft chip	Trench, 200 ft by 35 ft, fractured sandstone with minor breccia, fluorite, calcite; 45 cps.

Appendix A.-- Analytical results and sample descriptions for samples from the Red Cloud mining district, Lincoln County, New Mexico.--continued

Sample No.	Length type	Description
49	Grab select	Shaft, 85 ft deep; Fragments of brecciated sandstone and trachyte from dump, fluorite, barite, hematite-limonite pseudomorphs after pyrite; 65 cps.
50	Grab	Pit, 15 ft by 10 ft; Fragments of brecciated sandstone from dump, fluorite, hematite-limonite after pyrite; 40 cps.
51	Grab	Pit, 65 ft by 50 ft; fragments of brecciated trachyte from dump, fluorite, barite; 55 cps.
52	Grab	Shaft, 11 ft deep; fragments of brecciated sandstone from dump, fluorite, barite, hematite-limonite; 40 cps.
53	Grab	Trench, 150 ft by 12 ft; fragments of brecciated sandstone from dump, fluorite; 30 cps.
54	2.0-ft chip	Outcrop; trachyte, zoned feldspar phenocrysts averaging 4 mm in length in a purplish-gray aphanitic groundmass, mafics altered to hematite-limonite; 40 cps.
55	Grab	Pit, 15 ft by 10 ft; fragments of fenitized intrusive breccia from dump, subangular sandstone, trachyte, and granite clasts in a purplish-gray aphanitic matrix with crystal fragments; 40 cps.
56	Grab	Fragments of fenitized intrusive breccia; subangular to subrounded clasts of sandstone, trachyte, and granite as much as 6 in. in diameter in a gray aphanitic matrix with crystal fragments; hematite-limonite, manganese oxide; 50 cps. Rock slab examined under CL.
57	Grab	Fragments of intrusive breccia; subangular to subrounded clasts of sandstone, trachyte, and granite as much as 6 in. in diameter in a gray aphanitic matrix with crystal fragments; hematite-limonite, 40 cps.
58	4.0-ft chip	Opencut; iron skarn in contact with trachyte, hematite, fibrous green amphibole, feldspar, and allanite, calcite crystals on fractures; 80 cps.
59	Grab	Shaft, 50 ft deep; fragments of iron skarn from dump, magnetite, hematite, fibrous amphibole, pyroxene, and quartz; 80 cps.
60	Grab	Fragments of intrusive breccia; subangular to subrounded clasts of sandstone and trachyte in a tan aphanitic matrix with crystal fragments; hematite-limonite; 35 cps.
61	Grab	Pit, 10 ft by 10 ft; fragments of iron skarn from dump, gray radiating fibrous amphibole, greenish-black prismatic pyroxene, hematite, and calcite on fractures; 25 cps.
62	Grab	Fragments of intrusive breccia; subangular to subrounded clasts of sandstone and trachyte in a tan aphanitic matrix with crystal fragments; hematite-limonite; 40 cps.
63	Grab	Fragments of intrusive breccia; angular to subrounded clasts of sandstone and trachyte in a tan aphanitic matrix with crystal fragments; hematite-limonite; 35 cps.
64	0.4-ft chip	Pit, 6 ft by 6 ft; brecciated zone in sandstone, striking N. 3° W. and dipping 76° E., fluorite; 40 cps.

Appendix A.-- Analytical results and sample descriptions for samples from the Red Cloud mining district, Lincoln County, New Mexico.--continued

Sample No.	Length type	Description
65	Grab	Fragments of intrusive breccia; subangular to rounded clasts of sandstone, trachyte, and granite as much as 4 in. in diameter in a tan aphanitic matrix with crystal fragments; hematite-limonite; 35 cps.
66	Grab	Fragments of intrusive breccia; angular to rounded clasts of sandstone and trachyte as much as 6 in. in diameter in a tan aphanitic matrix with crystal fragments; hematite-limonite; 80 cps.
67	Grab	Fragments of intrusive breccia; subangular to subrounded clasts of sandstone, trachyte, and granite as much as 6 in. in diameter in a tan aphanitic matrix with crystal fragments; hematite-limonite; 70 cps.
68	Grab	Fragments of fenitized intrusive breccia; subangular to subrounded clasts of sandstone and trachyte as much as 2 in. in diameter in a tan aphanitic matrix with crystal fragments; hematite-limonite; 90 cps.
69	1.0-ft chip	Outcrop; altered intrusive breccia, subangular to subrounded clasts of sandstone and trachyte as much as 4 in. in diameter in a tan aphanitic matrix with crystal fragments; hematite-limonite; 170 cps.
70	Grab	Fragments of altered intrusive breccia; subangular to subrounded clasts of sandstone and trachyte as much as 6 in. in diameter in a tan aphanitic matrix with crystal fragments; hematite-limonite; 70 cps.
71	4.0-ft chip	Vuggy barite, fluorite, and quartz rich zone in intrusive breccia; broken bluish white barite crystals as much as 1 1/2 in. long in a finer mass of barite, fluorite and quartz, pyrite pyritohedrons altering to hematite-limonite; 65 cps.
72	2.0-ft chip	Fenitized intrusive breccia; trachyte clasts, hematite-limonite, manganese oxide; 85 cps.
73	2.0-ft chip	Fenitized intrusive breccia; trachyte and granite clasts, hematite-limonite; 105 cps.
74	Grab	Fragments of fenitized intrusive breccia; trachyte clasts, hematite limonite, manganese oxide, 70 cps.
75	Grab	Float fragment of vuggy barite, fluorite, and quartz rich rock similar to sample 71.
76	5.0-ft chip	Fenitized intrusive breccia, mainly angular to rounded trachyte clasts with a few sandstone clasts in a matrix of brown calcite, fluorite and quartz crystals, pyrite pyritohedrons altering to hematite-limonite; 75 cps.
77	5.0-ft chip	Fenitized intrusive breccia, mainly angular to rounded trachyte clasts with a few sandstone clasts in a matrix of brown calcite, fluorite and quartz crystals, pyrite pyritohedrons altering to hematite-limonite; 75 cps.
78	2.3-ft chip	Fenitized and carbonatized trachyte; brown trachyte block; 80 cps.
79	1.5-ft chip	Fenitized intrusive breccia; subangular trachyte clasts in a matrix of brown calcite and fluorite crystals, bastnaesite crystals as much as 1/8 in. in length; 80 cps.

Appendix A.-- Analytical results and sample descriptions for samples from the Red Cloud mining district, Lincoln County, New Mexico.--continued

Sample No.	Length type	Description
80	6.0-ft chip	Fenitized intrusive breccia; angular trachyte fragments in matrix of fluorite, barite, bastnaesite crystals as much as 1/2 in. in length, pyrite pyritohedrons altering to hematite- limonite, minor calcite; 380 cps.
81	3.0-ft chip	Fenitized intrusive breccia; angular to subrounded trachyte clasts in a matrix of brown calcite and fluorite, hematite-limonite; 175 cps.
82	3.0-ft chip	Fenitized intrusive breccia; angular trachyte clasts in a matrix of brown calcite and fluorite, hematite-limonite; 50 cps.
83	2.0-ft chip	Fractured and fenitized trachyte near edge of intrusive breccia; 100 cps.
84	Grab	Fragments of fenitized intrusive breccia; mainly subangular trachyte clasts and a few rounded sandstone clasts, hematite-limonite; 75 cps.
85	Grab	Fragments of fenitized trachyte in tree roots; 85 cps.
86	Grab	Fragments of fenitized intrusive breccia; angular trachyte clasts, hematite-limonite; 60 cps.
87	2.0-ft chip	Pit, 8 ft by 8 ft; fenitized intrusive breccia, trachyte clasts in a matrix of fluorite and barite, bastnaesite crystals as much as 1/8 in. in length; 130 cps.
88	3.0-ft chip	Outcrop; fractured trachyte, hematite-limonite; 150 cps.
89	4.0-ft chip	Fractured trachyte with minor breccia; fluorite in veinlets as much 2 in. in width and on fractures; 100 cps.
90	Grab select	Fragments of brecciated trachyte from dump; fluorite, chrysocolla, and malachite, 65 cps.
91	Grab	Fragment of brecciated sandstone in float; barite.
92	0.5-ft chip	Outcrop; fractured trachyte with minor breccia; striking N. 35° W. and dipping vertically, calcite; 55 cps.
93	3.0-ft chip	Outcrop; brecciated zone in trachyte, trending N. 30° W., calcite, minor fluorite; 65 cps.
94	5.0-ft chip	Outcrop; brecciated zone in trachyte, trending N. 25° E., fluorite, calcite; 75 cps.
95	Grab	Pit, 8 ft by 8 ft; fragments of trachyte from dump, zoned feldspar phenocrysts averaging 4 mm in length in a white to light gray aphanitic groundmass, mafics altered to hematite-limonite; 50 cps.
96	Grab	Shaft, 18 ft deep; fragments of magnetite-hematite with minor quartz from dump; 35 cps.
97	3.0-ft chip	Adit, 30 ft long; fenitized and carbonatized intrusive breccia, angular to rounded granite, sandstone, limestone clasts as much as 6 in. in diameter in a bleached white to light gray aphanitic matrix with crystal fragments, minor fluorite, calcite on fractures; 120 cps.

Appendix A.-- Analytical results and sample descriptions for samples from the Red Cloud mining district, Lincoln County, New Mexico.--continued

Sample No.	Length type	Description
98	5.0-ft chip	Adit, 30 ft long; fenitized and carbonatized intrusive breccia, mainly angular granite, trachyte, sandstone, limestone clasts as much as 12 in. in diameter in a bleached white to light gray aphanitic matrix with crystal fragments, minor fluorite, calcite on fractures; 120 cps.
99	Grab	Fragments of intrusive breccia in float; trachyte and sandstone clasts in a tan aphanitic matrix with crystal fragments; 40 cps.
100	3.0-ft chip	Intrusive breccia; angular to rounded granite, sandstone, limestone clasts as much as 12 in. in diameter in a tan to light gray aphanitic matrix with crystal fragments, calcite; 50 cps.
101	2.0-ft chip	Brecciated sandstone; angular sandstone clasts as much as 1/2 in. in diameter, calcite, minor fluorite.
102	3.0-ft chip	Brecciated sandstone; angular sandstone clasts, calcite, fluorite; 20 cps.
103	4.0-ft chip	Brecciated sandstone; angular sandstone clasts, calcite, minor fluorite; 55 cps.
104	Grab	Pit, 8 ft by 8 ft, fragments of fractured sandstone from dump, calcite on fractures.
105	2.0-ft chip	Pit, 7 ft by 7 ft, on edge of bulldozed area 130 ft by 100 ft; brecciated trachyte, fluorite; 170 cps.
106	1.5-ft chip	Bulldozed area, 130 ft by 100 ft; fractured and altered trachyte, hematite-limonite; 100 cps.
107	1.3-ft chip	Opencut, 10 ft by 5 ft; brecciated trachyte sandstone contact, trending N. 25° E. and dipping vertically, hematite-limonite, minor calcite; 70 cps.
108	4.0-ft chip	Pit, 10 ft by 10 ft; brecciated zone in sandstone, trending N. 85° W., fluorite, barite, hematite-limonite; 65 cps.
109	2.0-ft chip	Outcrop; brecciated zone in sandstone, trending N. 40° W., fluorite, barite, hematite-limonite; 50 cps.
110	7.0-ft chip	Brecciated sandstone; angular sandstone clasts, fluorite, barite, hematite-limonite; 40 cps.
111	6.0-ft chip	Brecciated sandstone; angular sandstone clasts, fluorite, barite, hematite-limonite; 55 cps.
112	6.5-ft chip	Brecciated sandstone; angular sandstone clasts, fluorite, barite, hematite-limonite; 50 cps.
113	6.5-ft chip	Brecciated sandstone; angular sandstone clasts, fluorite, barite, hematite-limonite; 40 cps.
114	9.0-ft chip	Brecciated sandstone; angular sandstone clasts, fluorite, barite, hematite-limonite; 40 cps.
115	2.5-ft chip	Brecciated sandstone; angular sandstone clasts, fluorite, translucent blue-green barite, greenish-yellow bastnaesite crystals as much as 1/16 in. in length, hematite-limonite pseudomorphs after pyrite; 55 cps.

Appendix A.-- Analytical results and sample descriptions for samples from the Red Cloud mining district, Lincoln County, New Mexico.--continued

Sample No.	Length type	Description
116	5.5-ft chip	Brecciated sandstone; few angular sandstone clasts, fluorite, translucent blue-green barite, hematite-limonite pseudomorphs after pyrite; 75 cps.
117	4.5-ft chip	Brecciated sandstone; angular sandstone clasts, fluorite, translucent blue-green barite, hematite-limonite pseudomorphs after pyrite; 125 cps.
118	5.0-ft chip	Brecciated sandstone; angular sandstone clasts, fluorite, barite, hematite-limonite pseudomorphs after pyrite; 175 cps.
119	4.0-ft chip	Brecciated sandstone; angular sandstone clasts, fluorite, calcite coatings on bedding planes, hematite-limonite pseudomorphs after pyrite; 125 cps.
120	3.5-ft chip	Brecciated sandstone; angular sandstone clasts, fluorite, calcite veinlets, hematite-limonite; 125 cps.
121	4.0-ft chip	Brecciated sandstone; angular sandstone clasts, fluorite, barite, hematite-limonite; 115 cps.
122	4.0-ft chip	Brecciated sandstone; angular sandstone clasts, fluorite, barite, hematite-limonite; 125 cps.
123	5.0-ft chip	Brecciated sandstone; angular sandstone clasts, fluorite, malachite, hematite-limonite pseudomorphs after pyrite; 115 cps.
124	4.0-ft chip	Brecciated sandstone; angular sandstone clasts, fluorite, hematite-limonite; 140 cps.
125	3.0-ft chip	Brecciated sandstone; angular sandstone clasts, fluorite, pink barite crystals, hematite-limonite; 75 cps.
126	3.0-ft chip	Brecciated sandstone; angular sandstone clasts, fluorite, pink barite crystals, hematite-limonite; 85 cps.
127	2.5-ft chip	Fractured sandstone; fluorite veinlets as much as 1/16 in. in width; 70 cps.
128	3.5-ft chip	Brecciated sandstone; angular sandstone clasts, fluorite, malachite, hematite-limonite pseudomorphs after pyrite; 125 cps.
129	3.0-ft chip	Fractured sandstone; minor breccia, minor fluorite; 70 cps.
130	4.0-ft chip	Brecciated sandstone; angular sandstone clasts, fluorite, barite, hematite-limonite; 130 cps.
131	5.0-ft chip	Brecciated sandstone; angular sandstone clasts, fluorite, barite, hematite-limonite; 95 cps.
132	6.0-ft chip	Brecciated sandstone; few angular sandstone clasts, fluorite, white to greenish-blue barite crystals, malachite, hematite-limonite pseudomorphs after pyrite; 75 cps.
133	4.0-ft chip	Brecciated sandstone; angular sandstone clasts, fluorite; 50 cps.

Appendix A.-- Analytical results and sample descriptions for samples from the Red Cloud mining district, Lincoln County, New Mexico.--continued

Sample No.	Length type	Description
134	7.0-ft chip	Brecciated sandstone; angular sandstone clasts, fluorite, barite, bastnaesite crystals as much as 1/8 in. in length, hematite-limonite, manganese oxide; 50 cps.
135	3.8-ft chip	Brecciated sandstone; angular sandstone clasts, fluorite, clay minor calcite; 70 cps.
136	3.0-ft chip	Brecciated sandstone; angular sandstone clasts, fluorite; 75 cps.
137	3.0-ft chip	Brecciated sandstone; angular sandstone clasts, fluorite, barite; 70 cps.
138	3.0-ft chip	Brecciated sandstone; angular sandstone clasts, fluorite, minor calcite; 55 cps.
139	3.0-ft chip	Brecciated sandstone; angular sandstone clasts, fluorite, barite, minor calcite; 75 cps.
140	5.0-ft chip	Brecciated sandstone; angular sandstone clasts, minor fluorite, clay, minor calcite; 85 cps.
141	3.0-ft chip	Brecciated sandstone; minor fluorite, clay, calcite; 85 cps.
142	3.0-ft chip	Brecciated sandstone; clay, calcite; 150 cps.
143	1.0-ft chip	Brecciated sandstone; clay; 68 cps.
144	1.7-ft chip	Brecciated sandstone; fluorite, clay, minor calcite; 40 cps.
145	4.0-ft chip	Brecciated sandstone; fluorite, malachite, chrysocolla; 55 cps.
146	1.0-ft chip	Brecciated sandstone; chalcocite, malachite, calcite, minor fluorite, hematite-limonite; 55 cps.
147	1.7-ft chip	Brecciated sandstone; chalcocite, malachite, calcite, minor fluorite, hematite-limonite; 60 cps.
148	0.6-ft chip	Brecciated sandstone; chrysocolla, azurite, malachite, calcite, minor fluorite, hematite-limonite; 50 cps.
149	Grab select	Fragments of brecciated sandstone and a few fragments of limestone from dump; chalcocite, chrysocolla, malachite, fluorite, calcite.
150	Grab select	Fragments of brecciated sandstone and a few fragments of limestone from dump; azurite, chrysocolla, malachite, fluorite, calcite; 65 cps.
151	5.0-ft chip	Brecciated sandstone; chrysocolla, azurite, malachite, calcite, fluorite, hematite-limonite; 130 cps.
152	Grab	Pit, 8 ft by 8 ft; fractured sandstone, minor breccia, hematite-limonite; 70 cps.
153	2.5-ft chip	Trench, 10 ft by 5 ft; brecciated sandstone, minor fluorite; 55 cps.

Appendix A.-- Analytical results and sample descriptions for samples from the Red Cloud mining district, Lincoln County, New Mexico.--continued

Sample No.	Length type	Description
154	4.0-ft chip	Brecciated limestone bed; brown calcite, fluorite, barite, hematite-limonite; 55 cps.
155	3.3-ft chip	Brecciated limestone bed; brown calcite, fluorite, hematite-limonite; 50 cps.
156	4.5-ft chip	Brecciated zone in sandstone; fluorite, hematite-limonite; 60 cps.
157	Grab	Fragments of brecciated sandstone and limestone from dump; brown calcite, fluorite, barite, hematite-limonite pseudomorphs after pyrite; 55 cps.
158	3.0-ft chip	Brecciated sandstone-limestone contact; fluorite, barite, sphalerite, hematite-limonite; 45 cps.
159	4.0-ft chip	Brecciated sandstone; fluorite, barite, hematite-limonite; 55 cps.
160	6.0-ft chip	Brecciated sandstone and limestone; brown calcite, fluorite, malachite, chrysocolla, hematite-limonite; 125 cps.
161	3.0-ft chip	Brecciated zone in sandstone; fluorite, anglesite, manganese oxide; 175 cps.
162	Grab select	Fragments of brecciated sandstone from dump; fluorite, chrysocolla, malachite, anglesite, minor calcite.
163	Grab select	Fragments of brecciated sandstone from dump; fluorite, hematite-limonite.
164	5.0-ft chip	Brecciated sandstone; angular sandstone clasts as large as 2 ft in diameter, fluorite, hematite-limonite, manganese oxide; 65 cps.
165	7.0-ft chip	Brecciated sandstone; angular sandstone clasts as much as 12 in. in diameter, fluorite, chrysocolla, malachite, hematite-limonite; 100 cps.
166	3.0-ft chip	Brecciated sandstone; fluorite, chrysocolla, hematite-limonite; 70 cps.
167	5.0-ft chip	Fluorite rich zone; few angular sandstone clasts, galena, malachite, chrysocolla, barite, hematite-limonite; 350 cps.
168	5.0-ft chip	Fluorite rich zone; few angular sandstone clasts, galena, malachite, chrysocolla, barite, hematite-limonite; 350 cps. Polished thin section and rock slab examined under CL.
169	5.0-ft chip	Fluorite rich zone; subangular sandstone clast 18 in. in diameter, galena, malachite, chrysocolla, barite, hematite-limonite; 350 cps.
170	3.0-ft chip	Fluorite rich zone; few angular sandstone clasts, galena, malachite, chrysocolla, barite, hematite-limonite; 350 cps.
171	4.0-ft chip	Brecciated zone in sandstone; fluorite, chrysocolla; 75 cps.
172	5.0-ft chip	Brecciated zone in sandstone; fluorite, chrysocolla, quartz coating fractures; 155 cps.

Appendix A.-- Analytical results and sample descriptions for samples from the Red Cloud mining district, Lincoln County, New Mexico.--continued

Sample No.	Length type	Description
173	2.5-ft chip	Brecciated sandstone; fluorite; 55 cps.
174	3.0-ft chip	Fractured sandstone with minor breccia; fluorite, chrysocolla; 80 cps.
175	4.0-ft chip	Brecciated sandstone; fluorite, chalcocite, chrysocolla; 140 cps.
176	5.0-ft chip	Brecciated sandstone; fluorite, chrysocolla, hematite-limonite; 130 cps.
177	4.0-ft chip	Brecciated sandstone; fluorite, hematite-limonite; 150 cps.
178	5.0-ft chip	Brecciated zone in sandstone; fluorite; 200 cps.
179	5.0-ft chip	Brecciated sandstone; fluorite, chrysocolla, malachite.
180	5.0-ft chip	Brecciated sandstone; fluorite, barite, chrysocolla; 250 cps.
181	5.0-ft chip	Brecciated sandstone; fluorite, chrysocolla; 210 cps.
182	Grab select	Fragments of brecciated limestone; brown calcite, fluorite, hematite-limonite, manganese oxide; 50 cps.
183	5.0-ft chip	Brecciated sandstone; fluorite, barite, chrysocolla; 110 cps.
184	7.0-ft chip	Brecciated sandstone; fluorite, malachite; 70 cps.
185	0.5-ft chip	Fractured sandstone with minor breccia; fluorite, anglesite; 80 cps.
186	5.0-ft chip	Brecciated sandstone; fluorite, barite, hematite-limonite; 70 cps.
187	2.0-ft chip	Brecciated sandstone; fluorite, bastnaesite, malachite, chrysocolla, hematite-limonite; 105 cps.
188	3.0-ft chip	Brecciated sandstone; fluorite, barite; that has been rebrecciated with calcite coating open space; 150 cps.
189	5.0-ft chip	Fluorite, barite, quartz rich zone, few angular sandstone fragments; 60 cps.
190	5.0-ft chip	Brecciated sandstone; fluorite, barite, quartz, hematite-limonite; 75 cps.
191	8.0-ft chip	Brecciated sandstone; angular sandstone clasts, fluorite, barite, hematite-limonite; 55 cps.
192	8.0-ft chip	Brecciated sandstone; angular sandstone clasts, fluorite, hematite-limonite; 50 cps.

Appendix A.-- Analytical results and sample descriptions for samples from the Red Cloud mining district, Lincoln County, New Mexico.--continued

Sample No.	Length type	Description
193	1.7-ft chip	Brecciated sandstone; fluorite, barite, hematite-limonite; 35 cps.
194	4.5-ft chip	Brecciated sandstone; fluorite, minor calcite on fractures, hematite-limonite; 60 cps.
195	3.0-ft chip	Brecciated sandstone; fluorite, hematite-limonite; 80 cps.
196	2.5-ft chip	Brecciated sandstone; fluorite, barite; that has been rebrecciated, calcite on fractures; 65 cps.
197	4.5-ft chip	Brecciated sandstone; fluorite, barite; that has been rebrecciated, clay, calcite on fractures; 110 cps.
198	3.5-ft chip	Brecciated sandstone; fluorite; that has been rebrecciated, clay, calcite on fractures, clay; 110 cps.
199	Grab	Brecciated sandstone; angular sandstone clasts, fluorite, barite, hematite-limonite.
200	Grab	Fragments of brecciated sandstone from dump; angular sandstone clasts, fluorite, barite, hematite-limonite, 50 cps.
201	5.0-ft chip	Brecciated sandstone; fluorite, hematite-limonite, 115 cps.
202	3.0-ft chip	Brecciated sandstone; fluorite, hematite-limonite, 65 cps.
203	4.0-ft chip	Brecciated sandstone; fluorite, hematite-limonite, 60 cps.
204	2.0-ft chip	Brecciated sandstone; fluorite, hematite-limonite, manganese oxide; 55 cps.
205	5.0-ft chip	Fractured and brecciated trachyte; fluorite, hematite-limonite; 160 cps.
206	9.0-ft chip	Brecciated sandstone and conglomeratic sandstone; fluorite, barite, hematite-limonite pseudomorphs after pyrite, drusy quartz coating open spaces; 100 cps.
207	5.0-ft chip	Brecciated sandstone; quartz, minor fluorite, hematite-limonite, manganese oxide; 45 cps.
208	Grab	Fragments of brecciated sandstone; fluorite, barite, malachite, late calcite, hematite-limonite pseudomorphs after pyrite; 60 cps.
209	2.6-ft chip	Brecciated sandstone; fluorite, barite, hematite-limonite; 115 cps.
210	1.5-ft chip	Fractured and brecciated sandstone; fluorite, barite; 44 cps.
211	2.5-ft chip	Brecciated sandstone-dolomite contact; brown calcite, fluorite; 40 cps.
212	1.5-ft chip	Pit, 8 ft by 8 ft; brecciated sandstone-dolomite contact, trending N. 45° E.; brown calcite, fluorite, malachite; 100 cps.

Appendix A.-- Analytical results and sample descriptions for samples from the Red Cloud mining district, Lincoln County, New Mexico.--continued

Sample No.	Length type	Description
213	7.0-ft chip	Brecciated sandstone-limestone contact; brown calcite; 65 cps.
214	4.0-ft chip	Brecciated sandstone; fluorite, quartz, chrysocolla, malachite, azurite, hematite-limonite, drusy calcite coatings; 115 cps.
215	4.0-ft chip	Brecciated sandstone-limestone contact; calcite, quartz, chrysocolla, malachite, azurite, hematite-limonite; 30 cps.
216	3.5-ft chip	Fractured sandstone; chrysocolla, malachite, hematite-limonite pseudomorphs after pyrite, minor calcite; 30 cps.
217	Grab	Fragments of vuggy trachyte; 55 cps.
218	7.5-ft chip	Brecciated sandstone; fluorite, barite, chrysocolla, minor calcite, hematite-limonite, manganese oxide; 100 cps.
219	6.0-ft chip	Brecciated sandstone; fluorite, barite, chrysocolla, minor calcite, hematite-limonite, manganese oxide; 120 cps.
220	3.0-ft chip	Brecciated sandstone; angular sandstone clasts, fluorite, barite, chrysocolla, malachite, minor calcite, hematite-limonite, manganese oxide; 110 cps.
221	Grab	Shaft, 25 ft deep; fragments of brecciated sandstone from dump, abundant brown calcite, barite, fluorite, hematite-limonite pseudomorphs after pyrite; 150 cps.
222	3.5-ft chip	Trench, 15 ft 8 ft; Fractured and brecciated siltstone, fluorite; 150 cps.
223	8.0-ft chip	Pit, 10 ft by 10 ft; brecciated siltstone and sandstone, fluorite; 45 cps.
224	1.7-ft chip	Pit, 15 ft by 7 ft; breccia zone in sandstone, striking N. 44° W. and dipping 45° S., calcite, fluorite, hematite-limonite pseudomorphs after pyrite; 55 cps.
225	1.0-ft chip	Pit, 10 ft by 10 ft; breccia zone in sandstone, trending N. 36° E., fluorite; 45 cps.
226	5.0-ft chip	Fractured and brecciated sandstone; fluorite, malachite; 65 cps.
227	5.0-ft chip	Fractured and brecciated sandstone ; fluorite, malachite, azurite; 130 cps.
228	1.0-ft chip	Brecciated sandstone; angular sandstone clasts, fluorite, chrysocolla, mimetite; 180 cps.
229	5.0-ft chip	Brecciated sandstone; angular sandstone clasts, fluorite, chrysocolla, malachite, azurite, hematite-limonite; 180 cps.
230	4.0-ft chip	Brecciated sandstone; angular sandstone clasts, fluorite, pyrite, chalcocite, chrysocolla, malachite, azurite, hematite-limonite; 500 cps.
231	3.0-ft chip	Brecciated sandstone; gouge, minor fluorite, hematite-limonite; 70 cps.

Appendix A.-- Analytical results and sample descriptions for samples from the Red Cloud mining district, Lincoln County, New Mexico.--continued

Sample No.	Length type	Description
232	Grab 20-ft grid	Fragments of brecciated sandstone from dump; fluorite, chrysocolla, malachite, azurite, wulfenite, hematite-limonite, manganese oxide; 55 cps.
233	5.0-ft chip	Brecciated sandstone; angular sandstone clasts as much as 5 in. in diameter, fluorite, bastnaesite, hematite-limonite, manganese oxide; 125 cps.
234	4.5-ft chip	Brecciated sandstone; angular sandstone clasts, fluorite, barite, hematite-limonite, manganese oxide; 125 cps.
235	5.0-ft chip	Brecciated sandstone; angular sandstone clasts, minor fluorite, hematite-limonite; 65 cps.
236	5.0-ft chip	Brecciated sandstone; angular sandstone, fluorite, barite, clumps of bastnaesite crystals, hematite-limonite; 165 cps.
237	Grab select	Fragments of brecciated sandstone; angular sandstone clasts, fluorite, pink barite, greenish yellow bastnaesite crystals as much as 1/4 in. in length, hematite-limonite; 95 cps.
238	Grab	Shaft, 40 ft deep; fragments of conglomerate from dump, fluorite, calcite, chrysocolla, malachite, hematite-limonite pseudomorphs after pyrite; 170 cps.
239	2.0-ft chip	Adit, 25 ft long; fractured and sheared, fenitized gneissic granite, minor calcite, hematite-limonite; 35 cps. Rock slab examined under CL.
240	1.0-ft chip	Opencut, 5 ft by 5 ft; trachyte dike-gneissic granite contact, minor gouge, calcite on fractures; 120 cps.
241	7.0-ft chip	Pit, 10 ft by 10 ft; calcite vein in sandstone, trending N. 40° W., white colloform calcite, vuggy; 20 cps.
242	Grab	Pit, 10 ft by 10 ft; fragments of sandstone containing calcite veinlets from dump, minor fluorite; 25 cps.
243	1.0-ft chip	Fractured sandstone; calcite veinlets as much as 1/4 in. in width, minor fluorite; 30 cps.
244	2.0-ft chip	Fractured sandstone with minor breccia; minor fluorite, quartz; 25 cps.
245	3.0-ft chip	Brecciated sandstone; angular sandstone clasts, fluorite, quartz; 25 cps.
246	2.0-ft chip	Opencut, 10 ft by 6 ft; fractured sandstone with minor breccia, fluorite, hematite-limonite; 45 cps.
247	5.0-ft chip	Brecciated sandstone; fluorite, calcite; 150 cps.
248	5.0-ft chip	Brecciated sandstone; fluorite, calcite; 125 cps.
249	3.0-ft chip	Brecciated sandstone; fluorite, rebrecciated, clay, hematite-limonite; 140 cps.

Appendix A.-- Analytical results and sample descriptions for samples from the Red Cloud mining district, Lincoln County, New Mexico.--continued

Sample No.	Length type	Description
250	2.3-ft chip	Brecciated sandstone; fluorite, calcite on fractures, hematite-limonite; 110 cps.
251	1.0-ft chip	Brecciated sandstone; fluorite, rebrecciated, calcite coating open spaces; 150 cps.
252	1.0-ft chip	fenitized and fractured trachyte dike, aphanitic groundmass with scattered feldspar phenocrysts cut by potassium feldspar veinlets with hematite-limonite; 150 cps.
253	1.0-ft chip	fenitized and fractured trachyte dike, aphanitic groundmass with scattered feldspar phenocrysts cut by potassium feldspar veinlets with hematite-limonite; 95 cps.
254	Grab select	Fragments of brecciated sandstone from dump; fluorite, chrysocolla, malachite, azurite, hematite-limonite; 60 cps.
255	1.0-ft chip	Brecciated sandstone; fluorite, chalcocite, malachite, chrysocolla; 80 cps.
256	5.0-ft chip	Brecciated sandstone; fluorite, hematite-limonite, manganese oxide; 80 cps.
257	Grab 10-ft grid	Fragments of sandstone and brecciated sandstone from dump; fluorite, hematite-limonite; 70 cps.
258	4.5-ft chip	Adit, 26 ft long; trachyte dike, feldspar and biotite phenocrysts in an aphanitic matrix, apatite crystals, mafics altered to hematite-limonite; 75 cps.
259	2.0-ft chip	Opencut, 5 ft by 5 ft; fractured sandstone and shale with minor breccia along bedding planes, calcite veinlets; 55 cps.
260	3.0-ft chip	Pit, 100 ft by 70 ft, magnetite-hematite, calcite; 30 cps.

Appendix B.-- Whole rock and oxide analysis of selected samples from the Red Cloud mining district, Lincoln County, N. Mex.

[BFPES, borate fusion plasma-emission spectroscopy; LECO, leco method; GRAV, gravimetric method; %, percent; xx, not applicable; na, not analyzed.]

Sample Number	SiO_2 (%) (BFPES)	TiO_2 (%) (BFPES)	Al_2O_3 (%) (BFPES)	Fe_2O_3 (%) (BFPES)	MnO (%) (BFPES)	MgO (%) (BFPES)	CaO (%) (BFPES)	Na_2O (%) (BFPES)	K_2O (%) (BFPES)	P_2O_5 (%) (BFPES)	LOI (%) (GRAV)	Total (%)	BaO (%) (BFPES)	Cr_2O_3 (%) (BFPES)	S Tot (%) (LECO)
2	na	na	na	na	na	0.09	29.09	0.28	3.51	na	na	xx	na	na	na
3	na	na	na	na	na	0.18	4.70	0.70	12.01	na	na	xx	na	na	na
8	na	na	na	na	na	0.16	7.24	3.19	7.86	na	na	xx	na	na	na
9	na	na	na	na	na	0.27	8.59	1.10	10.51	na	na	xx	na	na	na
18	na	na	na	na	na	0.40	4.49	0.05	0.75	na	na	xx	na	na	na
21	51.40	1.10	18.00	8.17	0.18	3.77	6.45	4.84	2.64	0.21	2.67	99.43	0.449	<0.01	0.04
23	60.20	0.36	18.70	3.11	0.17	0.15	0.38	4.60	8.46	0.18	1.34	97.65	na	na	na
26	na	na	na	na	na	0.01	1.07	9.37	2.26	na	na	xx	na	na	na
28	na	na	na	na	na	0.06	0.11	10.20	1.12	na	na	xx	na	na	na
29	67.90	0.16	15.50	1.19	0.03	0.08	0.41	5.16	6.25	0.15	0.69	97.52	na	na	na
30	na	na	na	na	na	0.07	0.31	6.17	6.27	na	na	xx	na	na	na
31	na	na	na	na	na	0.29	0.83	4.38	5.82	na	na	xx	na	na	na
32	na	na	na	na	na	0.43	1.35	3.49	5.19	na	na	xx	na	na	na
33	na	na	na	na	na	0.03	0.04	3.58	9.36	na	na	xx	na	na	na
34	na	na	na	na	na	0.09	0.19	5.80	8.16	na	na	xx	na	na	na
35	na	na	na	na	na	0.11	0.24	6.31	6.57	na	na	xx	na	na	na
36	63.90	0.34	11.70	2.63	0.34	0.17	4.70	3.17	5.88	0.26	4.63	97.72	na	na	na
37	na	na	na	na	na	0.24	5.26	5.57	5.19	na	na	xx	na	na	na
38	52.40	0.73	13.20	5.08	0.46	0.32	9.42	3.86	5.62	0.69	8.50	100.28	na	na	na
39	na	na	na	na	na	0.16	1.72	5.53	4.31	na	na	xx	na	na	na
40	na	na	na	na	na	0.22	0.77	4.46	5.97	na	na	xx	na	na	na
41	na	na	na	na	na	0.13	0.23	7.48	6.26	na	na	xx	na	na	na
42	na	na	na	na	na	3.64	1.17	4.16	0.89	na	na	xx	na	na	na
54	66.10	0.20	17.70	2.11	0.09	0.06	0.16	6.75	5.52	0.12	0.63	99.44	0.043	<0.01	<0.02
72	65.60	0.28	16.80	1.86	0.52	0.06	0.16	4.01	9.08	0.22	1.24	100.23	0.400	<0.01	0.09
73	na	na	na	na	na	0.11	0.10	1.32	12.29	na	na	xx	na	na	na
74	na	na	na	na	na	0.06	0.04	4.90	8.95	na	na	xx	na	na	na
76	na	na	na	na	na	0.18	31.25	2.05	3.02	na	na	xx	na	na	na
78	na	na	na	na	na	0.33	8.61	2.07	9.79	na	na	xx	na	na	na
79	na	na	na	na	na	0.17	43.82	0.95	2.01	na	na	xx	na	na	na
83	na	na	na	na	na	0.04	0.04	7.76	3.76	na	na	xx	na	na	na
84	na	na	na	na	na	0.05	0.01	3.10	8.70	na	na	xx	na	na	na
85	68.50	0.23	16.30	1.04	0.13	0.05	0.21	6.62	4.03	0.09	0.78	97.98	0.076	<0.01	<0.02
86	na	na	na	na	na	0.05	0.02	0.54	14.88	na	na	xx	na	na	na
95	68.34	0.28	17.01	0.84	0.16	0.05	0.55	9.41	0.98	0.10	0.83	98.74	0.190	<0.01	0.06
239	68.00	0.14	13.70	2.32	0.55	0.13	1.10	3.28	6.95	0.25	1.94	98.64	0.280	<0.01	0.10
258	60.25	0.61	17.39	5.07	0.13	0.21	0.13	8.35	2.45	0.37	2.02	98.21	0.220	<0.01	0.11

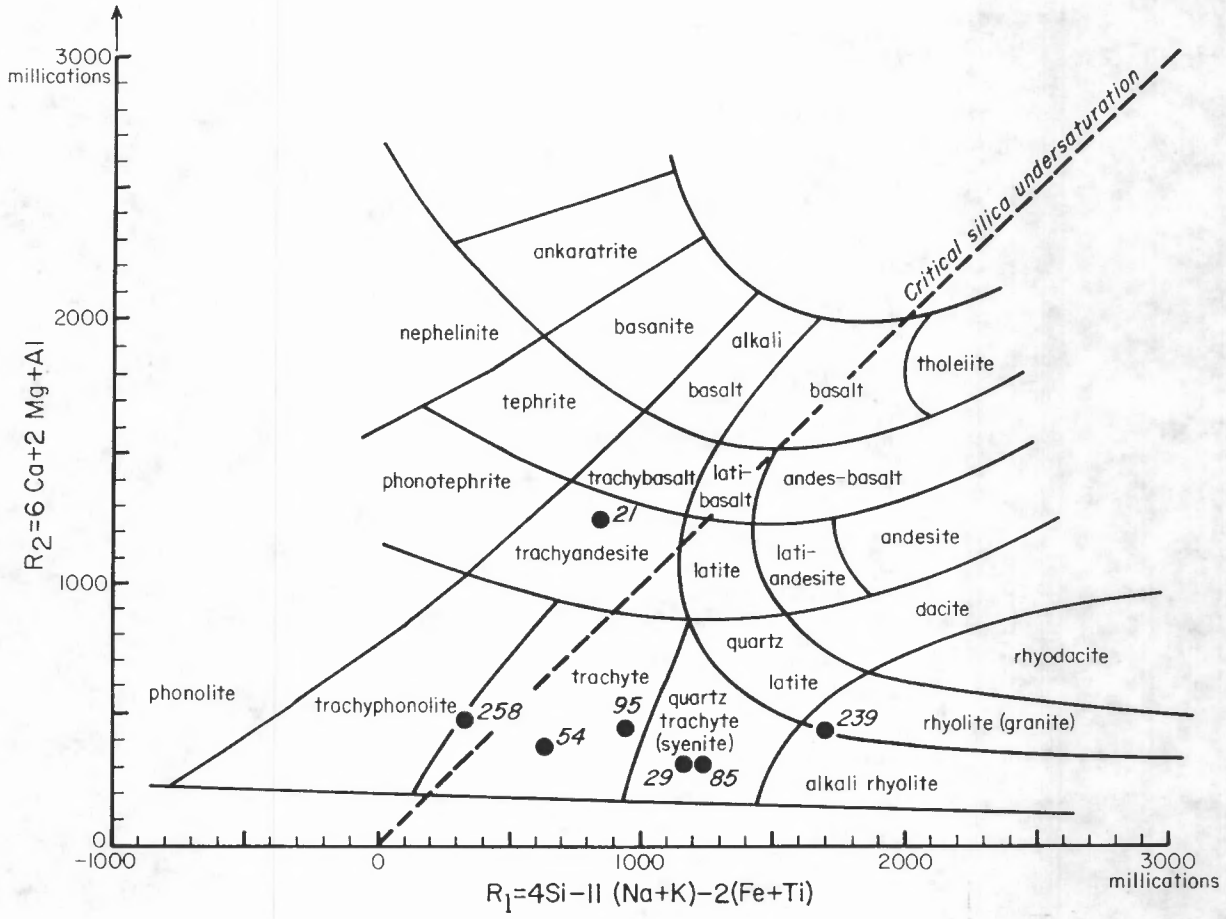

Appendix C.-- De La Roche R_1R_2 rock classification plot for samples 21, 29, 54, 85, 95, 239, and 258 from the Red Cloud mining district, Lincoln County, N. Mex. (De La Roche and others, 1980).

Appendix D.-- SEM-EDX analysis of fenite feldspar, crocidolite, and aegirine/aegirine-augite from selected samples from the Red Cloud mining district, Lincoln County, N. Mex.

[%, percent.]

Fenite Feldspar

Oxide (%)	Albite		Potassium Feldspar	
	Sample Number			
	29	76	32	73
SiO_2	71.3	68.0	65.4	64.1
TiO_2	0.0	0.0	0.0	0.0
Al_2O_3	18.1	19.5	17.6	16.0
FeO	0.0	0.0	0.0	0.0
MnO	0.0	0.0	0.0	0.0
MgO	0.0	0.0	0.0	0.0
CaO	0.0	0.7	0.1	0.0
Na_2O	10.0	10.4	0.1	1.2
K_2O	0.7	1.4	17.6	18.8

Crocidolite

Oxide (%)	Sample Number				
	32	32	32	42	42
SiO_2	54.1	54.6	50.7	58.0	59.6
TiO_2	1.5	0.8	1.2	0.2	0.1
Al_2O_3	1.0	1.2	2.4	1.2	0.8
FeO	25.0	22.4	25.0	15.4	12.0
MnO	<0.1	0.4	0.6	0.4	0.4
MgO	4.9	9.4	9.6	13.0	15.4
CaO	2.4	1.7	1.4	5.8	6.3
Na_2O	10.0	8.2	7.8	5.8	4.7
K_2O	0.5	0.8	1.0	0.4	0.7

Aegirine/aegirine-augite

Oxide (%)	Sample Number				
	29	32	32	32	32
SiO_2	50.3	53.1	49.4	52.0	50.3
TiO_2	0.1	0.1	0.0	0.2	0.3
Al_2O_3	2.2	0.8	1.1	1.0	1.1
FeO	33.0	26.5	24.8	28.5	25.6
MnO	0.0	0.6	2.8	0.4	0.1
MgO	0.9	3.2	2.6	2.1	4.2
CaO	1.0	4.8	11.4	3.5	9.9
Na_2O	12.3	10.4	7.6	11.7	8.3
K_2O	0.3	0.2	0.0	0.2	0.3

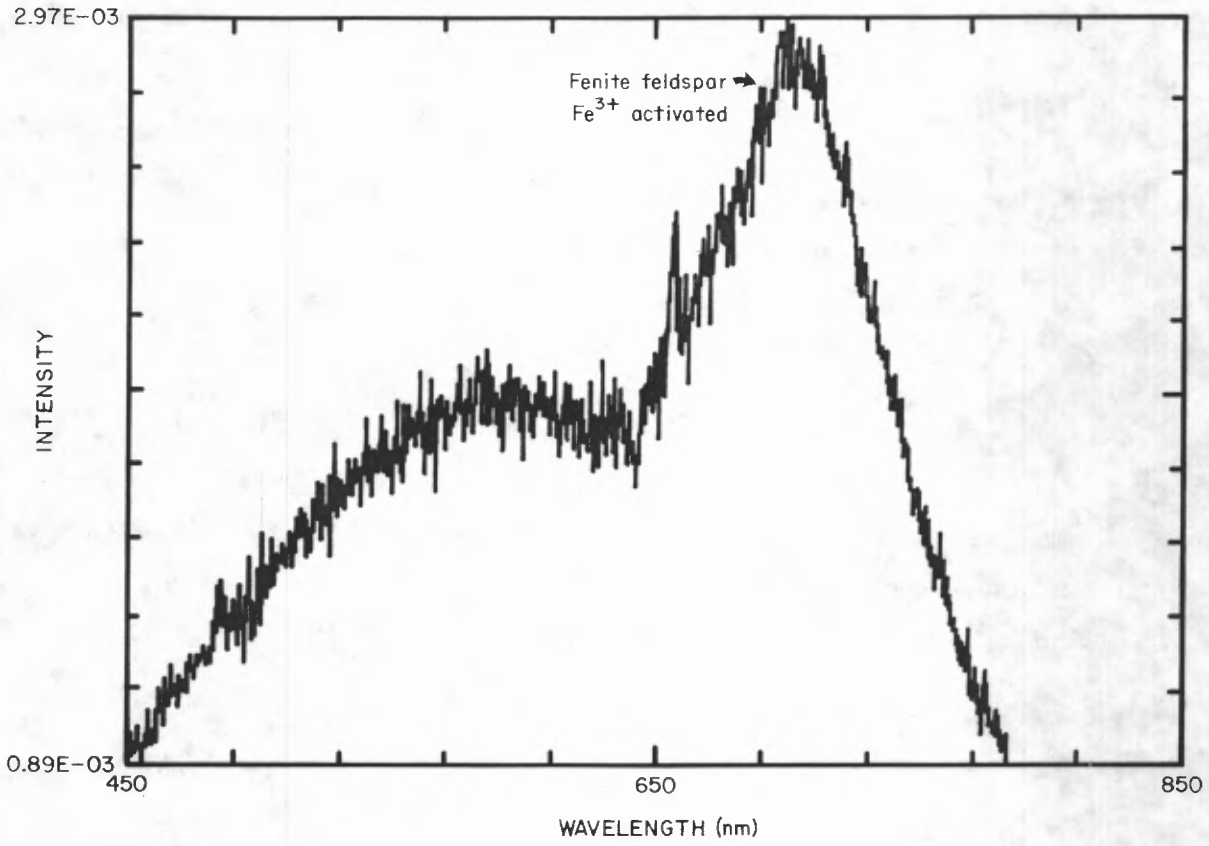

Appendix E.-- Cathodoluminescence emission spectra for tan luminescing fenite potassium feldspar from strongly fenitized intrusive breccia at sample site 73 from the Red Cloud mining district, Lincoln County, N. Mex. (provided by Anthony N. Mariano, consultant, Carlisle, Mass.).

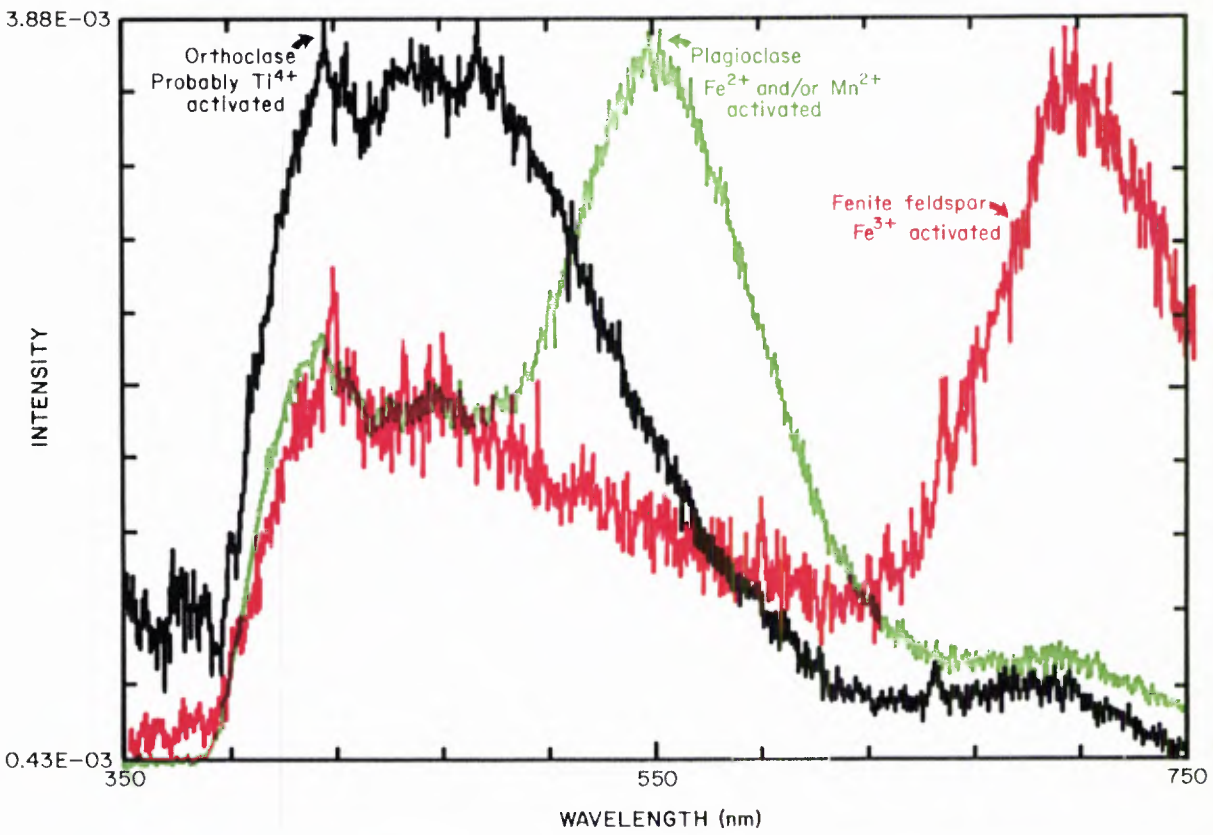

Appendix F.-- Cathodoluminescense emission spectra for brilliant red luminescing fenite feldspar, greenish yellow luminescing plagioclase, and blue luminescing orthoclase from weakly fenitized gneiss at sample site 32 from the Red Cloud mining district, Lincoln County, N. Mex. (provided by Anthony N. Mariano, consultant, Carlisle, Mass.).

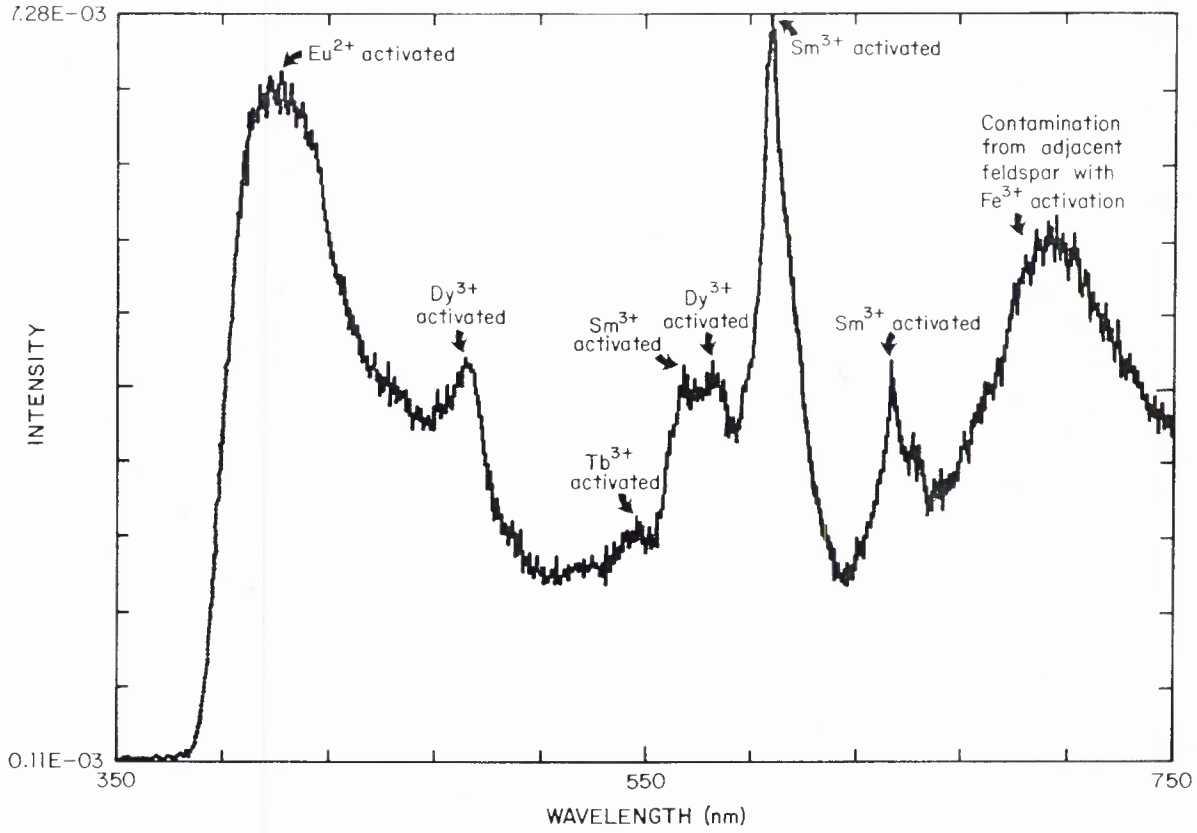

Appendix G.-- Cathodoluminescense emission spectra for blue luminescing apatite in strongly fenitized gneiss fragment found near sample site 32 from the Red Cloud mining district, Lincoln County, N. Mex. (provided by Anthony N. Mariano, consultant, Carlisle, Mass.).